National Library
of Canada

Acquisitions and
Bibliographic Services Branch

395 Wellington Street
Ottawa, Ontario
K1A 0N4

Bibliothèque nationale
du Canada

Direction des acquisitions et
des services bibliographiques

395, rue Wellington
Ottawa (Ontario)
K1A 0N4

Your file Votre référence

Our file Notre référence

NOTICE

The quality of this microform is heavily dependent upon the quality of the original thesis submitted for microfilming. Every effort has been made to ensure the highest quality of reproduction possible.

If pages are missing, contact the university which granted the degree.

Some pages may have indistinct print especially if the original pages were typed with a poor typewriter ribbon or if the university sent us an inferior photocopy.

AVIS

La qualité de cette microforme dépend grandement de la qualité de la thèse soumise au microfilmage. Nous avons tout fait pour assurer une qualité supérieure de reproduction.

S'il manque des pages, veuillez communiquer avec l'université qui a conféré le grade.

La qualité d'impression de certaines pages peut laisser à désirer, surtout si les pages originales ont été dactylographiées à l'aide d'un ruban usé ou si l'université nous a fait parvenir une photocopie de qualité inférieure.

Canada

Diffusion Coefficients at Infinite Dilution in Alcohol Solvents at Temperatures to 348 K and Pressures to 17 MPa

by

Elizabeth Cooper

A Thesis Submitted in Partial

Fulfillment of the Requirements for the

Degree of

Doctor of Philosophy

in the

Department of Chemical Engineering

University of Ottawa, 1992

National Library
of Canada

Acquisitions and
Bibliographic Services Branch

395 Wellington Street
Ottawa, Ontario
K1A 0N4

Bibliothèque nationale
du Canada

Direction des acquisitions et
des services bibliographiques

395, rue Wellington
Ottawa (Ontario)
K1A 0N4

Your file Votre référence

Our file Notre référence

ISBN 0-315-80052-6

Canada

UNIVERSITÉ D'OTTAWA
UNIVERSITY OF OTTAWA

ABSTRACT

A knowledge of diffusion coefficients in liquids is important from engineering as well as theoretical aspects. Molecular diffusivities can be used in predicting the mass transfer coefficients for the design of equipment for separation processes. The diffusion process may determine the rate at which these processes take place. The understanding of the diffusion process is important from a theoretical standpoint in helping us to understand the structure of liquids, the mechanism of diffusive transport and to test the validity of existing theories of diffusion.

This work examined the effect of temperature and particularly of pressure on the diffusion coefficients at infinite dilution of the solute gases, ammonia, propane, propene and carbon dioxide in the alcohol solvents, methanol, ethanol, propanol and butanol, using the dynamic Taylor dispersion method at temperatures of 298.15, 323.15 and 348.15 K and pressures up to 17 MPa (2500 psig). Solvent densities and some solvent viscosities were also measured over a similar range. The use of a data acquisition system for the collection and subsequent analysis of data using an IBM computer ensured that the data for molecular diffusivity, density, and viscosity were accurate and reliable. Also, because Taylor's method is a dynamic one, it is a relatively rapid method of measurement.

Although the measured diffusivities showed some differences from the diffusivities obtained from the literature, the diffusivities from this work are considered to be more reliable and accurate because of the experimental technique and type of analysis used. The measured densities and viscosities of the solvents showed excellent agreement with those reported in the literature.

It was found that the molecular diffusivities as well as the densities tended to increase linearly with increasing pressure, and the preliminary results for the viscosities showed that the viscosities tended to increase linearly with increasing pressure. Although the temperature effect on diffusivity, density and viscosity was larger than the pressure effect, there was a statistically significant effect of pressure.

It was found that the effects of hydrogen bonding, dipole moment, polarity, association, molecular mass, molecular size, shape and the resulting molecular interactions between the solute and the solvent molecules all appeared to influence

the diffusion of the gases through the solvents. The diffusion coefficients of the solutes increased in the order ammonia, propane, propene, and carbon dioxide. The diffusion coefficients in the solvents increased in the order butanol, propanol, ethanol, and methanol.

A generalized equation based on the RHS theory was developed for the systems studied in this work which requires only certain physical properties of the solute and the solvent and the temperature in order to predict the diffusion coefficient. This study provides the first systematic effort to generalize the RHS theory to predict infinite dilution coefficients of solutes and solvents of various polarities, dipole moments and degrees of association at high pressures.

With love to my husband Dave,

for his patience and support.

Acknowledgements

I am grateful to my husband Dave for his unwavering support and guidance throughout this degree.

I would like to thank Dr. Walter Hayduk for giving me the freedom to learn to think independently while always providing supervision and assistance when it was needed. His wise advice and encouragement always made those numerous large problems seem so much smaller.

I would also like to thank my parents, sisters and brothers and other members of my family. Words cannot express the depth of my gratitude for their constant encouragement and support both morally and financially.

My thanks also go to the technical support personnel of the Chemical Engineering Department who contributed much appreciated information and technical skills towards the successful completion of this project.

Financial assistance from the National Sciences and Engineering Research Council of Canada, the Ontario Graduate Scholarship program and the University of Ottawa is gratefully acknowledged.

Last but far from least I would like to express my thanks to my unforgettable friends and colleagues who were there when I needed them.

TABLE OF CONTENTS

LIST OF TABLES

LIST OF FIGURES

NOMENCLATURE

a	constant in equation (3.23)
a_1	constant in equation (3.28), (3.29) and (3.30)
A	constant in equation (3.26)
A'	constant in equation (3.31)
A_{VDW}	van der Waals area, $m^2 \cdot kmol^{-1}$
b	constant in equation (3.23)
B	constant in equation (3.37)
B_1	adjustable parameter in equation (4.41) approximately equal to $V_{max} \cdot t_R$
B_2	adjustable parameter in equation (4.41) approximately equal to 4 K
B_3, B_5	adjustable parameter in equation (4.41) accounting for baseline offset and drift
B_4	adjustable parameter in equation (4.41) equal to the average velocity of the solvent
B'	constant in equation (3.38)
C	concentration of solute at a radial distance, $mol \cdot L^{-1}$
C'	constant in equation (3.25)
C_m	radially averaged concentration of solute, $mol \cdot L^{-1}$
C_m^o	radially averaged concentration at t=0, z=0, $mol \cdot L^{-1}$
$C(\cdots)$	correction term in equation (3.9)
ΔC	difference in concentration between the sample cell and the reference cell
d	constant in equation (7.5)
D_{AA}, D_{BB}	self diffusion coefficient of A in A, and B in B, $m^2 \cdot s^{-1}$
D_{AB}	mutual diffusion coefficient of A in B, $m^2 \cdot s^{-1}$
D_{AB}^{CE}	Chapman-Enskog mutual diffusivity of a low density gas, $m^2 \cdot s^{-1}$
D_{AB}^{E}	Enskog mutual diffusivity of a moderately dense gas, $m^2 \cdot s^{-1}$
D_{AB}^{HSG}	mutual diffusion coefficient for a low density Hard Sphere Gas, $m^2 \cdot s^{-1}$
D_{AB}^{HSL}	mutual diffusivity of of a Hard Sphere Liquid, $m^2 s^{-1}$
D_{AB}^{RHS}	mutual diffusion coefficient based on rough hard sphere model, $m^2 \cdot s^{-1}$
D_{AB}^{o}	mutual diffusion coefficient at infinite dilution, $m^2 s^{-1}$
D_{BB}^{CE}	Chapman-Enskog self diffusivity of a low density gas, $m^2 \cdot s^{-1}$

D_{BB}^{E}	Enskog self diffusivity of a moderately dense gas, $m^2 \cdot s^{-1}$
D_{BB}^{HSG}	self diffusion coefficient for a low density Hard Sphere Gas, $m^2 \cdot s^{-1}$
D_{BB}^{HSL}	self diffusivity of of a Hard Sphere Liquid, $m^2 s^{-1}$
D_{BB}^{RHS}	self diffusion coefficient based on rough hard sphere model, $m^2 \cdot s^{-1}$
e	constant in equation (7.5)
E_{AA}^{j}, E_{BB}^{j}	activation energies of jumping for the solute and solvent, $J \cdot mol^{-1}$
E_D	free activation energy for the diffusion process, $J \cdot mol^{-1}$
E_η	free activation energy for the viscous process, $J \cdot mol^{-1}$
f	constant in equation (3.48)
f	frictional coefficient in equation (3.1)
F	roughness factor, correction term in equations (3.9) and (3.10)
$g(\sigma_B)$	radial distribution function in equation (3.10)
$g(\sigma_{AB})$	radial distribution function in equation (3.9)
ΔG_D	free energy of activation for diffusion compared to the equilibrium state, $J \cdot mol^{-1}$
ΔG_η	free energy of activation for viscosity compared to the equilibrium state, $J \cdot mol^{-1}$
h	Planck's constant
H	plate height
ΔH_A, ΔH_B	latent heat of vaporization of solute and solvent at their normal boiling points
ΔH_m	heat of fusion at melting point, $J \cdot kmol^{-1}$
J_r	flux density in the radial direction
J_z	flux density in the axial direction
k	Boltzmann's constant
K	Taylor diffusion coefficient
K′	constant in equations (3.34) and (3.36)
K_1	constant in equation (4.6) which is independent of temperature and pressure
K_2	constant in equation (4.10) which is independent of temperature and pressure
L	length of the dispersion column, m
M	mass of solute in sample injected, kg

$\dot{m}$	mass flow rate
$\dot{m}_1$, $\dot{m}_2$	known, 1, and unknown, 2, mass flow rates of solvent, $kg \cdot s^{-1}$
m_A, m_B	mass of one molecule of solute, A, and solvent, B, respectively
M_A, M_B	molecular weights of solute, A, and solvent, B, $kg \cdot kmol^{-1}$
n	number density of a dilute gas (molecules/volume)
n'	number density of a moderately dense gas (molecules/volume)
N	Avogadro's number
N_{De}	Dean number
N_{Re}	Reynolds number
N_{Sc}	Schmidt number
P	pressure
ΔP	pressure difference, psi
ΔP_1	pressure difference between P_1 and atmospheric pressure, psi
ΔP_2	pressure difference between P_2 and atmospheric pressure, psi
P_A, P_B	parachors of the solute and solvent
P_c	critical pressure, Pa
P_{tp}	triple point pressure, Pa
Q	volumetric flow rate of solvent, mls/min
Q_{trans}	transition volumetric flow rate for secondary effects, mls/min
r	any radial distance
R	inside radius of the dispersion column, m
r_A	radius of solute molecule, cm
R_A, R_B	radii of gyration of the solute and solvent, nm
R_c	radius of the coil or helix
R_g	gas constant, $kJ \cdot kmol^{-1} \cdot K^{-1}$
RHS	denotes the Rough Hard Sphere model
ΔR	refractive index difference between the sample cell and the reference cell
S	zeroth moment, equation (4.37)
S_i	surface tension of substance i, dynes/cm
t	time, s
$\bar{t}$	first moment, equation (4.38)
t_R	retention or residence time, s
$(t_R)_1$, $(t_R)_2$	known, 1, and unknown, 2, retention times, s
T	temperature, K
ΔT	temperature difference, K

T_1, T_2	temperatures at conditions 1 and 2, K
T_b	normal boiling point, K
T_c	critical temperature, K
T_{ref}	reference temperature for measurement of dispersion tubing, K
T_{tp}	triple point temperature, K
$\bar{u}$	average velocity, $m \cdot s^{-1}$
u_{max}	maximum centreline velocity, $m \cdot s^{-1}$
u(r)	velocity at a radial position r, $m \cdot s^{-1}$
V	molar volume of the liquid mixture, $m^3 \cdot mol^{-1}$
V_{bA}, V_{bB}	molar volumes of solute, A, and solvent, B, at their normal boiling points, $m^3 \cdot mol^{-1}$
V_o	close-packed hard sphere volume, $m^3 \cdot mol^{-1}$
V_A, V_B	molar volumes of solute, A, and solvent, B, $m^3 \cdot mol^{-1}$
V_{cA}, V_{cB}	critical volumes of solute and solvent, $cm^3 \cdot mol^{-1}$
V_D	molar volume at which diffusion is frozen, $m^3 \cdot mol^{-1}$
V_{VDW}	van der Waals volume, $m^3 \cdot kmol^{-1}$
V_i	molar volume of substance i, $L \cdot mol^{-1}$
V_η	molar volume at infinite viscosity, $L \cdot mol^{-1}$
$W_{1/2}$	peak width at half height
z	fixed axial coordinate
Z	axial coordinate moving with the mean velocity of flow, equation (4.23)
Z_c	critical compressibility factor

Superscripts

CE	Chapman-Enskog
E	Enskog
HSG	hard sphere gas
HSL	Hard Sphere Liquid
RHS	Rough Hard Sphere
o	initial condition for a dilute gas

Subscripts

A	solute
B	solvent
AB	solute and solvent or solute and surroundings
AA	solute and solute molecules
BB	solvent and solvent molecules
bA	at boiling point of A
bB	at boiling point of B
c	critical
De	Dean
i	substance i
m	average
obs	observed
ref	reference condition
Re	Reynolds
Sc	Schmidt
1	condition 1
2	condition 2

Greek symbols

α	thermal expansion coefficient
β	coefficient of sliding friction
β_{AB}	coefficient of sliding friction between A and B
δ	width of injected pulse, m
γ	constant in equation (3.37)
ϵ	constant in equation (3.36)
ϵ_A	number of solvent molecules around the central solute molecule
ζ	constant in equation (3.36)
η	viscosity of solution
η_1, η_2	known, 1, and unknown, 2, viscosities of the solvent
η_B	viscosity of solvent
λ	jump distance of the molecules in the activated state model
μ_1, μ_2	absolute viscosities of the solution at temperatures T_1 and T_2

ξ	packing factor for hard sphere assemblies
π	constant = 3.14159
ρ	density of solution, $kg \cdot m^{-3}$
ρ_1, ρ_2	known, 1, and unknown, 2, densities of fluid, $kg \cdot m^{-3}$
σ_{AB}	average molecular diameter of molecules A and B
σ_A, σ_B	molecular diameters of solute, A, and solvent, B, nm
σ_t^2	variance of the response curve
ϕ	ratio of the helix or coil radius to the tube radius
Φ	association parameter in the Wilke-Chang correlation
ω	Pitzer's acentric factor

CHAPTER 1

INTRODUCTION

Diffusion is the random thermal net movement (flux) of matter on a molecular scale within one or more phases under the influence of a physical stimulus, the most common of which is a concentration gradient of the diffusing component. When a concentration gradient, or more strictly, a gradient in chemical potential exists in a solution, the diffusing species will move from a region of higher chemical potential to one of lower chemical potential until the mixture is one of uniform concentration or chemical potential. Thus a gradient in chemical potential will cause molecular diffusion to occur until equilibrium is reached.

There are two general classes of binary diffusion coefficients with limiting cases within each class. The definitions associated with these two classes will be summarized below.

A. TYPES OF DIFFUSION COEFFICIENTS

The first general class of diffusion coefficients are referred to as mutual diffusion coefficients or interdiffusion coefficients. It is the most commonly measured type of diffusion coefficient and is used in many mass transfer calculations to determine the rates at which the unit operations take place. For a binary system of solute A and solvent B, the mutual diffusion coefficient, D_{AB}, describes the net rate of transfer of solute molecules (A) through solvent molecules (B) corresponding to the prevailing concentration gradient. The mutual diffusion is best defined by Fick's first law:

$$n_A = -D_{AB}\frac{\partial C_A}{\partial z} \tag{1.1}$$

In equation (1.1) D_{AB} is the proportionality constant between the flux, n_A, and the concentration gradient, $\partial C_A/\partial z$, in a system in which diffusion is taking place.

A limiting case of the mutual diffusion coefficient is normally referred to as the mutual diffusion coefficient at infinite dilution, D°_{AB}. The two limiting cases of the mutual diffusion coefficient thus refer to the diffusivities of each of the infinitely dilute components in the solvent. Thus, D°_{AB} refers to the case where the solute (A) is infinitely dilute in the solvent (B). This study focuses on this limiting case and

shall be referred to as the mutual diffusion coefficient at infinite dilution or the diffusivity at infinite dilution. Because the majority of gases are sparingly soluble in liquids, the diffusion coefficient normally measured for these systems is essentially the mutual diffusion coefficient at infinite dilution.

The second general class of diffusion coefficients are referred to as intradiffusion coefficients or tracer diffusion coefficients (Mills, 1965; Albright and Mills, 1965). Intradiffusion refers to the diffusion of single molecules within a uniform environment of the same type and concentration of molecules and is sometimes referred as tracer diffusion. If a solution of uniform composition was examined, the net mass flux observed would be zero although the molecules would still be in dynamic motion. By labelling a group of similar molecules by isotopic substitution, the diffusion of these labelled molecules can be observed and the intradiffusion or tracer diffusion coefficient, based on measured transfer rates, can be calculated. Hence, D_A^* refers to the tracer diffusion coefficient of isotopically labelled molecules, A, diffusing in a nearly identical solution of solute and solvent molecules. A limiting case of intradiffusion is self-diffusion which describes the diffusion within a pure liquid. Here $(D_A^*)^S$ refers to the self-diffusion coefficient of pure liquid A and represents the movement of isotopically labelled molecules of A in an otherwise pure liquid A. The diffusion process is considered to be the same whether the molecule is isotopically labelled or not.

Figure 1.1 represents one of the possible trends of both mutual and tracer diffusion coefficients with concentration for a binary system. Both tracer and mutual diffusion coefficients are generally strong functions of concentration.

A knowledge of diffusion coefficients in liquids is important from engineering as well as theoretical aspects. Limited diffusion data exist especially at temperatures and pressures above ambient because of the difficulties and expense associated with experimentally determining them. Thus high pressure diffusivity data were collected in this study.

The Chemical Engineer develops, designs and constructs equipment for industrial processes. In many unit operations involving mass transfer in the gaseous and/or liquid states, such as in gas absorption, distillation, leaching, and liquid extraction, the diffusion process within and/or between phases or states may determine the overall processing rate. Thus the diffusion coefficient may be useful in evaluating or predicting the mass transfer coefficient for the design of these separation processes. If no relevant diffusivity data exist, the molecular diffusivity may be

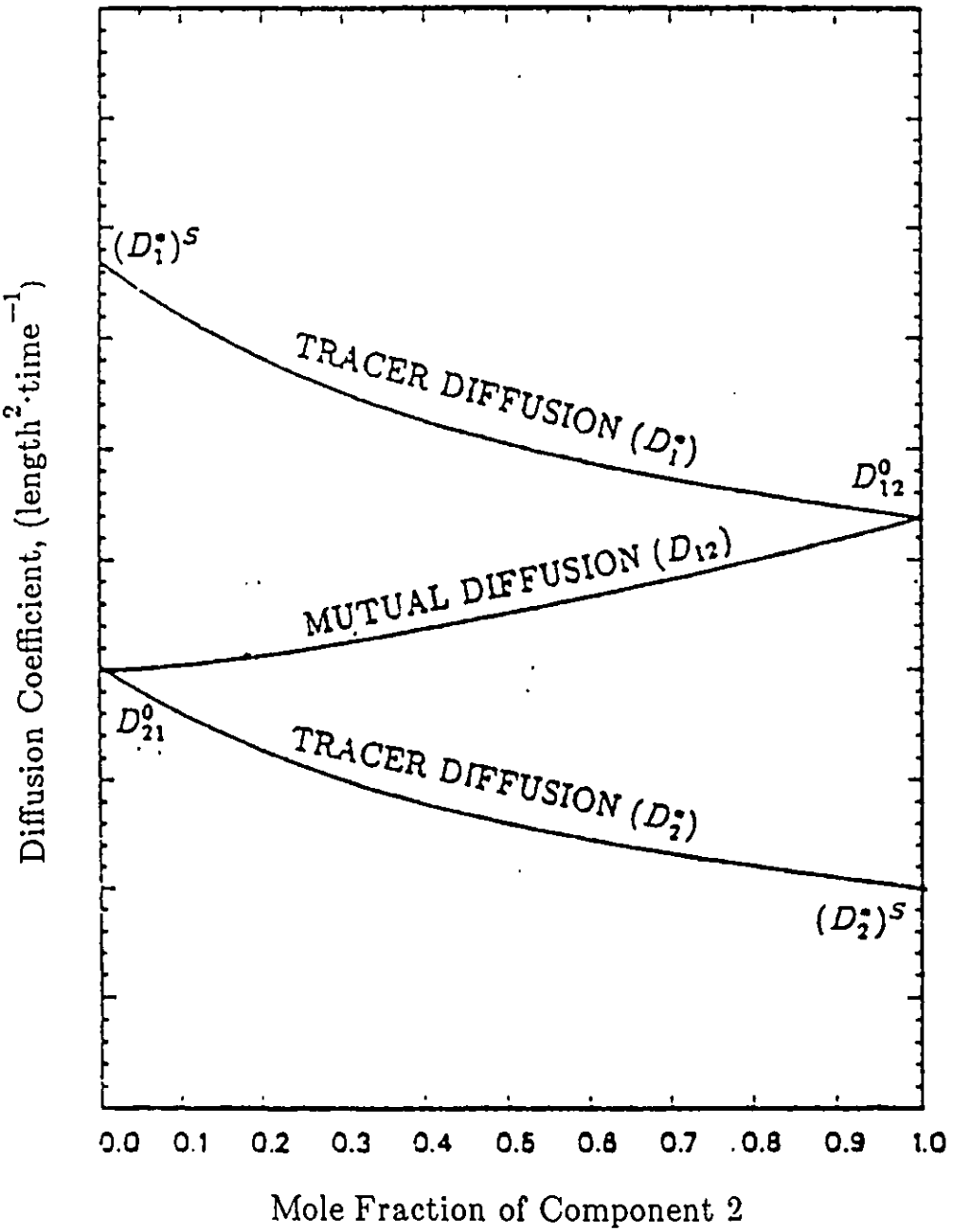

Figure 1.1: Qualitative Behavior of Diffusion Coefficients for a Highly Ideal Binary Liquid System, (Rodden, 1988)

obtained from correlations. High pressure diffusivity data would therefore be useful in the design of separation processes and in the development of high pressure correlations.

Diffusion is important from the theoretical standpoint in helping us to understand the structure of liquids, the mechanism of diffusive transport and to test the validity of existing theories of diffusion. Thus increasing the available diffusivity data to include high pressure data could lead to a better understanding of the diffusion process in liquids.

For my research a Taylor dispersion apparatus was constructed for the measurement of molecular diffusivities at infinite dilution of dissolved gases in liquids which was utilized for temperatures between 273.15 and 348.15 K and for pressures of up to 17 MPa (2,500 psi). As indicated in more detail in Chapter 2, this work entailed determining diffusivities for all combinations of four gases in four solvents at three temperatures and a range of pressures to 17 MPa. This large number of measurements could only have been possible in a reasonable time period using a relatively rapid experimental method such as the dynamic method of Taylor. Also, a computer connected directly to the analyzer of the diffusion apparatus ensured quick, and accurate collection and analysis of the data. The work involved overcoming the problems associated with connecting a computer to an experimental apparatus, as well as with writing the necessary programs to process the data. Furthermore, with some additional work, the diffusivity apparatus was modified to permit the determination of viscosity and density of the solvent at high pressures in conjunction with the determination of diffusivities. The density can be used to calculate the molar volume and together with the absolute viscosity can be used to calculate the kinematic viscosity. These two physical properties density and viscosity are required to solve problems in heat transfer and fluid flow, as well as testing the predictive capability and validity of correlations. Thus, the Taylor dispersion apparatus has become a versatile tool for obtaining transport data at high pressures. In this work, data for diffusivities were obtained for a number of polar and non-polar gases in a number of polar solvents. Subsequently, the data were analyzed to determine, if possible, the general behaviour of diffusivities in these complex solutions with respect to the effect of the molecular interactions in the solutions. The validity and predictive capability of the Rough Hard Sphere model as applied to these systems was examined.

CHAPTER 2

SCOPE OF RESEARCH

In this chapter the scope of my research will be described in five parts. First of all, modifications to the basic Taylor dispersion apparatus made over the last two years, before experimental measurements could begin, are described. Improvements in methods for deaeration of the solvent, control of solvent flow rate, and control of the system pressure allowed reliable diffusivity results to be obtained over a wide pressure range and at several temperatures. The experimental apparatus was also modified to measure viscosities and densities of the solvent over a wide pressure range.

Secondly, the application of a computerized data-logging and data-handling system, using an on-line IBM computer, an analog-to-digital converter, and a LabMaster signal processing unit, ensured improved accuracy, reliability and speed of collection of data. It was necessary to learn C-language in order to write programs to analyze the collected data. The data were analyzed using the analytical solution to the Taylor dispersion problem, instead of the alternate but less accurate graphical or moment methods sometimes used.

Thirdly, the solutes and solvents which were used were carefully chosen to contribute to the understanding of liquids by examining the effects of association and solute dipole moment on the diffusion process. The solutes which were used included propene, propane, carbon dioxide and ammonia. The alcohol solvents were chosen to examine the effect of the degree of association on the diffusion process. The solvents which were used included methanol, ethanol, 1-propanol, and 1-butanol.

The operating conditions were temperatures of 298.15, 323.15 and 348.15 K and pressures ranging from 0.1 to 17 MPa. Pressures of approximately 0.1, 3.5, 7.0, 10, 14, and 17 MPa were used since it was found that for pressures up to 3.5 MPa, the diffusivities were a linear function of pressure and it was of interest to see if this relationship continued to higher pressures.

Finally, the predictive capability along with any existing supporting theory of several semi-empirical and empirical equations, including the Rough Hard Sphere

(RHS) model were tested. Emphasis was placed on the RHS model because of its sound theoretical basis and because it has been used successfully by Chen et al. (1982), Wong (1989), Matthews (1986) and Rodden (1988). An attempt was made to develop an equation, most likely based on the RHS theory, to predict the diffusivities at infinite dilution for these and similar systems.

CHAPTER 3

LITERATURE REVIEW

3.1 Techniques for Measuring Diffusion Coefficients of Liquids

Several experimental techniques exist for the measurement of the diffusion coefficients in liquids. Diffusion coefficients in liquids include gaseous, solid as well as liquid solutes. The diffusion of dissolved gases in liquids is a special category with major experimental difficulties and thus will be discussed separately. In this section the diffusion of liquids in liquids will be discussed.

In the past, the diaphragm cell method was the most common one for measuring mutual diffusivities in liquids. It can also be used for tracer diffusion measurements of liquid and gaseous solutes and has been successfully used for high pressure conditions. In the diaphragm cell method, diffusion takes place across a porous disk which is usually made of glass or metal. Liquid mixtures of different compositions are placed on either side of the diaphragm. When steady-state conditions are attained, the concentration changes in the liquid solutions on either side of the diaphragm are measured and, based on the calibration constant for the diaphragm cell, the diffusion coefficient is calculated. The disadvantages of this method are:

(1) It is considered to be slow because several days may be required for steady-state conditions to be attained.

(2) Calibration of the cell is necessary to obtain the effective diffusion path length.

(3) Very precise concentrations and concentration differences are needed for accurate determinations.

(4) It is difficult to adapt this method to extreme conditions of high temperature because it is difficult to fill and obtain a sample from the cell without disturbing the liquid.

Optical interference techniques have also been used for liquid systems. This technique examines the refractive index gradient at the boundary between two miscible liquids using light beams, and measures the interferometric fringe patterns. Optical interference methods are especially suitable for measuring mutual diffusion

coefficients over the entire concentration range in a single experiment, but are not suitable for high temperatures and pressures. The difficulties in obtaining the initial sharp concentration gradient, in developing an optically clear window, and in the prevention of convection currents make it difficult to perform experiments at high pressures and temperatures. Another disadvantage of this method is that it is expensive. This technique of measuring diffusion coefficients is very accurate because the interference patterns produced can be measured very accurately.

Because of the theoretical significance of self-diffusion coefficients, the Nuclear Magnetic Resonance (NMR) technique of measurement will be briefly mentioned. The NMR method is fast, very accurate, and adaptable to high temperatures and pressures. These self-diffusion coefficients are measured using radioactive tracers and small samples. In the past this technique was used only for self-diffusion measurements in pure liquids, but attempts are now being made to measure tracer diffusion coefficients in solutions.

3.2 Techniques for Measuring Diffusion Coefficients of Dissolved Gases

Several techniques are described in the literature for the measurement of the diffusion coefficients of dissolved gases in liquids. The measurement of these types of diffusion coefficients involve a number of major experimental difficulties. On examining the diffusivity data in the literature, large differences are found in some cases depending on which measuring technique is used. This is due to the difficulties associated with the experiment techniques which then affect the reliability of the diffusivity results.

Techniques for the measurement of diffusion coefficients of gases in liquids generally involve the transfer of gas at a measurable rate over a known cross-sectional area and thickness of the solvent layer, as well as the imposed concentration gradient. Fick's first or second law is used to obtain the diffusion coefficients depending on the nature of the experiment. In all of these techniques, the concentration gradients and mass transfer rates are those either for the system at steady-state or for transient conditions leading to differences in the analytical procedures used to calculate the diffusivities. These techniques can be classified as those involving either stationary or moving solvents. Very few of the techniques are suitable for high

temperatures and pressures. A comprehensive review of these methods, summarized in Table 3.1, is given by Tyrrell and Harris (1984).

Because of the major experimental difficulties associated with the measurement of the diffusion coefficients of dissolved gases in liquids, only three of the most popular and most reliable techniques will be discussed in the following paragraphs. They include the capillary tube technique of Malik and Hayduk (1968), the technique for laminar flow systems, and the diaphragm cell method. The major limitation common to all three of these methods is that they require accurate gas-liquid solubility data, which can rarely be obtained, except at ambient conditions and for the simplest of systems.

The steady-state capillary cell technique devised by Malik and Hayduk (1968), has been used by several researchers. In this case the gas diffuses through a column of solvent confined at the bottom of a glass capillary while the gas is confined in the top section of the capillary by a bead of solvent. As the gas diffuses, its volume diminishes. The rate of steady-state absorption of the gas along with the system parameters are used to calculate the diffusion coefficient for this gas-liquid system where the liquid solvent is stationary.

Another popular technique for measuring gas-liquid diffusivities is the absorption of the gas in a wetted wall column (Kramers et al., 1959; Mazarei and Sandall, 1980), a laminar jet (Onda et al., 1960; Dim et al., 1971; Halmour and Sandall, 1984), or, in general one involving a laminar flow systems (Davidson and Cullien, 1957). In this case a controlled flow of solvent is permitted to flow along the inside surface of a tube, or discharged from a nozzle through the centre of an adsorption vessel as a smooth jet. In both of these devices the flow is laminar and a known area of solvent is exposed to the gas for absorption. Because the flow parameters can be accurately defined, the diffusivities can be calculated from the absorption rates.

The diaphragm cell method, though not the most popular method, has been used with some success for measurement of the diffusivity of a gas in a liquid where the liquid is stationary (Vivian and King, 1964; Tham et al., 1967; Clegg and Tehrani, 1973; Tham et al., 1973; Onda et al., 1975; Takahashi et al., 1982). It should be recalled, as previously mentioned, that this technique is more commonly used in liquid diffusivity measurements for mutual diffusivities, and has also been used by Collings et al. (1971), McCool et al. (1972), and McCool and Woolf (1972) to measure self- diffusivities at elevated pressures. The disadvantages of this method

TABLE 3.1

Techniques for Measuring Diffusion Coefficients of Gases in Liquids

Liquid in motion	Quiescent liquid
1. Gas absorption in laminar flow systems a. Laminar jet b. Wetted wall column c. Flow over a wetted sphere 2. Taylor dispersion in a capillary tube	1. Diaphragm cell technique with diffusion through the pores of the diaphragm 2. Open tube technique - transient rate of volumetric uptake of gas by the liquid at the gas-liquid interface 3. Techniques utilizing capillaries: a. Steady-state multiple capillary method, a modified version of the diaphragm cell b. Steady state capillary cell method c. Unsteady-state open-ended capillary cell method 4. Bubble dissolution technique with gas absorption from the gas bubble a. Flat surface with bubble adhering to it b. Constant bubble size

are the same as given before for liquid systems. However, it should be noted that with a gas as the solute, the possible loss of gas on sampling and the difficulty in accurately measuring small differences in concentration can introduce errors and affect the reliability of the measurement especially for sparingly soluble gases.

3.2.1 TAYLOR 'S DISPERSION TECHNIQUE

Taylor's dispersion technique which can be described as a chromatographic broadening technique, although in existence since 1953, has evolved in recent years, beginning in 1984, to be the fastest and most reliable and versatile method for measuring the diffusion coefficients of both gaseous and liquid solutes in liquid solvents. Taylor's technique was first used for the measurement of diffusivities in the gas phase (Giddings and Seager, 1962). Taylor's technique was soon modified by Ferrell and Himmelblau (1967) to measure the diffusivity of gases in liquids. Other researchers who also used Taylor's technique to measure the diffusivity of gases in liquids include Pratt et al. (1973), Evans et al. (1979), Chen et al. (1981, 1982), Matthews (1986) Rodden (1988) and Wong (1989). Taylor's technique was then further modified to measure the diffusivities of both gaseous and liquid solutes in liquid solvents at high temperatures and pressures (Jacob Sun and Chen, 1985, 1987; Matthews, 1986; Matthews and Akgerman, 1987; Rodden, 1988; and Wong, 1989).

Diffusion takes place in a liquid moving in laminar flow in a capillary tube. Taylor (1953, 1954) and Aris (1956) showed that if a pulse of solute is injected into a moving solvent, diffusion occurred in the radial direction and the combination of the bulk fluid flow in the axial direction and diffusion in the radial direction causes the solute to disperse axially. The resulting Gaussian type concentration distribution peak is measured at the end of the dispersion column and the diffusivity is inversely related to the variance of the Gaussian type peak. Thus this method examines the effect of diffusion superimposed on the bulk motion of the fluid. The difference between the effects of the controlled flow rate (motion effect) and the combined effect of motion and diffusion then gives the effect due to diffusion. In the diaphragm cell and optical interference methods, the bulk flow effect is eliminated since the solvent is stationary. The advantages of this method include:

(1) Taylor's method is relatively fast requiring 1 to 3 hours for each measurement.

(2) Taylor's method can be used for diffusivity measurements at high temperatures and pressures.

(3) Gas solubility data is not required.

(4) No calibration is necessary.

(5) No gas-liquid interface is present.

A detailed description of Taylor's method including the associated mathematical development will be discussed in Chapter 4, since it is the experimental method used in this study.

3.3 Theories of Diffusion

The theories and mathematics of diffusion in liquids is complicated because liquids exhibit properties intermediate between those of a gases and a solids and in which the molecules exhibit a mixture of randomness and structure. The close packing (as in solids) of the molecules in liquids creates large intermolecular forces and these forces are difficult to model mathematically because the molecules are not confined to fixed lattices (as in solids). Thus although several theories of diffusion have been proposed, none has proved entirely successful. However, these theoretical models do provide a basis for the development and testing of correlations for interpolation and extrapolation of data and thus for the prediction of diffusivities. The four most significant theories of diffusion, the hydrodynamic theory, the activated state theory, the free volume theory, and the kinetic theory of hard spheres will be presented along with some of the associated semi-empirical equations.

3.3.1 HYDRODYNAMIC THEORY

The hydrodynamic theory is based on the Nernst-Einstein equation and shows the relationship between frictional force, velocity and diffusivity of a sphere moving in a continuum by Brownian motion. Nernst and Einstein (1905; cf Rossi and Bianchi, 1961) showed that for a single spherical particle moving in a solution by Brownian motion, the diffusion coefficient is given by:

$$D_{AB} = \frac{kT}{f} \tag{3.1}$$

In the above expression f is the frictional coefficient of the diffusing particle and its value derived from the theory of hydrodynamics is given by:

$$f = 6\pi\eta_B r_A \left(\frac{2\eta_B + r_A \beta_{AB}}{3\eta_B + r_A \beta_{AB}} \right) \tag{3.2}$$

In equation (3.2), β_{AB} is the coefficient of sliding friction between the diffusing molecule and its surroundings, and r_A is the radius of the sphere which is moving through a medium of viscosity η_B.

The two limiting cases of β_{AB}, as shown by Furth (1931), include the possibilities of no slip or slip at the fluid surface:

(1) For $\beta_{AB}=\infty$ which represents the limiting case of no slip of the fluid at the surface of the sphere, equation (3.2) becomes Stokes's law:

$$f = 6\pi\eta_B r_A \tag{3.3}$$

Substitution into equation (3.1) gives the Stokes-Einstein equation:

$$D_{AB} = \frac{kT}{6\pi\eta_B r_A} \tag{3.4}$$

This equation has been shown by Sutherland (1905) to describe, with a reasonable degree of accuracy, the diffusion of spherical and rigid particles much larger than the solvent molecules.

(2) For $\beta_{AB}=0$ which represents the limiting case of slip of the fluid at the surface of the sphere, equation (3.2) becomes:

$$f = 4\pi\eta_B r_A \tag{3.5}$$

Substitution into equation (3.1) gives:

$$D_{AB} = \frac{kT}{4\pi\eta_B r_A} \tag{3.6}$$

Equation (3.6) has been found to correlate diffusion data fairly well if the diffusing particle is of the same order of size as the solvent molecules.

These resulting semi-empirical models represent only a limited number of systems, and do not describe the behaviour for systems in which the solute molecules have a relatively small diameter as, for example, for gases although the theory predicts that D_{AB} does vary with r_A. Nor does this equation describe the behaviour for solutes which are not spherically symmetrical since three frictional coefficients, not one, are involved (Tyrrell and Harris, 1984), or for elevated temperatures. Hildebrand (1971) stated that because viscous forces are based on a macroscopic nature, the frictional coefficient is meaningless because it is based on a microscopic level.

However, the hydrodynamic approach predicts that the factor, $D\eta_B/T$, is a constant and it has been used as a starting point for several well known correlations such as those of Wilke and Chang (1955), and Lusis and Ratcliff (1968). It should be noted, though, that the hydrodynamic-based correlations are not successful in predicting diffusivities at elevated temperatures or over a wide temperature range. Other correlations such as the Sovova equation (3.48) and the Hayduk-Cheng relation (3.47) empirically relate D_{AB} to viscosity raised to some power. These hydrodynamically based correlations are mostly empirical in form.

3.3.2 ACTIVATED STATE THEORY

The process of diffusion was first explained utilizing activated state theory by Eyring and co-workers (Eyring, 1936; Hirschfelder, 1937) similar to the activated state approach for describing kinetic reaction rates. It is also known as the Eyring rate theory. In the Eyring theory, diffusion is described as the movement of molecules, one molecule at a time, from a given position to a new and more stable equilibrium position, in an adjacent "hole", which only occurs when the molecules attain a sufficiently high energy to overcome a potential barrier. If a cubic lattice configuration of the liquid is assumed, the diffusion coefficient is expressed in an exponential relationship (Glasstone et al., 1941), and the following equation results:

$$D_{AB} = \frac{kT\lambda^2}{h} \exp\left(-\frac{\Delta G_D}{R_g T}\right) \tag{3.7}$$

In the above equation ΔG_D is the Gibbs energy of activation and is the energy required to form a hole, and λ is the distance the molecules jump.

Many researchers using theoretical arguments have questioned the validity of this theory, namely Tyrrell and Harris (1984), Hildebrand (1971), and Alder and Hildebrand (1973). They point out that their understanding of the facts put forward suggests that activated and un-activated molecules do not exist since the potential field of all the molecules is almost uniform. Also, the activation energies actually observed are low, of the order of 10 kJ/mol, which suggests that a large percentage of molecules will be in the activated state and Eyring's theory suggests that the number of molecules in the activated state should be small. Another argument put forward is that all molecules diffuse at all times and is not a unimolecular process as presented by Eyring.

Because there are no reliable methods of estimating the activation energy, ΔG_D, and the jump distance, λ, equation (3.7) can only be used for extrapolation and interpolation of data. The activation theory has not often been used but has successfully been used by Akgerman and Gainer (1972a,b) as the basis for correlating the exponential dependence of binary diffusivity data on temperature over a wide temperature range for dissolved gases in liquids. This theory was also used by Olander (1963), and Gainer and Metzner (1965).

Subsequently the Eyring rate theory for diffusion was modified as follows:

$$D_{AB} = \frac{k'_1}{\eta}\left(\frac{N}{V}\right)^{1/3} \tag{3.8}$$

This equation was obtained from Eyring's expression for viscosity and does not require a knowledge of ΔG_D and λ. However, the values predicted from this equation differ greatly from experimental values and thus equation (3.8) can only be used to give values of diffusivity of the correct order of magnitude.

3.3.3 ROUGH HARD SPHERE (RHS) THEORY

The Rough Hard Sphere (RHS) theory which is based on the kinetic theory of gases is referred to as the Chapman-Enskog theory and is discussed in mathematical detail by Chapman and Cowling (1970). In this section the RHS theory as applied to diffusion will be discussed; the mathematical details will not be included here. The RHS approach is possibly more realistic than the activated state theory and the

hydrodynamic theory and, although not perfect, it has been found to be useful in the interpretation of data for different systems.

The RHS mutual diffusion coefficient, D_{AB}^{RHS}, is written as a product of four terms:

$$D_{AB} = D_{AB}^{RHS} = (D_{AB}^{HSG}) \cdot \frac{1}{g(\sigma_{AB})} \cdot C(\sigma_A, \sigma_B, m_A, m_B, V_B) \cdot F \qquad (3.9)$$

Similarly, the RHS self diffusion coefficient, D_{BB}^{RHS}, which can be deduced from equation (3.9) is written as:

$$D_{BB} = D_{BB}^{RHS} = (D_{BB}^{HSG}) \cdot \frac{1}{g(\sigma_B)} \cdot C(\sigma_B, m_B, V_B) \cdot F \qquad (3.10)$$

The terms are listed in order of their development, beginning with the diffusivity in a low density gas and concluding with the diffusivity in a liquid and will be discussed separately.

The expressions for the mutual diffusion coefficient of a low density (dilute) hard sphere gas (HSG), (D_{AB}^{HSG}), and the self diffusion coefficient of a low density HSG, (D_{BB}^{HSG}) were derived by Chapman and Enskog with the following assumptions:

(1) The gas is "dilute" or of low density and thus the mean free path between molecules is large compared to their diameters.

(2) The gas is in a state of molecular chaos, in that there is no correlation between the position and velocity of the molecules.

(3) The molecules are spherically symmetrical and smooth.

(4) All molecules collide with only one other molecule at any time; multiple interactions are negligible.

(5) The collisions are perfectly elastic and instantaneous.

(6) There are no attractive or repulsive force fields affecting the molecules on their flight between collisions.

The HSG diffusivity is sometimes referred to as the Chapman-Enskog (CE) diffusivity and written as (D_{AB}^{CE}) and (D_{AB}^{HSG}) for mutual diffusivity and (D_{BB}^{CE}) and (D_{BB}^{HSG}) for self diffusivities, respectively. For the above assumptions, the expression of (D_{AB}^{HSG}) was written by Chapman and Cowling (1970) as:

$$(n D_{AB}^{HSG}) = \frac{3}{8\sigma_{AB}^2}\left[\frac{kT}{2\pi}\frac{(m_A + m_B)}{m_A m_B}\right]^{1/2} \tag{3.11}$$

In the above expression, σ_{AB} is the average molecular diameter of molecules A and B on collision ($=(\sigma_A + \sigma_B)/2$), m_A and m_B are the molecular masses of the solute and solvent molecules and n is the number density (molecules/volume).

From equation (3.11), the expression for self diffusion can be obtained (Chapman and Cowling, 1970):

$$(n D_{BB}^{HSG}) = \frac{3}{8\sigma_B^2}\left[\frac{kT}{\pi m_B}\right]^{1/2} \tag{3.12}$$

As the density of the gas increases, the above six assumptions for the kinetic theory of gases become more and more invalid or unrealistic. It was considered by Enskog (cf. Chapman and Cowling, 1970) that as the density of the gas increased, the assumption of molecular chaos became more unrealistic and to compensate the radial distribution function, $g(\sigma_{AB})$ for mutual diffusion and $g(\sigma_B)$ for self diffusion, was introduced as correction terms relating diffusivity in a dilute gas to that in a moderately dense gas. Enskog relaxed the assumption of uncorrelated positions and showed analytically that the self diffusion coefficient for a dense gas could be predicted by correcting for the increased frequency of collisions in a dense gas with the resulting equation:

$$\frac{n' D_{BB}{}^{E}}{(n D_{BB}^{HSG})} = \frac{1}{g(\sigma_B)} \tag{3.13}$$

In equation (3.13), $n' D_{BB}{}^{E}$ is the number density times the Enskog self diffusivity at moderate density, and $g(\sigma_B)$ is the radial distribution function of pure B. Thorne (cf. Chapman and Cowling, 1970) derived the analogous expression for mutual diffusion:

$$\frac{n' D_{AB}{}^{E}}{(n D_{AB}^{HSG})} = \frac{1}{g(\sigma_{AB})} \tag{3.14}$$

In equation (3.14), $n' D_{AB}{}^{E}$ is the product of the number density and the Enskog mutual diffusivity of a moderately dense gas, $(n D_{AB}^{HSG})$ is the product of the number density and the CE mutual diffusivity of a dilute gas, and $g(\sigma_{AB})$ is evaluated at the

average collision diameter.

The radial distribution function depends on the composition and molar volume of the mixture and on the diameters of the all of the molecules in the mixture. The form for $g(\sigma_{AB})$ when component A is present in trace amounts was given by Evans et al. (1981) and Alder et al. (1974):

$$g(\sigma_{AB}) = \frac{1}{1-\xi} + \frac{3\xi\sigma_A}{(1-\xi)^2(\sigma_A+\sigma_B)} + \frac{\xi^2\sigma_A}{2(1-\xi)^3\sigma_B} \tag{3.15}$$

In the above equation ξ is the packing factor for hard sphere assemblies and for the infinitely dilute case, that is, for $n_A = 0$, ξ is given by the following expression:

$$\xi = \frac{\pi\eta_B\sigma_B^3}{6} \tag{3.16}$$

The expression is based on the Percus-Yevick equation of state for hard spheres (Lebowitz, 1964).

At liquid densities, the assumption of uncorrelated velocities of the molecules is completely unrealistic and the third term, $C(\sigma_A, \sigma_B, m_A, m_B, V_B)$, was introduced to correct for the deviation from the Chapman-Enskog theory. This term considers such effects as backscattering and vortex formation and thus accounts for correlated molecular motions. Alder et al. (1974) and Esteal et al. (1983) found that the mutual diffusion coefficients obtained from the first two terms of equation (3.9) by computer simulation, and those obtained experimentally, differed greatly. Alder et al. (1970) and Dymond (1972) found a similar trend for self-diffusion from equation (3.10). At high densities (greater than 1.5 to 2 times the critical density, ρ_c) and for low solute to solvent mass ratios (for dilute solutions), the diffusion coefficient is decreased by backscattering; that is, the diffusion coefficient is lower than that predicted from the Chapman-Enskog theory. Backscattering is the multiple successive collisions of the solute with its neighbouring molecules where the solute is said to be temporarily trapped in a cage for the time of several collisions after which the molecule can move on. At lower liquid densities (less than 1.5 times the critical density) and for higher solute to solvent mass ratios, Alder and Wainwright (1970) showed that the neighbouring molecules form a vortex around the diffusing molecule acting to increase its velocity and thus effectively increasing its diffusion coefficient

above that predicted by the Chapman-Enskog theory.

Instead of trying to obtain the complicated expressions for the analytical solutions of the correction term $C(\sigma_A, \sigma_B, m_A, m_B, V_B)$, this term is obtained from the ratio of the actual diffusivity which is referred to as the Hard Sphere Liquid (HSL) diffusivity and is obtained from computer calculations, to the Enskog diffusivity. The expression for C for mutual diffusion is:

$$C(\sigma_A, \sigma_B, m_A, m_B, V_B) = \frac{D_{AB}^{HSL}}{(D_{AB}^{HSG})/g(\sigma_{AB})} = \frac{D_{AB}^{HSL}}{(D_{AB}^{E})} \tag{3.17}$$

In equation (3.17), D_{AB}^{HSL} represents the mutual diffusion coefficient for a hard sphere liquid. Similarly C for self-diffusion is expressed as:

$$C(\sigma_B, m_B, V_B) = \frac{D_{BB}^{HSL}}{(D_{BB}^{E})} \tag{3.18}$$

In equation (3.18), D_{BB}^{HSL} represents the self diffusion for a HSL. Molecular dynamics computer simulations were carried out by Alder et al. (1970) to determine C for self diffusion coefficients. Alder et al. (1974) and Esteal et al. (1983) similarly determined C for infinite dilution mutual diffusion coefficients. Chen (1981) compiled and graphed the values of C for the few available solute-solvent systems by interpolating and extrapolating from the existing computer simulation results of Alder et al. (1974), Herman and Alder (1972), Shelton (1981) Alder et al. (1970). Czworniak et al. (1975) expressed C as a polynomial function of m_A/m_B, σ_A/σ_B, and ξ. The complex nature of the calculations limits the use of the computer in calculating the diffusivity of every possible system. The few available results are given as a function of σ_A/σ_B, m_A/m_B, and V/V_o. V_o is the closed packed hard sphere volume and is given by:

$$V_o = \frac{N\sigma_B^3}{\sqrt{2}} \tag{3.19}$$

The smoothness assumption of Enskog is no longer valid for polyatomic molecules because of the possibility of exchange of kinetic and rotational energy on collision of irregular shaped molecules (Chandler, 1975). Chandler (1975) has shown that the fourth term in equations (3.9) and (3.10), the roughness factor, F, should be

used to account for kinetic and rotational energy transfer between molecules if the molecules were not smooth. The factor F, which according to Chandler (1975), is independent of density and temperature reduces the diffusion coefficient, so that:

$$0 \leq F \leq 1 \tag{3.20}$$

Thus the diffusivity obtained on utilizing all four terms results in the diffusivity in a liquid where the constituent molecules are irregular in shape or "rough", that is D_{AB}^{RHS}. Several researchers have obtained values of F. Chandler found that a value of F=0.54 satisfies the intradiffusion coefficient in carbon tetrachloride and Parkhurst and Jonas (1975) used a value of F=0.59 for tetramethylsilane. From geometric considerations, Baleiko and Davis (1974) calculated F for rough spheres and found that theoretically $0.71 < F \leq 1$. Evans et al. (1981) found that the values of F of either 1, 0.78, or 0.70 fitted several sets of diffusivity data. Bertucci and Flygare (1975) similarly fitted diffusivity data and found values of F ranging from 0.44 to 0.552.

Thus the rough hard sphere theory begins with an analytical expression for diffusion in a dilute gas, (D_{AB}^{HSG}), is then modified for a moderately dense gas using the radial distribution function $g(\sigma_{AB})$, then corrects for backscattering and vortex formation which arises form correlated motions in liquids, which is represented by term C, and then finally corrects for rotational and kinetic energy transfer which arises from molecules that are not smooth and is represented by F.

As shown by Dymond and Woolf (1982), the RHS diffusion coefficient can be rewritten for mutual and self diffusion. The expression for the RHS mutual diffusion coefficient can be obtained by substituting equations (3.11) and (3.17) into equation (3.9):

$$D_{AB}^{RHS} = \frac{3}{8 n \sigma_{AB}^2} \left[\frac{kT}{2\pi} \frac{(m_A + m_B)}{m_A m_B} \right]^{1/2} \cdot \frac{F}{g(\sigma_{AB})} \left[\frac{D_{AB}^{HSL}}{D_{AB}^{E}} \right]_{MD} \tag{3.21}$$

Similarly the expression for the RHS self diffusion coefficient can be obtained by substituting equations (3.12) and (3.18) into equation (3.10):

$$D_{BB}^{RHS} = \frac{3}{8 n \sigma_{B}^2} \left[\frac{kT}{\pi m_B} \right]^{1/2} \cdot \frac{F}{g(\sigma_{B})} \left[\frac{D_{BB}^{HSL}}{D_{BB}^{E}} \right]_{MD} \tag{3.22}$$

The subscript MD represents the molecular dynamics computer calculations for the determination of C.

Instead of expressing D_{AB}^{RHS} and D_{BB}^{RHS} in terms of σ_A, σ_B, n , and C, it has been found to be more convenient to calculate the diffusivity in terms of the molar volume of the liquid. The molecular dynamics calculations of Alder (1970) for the term C for self diffusion data was used by Dymond (1974). The group $C/g(\sigma_B)$ was fitted to a straight line as given below:

$$\frac{V}{V_o}\cdot\frac{1}{g(\sigma_B)}\cdot\left[\frac{D_{BB}^{HSL}}{D_{BB}^{E}}\right]_{MD}=a\left[\frac{V}{V_o}-b\right] \tag{3.23}$$

In the above equation V is the molar volume of the pure liquid for the case of self diffusion, and a is a constant for every solute-solvent pair. From the linear relationship, b was empirically determined by Dymond (1974) to be equal to 1.384 and by Tyrrell and Harris (1984) to be equal to 1.358. Substituting for the group $C/g(\sigma_B)$ from equation (3.23) into equation (3.10) results in Dymond's expression for diffusivity, D_{BB}^{DYM}, based on the RHS model:

$$D_{BB}^{DYM}=F\cdot\frac{3}{8n\sigma_B^2}\left[\frac{kT}{\pi m_B}\right]^{1/2}\cdot\frac{V_o}{V}\left[a\left(\frac{V}{V_o}-b\right)\right] \tag{3.24}$$

The product nV is a constant and represents the number of molecules in a volume V. Also m_B, k, and π are all constants. Equation (3.24) can thus be expressed as:

$$\frac{D_{BB}^{DYM}}{\sqrt{T}}=F\cdot\frac{C'}{\sigma_B^2 m_B^{1/2}}\cdot[a(V-bV_o)] \tag{3.25}$$

In equation (3.25), C' is a constant.

Dymond (1974) found that for an $a=1.271$, equation (3.25), after some rearranging, becomes:

$$\frac{10^9 D_{BB}^{RHS}}{\sqrt{T}}=\frac{A\cdot 2.527\,k^{1/2}}{V_o^{2/3}M^{1/2}}\cdot(V-1.384V_o) \tag{3.26}$$

In equation (3.26), k is the Boltzmann's constant, and M is the molecular weight of the liquid. Dymond found that the data for self diffusion coefficients could be fitted accurately to equation (3.26) but did not develop the expression for mutual diffusivities. Although Esteal et al. (1983) determined the term C from molecular dynamics calculations, for infinite dilution mutual diffusion coefficients, nothing has

dynamics calculations, for infinite dilution mutual diffusion coefficients, nothing has been done to correlate these values of C to the molar volume. The incomplete study of the MD simulations does not allow for the development of a general RHS correlation. If the narrow range of σ_A/σ_B, m_A/m_B, and V/V_o is increased in the MD calculations, a comprehensive study can be initiated on the study of the translational -rotational coupling parameter, F, as well as possibly obtaining a general RHS correlation. Also the few experimental diffusivity data above ambient conditions does not allow for the testing of these possible studies.

Chen et al. (1982) claimed that Dymond's equation for self diffusivity, equation (3.26), could be applied to mutual diffusion coefficients at infinite dilution with the resulting equation:

$$\frac{D^{\circ}_{AB}}{\sqrt{T}} = \beta(V - V_D) \tag{3.27}$$

In the above equation β is the slope of $D^{\circ}_{AB}/\sqrt{T}$ versus V, and V_D is the intercept where the diffusivity is effectively zero. Chen found a linear relationship for all of the solute-n-alkane systems examined Expressions for β and V_D will be given later.

Matthews (1986) and Rodden (1988) also found that this linear relationship of equation (3.27) was valid for their n-alkane systems and predicted the mutual diffusivities at infinite dilution to a higher degree of accuracy than the other correlations. The equation of Matthews is:

$$\frac{10^9 D^{\circ}_{AB}}{\sqrt{T}} = a_1 M_A^b \left(\frac{\sigma_A}{\sigma_B}\right)^3 (V - V_D) \tag{3.28}$$

The equation of Rodden is:

$$\frac{10^9 D^{\circ}_{AB}}{\sqrt{T}} = \frac{a_1}{M_A^b M_B^c (\sigma_A \sigma_B)^d} (V - V_D) \tag{3.29}$$

Wong (1989) found a similar linear relationship for infinitely dilute propene in various solvents. The equation of Wong is:

$$\frac{10^9 D^{\circ}_{AB}}{\sqrt{T}} = a_1 M_A^b M_B^c \left(\frac{V_{bA}}{V_{bB}}\right)^d (V - V_D) \tag{3.30}$$

Equations (3.28), (3.29) and (3.30) all accurately predicted the experimental diffusivities and are based on the RHS theory.

To test the validity of equation (3.27) to the RHS theory, equation (3.27) has to be expressed in terms of the RHS parameters. As shown by Rodden (1988), the first step requires the use of Dymond's equation and after the collection of constant terms, equation (3.25) can be written as:

$$\frac{D_{BB}^{DYM}}{\sqrt{T}} = F \cdot \frac{A'}{\sigma_B^2 m_B^{1/2}} \cdot (V - bV_o) \tag{3.31}$$

A generalized expression for D_{AB} can be obtained using equation (3.31):

$$D_{AB} = \frac{D_{AB}^{RHS}}{D_{BB}^{RHS}} \cdot D_{BB}^{DYM} \tag{3.32}$$

Equation (3.32) represents the ratio of the RHS mutual diffusion coefficient at any concentration and the RHS self diffusion coefficient for a pure solvent multiplied by the self diffusion coefficient of Dymond.

Substituting equations (3.21), (3.22), and (3.31) into equation (3.32) results in :

$$\frac{D_{AB}}{\sqrt{T}} = \beta \cdot (V - bV_o) \tag{3.33}$$

In equation (3.33), β is represented by:

$$\beta = \frac{K'}{\sigma_{AB}^2} \left(\frac{m_A + m_B}{m_A m_B} \right)^{1/2} \cdot F \cdot \frac{g(\sigma_B)}{g(\sigma_{AB})} \frac{[D_{AB}^{HSL}/D_{AB}^{E}]_{MD}}{[D_{BB}^{HSL}/D_{BB}^{E}]_{MD}} \tag{3.34}$$

In equation (3.34), K' is a collection of constants. The subscript MD represents the molecular dynamic calculations for mutual and self diffusion data and this equation could be used to predict concentration dependent mutual diffusion coefficients if the MD calculations exist. However, no such data exist, but some MD data exist for infinitely dilute systems. Equations (3.33) and (3.34) can be written for the infinitely dilute case as follows:

$$\frac{D_{AB}^{\circ}}{\sqrt{T}} = \beta \cdot (V - bV_o) = \beta \cdot (V_B - V_D) \tag{3.35}$$

In equation (3.35), β is represented by:

$$\beta = \frac{K'}{\sigma_{AB}^2}\left(\frac{m_A + m_B}{m_A m_B}\right)^{1/2} \cdot F \cdot \frac{g(\sigma_B)}{g(\sigma_{AB})} \frac{[D_{AB}^{HSL}/D_{AB}^{E}]_{MD}^{o}}{[D_{BB}^{HSL}/D_{BB}^{E}]_{MD}} \qquad (3.36)$$

In equation (3.35), for the infinitely dilute solvent, V_B represents the molar volume of the pure solvent B, and V_D is equivalent to the product bV_o and $g(\sigma_{AB})$ is the radial distribution function for the case of infinitely dilute A in B. Equations (3.35) and (3.36) could be used to predict infinitely dilute mutual diffusion coefficients if the MD data is available from the literature. Equation (3.35) thus proves the validity of equation (3.27).

Examining the above equations based on the RHS theory, leads to the following observations. Dymond's analysis using self diffusivity data showed that V_D is a constant and depends only on the properties of the solvent. Hildebrand (1977), Chen (1982), Matthews (1986), Rodden (1988) and Wong (1989) have all found V_D to depend on the solute as well as the solvent properties for infinitely dilute diffusivity data. The molar volume, V_D, was considered by Hildebrand (1971) to be a hypothetical molar volume of the solvent in which there is no free space left for molecular diffusion and, at the same time, that the solute diffusivity is zero. This is analogous to the close packed, hard core volume V_o where the effective solute diffusivity is zero. The constant β should depend on both the solute and solvent properties; further it is observed that β is inversely proportional to σ_{AB}^2 and directly proportional to $\sqrt{(m_A + m_B)/m_A m_B}$, and contains the constant, a, from equation (3.25). Chen and Chen (1985), Matthews (1986) and Rodden (1988) have all found that a is constant for a given solute-solvent pair.

Equation (3.35) will be utilized in the analysis of the experimental results obtained in this study. The linear relationship between $D_{AB}/\sqrt{T}$ and molar volume will be examined using the experimental results obtained in this study. Both Batchinski (1913) and Hildebrand (1971) observed this linear behaviour. This is further discussed in the next section on the Free Volume Theory. In order to predict the molecular diffusivities at infinite dilution without prior knowledge of MD data, the expression for β has to be simplified using parameters which can be easily obtained from the literature.

3.3.4 FREE VOLUME THEORY

The free volume is the difference between the molar volume at the operating conditions V_B, and the limiting closed packed hard sphere volume, V_o. The free volume theory was originally proposed by Batchinski (1913) for describing viscosity relationships and later by Hildebrand (1971) for diffusivity.

Batchinski (1913) plotted the viscosity versus the molar volume for 87 non-associated liquids and observed straight lines. Thus Batchinski found that this relationship could be expressed as:

$$\frac{1}{\eta} = B \cdot \frac{V_B - V_\eta}{V_\eta} \tag{3.37}$$

In the above expression B is a constant and its values are dependent on the solvent. V_B is the liquid molar volume and V_η is the hypothetical liquid molar volume at infinite viscosity. Batchinski found from his experiments that V_η is the molar volume of either the liquid or the solid at its melting point and that the difference $V_B - V_\eta$ can be thought of as the free volume that exists between the fluids actual volume and the closed packed volume at its melting point.

Hildebrand applied this reasoning to diffusivity and observed that both the self diffusion coefficient and the infinite dilution coefficient may be expressed by a similar relationship:

$$D = B' \cdot \frac{V_B - V_D}{V_D} \tag{3.38}$$

In this case V_D is equivalent to V_η and is the molar volume at its melting point at which diffusion is considered to cease. The difference $V_B - V_D$ is also analogous to the free volume of the system. The simple form of the free volume equation is seldom used. However, several empirical equations use the free volume theory as the basis of development. It is noted that although Hildebrand's explanation of the linear relationship between D and V_B has no theoretical basis, the RHS theory which shows the same linear relationship suggests the existence of some theoretical basis for this relationship.

3.4 Literature Review for Molecular Diffusivities in Liquids

In this section, the diffusivity data reported by a number of researchers will be mentioned. Of all the types of diffusivity data available in the literature, diffusivities for alkane systems at ambient conditions are perhaps the most plentiful. Of these, only a few measurements have been reported for gaseous solutes in alkane or alkanol solvents. The systems consisting of gaseous solutes and alkane or alkanol solvents are of special interest because they constitute the main interest of my research.

A large portion of the available data for molecular diffusivities was reported over thirty years ago especially for n-alkanes. Using a capillary-type apparatus Fishman (1955) measured the self-diffusivities for n-pentane and n-heptane at temperatures between 193.15 and 373.15 K. Peter and Weinert (1956) measured the diffusivity of hydrogen in molten paraffin wax at 373 and 473.15 K and at several pressures up to 96.5 MPa. These were the first diffusion measurements done at high pressures. From 1960 to 1980, very few measurements of mutual diffusivity were reported for any system for temperatures above 298.15 K.

The data for gases dissolved in alkane and alkanol solvents most relevant to my research will now be summarized. The diffusivity of propene in n-butanol was measured by Wong and Hayduk (1990b). The diffusivity of propane in n-butanol was measured by Hayduk et al. (1973). The diffusivity of carbon dioxide in several solvents were measured in ethanol by Onda et al. (1960), Tang and Himmelblau (1965), Dim et al. (1971), Pfeiffer and Krieger (1974), and Malik and Hayduk (1968), in ethylene glycol by Hayduk and Malik (1971), in propanol by Takahashi et al. (1982), and Takenihi et al. (1975), and in n-butanol by Dim et al. (1971), and Takenihi et al. (1975). All of the above-mentioned measurements were done at atmospheric pressure and in the temperature range 273.15 to 323.15 K, and the gaseous solutes were infinitely dilute in the solvents.

Moore and Wellek (1974) measured the diffusivities for the solutes n-heptane and n-decane in the solvents n-hexane to n-decane, n-hexanol and n-heptanol at 293.15 to 313.15 K.

The diffusivity data collected using the Taylor dispersion apparatus will now be described. Evans et al. (1979) were among the first in the use of the Taylor

dispersion apparatus. They measured the diffusion coefficients at infinite dilution for the gases argon, krypton, xenon, and methane in n-hexane, n-decane and n-tetradecane at 298.15 K, as well as the diffusivities for several liquid solutes. The Taylor dispersion apparatus was also used by Alizadeh and Wakeham (1982), to measure the mutual diffusion coefficients above ambient conditions at 293.15 and 343.15 K, and at 0.1 MPa over the entire concentration range of all binary combinations of n-hexane, n-heptane, and n-octane. Chen et al. (1982) collected diffusivity data for the solutes argon, krypton, xenon, methane, carbon tetrachloride and several n-alkanes in n-alkane solvents at 298.15 to 333.15 K. Matthews (1986) measured diffusivities for n-octane, n-decane, n-dodecane, n-tetradecane and n-hexadecane in the solvents n-heptane, n-dodecane and n-hexadecane as well as for the gases hydrogen, carbon monoxide and carbon dioxide in n-heptane, n-dodecane and n-hexadecane over the temperature range 323.15 to 564.15 K and at pressures of 1.38 and 3.45 MPa. Following this, diffusivities were measured by Rodden (1988) for hydrogen, carbon monoxide, carbon dioxide and several n-alkane solutes in the solvents n-eicosane, n-octacosane and a Fischer-Tropsch wax, which was a mixture of paraffins with an average carbon number of 28, at 1.38 MPa and up to 533.15 K. Wong and Hayduk (1990b) measured the diffusivities of propene in acetic acid, acetone, n-butanol, chlorobenzene, ethylene glycol and n-octane for a range of temperatures and for pressures ranging to 6.89 MPa. Bartle et al. (1989) measured the diffusivities for the n-alkanes solutes ranging from ethane to octacosane in the solvents propan-2-ol and tetrahydrofuran at 300.15 K and atmospheric pressure.

3.5 Correlations for Diffusivities in Liquids at Infinite Dilution

This section will now deal with the correlations available for the calculation of the diffusivities of dissolved solutes in liquid solvents where the solute is considered to be infinitely dilute. The solute is said to be infinitely dilute in the solvent when each solute molecule is surrounded by many solvent molecules. In engineering applications, infinite dilution is said to occur when the concentration of the solute is less than 5 mole percent in a binary mixture. Most of the correlations reported are either semi-empirical or empirical. The semi-empirical equations are based on a modified version of one of the theories of diffusion explained previously and were

tested using experimental data. Many of these correlations are applicable only to certain types or families of liquids, and relatively low temperatures and pressures. Thus large percent errors are usually incurred when these correlations are used outside their proven range of applicability. Properties which can be measured or estimated, such as viscosity, molar and critical volumes are necessary to obtain the diffusivity in most of these correlations. Ghai et al. (1973), Ertl et al. (1974), Reid et al. (1977, 1987) and Hayduk (1986), reviewed correlations for the prediction of diffusivities at infinite dilution. Generalized correlations for all types of solutes in all types of solvents, as well as correlations for dissolved gases in liquids will now be discussed. Two other important classes of correlations which will not be discussed include correlations for liquid n-alkane systems and correlations for water as the solvent. Correlations classified according to specific solute and/or solvent usually yield lower precent errors than those for general correlations applicable for all types of solutes and solvents which have widely varying properties. It should be noted that for the correlations which will now be presented, the units for diffusivity are cm^2/s, viscosity are *cp*, and molar volume are $cm^3/mole$.

3.5.1 GENERAL CORRELATIONS FOR DIFFUSIVITIES IN LIQUIDS

The generalized correlations for diffusivities in liquids were formulated by Wilke and Chang (1955), Lusis and Ratcliff (1968), King et al. (1965), Tyn and Calus (1975), Hayduk and Minhas (1982), and Siddiqi and Lucas (1986). The two equations of Wilke-Chang and Lusis-Ratcliff which are based on hydrodynamic theory, but are nevertheless classified as empirical equations, are well known for their use in estimating the diffusivities for a wide variety of systems. The Wilke-Chang correlation which is best suited for dilute solutions of nonelectrolytes is:

$$D_{AB}^{\circ} = 7.4 \times 10^{-8} \frac{(\Phi M_B)^{1/2} T}{\eta V_{bA}^{0.6}} \tag{3.39}$$

In this expression Φ is the "association constant" and accounts for solvation effects in systems with strong chemical attractions like hydrogen bonding. η is the viscosity of the solution and ΦM_B is the "effective molecular weight". The value of Φ varies: $\Phi = 1.0$ for non-associated solvents as in alkanes, $\Phi = 2.6$ for water, $\Phi = 1.9$ for methanol, and $\Phi = 1.5$ for ethanol. The association parameter for water was later

revised by Hayduk and Laudie (1974) to be 2.26. Hayduk and Laudie examined 285 diffusivity data in aqueous solution at 298.15 K and found that the 10% error obtained using $\Phi = 2.26$ was lower than that with $\Phi = 2.6$. The Wilke-Chang correlation yields poor predictions of diffusivity for water as the solute and for highly viscous solvents.

The Lusis-Ratcliff (1968) equation is similar to the Wilke-Chang equation but is not used as frequently:

$$D^{\circ}_{AB} = 8.52 \times 10^{-10} (V_B)^{-1/3} \frac{T}{\eta} \left[1.40 \left(\frac{V_B}{V_A} \right)^{1/3} + \frac{V_B}{V_A} \right] \tag{3.40}$$

King et al. (1965) obtained an empirical correlation for self diffusivity based on their observation that $D\eta/T$ was, for the most part, constant and used the latent heat of vaporization as a measure of the intermolecular attractions present. The King et al. (1965) correlation is:

$$D^{\circ}_{AB} = 4.4 \times 10^{-8} \left(\frac{T}{\eta_B} \right) \left(\frac{V_{bB}}{V_{bA}} \right)^{1/6} \left(\frac{\Delta H_B}{\Delta H_A} \right)^{1/2} \tag{3.41}$$

This correlation has been found to predict diffusivities relatively well for polar solutes or for solutes of small molecular size. However, this correlation does not predict diffusivities accurately for aqueous systems and for polar solvents of high viscosity.

The Tyn and Calus (1975) correlation which is based on the Stokes-Einstein equation utilizes the ratios of molecular sizes and the ratio of the parachors as a measure of the intermolecular forces:

$$D^{\circ}_{AB} = 8.93 \times 10^{-8} \left(\frac{V_{bA}}{V_{bB}^2} \right)^{1/6} \left(\frac{P_B}{P_A} \right)^{0.6} \left(\frac{T}{\eta_B} \right) \tag{3.42}$$

In this expression V_{bA} and V_{bB} represent the molar volumes of the solute and solvent at the normal boiling points, respectively, and are a measure of the molecular sizes. The parachors of the solute and solvent, P_A and P_B, are related to the surface tension as follows:

$$P_i = V_i S_i^{1/4} \tag{3.43}$$

In the above expression V_i is the molar volume of substance i in cm^3/mol, and S_i is the surface tension in dynes/cm. Both V_i and S_i are measured at the same temperature. The parachor values have been found to be essentially constant over a moderate temperature range. The Tyn and Calus correlation is bounded by several conditions. The correlation gives poor results for solvents of viscosity greater than 20 cp, and the values of V_A and P_A have to be adjusted for specific solutes and/or solvents. It should be noted that for nonpolar solutes and alcohols with one hydroxyl group, the values of V_B and P_B should be multiplied by a factor of $8\eta_B$.

After testing this correlation for a variety of systems Reid et al. (1987) found errors of less than 10% in predictability.

With some modification to the Tyn and Calus correlation, Hayduk and Minhas (1982) observed better results. Their correlation which is based on the parachor values and in which the same boundary conditions were used as in the Tyn-Calus equation is:

$$D^{\circ}_{AB} = 1.55 \times 10^{-8} T^{1.29} \eta_B^{-0.92} V_{bB} - 0.23 P_A - 0.42 P_B^{0.5} \qquad (3.44)$$

Hayduk and Minhas also obtained another correlation using the radius of gyration, R, to describe the effects of molecular size and shape on the diffusivity. This latter proposed equation is:

$$D^{\circ}_{AB} = 6.916 \times 10^{-10} T^{1.7} \eta_B^{-0.8} R_A^{-0.4} R_B^{0.2} \qquad (3.45)$$

Hayduk and Minhas tested the correlation given by equation (3.44) for 756 data points and found an average error of 13.9%.

Siddiqi and Lucas (1986) developed a correlation using the viscosity of the solvent, η_B, and the molar volumes of the solute and solvent, V_{bA} and V_{bB}, as two important parameters which are measures of the intermolecular forces affecting the diffusion process. The equation which was developed for organic liquid mixtures is:

$$D^{\circ}_{AB} = 9.89 \times 10^{-8} T \eta_B^{-0.907} V_{bA}^{-0.45} V_{bB}^{0.265} \qquad (3.46)$$

Siddiqi and Lucas tested their correlation using 1275 data points and observed an average percent error of 13.1%.

The generalized correlations are applicable for all types of solutes, solvents, a limited temperature and pressure range, and usually yield relatively large errors of

prediction because of all of the the chemically different systems which are considered together. Thus more accurate estimates of diffusivity may usually be obtained by using correlations that are restricted in some way say, for example, the correlation is applicable only to systems where water is the solvent. Another possible restriction is that the correlation is limited to the prediction of diffusivities of a solute which is a gas at normal temperatures and pressures. These correlations will be discussed in the next section.

3.5.2 CORRELATIONS FOR DIFFUSIVITIES OF DISSOLVED GASES IN LIQUIDS

A review of the correlations for diffusivities of dissolved gases in liquids is given by Himmelblau (1964), and more recently by Sovova (1976). The correlations which have been the most used by researchers will now be mentioned.

Sovova modified the Hayduk and Cheng correlation (1971). Hayduk and Cheng proposed that the viscosity of the solvent in a dilute solution is a measure of the molecular interactions and thus influences the diffusivity. They expressed diffusivity as proportional to viscosity to some power ς. The resulting correlation which is an empirical one based on the hydrodynamic theory is:

$$D^{\circ}_{AB} = \epsilon \eta_B^{\varsigma} \tag{3.47}$$

Hayduk and Cheng (1971) suggest that ς and ϵ are constants for a given solute in any solvent. These constants can only be determined by experimental means. If the diffusivity and viscosity values are known for at least two solvents, the constants ς and ϵ can be determined for a particular solute and thus equation (3.47) can be used to predict diffusivities in other solvents. This relationship has been found to predict the diffusivity of a dissolved gas in a liquid at infinite dilution reasonably well when no complexing or no association exists. Hayduk and Cheng provided the constants for their systems but since no theoretical or empirical basis was provided for generalizing the constants for other solute and solvent mixtures, this equation cannot be used to predict diffusivities unless at least two experiments are done to obtain the new constants.

It should be noted that the Hayduk and Cheng (1971) correlation has also been used for other systems other than dissolved gases in liquids. Moore and Wellek

(1974) experimented with two infinite dilute solutes n-heptane and n-decane in the series of alkane solvents n-hexane through n-decane and in the alcohol solvents n-hexanol and n-hep anol and then used the Hayduk and Cheng correlation on these alkane and alcohol systems.

Sovova's correlation which is a modified version of equation (3.47) and which was originally proposed for the infinite dilution diffusion coefficients of gases in alkane solvents is:

$$D^{\circ}_{AB} = 14.8 \times 10^{-5} \frac{f \eta_B^{\gamma}}{V_{bA}^{0.6}} \tag{3.48}$$

In the above equation V_{bA} is the molar volume of the gas at its normal boiling point, and the values of f and γ were specific for different types of solvents. For example $f = 1.0$ and $\gamma = -1.15$ for water, $f = 1.8$ and $\gamma = -1.15$ for aromatic hydrocarbon solvents and their derivatives, and $f = 2.28$ and $\gamma = -0.5$ for alcohols and alkanes.

The equation proposed by Akgerman and Gainer (1972a, 1972b) for the diffusion of gases in liquids is based on the activated state approach (Glasstone et al., 1941) and has no adjustable parameters.

$$D^{\circ}_{AB} = \frac{kT}{\epsilon_A \eta_B} \left(\frac{N}{V_B}\right)^{1/3} \left(\frac{M_B}{M_A}\right)^{1/2} \exp\left(\frac{E_\eta - E_D}{R_g T}\right) \tag{3.49}$$

In equation (3.49), k is Boltzmann's constant, T is the absolute temperature, N is the Avogadro's number and ϵ_A is the number of solvent molecules surrounding the central solute molecule where ϵ_A is defined as:

$$\epsilon_A = 6 \left(\frac{V_{bA}}{V_{bB}}\right)^{1/6} \tag{3.50}$$

The term $E_\eta - E_D$ represents the free energy of activation between the viscous (E_η) and the diffusion process (E_D) and is calculated from the activation energies of "jumping" of the solute and solvent molecules, represented by E^j_{AA} and E^j_{BB}, respectively.

$$E_\eta - E_D = E^j_{BB} \left[1 - \left(\frac{E^j_{AA}}{E^j_{BB}}\right)^{\frac{1}{\epsilon_A + 1}}\right] \tag{3.51}$$

$$E_{BB}^{j} = \frac{-R_g \ln\left(\frac{\mu_2}{\mu_1}\right) + \frac{R_g}{2}\ln\left(\frac{T_1}{T_2}\right)}{\frac{1}{T_1} - \frac{1}{T_2}} \tag{3.52}$$

$$E_{AA}^{j} = 5875.3\, M_A^{-0.186} \tag{3.53}$$

In equation (3.52), μ_1 and μ_2 represent the absolute viscosities of the solution at absolute temperatures T_1 and T_2, respectively.

The Akgerman and Gainer(1972a, 1972b) correlation has been found more successful in predicting diffusivities for solutes such as hydrogen and helium in which the solute molecules are small, and also for solvents of high viscosity ($\eta_B > 5cp$).

The correlation of Sridhar and Potter (1977a,b) is:

$$D_{AB}^{\circ} = 0.088 \frac{V_{cB}}{N^{2/3}} \cdot \frac{R_g T}{\eta_B V^*} \cdot \frac{1}{V_{cA}^{2/3}} \tag{3.54}$$

where:

$$V^* = 0.31\, V_{cB} \tag{3.55}$$

In the above expressions, V_{cA} and V_{cB} represent the critical molar volumes of the solute and solvent. The empirical correlation of Sridhar and Potter resulted from the combination of the empirical expressions for gas-liquid diffusivity of Hildebrand and self-diffusivity of Dullien. This is a poor correlation for solute gases of small molecular size such as hydrogen and helium.

The correlation of Umesi and Danner (1981) which was developed for hydrocarbon gases in nonpolar solvents is:

$$D_{AB}^{\circ} = 2.75 \times 10^{-8} \cdot \frac{T}{\eta_B} \left[\frac{R_B}{R_A^{2/3}}\right] \tag{3.56}$$

Here the authors proposed that the size-shape relationship is the dominant factor affecting the intermolecular forces and thus the diffusivity. Umesi and Danner used the viscosity of the solvent B, η_B, and the radius of gyration, R_A and R_B to define the

size-shape relationship. This equation can also be used for dilute nonpolar or polar solutes in polar solvents.

Finally, the correlation of Wong and Hayduk (1990a) which was proposed for dissolved gases (polar, non-polar, and hydrocarbon solutes) in hydrocarbon solvents is:

$$D^{\circ}_{AB} = 2.77 \times 10^{-3} \eta_B^{-0.559} \left(\frac{V_{cB}}{V_{cA}^{1.59}} \right)^{0.335} \cdot \left(M_A M_B^{1.31} \right)^{-0.166} \cdot \exp\left(- \frac{685.5}{T} \right) \quad (3.57)$$

Wong and Hayduk (1990a) examined 421 data points, in the temperature range of 273.15 to 567.15 K and obtained an average percent error of fit of 14.64%. The data did not include values for the solutes hydrogen and helium.

These correlations all have some limitation with respect to the temperature and pressure ranges in which they can be utilized. On the other hand, the equations have usually been found to yield reasonably accurate predictions of diffusivity for specific classes of solutes and solvents.

CHAPTER 4

DENSITY AND VISCOSITY MEASUREMENT AND TAYLOR DISPERSION THEORY

The theories and equations for density, and viscosity in conjunction with the Taylor theory of dispersion in capillary flow will be discussed in this chapter, as well as the theory and mathematics of the Taylor method for measuring and calculating molecular diffusivities.

4.1 Density Measurement

It is of interest to measure the actual solvent densities and viscosities in addition to the dissolved gas diffusivities at high pressure. The measurement of density involves a technique based on the retention time of the dispersion peak, t_R, and the solvent mass flow rate, $\dot{m}$. It was Griffiths, (1911), who first observed that the centre of gravity of the peak moves with the average speed of flow of the solvent, $\bar{u}$, for the entire length, L, of the diffusion tube and the retention time can therefore be obtained as follows:

$$t_R = \frac{L}{\bar{u}} \tag{4.1}$$

At steady state the mass flow rate, $\dot{m}$, is constant:

$$\dot{m} = \pi R^2 \bar{u} \rho = \frac{\pi R^2 L \rho}{t_R} \tag{4.2}$$

The density of the solvent can be calculated from equation (4.2) if an accurate value for L and r are known. However because L is typically tens of meters and r is typically a fraction of a centimeter, these quantities are usually difficult to measure accurately. To eliminate the need of knowing L and r, an expression was obtained for the ratio of the density at condition 1 using a fluid of known density, ρ_1, to that at condition 2 where ρ_2 is unknown. Equation (4.2) may then be rewritten in terms of the thermal coefficient of expansion for stainless steel, α, (Matthews, 1986):

$$\frac{\rho_2}{\rho_1} = \frac{(t_R)_2 \dot{m}_2 (R^2L)_1}{(t_R)_1 \dot{m}_1 (R^2L)_2} \tag{4.3}$$

$$= \frac{(t_R)_2 \dot{m}_2 [1 + \alpha(T_1 - T_{ref})]^3}{(t_R)_1 \dot{m}_1 [1 + \alpha(T_2 - T_{ref})]^3} \tag{4.4}$$

In these expressions $R = R_{ref}[1 + \alpha(T - T_{ref})]$ and $L = L_{ref}[1 + \alpha(T - T_{ref})]$. The reference temperature, T_{ref}, at which the length and diameter of the diffusion tube were measured was assumed to be 295 K or essentially room temperature. Rearrangement gives:

$$\rho_2 = \left(\rho_1 \frac{[1 + \alpha(T_1 - T_{ref})]^3}{(t_R)_1 \dot{m}_1} \right) \frac{(t_R)_2 \dot{m}_2}{[1 + \alpha(T_2 - T_{ref})]^3} \tag{4.5}$$

$$= K_1 \frac{(t_R)_2 \dot{m}_2}{[1 + \alpha(T_2 - T_{ref})]^3} \tag{4.6}$$

In the above expression K_1 is a constant that may be determined from a calibration performed with a substance of known density at temperature T_1.

Because with this equipment it was not possible to measure density at atmospheric pressure at which pressure an actual reference density could be used, I devised an alternate method. In this method an assumed value was used for K_1 and the value of ρ_2 was then obtained as a function of pressure at the temperature T_2. A linear regression of ρ_2 as a function of pressure was then performed. The intercept of this line then represented the density at 0 gauge pressure. The value of K_1 was then adjusted so that the value of the intercept corresponded to the solvent density of the reference substance at $T = T_1 = T_2$.

A similar method was used by Matthews (1986) to obtain the density of the solvent using the same design of experimental apparatus as was used in this study. Matthews used an equation similar to equation (4.3) but did not calculate a calibration constant K_1. Instead, he performed the Taylor's dispersion experiment twice; first at condition 1 using a fluid of known density ρ_1, then again at condition 2 where ρ_2 is unknown. The volume correction term $(R^2L)_1/(R^2L)_2$ which eliminates the need to know L and R can be accurately accounted for using the thermal expansion coefficient for the stainless steel tube. This correction term

$(R^2L)_1/(R^2L)_2 = (1 + \alpha\Delta T)^{-3}$ where $\Delta T = T - T_1$. Thus T_1 was used in place of T_{ref}. Matthews used distilled, deionized water as the calibration fluid since accurate data for densities over a wide range of temperatures and pressures are available. It was necessary to use a small quantity of tracer in the water to be able to detect a peak. He performed two calibration experiments at 303.2 and 303.0 K for reproducibility using a 2% by weight solution of methanol in water. He then verified the procedure by performing the Taylor dispersion experiment again at different temperatures and pressures and then calculating the densities of the water. Matthews found that on comparing the calculated and literature values of water densities, the agreement was excellent with an average absolute error of 0.025%. Thus Matthews found that this method of calculating the densities of solvents using Taylor dispersion experiment gave accurate results. Therefore it has already been shown that the Taylor dispersion experiment has been adequately designed for accurate density measurements. The results from this work will also prove this to be true.

4.2 Viscosity Measurement

The solvent viscosities at high pressures were determined on the basis that the flow through the capillary tubing was laminar. This technique can thus be suitably used in conjunction with the Taylor technique of diffusivity measurements since both require that the solvent be moving in laminar flow. On that basis the Hagen-Poiseuille equation applies:

$$\eta = \frac{\pi \rho \Delta P R^4}{8 \dot{m} L} \tag{4.7}$$

The Hagen-Poiseuille equation is obtained from a momentum balance on the flow through a circular tube. The assumptions for this equation include: (1) laminar flow, (2) constant density, (3) flow is not a function of time, (steady state), (4) Newtonian fluid, and (5) end effects can be neglected. The ratio of η_2 to η_1 gives the following expression:

$$\eta_2 = \eta_1 \frac{\rho_2 \Delta P_2 R_{ref}^4 [1 + \alpha(T_2 - T_{ref})]^4}{\dot{m}_2 L_{ref} [1 + \alpha(T_2 - T_{ref})]} \frac{\dot{m}_1 L_{ref} [1 + \alpha(T_1 - T_{ref})]}{\rho_1 \Delta P_1 R_{ref}^4 [1 + \alpha(T_1 - T_{ref})]^4} \tag{4.8}$$

Rearrangement yields:

$$\eta_2 = \left(\eta_1 \frac{\dot{m}_1}{\rho_1 \Delta P_1 [1 + \alpha (T_1 - T_{ref})]^3} \right) \frac{\rho_2 \Delta P_2 [1 + \alpha (T_2 - T_{ref})]^3}{\dot{m}_2} \tag{4.9}$$

Because the first term on the right hand side is constant, we can write:

$$\eta_2 = K_2 \frac{\rho_2 \Delta P_2 [1 + \alpha (T_2 - T_{ref})]^3}{\dot{m}_2} \tag{4.10}$$

The reference temperature was again assumed to be 295 K. The method of obtaining the constant K_2 was the same as that used for determining the density. The value of the viscosity of the fluid for calibration was taken from the literature (Daubert and Danner, 1985).

Marvin (1971), reviewed the capillary viscometer technique and discussed the experimental error in great detail. He found an accuracy of $\pm 2\%$ or better. The accurate determination of ΔP is quite critical since the end effects can greatly influence the differential pressure. The experimental setup used in this work was designed to minimize end effects. Another critical factor is the determination of the value of R which can be used in equation (4.7). Because the radius cannot be accurately determined directly, it is indirectly determined by calibrating the capillary tube with a fluid of known density. Matthews (1986) followed this procedure using the universal calibration fluid, water, at a reference temperature. He was then able to correct for the length and radius at other temperatures using the thermal coefficient of expansion and found that the calculated viscosities differed from the literature values by less than 1%.

4.3 Taylor Dispersion Model

4.3.1 MATHEMATICAL DESCRIPTION OF THE MODEL

Taylor's dispersion technique can be likened to a dynamic chromatographic technique. It was Griffiths (1911) who first observed that on injecting a pulse of a dye solution into a slow stream of water confined in a glass capillary tube, the coloured solution dispersed symmetrical about a plane moving with the mean speed

of the flow, with time, slowly increasing in length. It was not until 1952 when Sir Geoffrey Taylor was asked by a veterinarian for a method of obtaining the mean velocity of blood in the arteries of animals using a tracer (Taylor, 1954a). Taylor in his solution to this problem (Taylor, 1953) explained the method for obtaining the mean velocity as well as the tracer diffusion coefficient which resulted in what is known as Taylor's dispersion method. Taylor (1953) noted that there appeared to be a discrepancy between Griffiths observation and the proven existence of a parabolic distribution of velocities for a fluid in laminar flow in a tube, with the fluid at the centre moving with twice the average velocity of flow. If this was all that was happening, the bulk movement of the fluid alone should have reshaped the pulse of coloured solution into the shape of a parabola (Figure 4.1). Figure 4.1 illustrates the case for a pulse of a sample of thickness δ injected at the tube inlet into a fluid in laminar flow. The pulse of width δ which initially can be considered to be a line across the diameter, tends to be distorted by the flowing fluid into a parabola of width δ with the centerline velocity of this parabolic velocity profile u_{max} being equal to twice the average velocity $\bar{u}$. As shown in Figure 4.1, if no other transport process were occurring, the parabola would simply lengthen with time. Taylor explained this observed discrepancy by recognizing that the mass transport processes included the bulk movement of the fluid as well as diffusion, both along and perpendicular to the tube axis. It is the concentration gradients which lead to diffusion and this is a very rapid mass transport process if the ratio of the tube diameter to the length of travel of the injected solute is small. Diffusion in the axial direction is then negligible compared to the radial diffusion. The longitudinal diffusion is also negligible in comparison to the significant movement of mass from one point to another in the direction of flow for the bulk transport process. At, and in the vicinity of the apex of the parabola, the diffusion is primarily towards the wall and near the wall it is towards the center (Figure 4.1). Taylor (1953, 1954), explains this as follows: "this means that the central part of the pipe fluid which is free of the dissolved substance passes into the zone where the concentration is rising. The dissolved substance is then absorbed till the concentration C, reaches its maximum value at $z = \bar{u}t$. The fluid then passes through the region where C decreases with z and finally leaves this zone, having yielded up the whole of the dissolved substance it had acquired." It can be thought that the movement of mass in the radial direction by diffusion, in effect decreases the movement of mass in the axial direction which would by itself be large

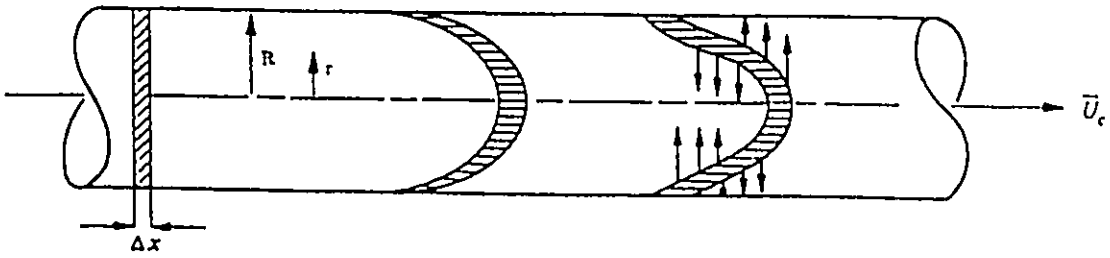

Figure 4.1: Taylor Diffusion Laminar Flow in a Round Tube

due to the velocity profile. The resulting radially averaged concentration distribution is said to be a normal or Gaussian distribution. Because of the radial diffusion, the average concentration at any distance z along the Gaussian peak is very sharp and distinct from another point on the peak. Further, although the maximum point on the peak which represents the maximum in the average concentrations moves at the average velocity of flow of the fluid, $\bar{u}$, portions of the fluid are moving more slowly and others more rapidly than $\bar{u}$. In the absence of molecular diffusion the mean concentration is uniform and varies inversely over the length $u_{max}t$.

Consider theoretically a δ pulse of solution of any concentration injected suddenly into a fluid in laminar flow of either a pure solvent or of a solution of different composition in a straight tube. The velocity of the injected pulse at a radial distance r in a tube of radius R is given by u(r). The resultant parabolic profile is:

$$u(r) = 2\bar{u}\left[1 - \left(\frac{r}{R}\right)^2\right] \tag{4.11}$$

The flux density J_z along the tube axis is comprised of the diffusive and the convective term:

$$J_z = -D_{AB}\left(\frac{\partial C}{\partial z}\right) + C \cdot 2\bar{u}\left[1 - \left(\frac{r}{R}\right)^2\right] \tag{4.12}$$

In the above equation the diffusivity is D_{AB} which is assumed to be independent of concentration, and C is the concentration in mass per unit volume and is a function of the radial position r. The flux in the radial direction J_r, which is due only to diffusion, is given by:

$$J_r = -D_{AB}\left(\frac{\partial C}{\partial r}\right) \tag{4.13}$$

In these equations the units of J_z and J_r are mass per unit area per unit time. To evaluate the effect of diffusion on the flow, the law of conservation of mass is applied to the diffusing species in a ring-shaped element with the inner radius r, outer radius r+dr, and thickness dz for a binary mixture of A and B. The mass balance considers the rate of accumulation of the mass of solute in the ring-shaped element being the result of the rate of change of mass at which the solute enters and leaves the

ring by mass transport along the z and r axes. The change of mass of A with respect to time is obtained by applying equations (4.12) and (4.13). The resulting continuity equation for component A in a binary mixture with constant diffusivity and density with no chemical reaction is given by:

$$D_{AB}\left[\frac{1}{r}\frac{\partial}{\partial r}\left(r\frac{\partial C}{\partial r}\right)+\frac{\partial^2 C}{\partial z^2}\right]=2\bar{u}\left[1-\left(\frac{r}{R}\right)^2\right]\frac{\partial C}{\partial z}+\frac{\partial C}{\partial t} \qquad (4.14)$$

The continuity equation describes the rate of change of concentration of A at a fixed point resulting from changes due to bulk movement and diffusion.

The measured concentration, C_m, is an average concentration across the cross section of the tube and is given by:

$$C_m=\frac{2}{R^2}\int_0^R C(r)\,r\,dr \qquad (4.15)$$

Multiplying equation (4.14) by $2r/R^2$ and integrating with respect to r from 0 to R gives the averaged continuity equation:

$$D_{AB}\frac{\partial^2 C_m}{\partial z^2}+\frac{4\bar{u}}{R^4}\frac{\partial}{\partial z}\int_0^R (C-C_m)\,r^3\,dr=\frac{\partial C_m}{\partial t}+\bar{u}\frac{\partial C_m}{\partial z} \qquad (4.16)$$

Taylor (1953, 1954a) showed that the axial diffusion term $\partial^2 C_m/\partial z^2$ can be neglected if the following conditions are satisfied:

$$\frac{4L}{R}\gg\frac{R\bar{u}}{D_{AB}}\gg 6.9 \qquad (4.17)$$

Equation (4.16) is then reduced to:

$$\frac{4\bar{u}}{R^4}\frac{\partial}{\partial z}\int_0^R (C-C_m)\,r^3\,dr=\frac{\partial C_m}{\partial t}+\bar{u}\frac{\partial C_m}{\partial z} \qquad (4.18)$$

Taylor (1954) showed that for this case the concentration profile is expressed by:

$$C-C_m=\frac{R^2\bar{u}}{4D_{AB}}\frac{\partial C_m}{\partial z}\left[-\frac{1}{3}+\left(\frac{r}{R}\right)^2-\frac{1}{2}\left(\frac{r}{R}\right)^4\right] \qquad (4.19)$$

Substituting equation (4.19) into equation (4.18) and integrating gives:

$$K \frac{\partial^2 C_m}{\partial z^2} = \bar{u} \frac{\partial C_m}{\partial z} + \frac{\partial C_m}{\partial t} \tag{4.20}$$

The effective dispersion coefficient, K, is given by:

$$K = \frac{\bar{u}^2 R^2}{48 D_{AB}} \tag{4.21}$$

Aris (1956) provided a more generalized mathematical approach and his expression for K which included the effect due to axial diffusion:

$$K = D_{AB} + \frac{\bar{u}^2 R^2}{48 D_{AB}} \tag{4.22}$$

Although Aris' definition of K is more rigorously correct, Taylor's assumption of ignoring the axial diffusion effect is reasonable because on performing calculations using equation (4.22) the first term is usually orders of magnitude smaller than the second term.

Because it was observed experimentally that the peak disperses about a point which moves at the mean speed of the flowing fluid, a new coordinate Z is defined to move with the mean speed of flow:

$$Z = z - \bar{u} t \tag{4.23}$$

The expressions for the partial derivatives for t held constant is:

$$\frac{\partial}{\partial Z} = \frac{\partial}{\partial z} \quad \text{and} \quad \frac{\partial^2}{\partial Z^2} = \frac{\partial^2}{\partial z^2} \tag{4.24}$$

Also the total time derivative of C_m which is dependent on position and time is given by:

$$\frac{d C_m}{d t} = \frac{\partial C_m}{\partial t} + \frac{\partial C_m}{\partial z} \frac{\partial z}{\partial t} \qquad \frac{d^2 C_m}{d z^2} = \frac{\partial^2 C_m}{\partial z^2} + \frac{\partial^2 C_m}{\partial t^2} \cdot \frac{\partial t^2}{\partial z^2} = \frac{\partial^2 C_m}{\partial z^2} \tag{4.25}$$

In this expression $\partial z/\partial t$ is the average velocity $\bar{u}$. Applying equations (4.24) and (4.25) to (4.20) gives:

$$K \frac{d^2 C_m}{dZ^2} = \frac{dC_m}{dt} \tag{4.26}$$

Equation (4.26) can be solved analytically for at least three different initial conditions where the diffusivity is assumed to be independent of concentration. There are considered to be three possible types of injections: (1) a delta or impulse injection of concentrated solute at time $t = 0$, (2) a square pulse injection at time $t = 0$ and (3) a step-change injection at time $t = 0$. The analysis and solutions to equation (4.26) for these three different cases have been determined by Baldauf and Knapp (1983). The solutions to this equation for both the delta and the step-change injection were originally performed by Taylor (1953).

The solutions for the delta and the square injections have been used much more than the step-change because the step-change injection has very little practical significance compared to the other types of injections. Because the solution for the delta type injection is much simpler than that for the square pulse injection, which contains a linear combination of terms involving the error function, it has been used by many researchers. Evans and Kenney (1905) found that when the ratio of the volume of the injected sample to the volume of the dispersion column is less than 1%, the solutions for the delta and the square-pulse injections are identical, and the extreme accuracy in agreement justifies using the delta solution although a pure impulse cannot be achieved in practice. Thus by satisfying the condition of Evans and Kenney (1905) the Taylor dispersion apparatus can be said to operate with an impulse or delta injection.

For a pulse of solute of concentration C_m^o injected into a cylindrical tube of infinite length at time $t = 0$ and position $z = 0$, the initial and boundary conditions are respectively:

$$C_m(0,0) = C_m^o \qquad C_m(\infty, t) = 0 \tag{4.27}$$

Solving equation (4.26) using these conditions and where the ratio of the pulse width, h, to the length of the tube is very small, then a delta pulse yields the solution:

$$C_m = C_m^o \left[\frac{h}{(4\pi K t)^{1/2}} \exp\left[-\frac{Z^2}{4Kt} \right] \right] \tag{4.28}$$

Since the mean concentration is measured at a distance L along the dispersion column, the equation can be rewritten as:

$$C_m = C_m^{\circ}\left[\frac{h}{(4\pi Kt)^{1/2}}\exp\left[\frac{-(L-\bar{u}\,t)^2}{4Kt}\right]\right] \qquad (4.29)$$

Equation (4.29) can also be rewritten in terms of the mass M of the solute in the injected pulse:

$$C_m = \frac{M}{\pi R^2(4\pi Kt)^{1/2}}\exp\left[-\frac{(L-\bar{u}\,t)^2}{4Kt}\right] \qquad (4.30)$$

In summary, equation (4.30) represents the radially averaged concentration at a distance L from the injection point which can be applied at the end of the dispersion tube for a delta injection containing a mass M of solute. Immediately after injection, the pulse of sample disperses into a Gaussian shape whose center of gravity moves with the mean velocity of the fluid and whose variance is σ^2 and is equal to $2Kt$ as was experimentally observed by Griffiths. It has been found experimentally that the observed variance is inversely proportional to the diffusion coefficient in liquid systems.

Equation (4.30) can be directly used to determine K and thence D_{AB} by the method of non-linear regression analysis for the estimation of all the parameters. Prior to the age of computers these non-linear techniques were not practical. Two general techniques, the moment method and the graphical method, which are both approximate solutions of equation (4.26), are the most popular methods for the Taylor analysis of dispersion data.

The graphical method, originally developed by chromatographers to obtain the diffusivities directly from the dispersion peak recorded by a chart recorder, is clearly and extensively described by Giddings and Seager (1962) and later by Grushka and Kikta (1974). This method is popular with many researchers because of its simplicity. In the graphical method the approximation is made that the variance is a constant independent of time. From the exact analytical expression of Taylor, the variance $\sigma^2 = 2Kt$ is approximated by the graphical method to $\sigma^2 = 2Kt_R$. Thus using the expression for K, the effective dispersion coefficient from equation (4.21) and replacing t with t_R, the variance is:

$$\sigma^2 = \frac{R^2 \bar{u}^2 t_R}{24 D_{AB}} \tag{4.31}$$

The first term of equation (4.22) is usually ignored for diffusion in liquids. The theoretical plate height, H, is defined from the chromatographic analysis as (Grushka and Kikta, 1974):

$$H = \frac{\sigma^2}{L} \tag{4.32}$$

Utilizing the retention time $t_R = L/\bar{u}$, and the theoretical plate height H, equation (4.31) can be rearranged to give:

$$D_{AB} = \frac{R^2 \bar{u}}{24 H} \tag{4.33}$$

The plate height is obtained from an expression involving the retention time and the the width of a Gaussian-shaped peak at half height, $W_{1/2}$, and is given by the following relationship (Cloeta et al., 1976):

$$H = \frac{L W_{1/2}^2}{5.54 t_R^2} \tag{4.34}$$

Substituting Equation (4.34) and the expression for t_R into equation (4.33) gives:

$$D_{AB} = 0.231 \frac{R^2 t_R}{W_{1/2}^2} \tag{4.35}$$

The graphical method is so called because the peak height and the subsequent peak width at half height are measured from the chart recorder using a ruler. The disadvantages of this method are: (1) the mathematics of the method are approximate, (2) the variance can only be independent of time for very narrow peaks and (3) the human measurement errors are undesirable but present.

The moment method solution, an approximate solution to equation (4.26) as given by Aris (1956) and later by Alizadeh et al. (1980) shows that:

$$D_{AB} = \frac{R^2 \bar{t}}{24 \sigma_t^2} \tag{4.36}$$

The zeroth, first and second temporal moments which are the sum function S, the center of gravity $\bar{t}$, and the variance σ_t^2, respectively, are defined as:

$$S = \int_0^\infty C_m(t)dt \tag{4.37}$$

$$\bar{t} = \frac{1}{S}\int_0^\infty t.C_m(t)dt \tag{4.38}$$

$$\sigma_t^2 = \frac{1}{S}\int_0^\infty (t - \bar{t})^2 C_m(t)dt \tag{4.39}$$

The moments are calculated from the raw peak data by finite summation using the trapezoidal rule. Examination of equation (4.39) shows that the variance is heavily weighted at the extremities of the peak by the difference term. Because it is at the peak ends that the uncertainty in measurement is greatest, this method can result in large errors in the diffusivities. The disadvantages of the moment method are discussed by Radeke (1981).

In practice, for a more complete analysis a few additional factors may be considered: (1) for large diffusivities, axial diffusion should be accounted for, (2) the observed variance is a function of time and transient effects such as, that the diffusion continues during the passage of the peak through the detector should be accounted for, (3) the contributions to the variance due to the finite width of the injection pulse, mixing in the detector cell, and the length of the tubing connecting the dispersion tube to the detector should all be accounted for. These corrections are discussed in detail by Alizadeh et al. (1980). Alizadeh and Wakeham (1982), and Rodden (1988), all found that their calculated diffusion coefficients to be strongly dependent on the selection of end points and thus they both discontinued using the moment method in favour of fitting the raw data to the fundamental analytical equation of Taylor, equation (4.30).

The analysis used in this work is based on the analytical solution of Taylor and was used in order to avoid the errors associated with the graphical and moment method. Since this method uses the fundamental solution of Taylor, unlike the moment and graphical methods, the diffusivities so calculated are considered to be better estimates of the true values.

Recalling Taylors analytical solution to the dispersion problem:

$$C_m = \frac{M}{\pi R^2 (4\pi K t)^{1/2}} \exp\left[-\frac{(L - \bar{u}t)^2}{4Kt} \right] \tag{4.30}$$

In this expression $\bar{u}$ is the average velocity at which the centre of the peak moves and K is the Taylor dispersion coefficient. In my experimental setup, a refractive index detector is used to measure the solute concentration at a distance L from the point of injection at the end of the dispersion tube. The detector generates a voltage which is proportional to the solute concentration. A test was devised to show that a linear response of the detector was obtained. The area under the peak was calculated and plotted versus the solute concentration in mole fraction, in this case using the test solute n-hexane and a straight line with zero intercept was obtained, indicating the linear response of the detector. With the voltage, V, directly proportional to the solute concentration, equation (4.30) can be modified to express the changing concentration in terms of a measured voltage as follows:

$$V = \frac{B_1}{t^{1/2}} \exp\left[-\frac{(L - B_4 t)^2}{B_2 t} \right] + B_3 + B_5 t \tag{4.40}$$

In the above expression, B_1 to B_5 are adjustable parameters with B_3 and B_5 accounting for baseline offset and drift, B_4 ($\equiv\bar{u}$) is the average velocity of the solvent and B_2 is equal to 4K. Recalling Aris' (1956) definition of K:

$$K = D_{AB} + \frac{\bar{u}^2 R^2}{48 D_{AB}} \tag{4.22}$$

Finally, the solution of the above quadratic equation in D_{AB} gives:

$$D_{AB} = \frac{B_2}{8} - \left[\frac{B_2^2}{64} - \frac{(R B_4)^2}{48} \right]^{1/2} \tag{4.41}$$

It is apparent that if the voltage-time data is recorded, preferably by a computer at regular time intervals, and the optimum values of the parameters have been found for equation (4.40), the value of D_{AB} may be determined using equation (4.41). Please refer to Chapter 6 in the section on Data Handling and Computational Analysis for more details.

4.3.2 LITERATURE REVIEW OF TAYLOR METHOD

Taylor (1953, 1954) not only performed experiments confirming his theory but successfully developed the first mathematical analysis for this phenomenon described by Griffiths. A more general approach was provided later by Aris (1956) and this subsequently led to applying Taylor's method to measure and calculate diffusion coefficients. The mathematical treatment was confirmed with many experiments. The first set of experiments performed using Taylor's technique was in the determination of gaseous diffusivities ($D \approx 1\ cm^2 \cdot s^{-1}$), by vapour phase chromatography using packed or unpacked columns (Giddings and Seager, 1960; Wakeham and Slater, 1973; Maynard and Grushka, 1965). Ouano (1972), was the first to use Taylor's technique for the determination of liquid diffusivities ($D \leq 10^{-5}\ cm^2 \cdot s^{-1}$). Many other experiments have been performed for liquid systems. This includes the interdiffusion coefficient of an infinitely dilute solute in a solvent (Ouano, 1972; Komiyama and Smith, 1974; Grushka and Kikta, 1974; Grushka and Kikta, 1975; Ouano and Carothers, 1975; Grushka and Kikta, 1976) and the differential interdiffusion coefficients as a function of solution composition (Pratt and Wakeham, 1974; Pratt and Wakeham, 1975a; Pratt and Wakeham, 1975b). The injection of one solution into another solution where the two solutions vary slightly in composition allows for the determination of the differential interdiffusion coefficient. The major problem associated with the measurement of the intradiffusion coefficient is the practical problem of detecting the concentration distribution of an isotopically labelled species. Taylor's technique was also confirmed by numerical simulation as is shown in the papers by Ar[illegible]thakrishnan et al. (1965) and Bailey and Grogarty (1962).

4.3.3 DESIGN CRITERIA FOR THE APPLICATION OF TAYLOR METHOD

4.3.3.1 Laminar Flow Criterion, Impulse (delta) injection, Negligible Axial Diffusion and Coiling Effect

To ensure that the Taylor dispersion model is applicable to the coiled capillary tube, several criteria must be satisfied. The first is that the flow must be laminar, the second is that the injected sample should be a delta type injection, the third is

that the rate of axial diffusion must be negligible and lastly that the effect of curvature of the capillary tube on the diffusivity must also be negligible.

1. Laminar Flow Criterion

It is normally easy to satisfy the criterion that the flow in the capillary tubing is laminar, because flow rates which are very low are normally utilized. In my experiments the Reynolds number was calculated for each experiment to ensure that the flow was laminar and it was found that the Reynolds number ranged from 2 to 65. Since the intermediate flow region occurs for $N_{Re} \geq 2000$ this criteria is not a limiting one.

2. Impulse (delta) Injection

Although in my experiments the injection more closely approximated a square pulse injection of finite length, Taylor assumed an impulse injection because the solution for an impulse injection was much simpler than the solution for a square pulse which contained a linear combination of terms containing the error function. Both Levenspiel and Smith (1957) and Evans and Kenney (1965) have shown that if the volume of the injected sample to the volume of the dispersion column is less than 1%, then there is no difference between the impulse and the square pulse solutions. Thus, although in practice it is impossible to obtain a pure impulse type injection, the error from this assumption for my experiments is negligible. For my experimental setup, the volume of the injected sample was 2.0×10^{-8} m^3, the volume of the dispersion column was 1.54×10^{-5} m^3 and the ratio of the two volumes was 0.13% thus satisfying the above-mentioned criterion.

3. Flow Criteria Based On Negligible Axial Diffusion

In his original work, Taylor specified two conditions for which axial diffusion is negligible (1953, 1954a). These are:

$$4\frac{L}{R} \gg \frac{\bar{u}R}{D_{AB}} \gg 6.9 \qquad (4.42)$$

Equation (4.42) was obtained by examining equation (4.22):

$$K = D_{AB} + \frac{\bar{u}^2 R^2}{48 D_{AB}} \tag{4.22}$$

Since the first term of equation (4.22) represents the effect of diffusion in the axial direction, and the second term represents the contribution due to radial diffusion and the dispersive effect due to the velocity profile, then in order that the longitudinal molecular diffusion be negligible compared to the dispersive effects expressed by K, the following condition must be met:

$$D_{AB} \ll \frac{\bar{u}^2 R^2}{48 D_{AB}} \tag{4.43}$$

Taking the square root gives:

$$\frac{\bar{u} R}{D_{AB}} \gg \sqrt{48} = 6.9 \tag{4.44}$$

$$4\frac{L}{R} \gg \bar{u}\frac{R}{D_{AB}} \gg 6.9 \tag{4.45}$$

In the above expressions $4L/R$ is a constant and equal to 357,900. The final form of the equation as specified by Taylor is:

$$\frac{D_{AB} L}{\bar{u} R^2} \gg 1 \tag{4.46}$$

This equation is obtained by taking the ratio of the the two groups of terms from equation (4.45). Alizadeh and Wakeham (1982) applied a different mathematical method for the moment method solution and obtained the same expression except that their criteria was a factor of 10 more limiting. The Taylor's solution is thus less limiting in velocity of flow than the moment solution of Alizadeh et al. (1980). In all of the experiments performed in this research, care was taken to ensure that the above-mentioned conditions of both Taylor and Alizadeh and Wakeham (1982) were satisfied thus ensuring negligible axial diffusion. For the experiments with propanol at 348.15 K, the ratio $D_{AB} L/\bar{u} R^2$ was 240 for propene, 200 for propane, 150 for ammonia, and 370 for carbon dioxide. At 298 K, for the same solvent, the ratio was 178 for propene, 134 for propane, 84 for ammonia and 235 for carbon dioxide.

4. Coiling Effects

Taylor's solution which resulted in equations (4.21) and (4.22) was for a straight tube. Because this is not practical for long lengths of tubing it is necessary to either shape the tubing into a helical form (Nunge et al., 1972; Pratt and Wakeham, 1974, 1975; Alizadeh et al., 1980) or into a U-shape (Ouano, 1972; Ouano and Carothers, 1975). Nunge et al. studied the two additional but opposing modes of mass transport that need to be considered for helical (curved) systems. Nunge et al. (1972) analytical treatment of dispersion in curved tubes using the velocity distribution of Topakoglu (1967) resulted in the observation of the two competing mechanisms. For curved tubes, the fluid travels different path lengths at different radial positions (fluid flowing near the outside wall travels a farther distance than that near the inside wall), with an associated disturbance of the true laminar flow profile and the increase in the variation in residence time across the flow when compared with straight tubes. The net effect results in an increase in the dispersion coefficient. Curved tubes also create secondary flow due to transverse mixing of the fluid and this has the effect of decreasing the dispersion coefficient. Nunge et al. (1972) demonstrated that the relative importance of these two effects are dependent on the Reynolds number: as the Reynolds number increases, the dispersion coefficient first increases and then decreases. The mechanisms contributing to the variation of the dispersion coefficient with Reynolds number are the asymmetric axial velocity distribution which tends to increase the dispersion coefficient and the secondary flow which decreases it. The secondary flow effect in the diffusion tube as a result of the circular path of the fluid is one of the greatest potential sources of error. This implies that it would be prudent to ensure the solvent flow rate is low and that the ratio of the coil radius, R_c, to the inside radius of the tube, R, be large. If the ratio of R_c/R is large this suggests that the curvature of the tube is more closely approximating a straight tube with a laminar parabolic velocity profile as in Taylor's model. Also since secondary flows are more likely to occur at higher Reynolds numbers it is good experimental practice to keep the velocity of flow as low as possible.

The resulting effect of these two mass transport mechanisms is that equation (4.22) must be corrected for coiling effects:

$$K = D_{AB} + \frac{\bar{u}^2 R^2 [1 + 192 f(\phi, Re, Sc)]}{48 D_{AB}} \qquad (4.47)$$

In equation (4.47) the correction term f is an expression involving the radius ratio:

$$\phi = R_c / R \tag{4.48}$$

The other terms used in equation (4.47) are as follows: Reynolds number:

$$N_{Re} = 2\bar{u}R\rho/\eta \tag{4.49}$$

Schmidt number:

$$N_{Sc} = \eta/\rho D_{AB} \tag{4.50}$$

Dean number:

$$N_{De} = N_{Re}\phi^{-1/2} \tag{4.51}$$

It has been found experimentally that the observed variance for liquid systems, $\sigma^2 (= 2K t_R)$, is inversely proportional to the diffusion coefficient and thus the first term of equation (4.47) can be ignored and expressed in terms of the true variance for a curved tube:

$$\sigma^2 = \frac{\bar{u}^2 R^2 [1 + 192 f(\phi, Re, Sc)]}{48 D_{AB}} \tag{4.52}$$

Thus, the apparent or experimentally observed diffusion coefficient, $D_{AB,obs}$, can be calculated from the following expression for the diffusion in a straight tube:

$$\sigma^2 = \frac{\bar{u}^2 R^2}{48 D_{AB,obs}} \tag{4.53}$$

The ratio of the deviation between the apparent and true diffusion coefficients to the apparent diffusion coefficient is given by:

$$(D_{AB,obs} - D_{AB})/D_{AB,obs} = -192 f(\phi, Re, Sc) \tag{4.54}$$

The expression for the function f which was obtained by Nunge et al. (1972) tends to zero at low Reynolds numbers and showed excellent fit with experimental data. Nunge et al. (1972) found that for their experimental setup under specific operating conditions for dispersion times > 3000 seconds, the function f was approximately zero and thus could be neglected. Both Nunge et al. (1972) and Golay (1979) obtained approximate analytical solutions for a curved tube as applied to Taylor's

method. Although the Nunge et al. (1972) solution is more accurate than that of Golay (1979) neither solution is accurate enough to be used to determine the diffusion coefficients. Both approximate solutions suggest that it would be better to use the results to establish operating conditions to ensure that the effect of tube curvature is negligible or has little effect on the true value of the experimental results, rather than to redefine Taylor's solution for curved tubes. The operating conditions for ensuring that the solvent flow rate is low and that the ratio of the coil diameter, R_c, to the inside diameter of the tube, R, should be relatively large are therefore essential.

For the purpose of using the analytical solutions to define operating conditions, Atwood and Goldstein (1984) using the solutions of Nunge et al. (1972) and Golay (1979) showed that both solutions could be approximated by the following form:

$$\frac{D_{AB,obs}}{D_{AB}} = \frac{1}{1 - \alpha(Q/Q_{trans})^4} \tag{4.55}$$

In the equation $\alpha = 0.184$ for Golay's solution and $\alpha = 0.1034$ for Nunge's solution. The apparent or experimentally determined diffusion coefficient, $D_{AB,obs}$, is that observed using Taylor's solution for a straight tube. The variable Q_{trans} was defined by Golay (1979) as the transition flowrate in a curved tube above which the dispersion effects due to secondary flows become significant. The transition flowrate was defined by the following expression:

$$Q_{trans} = (518 R R_c D_{AB} \eta / \rho)^{1/2} \tag{4.56}$$

Figure 4.2 shows a plot of equation (4.56) where the ratio of the diffusivities and the flowrates are plotted for the Nunge and the Golay solutions. As indicated in the plot, it is important to choose the correct flowrate to avoid erroneous diffusion coefficients.

Atwood and Goldstein (1984) suggest that the Nunge criterion should be used as the upper bound for the effects of secondary flow. They found using experimental data for several solute-solvent systems, that all of the data fell to the right of both curves in Figure 4.2 indicating that both criteria were too stringent and thus limited the velocity of flow to a much lower flow than the experimentally determined values. Also at any one particular flowrate, the ratio of the calculated to the true diffusivity was larger than the experimentally determined values. They found however that the

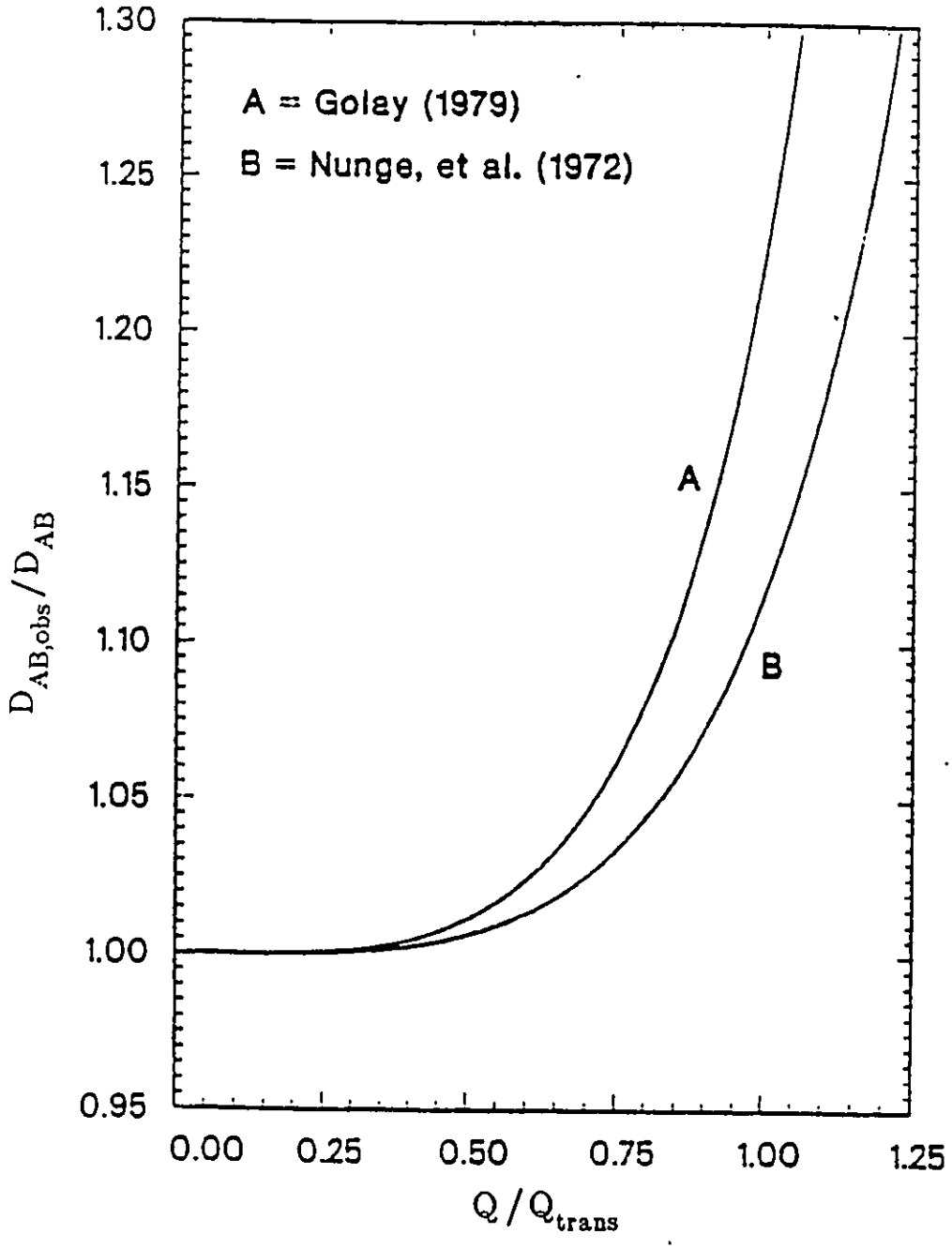

Figure 4.2: Effect of Tube Curvature on the Calculated Diffusion Coefficients

Nunge criterion fit the data well for $Q/Q_{trans} < 1$.

Thus using Atwood and Goldstein's (1984) method, flowrates of 0.08 to 0.16 mL/min in a tube having a diameter of 0.00076 m were used to calculate the percentage deviation in diffusivity due to secondary flows for all combinations of solvents and flow rates. The flow rates actually used were chosen to ensure that the effects of secondary flow were kept to a minimum. The largest deviation was 0.6% for the solvent methanol at 348.15 K. For the solvent methanol at 348.15 K, the estimated errors ranged from 0.37% for ammonia, 0.06% for propane, and 0.6% for carbon dioxide at the flowrate of 0.16 mL/min. At 298.15 K, the estimated errors ranged from 0.02% for ammonia, 0.04% for propane and 0.07% for carbon dioxide at a flowrate of 0.08 mL/min. Whereas the solvent methanol at 348.15 K showed the largest deviation, propanol showed the smallest deviation. For propanol at 348.15 K, the estimated errors ranged from 0.03% for propene, 0.045% for propane, 0.08% for ammonia, and 0.01% for carbon dioxide at 0.13 mL/min. At 298.15 K, the estimated errors ranged from 0.003% for propene, 0.005% for propane, 0.015% for ammonia, and 0.002% for carbon dioxide at 0.08 mL/min. Thus it can be concluded that the error due to coiling effects is dependent on the temperature and the solute used but that it is negligible for the selected, low flowrates.

Alizadeh et al. (1980) also defined conditions for which the effect of secondary flows would be negligible and which lead to results essentially identical to those of Atwood and Goldstein (1984). These are:

$$N_{De}^2 N_{Sc} \leq 20 \tag{4.57}$$

for the range of ϕ, $100 \leq \phi \leq 500$ with $\phi = R_c/R = 276$ and the percentage deviation from the true diffusion coefficient of approximately 10%. Several calculations were made and it was found that for a value of the parameter $N_{De}^2 N_{Sc} < 20$, the percentage deviation from the true diffusion coefficient was approximately equal to the one obtained by Atwood and Goldstein (1984).

The effect of increasing the flowrate (or decreasing the retention time) on the observed diffusion coefficient was examined by many researchers (Wong, 1989, Matthews, 1986 and Rodden, 1988). They observed that as the retention time decreased the experimentally obtained diffusivity increased well above the true value. Thus for flowrates below a certain value there is no change in the observed diffusivity and it is at these flowrates that the experiments should be performed to

minimize errors. This was also used in this study as a means of determining the choice of flowrates. Experiments were performed for the solvents and solutes in this study and the same trend was observed. It can be concluded that the laminar flow criterion and the coiling effects define the upper limit of the velocity of flow of the solvent, and that the axial diffusion criterion defines the lower limit of the velocity.

Alizadeh et al. (1980) found that for the proper design and operation of the Taylor dispersion apparatus, the necessary corrections result in a total combined error of only 0.5% in the diffusivity measurements.

As part of the calculations for determining the operating conditions, the design criteria was evaluated for each experiment and it was verified that the operating conditions were within the necessary limits. Another reason for checking the design criteria is that the diffusivity does vary with temperature and possibly because of the solute-solvent interactions. Pratt and Wakeham (1974, 1975b) found that the percent error in repetitive measurements of diffusion coefficients was about 2.5%. Grushka and Kikta (1976) observed a precision between 1 and 3% depending on the system studied. A large portion of the experimental error lies in the determination of the variance (Pratt and Wakeham, 1974, Ouano and Carothers, 1975, and Pratt and Wakeham, 1975).

CHAPTER 5

EXPERIMENTAL METHOD

5.1 Properties of Materials

The physical properties of the solutes and solvents used in this study are tabulated. Tables 5.1A and 5.1B are a summary of the properties of the solvents methanol, ethanol, propanol and butanol. Tables 5.1C and 5.1D are a summary of the properties of the solutes carbon dioxide, propane, propene and ammonia. The specified purities of these substances were at least 99%. The solvents were obtained from the Aldrich Chemical Company and the solutes were obtained from Air Products.

5.2 Apparatus and Procedure

The diffusivities of the each of the solutes gases propene, propane, carbon dioxide and ammonia were measured in each of the solvents methanol, ethanol, 1-propanol, and 1-butanol at temperatures of 298.15K, 323.15K, and 348.15K and pressures of approximately 0.1, 3.5, 7.0, 10, and 14 MPa. The densities of the solvents were also measured at the operating conditions given above. Preliminary viscosity measurements were done on the solvents methanol and ethanol at 298.15, 323.15 and 348.15 K and pressures up to 14 MPa. The apparatus used in this study was based on Taylor's dispersion phenomenon.

The Taylor dispersion apparatus is discussed by Matthews (1986), and Akgerman and Gainer (1972b). In this chapter, the design and operation of the original apparatus are reviewed along with the modifications made to the apparatus to improve its performance.

The essential features of the Taylor dispersion technique consist of injecting a pulse of dilute solution into a stream of solvent in laminar flow in a long capillary column. The extent of the dispersion of the pulse in the column is related to the diffusion coefficient. The important assumptions of Taylor which finally led to the application of the dispersion equations include: (1) the injected pulse is of negligible width, (2) the centre of gravity of the peak moves with the mean velocity of flow, (3) a laminar velocity profile is obtained, and (4) axial diffusion is negligible. Accord-

Table 5.1A

Physical Properties of Methanol and Ethanol
(Daubert and Danner, 1985)

PROPERTY	UNITS	METHANOL	ETHANOL
Molecular Weight, M.W.	$kg \cdot kmol^{-1}$	32.042	46.069
Critical Temperature, T_c	K	512.58	516.25
Critical Pressure, P_c	Pa	8.0959×10^{6}	6.3835×10^{6}
Critical Volume, V_c	$m^3 \cdot kmol^{-1}$	0.11780	0.16692
Critical Compress. Factor, Z_c		0.224	0.248
Melting Point, M.P.	K	175.47	159.05
Triple Point Temperature, T_{tp}	K	175.59	159.05
Triple Point Pressure, P_{tp}	Pa	1.0768×10^{-1}	7.1775×10^{-4}
Normal Boiling Point, T_b	K	337.85	351.44
Liquid Molar Volume, V at T_b	$m^3 \cdot kmol^{-1}$	0.040691	0.058515
Heat Fusion at Melt. Point, ΔH_m	$J \cdot kmol^{-1}$	3.2049×10^{6}	5.0124×10^{6}
Acentric Factor, ω		0.5656	0.6371
Radius of Gyration, R_B	m	1.5520×10^{-10}	2.2590×10^{-10}
Solubility Parameter	$(J \cdot m^{-3})^{1/2}$	2.9619×10^{4}	2.6421×10^{4}
Dipole Moment	$C \cdot m$	5.6706×10^{-30}	5.6372×10^{-30}
van der Waals Volume, V_{VDW}	$m^3 \cdot kmol^{-1}$	0.02171	0.03194
van der Waals Area, A_{VDW}	$m^2 \cdot kmol^{-1}$	3.5800×10^{8}	4.9300×10^{8}
Refractive Index at T=298.15K		1.3265	1.3594

Table 5.1B

Physical Properties of Propanol and Butanol
(Daubert and Danner, 1985)

PROPERTY	UNITS	PROPANOL	BUTANOL
Molecular Weight, M.W.	$kg \cdot kmol^{-1}$	60.096	74.122
Critical Temperature, T_c	K	536.71	562.93
Critical Pressure, P_c	Pa	5.1696×10^{6}	4.4127×10^{6}
Critical Volume, V_c	$m^3 \cdot kmol^{-1}$	0.21853	0.27453
Critical Compress. Factor, Z_c		0.253	0.259
Melting Point, M.P.	K	146.95	183.85
Triple Point Temperature, T_{tp}	K	146.95	184.51
Triple Point Pressure, P_{tp}	Pa	6.5112×10^{-7}	6.3772×10^{-4}
Normal Boiling Point, T_b	K	370.35	390.81
Liquid Molar Volume, V at T_b	$m^3 \cdot kmol^{-1}$	0.074939	0.091943
Heat Fusion at Melt. Point, ΔH_m	$J \cdot kmol^{-1}$	5.1965×10^{6}	9.3722×10^{6}
Acentric Factor, ω		0.6279	0.5945
Radius of Gyration, R_B	m	2.8250×10^{-10}	3.2510×10^{-10}
Solubility Parameter	$(J \cdot m^{-3})^{1/2}$	2.4557×10^{4}	2.3289×10^{4}
Dipole Moment	C · m	5.6039×10^{-30}	5.5372×10^{-30}
van der Waals Volume, V_{VDW}	$m^3 \cdot kmol^{-1}$	0.04217	0.05240
van der Waals Area, A_{VDW}	$m^2 \cdot kmol^{-1}$	6.2800×10^{8}	7.6200×10^{8}
Refractive Index at T=298.15K		1.3837	1.3971

Table 5.1C

Physical Properties of Carbon Dioxide and Propane
(Daubert and Danner, 1985)

PROPERTY	UNITS	CARBON DIOXIDE	PROPANE
Molecular Weight, M.W.	$kg \cdot kmol^{-1}$	44.010	44.096
Critical Temperature, T_c	K	304.19	369.82
Critical Pressure, P_c	Pa	7.3815×10^6	4.2492×10^6
Critical Volume, V_c	$m^3 \cdot kmol^{-1}$	0.09400	0.20288
Critical Compress. Factor, Z_c		0.274	0.280
Melting Point, M.P.	K	216.58	85.46
Triple Point Temperature, T_{tp}	K	216.58	85.44
Triple Point Pressure, P_{tp}	Pa	5.1351×10^5	2.0744×10^4
Normal Boiling Point, T_b	K	-	231.11
Liquid Molar Volume, V at T_b	$m^3 \cdot kmol^{-1}$	0.037417	0.075642
Heat Fusion at Melt. Point, ΔH_m	$J \cdot kmol^{-1}$	9.0190×10^6	3.5238×10^6
Acentric Factor, ω		0.2276	0.1517
Radius of Gyration, R_B	m	1.0400×10^{-10}	2.4310×10^{-10}
Solubility Parameter	$(J \cdot m^{-3})^{1/2}$	1.4564×10^4	1.3091×10^4
Dipole Moment	C·m	0.0	0.0
van der Waals Volume, V_{VDW}	$m^3 \cdot kmol^{-1}$	0.01970	0.03757
van der Waals Area, A_{VDW}	$m^2 \cdot kmol^{-1}$	3.2300×10^8	5.5900×10^8
Refractive Index at T=298.15K		1.0004	1.2898

Table 5.1D

Physical Properties of Propene and Ammonia
(Daubert and Danner, 1985)

PROPERTY	UNITS	PROPENE	AMMONIA
Molecular Weight, M.W.	$kg \cdot kmol^{-1}$	42.080	17.030
Critical Temperature, T_c	K	364.76	405.65
Critical Pressure, P_c	Pa	4.6126×10^6	1.1278×10^7
Critical Volume, V_c	$m^3 \cdot kmol^{-1}$	0.18100	0.07247
Critical Compress. Factor, Z_c		0.275	0.242
Melting Point, M.P.	K	87.90	195.41
Triple Point Temperature, T_{tp}	K	87.90	195.41
Triple Point Pressure, P_{tp}	Pa	9.1812×10^{-4}	6.1177×10^3
Normal Boiling Point, T_b	K	225.43	239.72
Liquid Molar Volume, V at T_b	$m^3 \cdot kmol^{-1}$	0.068802	0.024993
Heat Fusion at Melt. Point, ΔH_m	$J \cdot kmol^{-1}$	3.0029×10^6	5.6568×10^6
Acentric Factor, ω		0.1424	0.2520
Radius of Gyration, R_B	m	2.2540×10^{-10}	$8.5330\,10^{-11}$
Solubility Parameter	$(J \cdot m^{-3})^{1/2}$	1.3152×10^4	2.9217×10^4
Dipole Moment	$C \cdot m$	1.2208×10^{-30}	4.9034×10^{-30}
van der Waals Volume, V_{VDW}	$m^3 \cdot kmol^{-1}$	0.03408	0.01380
van der Waals Area, A_{VDW}	$m^2 \cdot kmol^{-1}$	5.0600×10^8	2.4500×10^8
Refractive Index at T=298.15K		1.3625	1.3250

ingly, the mathematical model of Taylor shows that the concentration profile which is detected at the end of the column by a Differential Refractometer, in the case of my equipment, is a Gaussian-shaped curve with the variance related to the diffusion of the solute in the solvent. Thus, consideration of the theory of Taylor dispersion shows that the most important experimental features are maintaining a steady, laminar flow, injection of a sample pulse, maintaining a constant temperature and pressure in the dispersion tube and the detection of the response peak. High pressures were obtained by throttling the flow at the discharge end of the capillary tubing with a needle valve. Pressure was measured using a transducer. Constant temperature of the capillary column was obtained by immersing the coiled column in a water bath. The coiled column which is known as the dispersion column, consisted of 34.0 m of capillary tubing of outside diameter 15.9×10^{-4} m and inside diameter 7.60×10^{-4} m. The dispersion column was wound into a coil of radius 0.105 m. The capillary tubing used for the entire experimental setup was made of stainless steel.

A schematic diagram of the apparatus is given in Figure 5.1. The details of the operation will now be presented. After the feed tank was filled with the desired solvent, the solvent was degassed with helium to remove any volatile impurities including absorbed moisture. A stirrer was also used in the feed tank to assist in the distribution of helium throughout the solvent, which was maintained at room temperature. The solvent was slowly and continuously degassed during the entire experiment. The degassed solvent was pumped from the reservoir by a dual-piston, metering pump via the capillary tubing which had an internal diameter of 7.6×10^{-4} m, to the pulse damper. The LDC CM3200 pump was designed for precise solvent delivery from 10 μL to 10 mL/min with a flow rate precision of 0.3% to guarantee reproducible peak retention times. Flow rates which were used ranged from 0.07 to 0.12 mL/min. The pulse damper (SSI model LP-21 LO-Pulse) was installed to reduce pressure pulsations from the pump. Three on-line filters, of pore sizes 2 and 0.5 micron were used to remove any particles that were present. The 2 micron filter was placed upstream of the pump and the other two filters were situated immediately after the pump. The solvent, after flowing through the filters, was divided into two streams by means of a three-way valve. One portion of the solvent stream was sent to the reference side of the Differential Refractometer. The other portion of the solvent stream was pumped to the temperature controlled water bath, which controlled the temperature to ± 0.01 K and contained the conditioning columns for the capillary viscometer, the capillary viscometer column, and the dispersion column. The

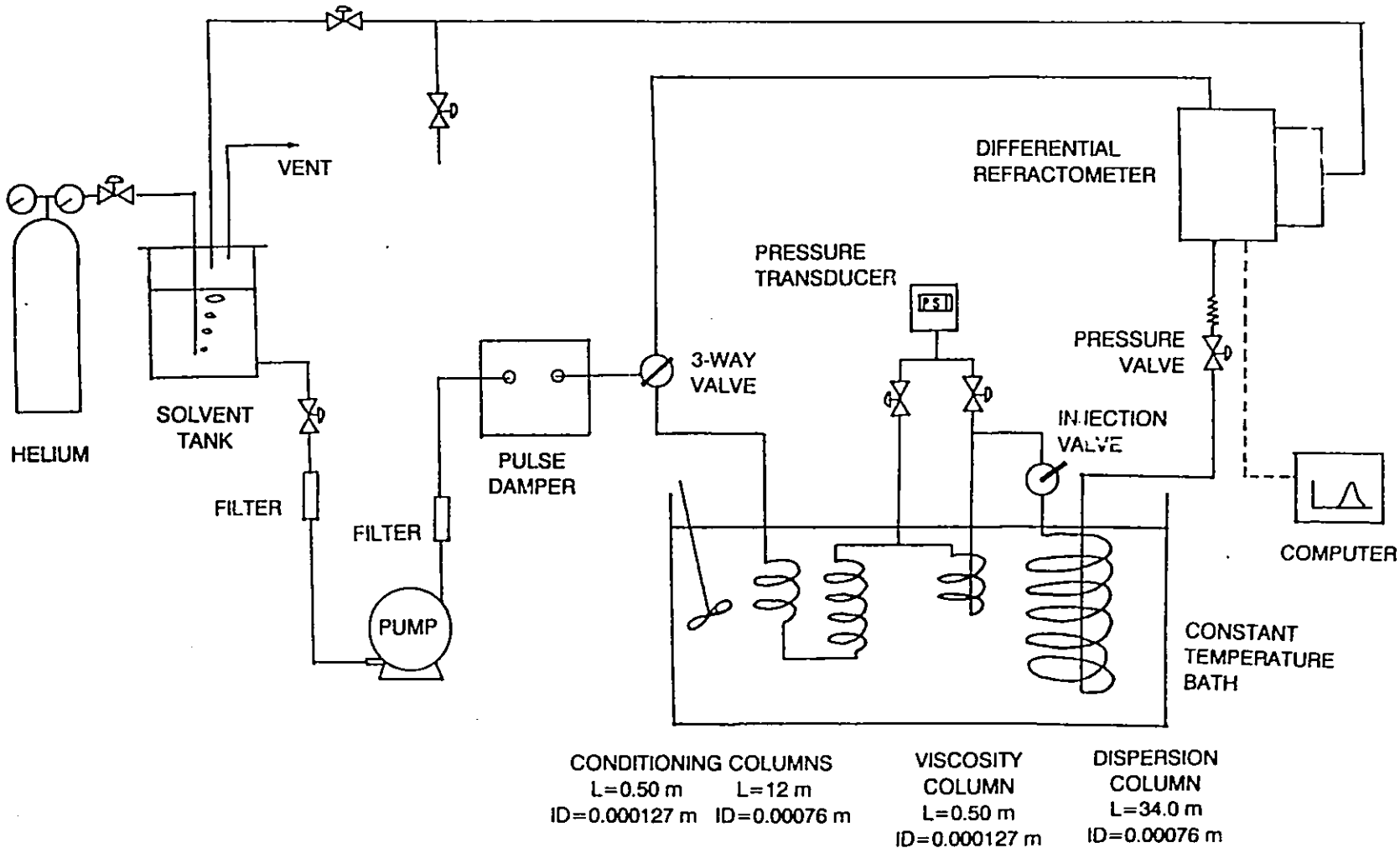

Figure 5.1: Schematic Diagram of Taylor Dispersion Apparatus

conditioning columns, one of length L = 0.50 m, and internal diameter 12.7×10^{-5} m and the other of L = 12 m and internal diameter 7.6×10^{-4} m served the purpose of preheating the solvent before it flowed into the capillary viscometer. A calibrated Viatran differential pressure transducer was installed across the 0.50 m long viscosity column of internal diameter 12.7×10^{-5} m, to measure the pressure drop across this length of column. The values of ΔP could then be used to obtain the viscosity of the solvent using the Hagen-Poiseuille equation. The solvent was allowed to flow to the Reodyne Model 7125 syringe loading sample injection valve. The sample loop of the injection valve had a volume of 2.0×10^{-8} m^3. A solution of approximately 5 mole percent solute was prepared separately by weighing the solvent initially and then bubbling the appropriate quantity of solute gas through and partially saturating the solvent. This prepared sample of a dissolved gas in the solvent was then injected into the sample loop ensuring that the loop was filled completely. The solute pulse then flowed to the dispersion column. The dispersion column was supported in the water bath so as to provide a minimum hindrance to the circulation of water. An average retention time for these experiments was approximately 3 hours. Thus after approximately 3 hours from the time of injection, the solution containing the injected pulse passed through a fine metering valve. The metering valve provided a constriction for control of the pressure of the system of up to 20 MPa. A high pressure transducer was installed upstream of the injection valve to measure the upstream pressure which was also considered to be the pressure at which the experiment took place since the pressure loss in the capillary column at the low flow rates used was negligible. The dispersed solute in the solvent was then allowed to flow to the sample side of the refractive index detector where a signal was produced. The voltage signal produced by the detector was proportional to the difference in the refractive indices of the pure solvent in the reference cell and the solution in the sample cell which in turn was proportional to the concentration of the sample. The temperature in the detector cell was maintained at 303 K with a circulating water bath for all the experiments. The concentration profile was initially monitored by a chart recorder but was later monitored by a computer. The linearity test for the differential detector was performed according to the instructions in the operating manual before the actual diffusivity experiments were initiated (Appendix A). After leaving the detector, the solvent was either recirculated to the feed tank through one valve or diverted through another valve for mass flow rate measurements. A tee

placed just upstream of the feed tank allowed for possible diversion of solvent to an external container. By weighing the container before and after the collection of the solvent, and recording these values along with the time for collection of the solvent, the mass flow rates for density and viscosity measurements were obtained. The mass of solvent collected was timed for approximately one retention time of one of the peaks. The exact retention time for this peak was also necessary in the calculation of the density and viscosity. The differential pressure required for the viscosity measurement was also recorded by the computer. The continuous re-circulation ensured that the solvent was continuously being degassed which thus facilitated the continuous collection of data.

The Taylor dispersion experiment was automated for data acquisition by means of a computer. The computer was interfaced both to the detector and the differential pressure transducer. The voltage signals from these instruments were monitored and data were stored for selected periods of operation. After a series of experiments, all calculations were performed by means of the computer. Chapter 6 examines the data handling and computational analysis in more detail. For their calculation, the diffusivities, viscosities and densities all required the retention time, t_R, which was also obtained from the collected data. It should be noted that for each solvent, the retention time used in the calculation of the diffusivity was the retention time of each individual peak for each solute while the retention time used in the calculation of the density and viscosity was the retention time of one of the peaks. For a particular solvent, temperature and pressure, the data was continuously collected for all the solutes examined in this study. Two or three sample pulses were injected in series at approximately one hour time intervals for each solute. All of the response curves for all of the solutes at one operating condition were collected together. After all the data for one solvent and for all the different solutes were collected, the effect of pressure on the diffusivity along with the effect of pressure on the densities and viscosities of the solvents at the three temperatures were calculated. This was repeatedly done for all of the solvents examined. This resulted in a rapid accumulation of data.

5.2.1 MODIFICATIONS TO THE ORIGINAL APPARATUS

The Taylor apparatus, originally constructed by Wong (1989), was modified before the data were collected. The modifications will now be described.

The pre-heat tubing upstream of the capillary viscometer, the capillary viscometer and the valves to allow for the measurement of mass flow rate for the determination of density were added. The pre-heat tubing serves two purposes. Its major function is to preheat the solvent to the operating temperature before measurements were begun. It also dampened out pressure fluctuations upstream of the diffusion column resulting in the operating pressure being almost constant. Previously, pressure variations as large as 1.2 MPa (200 psi) were observed. The equipment was also modified to obtain the density and viscosity of the solvents at all operating conditions. This was done by diverting the recycled solvent stream to an external vessel so that the mass flow rate, and subsequently the density and viscosity could be obtained. Another modification was the installation of a data acquisition system, LabMaster, and the interfacing of the differential refractometer and the differential pressure cell for the measurement of viscosity with LabMaster through the use of an analog-to-digital converter. This allowed collection of voltage-time data which was stored by means of an IBM computer. A new procedure was also initiated. During the experiment, a series of sample pulses for all the solutes in one solvent, at one temperature and one pressure were injected so that several response curves could be obtained approximately one hour apart. This allowed for rapid accumulation of diffusivity data. This method of collection of data ensured greater accuracy and reliability than other methods used to obtain diffusivity as well as a high efficiency in obtaining data.

CHAPTER 6

DATA HANDLING AND COMPUTATIONAL ANALYSIS

The basic data for determining the molecular diffusivities consisted of a continuous analysis of the effluent from the dispersion tube, and the controlled values of the pressure, temperature and flow rate of solvent through the tube. It is the data from the continuous analyzer, generated as a variable voltage, that is best handled using a computer. The reason is that many (about one hundred and fifty) values of the analyzer voltage readings are required to obtain a well-defined normal distribution curve which can be suitably described by the parameters discussed earlier in Chapter 5. It is also necessary to obtain an accurate value for the average residence time of a solute pulse. It is apparent therefore, that a computer is most useful for recording the injection times, collecting all the nearly constant analyzer output data during a period of up to six hours and including, finally, the Gaussian dispersion curve which is obtained in a time period of about twenty minutes. The function of the computer programs is then to detect any drift of the analyzer data, to detect any injections, to detect any upward or downward shifts in the baseline, to detect the onset of the dispersion curve, to fit statistically the best parameters to the particular Gaussian curve, as well as finally to calculate the diffusion coefficient in each case. The major emphasis of these experiments was to obtain the diffusivities. Density and viscosity values were also calculated from the logged data. The methodology for storing and handling the data by means of the computer will be briefly discussed in this chapter. Injection times and baseline shifts are also manually recorded on paper as a precautionary measure.

The data from each run are saved in three files by the data acquisition system. The SETUP file contains data that are not required for processing the data such as the frequency that the readings are recorded. In this case, the signal from the differential refractometer is saved in a file called CHANNEL.0. Also the signal from the differential pressure transducer is saved in a file called CHANNEL.1. A series of two programs is then used to analyze the logged data.

The first program, PROGRAM 1, begins the analysis of each individual run using the logged data. This program which generates three text files checks for

injections, baseline shifts and searches for and selects the peak data. It first reads the SETUP and CHANNEL.0 files and creates a temporary data file, the TMP file, in which matching times and voltages are stored for all the data from the run. The data from this temporary data file is useful for referring to after the run but is replaced each time the program is initiated. Each individual run contains the logged data for all of the solutes in one solvent at one temperature and pressure.

The voltage change produced during an injection is shown in Figure 6.1. An upward change in the baseline voltage is shown in Figure 6.2. To identify whether an injection or a baseline shift occurs, a linear regression is performed with ten data pairs (50 s to 140 s in Figure 6.1) and the voltage of the next data point (150 s) is estimated by extrapolation. If the recorded voltage exceeds or falls short of this estimated value by more than a given amount, usually 0.35 V and termed "delta" in the program, then an injection or a change of baseline is assumed to have occurred. To identify an injection, the voltage at the seventh data point after the last one in the regression analysis (210 s) is compared to the predicted value using the linear regression. If the voltage difference is less than 'delta' then an injection is considered to have occurred, otherwise a change in the baseline voltage is said to have occurred. In the case that an injection is identified, an injection time is recorded. The data surrounding the injections and baseline shifts are stored in the ABV file. This file is useful as a means of checking for extraneous injections which occur frequently and is thus used to ensure that the correct values are being used.

The first program which also selects the data to be used for the curve-fitting regression analysis of the peak, identifies the beginning of a peak by comparing the slopes of successive groups of data taking ten points at a time as shown in Figure 6.3. The beginning of a peak is identified by finding four consecutive groups of data for which the slope is increasing. The data is saved in the RLT file for analysis by the second program, PROGRAM 2. Thus the RLT file is a brief summary of the data from the files produced previously, and is necessary for completing the analysis of the run. A schematic diagram of the analysis of the data so far is shown in Figure 6.4.

After checking the RLT file for errors, and adding the run temperature, downstream pressure, and mass flow rate data for the calculation of density and viscosity, the second program is run. The RLT file and the CHANNEL.1 files are used as the inputs for the second program as shown in Figure 6.5. The program utilizes a

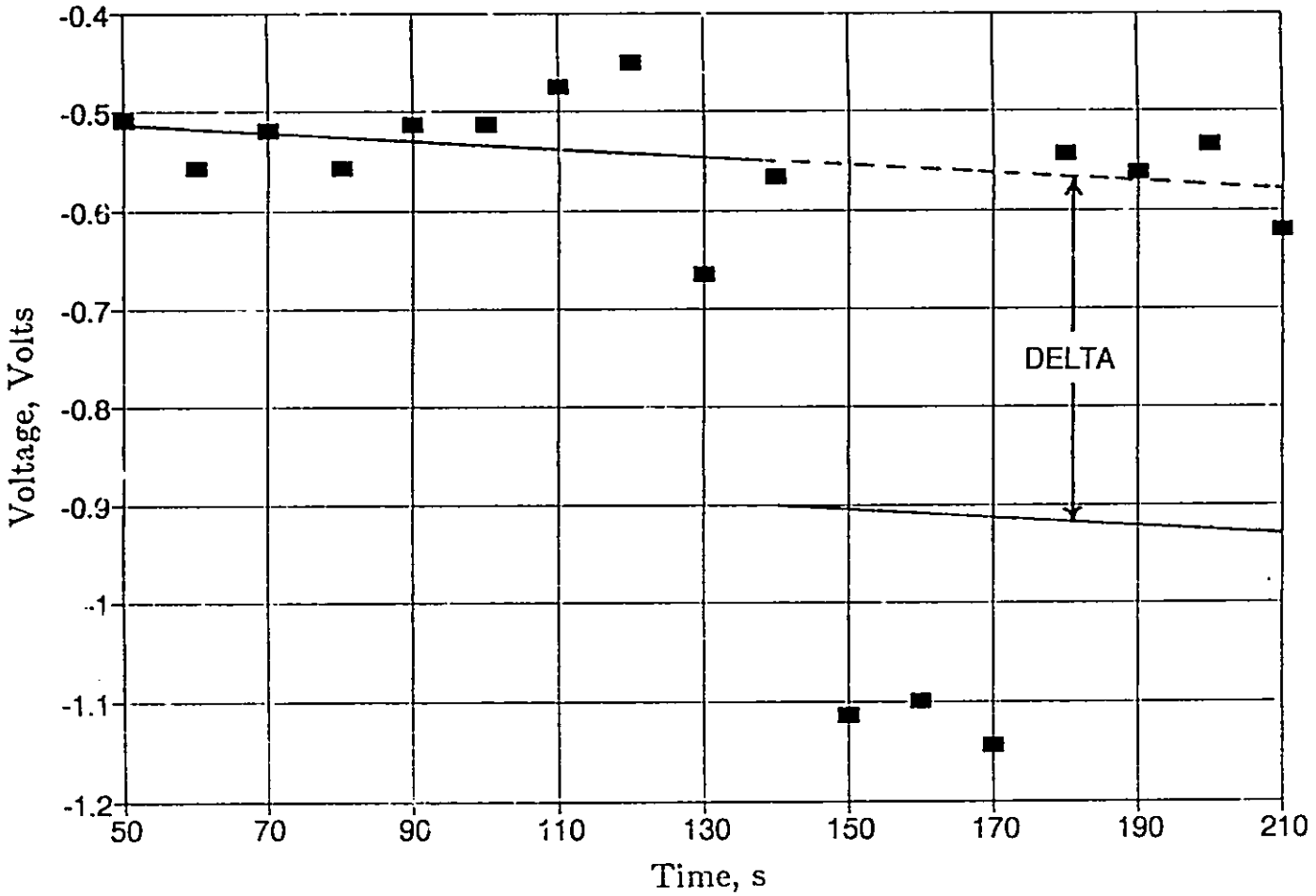

Figure 6.1: Voltage vs. Time for an Injection

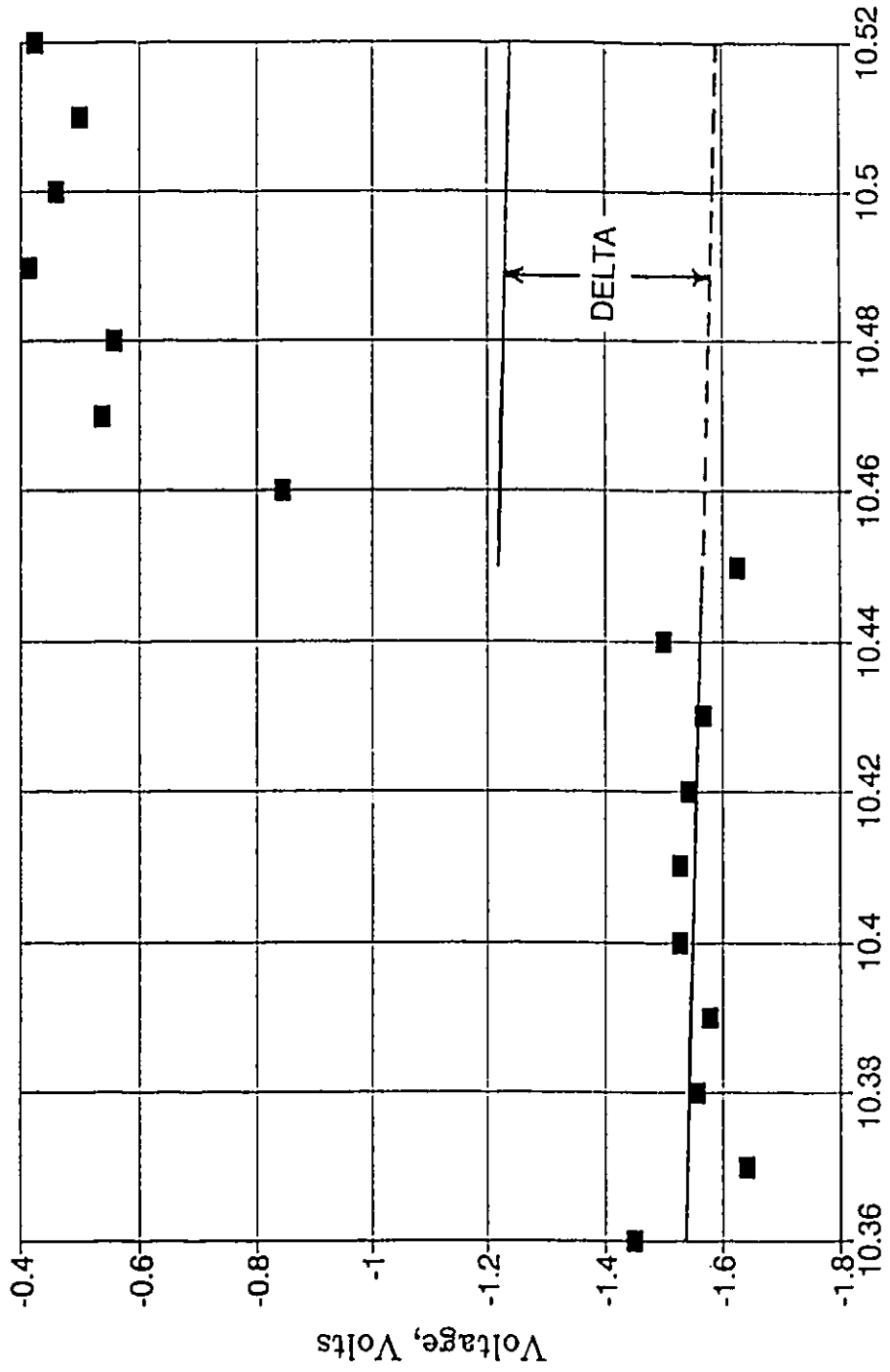

Figure 6.2: Voltage vs. Time for a Baseline Shift

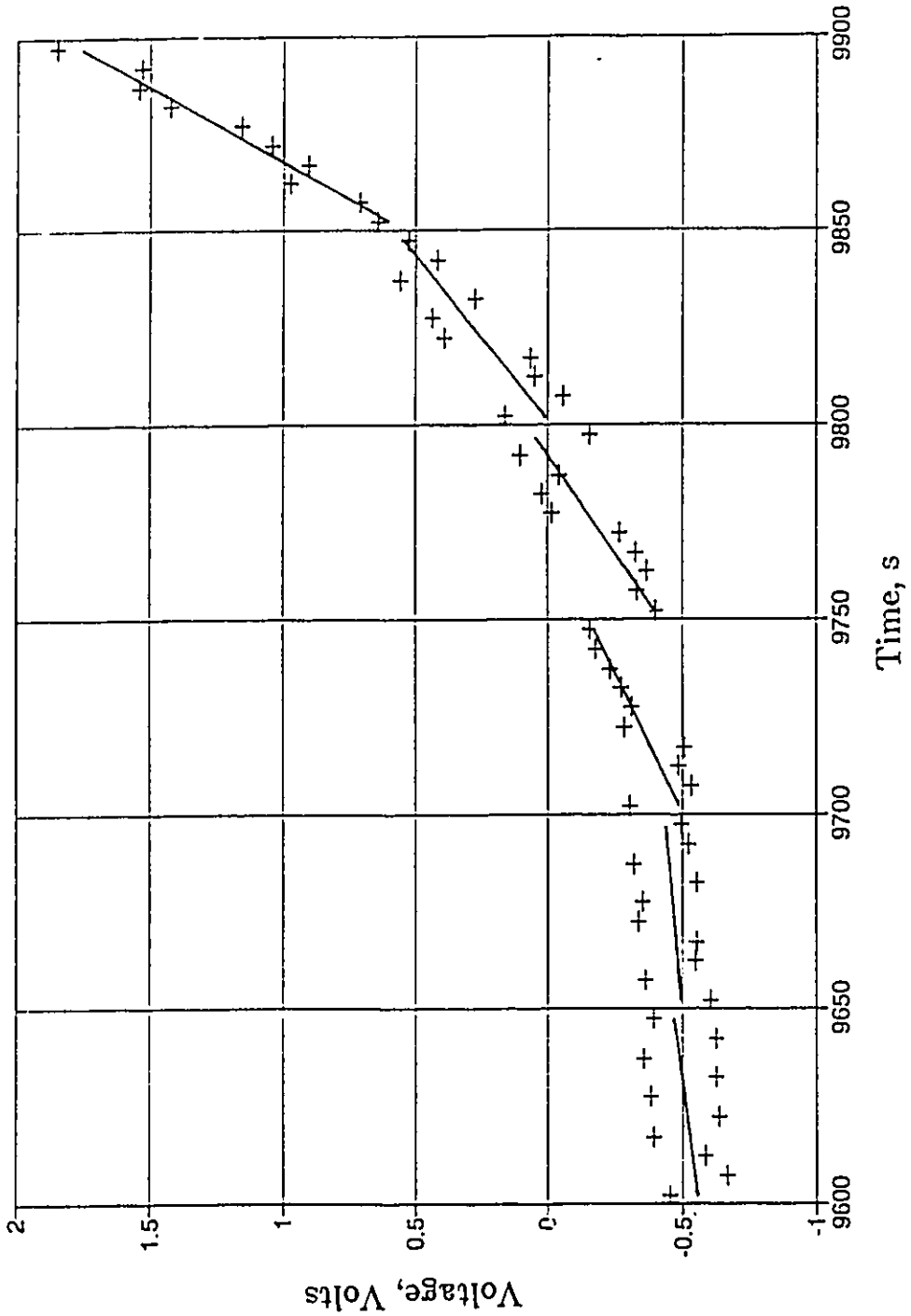

Figure 6.3: Identification of Peak Beginning

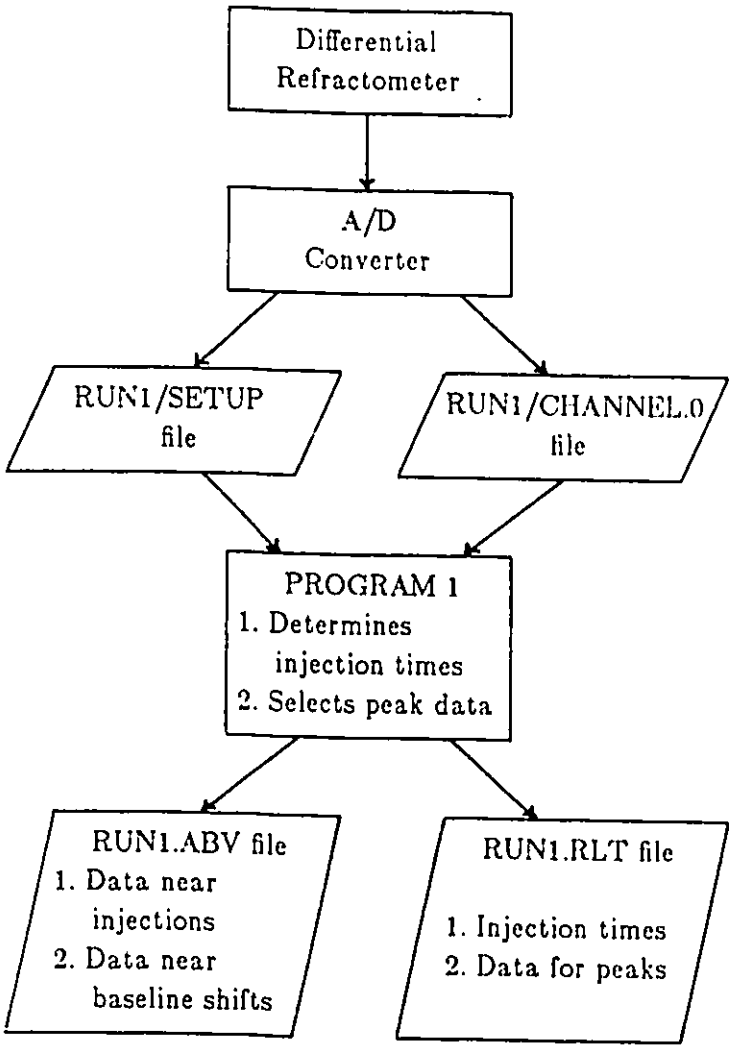

Figure 6.4: Schematic Diagram of PROGRAM 1

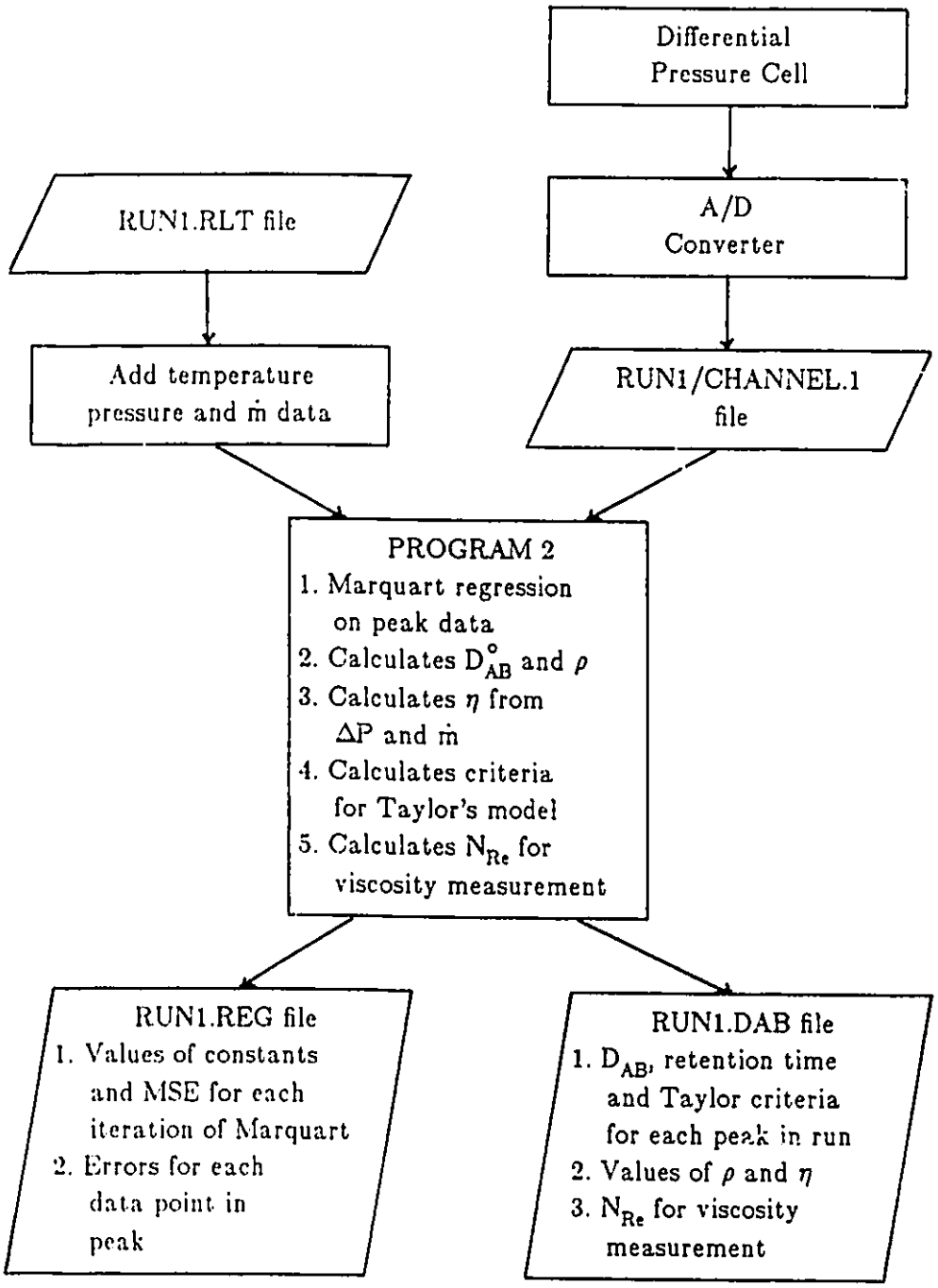

Figure 6.5: Schematic Diagram of PROGRAM 2

Marquardt regression algorithm to fit the peak data to equation (4.40) and then calculates the diffusivity utilizing Equation (4.41). Figure 6.6 shows the results of a typical curve-fitting calculation with the line representing the fitted curve, and the +'s representing the experimental points. The details of the regression analysis are saved in the REG file. This includes all the values of the constants B_1 to B_5 (intermediate and final), and the Mean Sums of Squares Error of the fit for each iteration of the regression. The REG file also contains the data showing the comparison between the actual voltage and the voltage predicted using the constants from the regression analysis for each data point in the peak. After the constants are obtained, the diffusivity for each peak can finally be calculated.

The method of obtaining the initial estimates for the regression is as follows. All of the initial estimates for all of the constants, B_1, to B_5, were generated within the program. The baseline slope, B_5, was initially estimated to be zero. The baseline drift or intercept, B_3, was estimated to be the voltage of the first point at the beginning of the peak. PROGRAM 2 searches for the maximum peak voltage, V_{max} and the retention time corresponding to this, t_R. The values, V_{max} and t_R, were then used in simple algebraic expressions to obtain the initial estimates of of B_1, B_2, and B_4. The last constant, B_4 which is the average velocity, $\bar{u}$, was estimated from the ratio of L to t_R (equation (4.1)). The estimation of B_2 was more involved than the other parameters because B_2 is equal to 4 times the Taylor's dispersion constant, K. From equation (4.22), in order to determine K, the values of D_{AB} and $\bar{u}$ (=B_4) are needed. An estimate already exists for B_4. Since very little diffusivity data exist for the systems being studied, an estimate of D_{AB} was obtained by utilizing the more approximate graphical method and equation (4.35). Equation (4.35) relates D_{AB} to retention time at the peak maximum, t_R, and the peak width at half height, $W_{½}$. Thus a computerized algorithm of the graphical method was used in PROGRAM 2 to estimate K and hence B_2. The algebraic expression for the determination of B_1 can be obtained from equation (4.40) at $t=t_R$, that is, at the maximum in the peak. Thus B_1 is the product of the square root of the retention time and the difference between the maximum peak voltage and the voltage due to baseline offset and drift ($=t_R[V_{max} - (B_3 + B_5 t_R)]$). In this case the voltage due to the baseline shift was estimated by using the average of the voltages at the beginning and the end of the peak.

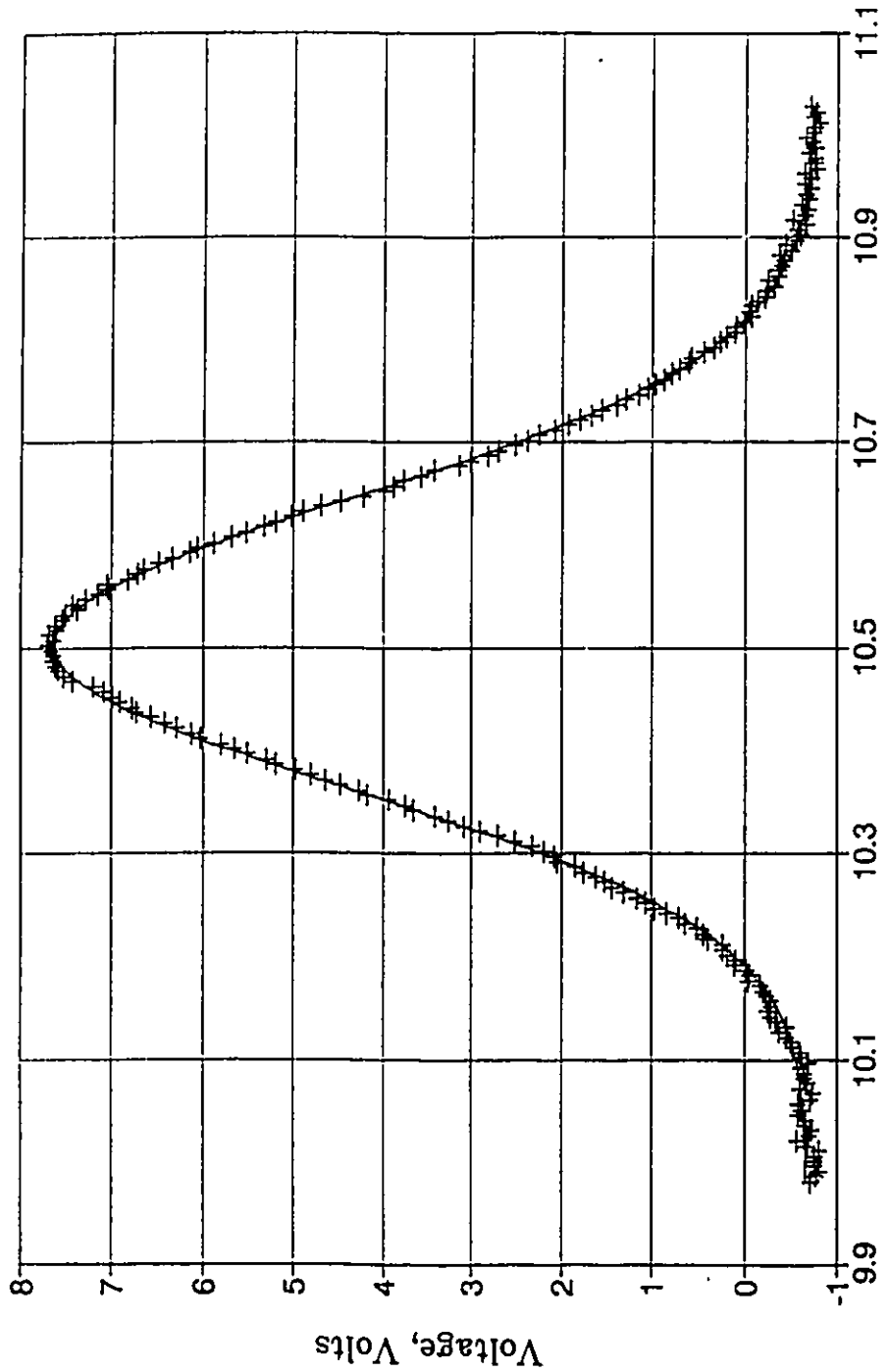

Figure 6.6: Experimental Data and Fitted Curve

The diffusivity results for each peak which includes the diffusivities, and retention times were saved in a DAB file. The density and viscosity were also calculated from the retention times and mass flow rate data using equations (4.6) and (4.10) respectively, and saved in the DAB file. The mass flow rate used in both of these calculations involved the collection of a mass of solvent over a timed interval from the point of injection to the point of elution for one of the peaks. Consequently, the retention time used in both of these calculation was for a specific peak. PROGRAM 2 is also used to check whether the criteria required for the application of the Taylor dispersion model as well as the laminar flow criteria for the viscosity measurement were satisfied. The values obtained from the equations used to check the criteria were saved in the DAB file. Thus the DAB file contained the final useful data from the regression analysis for all solutes in one solvent, at one temperature and one pressure. The diffusivities for each peak as well as the retention times and the values from the criteria for the validity of Taylor's model were listed and subsequently printed. Also the density and viscosity of the solvent were also listed, as well as the Reynolds number for the viscosity measurement.

It should be noted that for the density and diffusivity measurements, the downstream pressure at the beginning of the column is the pressure at which the experiment is said to take place, since there is very little pressure drop across the 34 m length of capillary dispersion column at a very low velocity of flow, (internal diameter $=7.6 \times 10^{-4}$ m). However, for the viscosity measurement, the experiment is said to take place at the average of the upstream and the downstream pressure. This pressure is obtained from the sum of the downstream pressure and one-half the pressure difference between the upstream and the downstream pressure, (the ΔP recorded by the computer). This pressure is used because it is a better estimate than the downstream pressure of the average pressure in the viscosity capillary since the pressure drop across this capillary is significant. A more detailed description of the calculations performed by these programs will be found in Appendix B.

CHAPTER 7

RESULTS AND DISCUSSION

7.1 Measured Densities and Diffusivities

The results for the measured densities of the solvents and the molecular diffusivities of the dilute solutes in the solvents, are examined and discussed in this section.

The measured values of density will be discussed first. The densities of methanol, ethanol, propanol and butanol as measured in this research can be found in Appendix C, Tables C.1A to C.1D, respectively, for the temperatures 298.15, 323.15 and 348.15 K and over the entire pressure range. Each value of density is the result of one measurement. Plots of density versus pressure can also be found in Appendix D, Figures D.1A to D.1D. The measured densities of the solvents are found to be in excellent agreement with those from the literature (Wilhoit and Zwolinski, 1973). Figures D.1A and D.1B show that over the entire pressure range the density of methanol is greater than the density of ethanol at 298 K. Although the difference in densities between methanol and ethanol is small, a definite trend exists. A possible explanation is that the degree of association is greater for methanol than ethanol at 298 K and this difference decreases as the temperature increases. Excluding the abnormal behaviour of methanol and ethanol at 298 K, Figures D.1A to D.1D show that the densities of the solvents increase as the pressure and the length of the carbon chain increases, and decrease as the temperature increases. This will be discussed in more detail later.

The effect of changing density on molecular diffusivity will now be discussed. For any one solvent at one temperature the increase in density with increasing pressure means that the molar volume of the solvent decreases with a consequent decrease in the free space between the molecules available for diffusion. This is considered to be true for each solvent and at each temperature. For any one solvent at a fixed pressure, the decrease in density as the temperature increases means that the molar volume increases with a consequent increase in the free space available for diffusion; if the solvent has an associating tendency as for example in short chain alcohols, it is also considered that the effect of increasing the temperature results in

a decrease in the degree of association within the solvent with a consequent increase in the molar volume. Comparing the solvents, at the same temperature and pressure, it is observed that as the chain length of the solvent molecule increases, the density increases. This is associated with an increase in the molar volume and a decrease in the free space available for diffusion.

A linear regression analysis was performed on the measured densities as given in Tables C.1A to C.1D and it was observed that, as expected, the density increases linearly with increasing pressure and decreases with increasing temperature. There is an increase in density of approximately 0.05 to 0.1% per MPa increase in pressure, and a decrease in density of 2.7 to 3.5% resulting from an increase in temperature from 298.15 to 323.15 K at 2MPa depending on the solvent used. An F-test shows that the effect of pressure on density is significant at the 95% confidence level. A similar linear trend was observed for the preliminary viscosity data. The effect of pressure on the viscosity data is summarized in Appendix J.

From the linear regression analysis, the percent increase in density as pressure increases from 2 MPa to 12 MPa was calculated as well as the slopes of the curves of density versus pressure for each temperature and solvent. These values are summarized in Table D.1. The trends observed in the measured densities as mentioned previously are also shown in Table D.1. The following observations were noted from Table D.1. For any one solvent as the temperature increases, there is an increase in the percentage change in density, and thus an increase in the change in density with pressure (slope). Because of the proportional relationship between density and molar volume, this translates to an increase in the percentage change in the molar volume as well as an increase in the change in molar volume with pressure of the solvent as the temperature increases for any one solvent. First, this shows that the increase in pressure at one temperature causes a decrease in the molar volume and hence a decrease in the free space available for diffusion. Secondly, it shows that as the temperature increases, the change and the percent change in the molar volume increases which increases the change in the free space. Thus at the higher temperatures, there is a greater influence on the reduction of the free space as the pressure increases. However it should be noted that the decrease in density with increasing temperature and the consequent increase in molar volume means that there is more free space available for diffusion at the higher temperatures. Thus for the solvent methanol for example, although the percentage change in molar volume was greater at 348 K than at 298 K the larger molar volumes at 348 K for all pressures means that there is more free space available for diffusion. This is true for all solvents.

Comparison between solvents at the same temperature and for a pressure increase from 2 to 12 MPa the following were noted as summarized in Table D.1. As the chain length of the solvent molecule increases, the percentage change in density and the change in density decreases. This is equivalent to a decrease in the percentage change in the molar volume. However, because of the increasing molecular weight of the solvents as their chain length increases, the change in molar volume also increases. Thus butanol shows the largest change in molar volume at each temperature over the pressure range and methanol the smallest. Compared to the other solvents of smaller chain lengths, butanol has the largest density and the largest molar volume at any pressure. Butanol also has the largest change in molar volume as pressure increases. This means that butanol has the largest reduction in free space as the pressure increases. Thus the effect of pressure on the free space available for diffusion increases as the chain length increases from methanol to butanol. Thus as the chain length of the solvents increases, the density and molar volume also increase. However this does not imply that as the chain length increases, the free space decreases.

The diffusion data will now be discussed. The infinite dilution diffusion coefficients of carbon dioxide, propene, propane, and ammonia in methanol, ethanol, propanol and butanol as measured in this research can be found in Appendix E, Tables E.1A to E.4C. Tables E.1A to E.1C for example contains the diffusivity-pressure data for all solutes examined in methanol at 298, 323, and 348.15 K respectively. Each value of diffusivity is the result of one measurement. A linear regression analysis was performed on the measured diffusivity values for each solute-solvent pair at each temperature and from this analysis the percent decrease in diffusivity as pressure increases from 2 MPa to 12 MPa was calculated as well as the slopes of the curves of diffusivity versus pressure. These values are summarized in Appendix F, Tables F.1A to F.1D for methanol, ethanol, propanol and butanol, respectively. It may be observed that the diffusivities decrease linearly with an increasing pressure and increase with increasing temperature. There is a decrease of approximately 0.3 to 1.2% in diffusivity corresponding to an increase in pressure of 1 MPa, and an increase in diffusivity of approximately 30-90% resulting from an increase in temperature from 298 to 323 K at atmospheric pressure, depending on the solute-solvent pair. An F-test of the slope of the straight line for each temperature indicates that the slope is significantly different from zero at the 95% confidence

level, leading to the conclusion that there is a significant effect of pressure on diffusivity.

Several types of graphs of diffusivity versus pressure were made. The first set of graphs which can be found in Appendix G, Figures G.1A to G.1O, shows the results for the molecular diffusivities as a function of pressure for one solute-solvent pair with temperature as a parameter in each graph. The next set of graphs, Figures H.1A to H.1H in Appendix H and Figures 7.1A to 7.1D, show the results for the molecular diffusivities as a function of pressure for the four gases in one solvent and at one temperature, in each case, with Figures 7.1A to 7.1D showing this effect at 298.15 K. These plots compare the behaviour of the different solutes in one solvent and for one temperature, in each case. The final set of diffusivity versus pressure graphs, Figures I.1A to I.1H in Appendix I, and Figure 7.2A to 7.2D compare the behaviour of one solute in all of the solvents examined with Figures 7.2A to 7.2D showing this effect at 323.15 K.

The free volume theory will now be examined because of its relationship to the diffusion process. Batchinski (1913) reasoned that the inverse of the viscosity or fluidity should be directly proportional to the free intermolecular volume, $(V-V_\eta)$, available for viscous flow (equation (3.37)). The reference volume V_η, represents the limiting volume at a temperature such that the molecules become so crowded that the viscosity is infinitely large. Batchinski observed this relationship for 87 non-associated liquids. Hildebrand observed a similar relationship for diffusivity (equation (3.38)). Hildebrand examined the self-diffusion of benzene and tetrachloromethane and the mutual diffusion at infinite dilution of iodine in tetrachloromethane. The diffusivity was observed to be a linear function of the free volume available for diffusion $(V-V_D)$, where the reference volume V_D represents that limiting volume at which the diffusion is zero. Both Batchinski and Hildebrand claimed that the temperature at which the fluidity and the diffusivity were zero was at the melting point of the solvent. In this case V_D is equivalent to V_η.

Thus, as the free volume for the viscous flow increases, the viscosity decreases or the fluidity increases. Similarly as the free volume for diffusion increases, the diffusivity increases. It should be noted that V_D appears to depend only on the solvent properties. However, the effect of different solutes on the value of V_D was not examined by either Batchinski or Hildebrand. Some researchers (Matthews ,1986; Akgerman, 1972a, 1972b; Wong, 1989) claim from their experimental observations

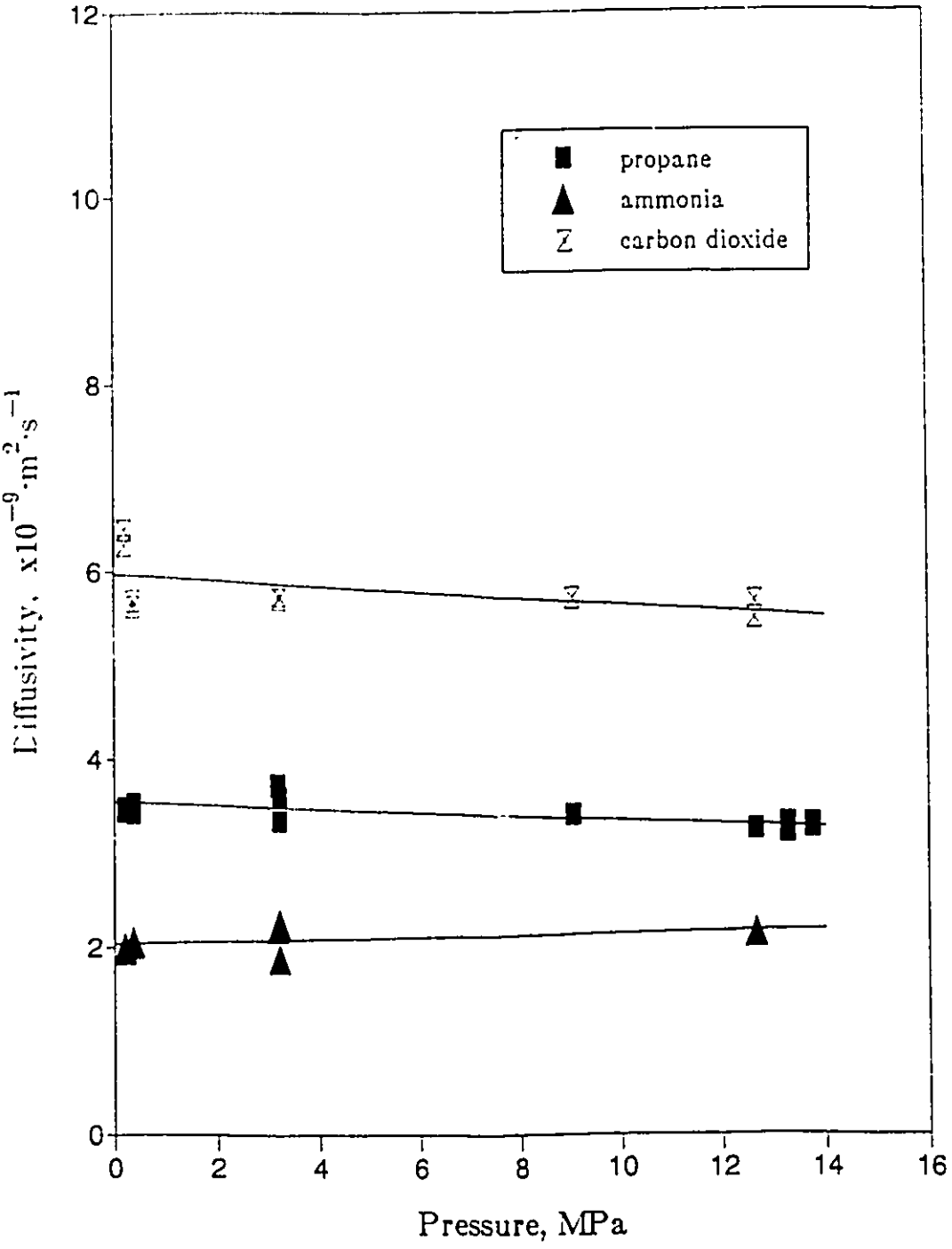

Figure 7.1A: Effect of Pressure on the Diffusivity of All Solutes in Methanol at 298.15 K

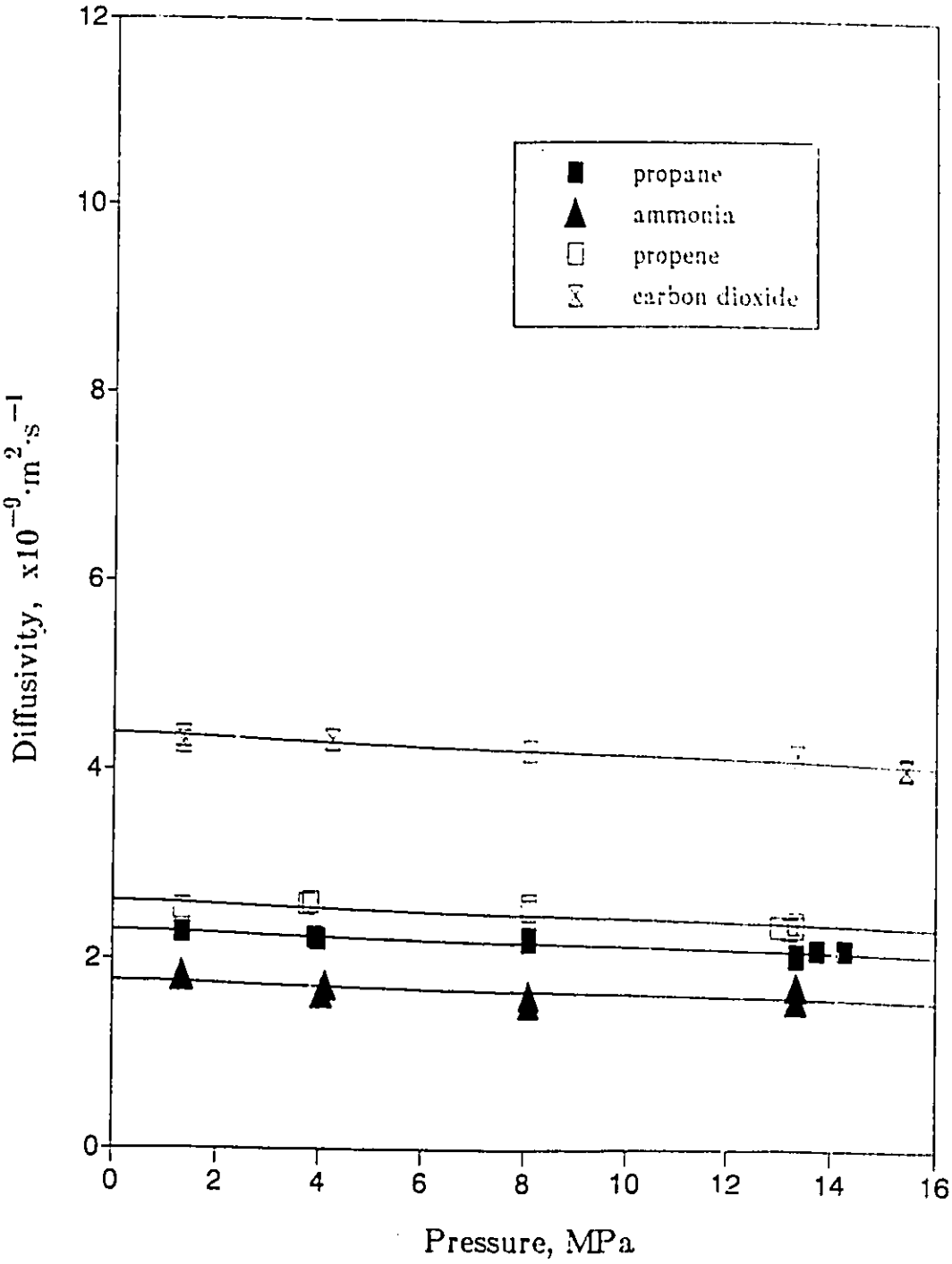

Figure 7.1B: Effect of Pressure on the Diffusivity of All Solutes in Ethanol at 298.15 K

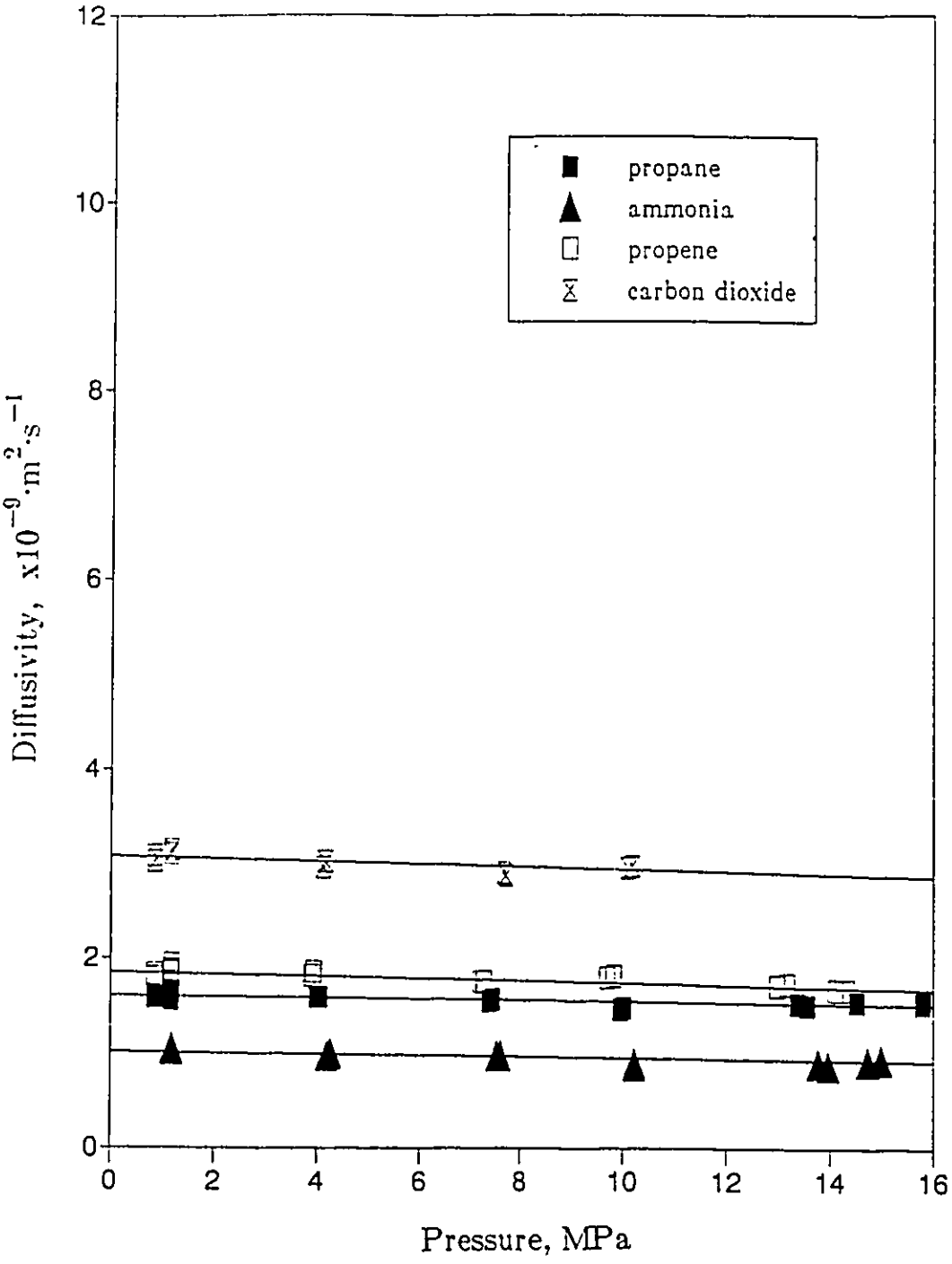

Figure 7.1C: Effect of Pressure on the Diffusivity of All Solutes in Propanol at 298.15 K

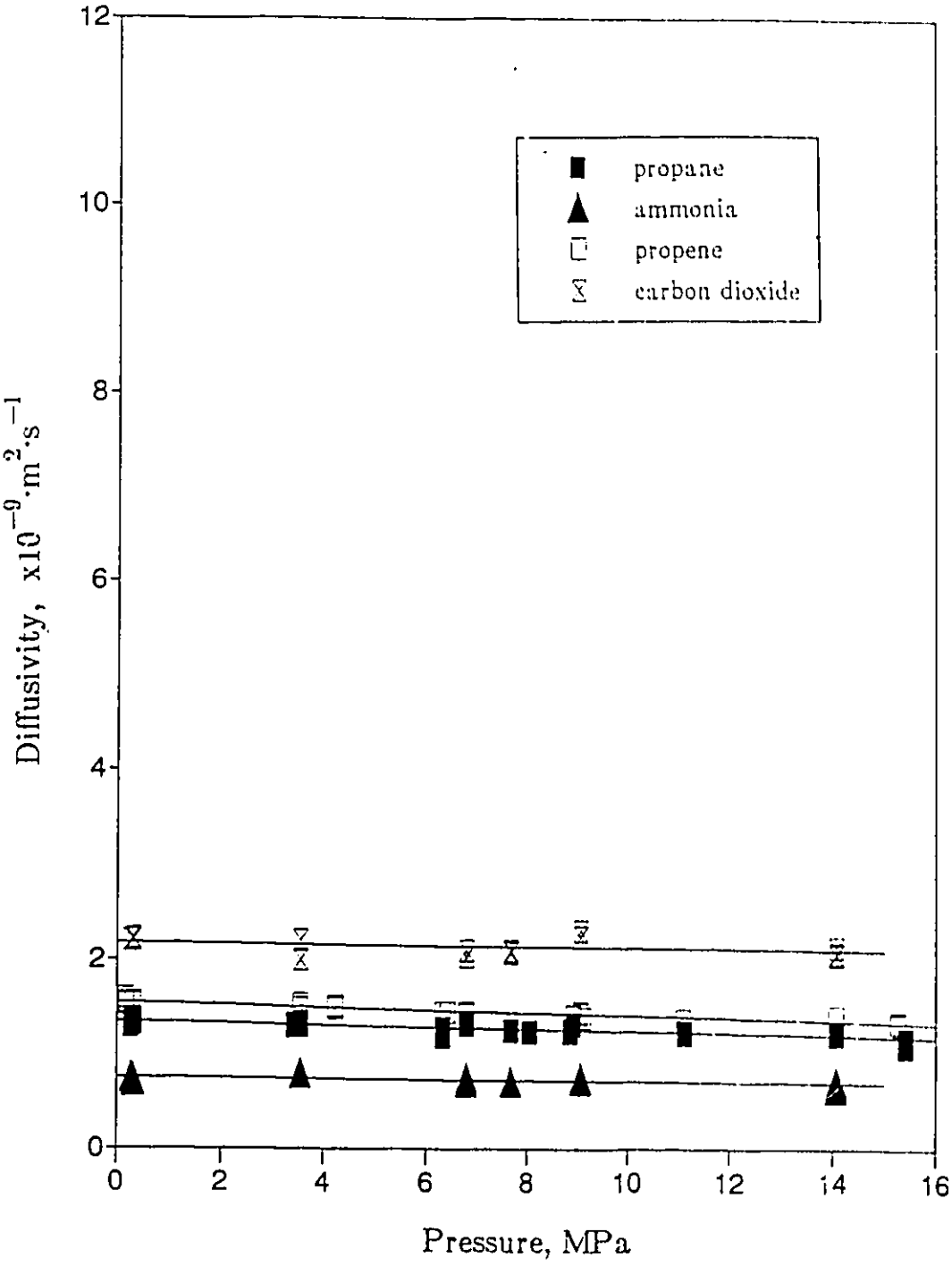

Figure 7.1D: Effect of Pressure on the Diffusivity of All Solutes in Butanol at 298.15 K

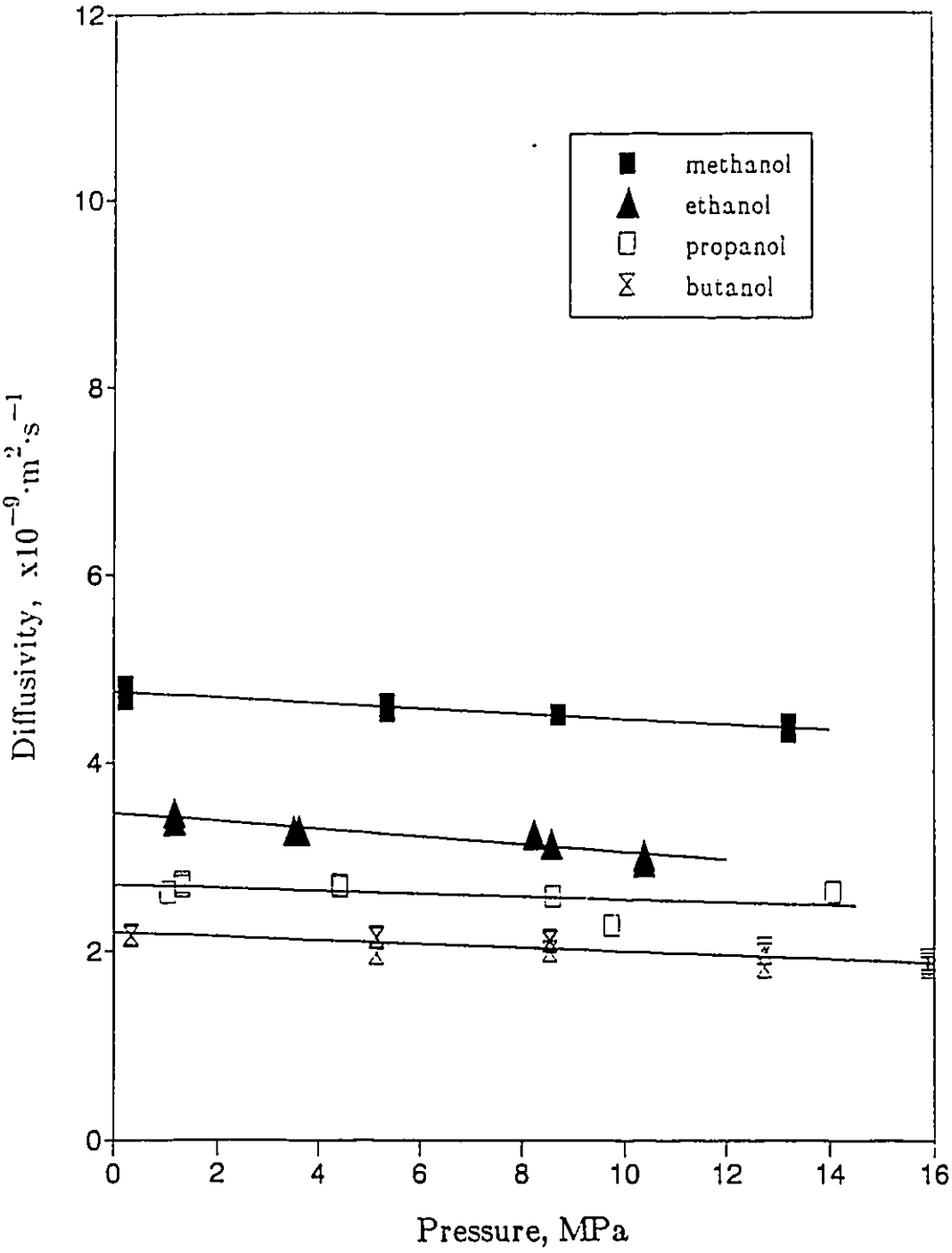

Figure 7.2A: Effect of Pressure on the Diffusivity of Propane in All Solvents at 323.15 K

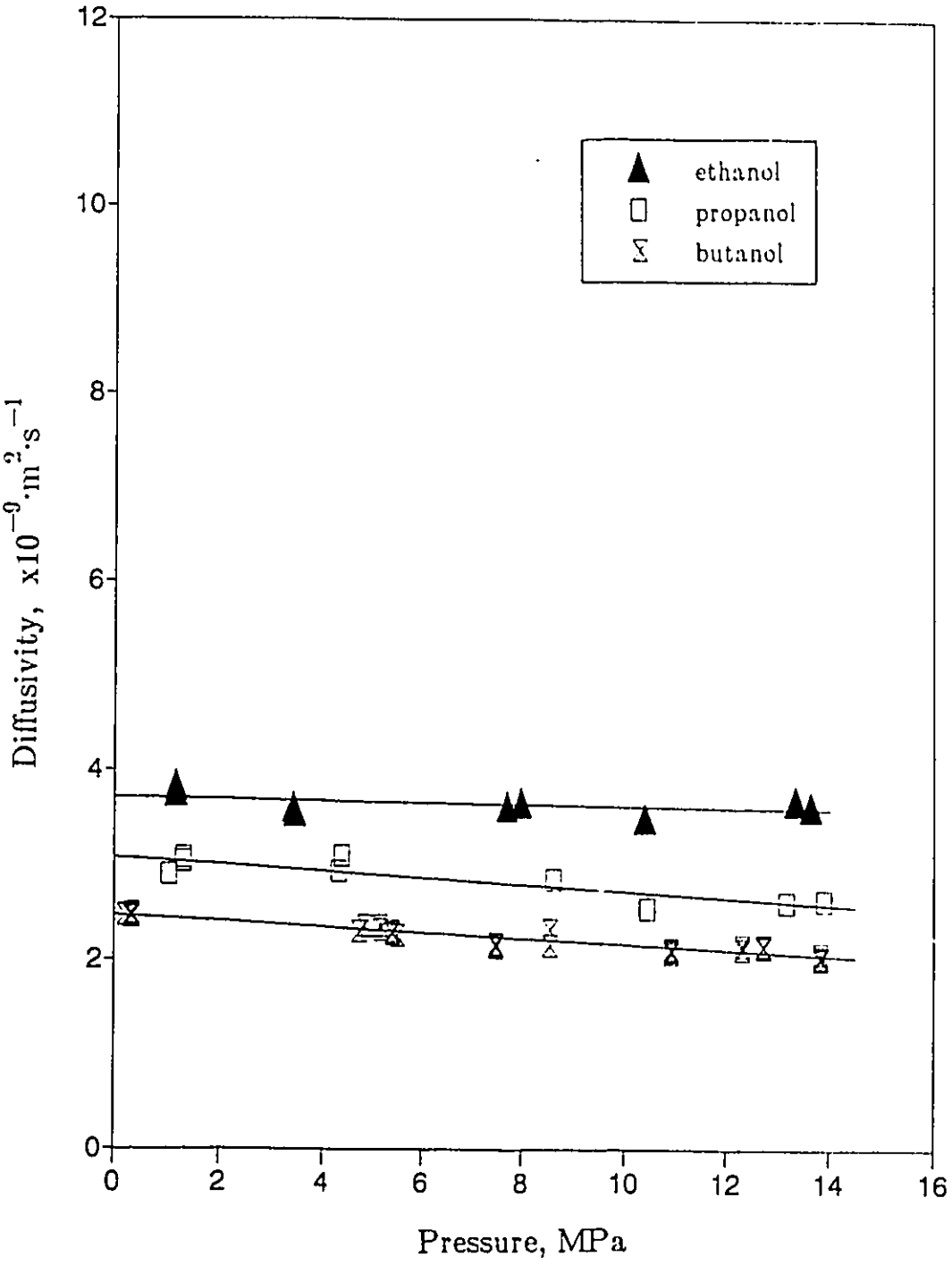

Figure 7.2B: Effect of Pressure on the Diffusivity of Propene in All Solvents at 323.15 K

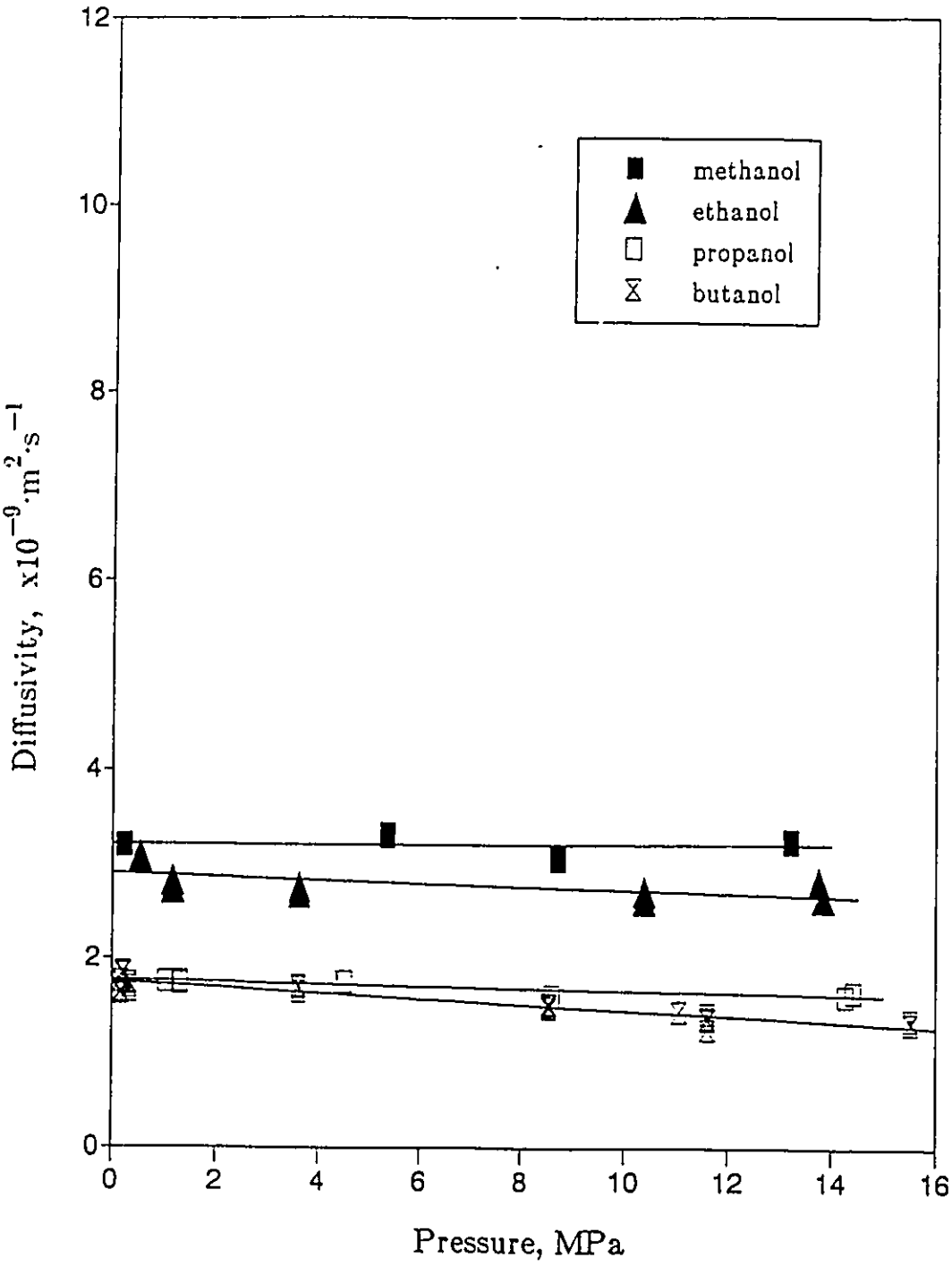

Figure 7.2C: Effect of Pressure on the Diffusivity of Ammonia in All Solvents at 323.15 K

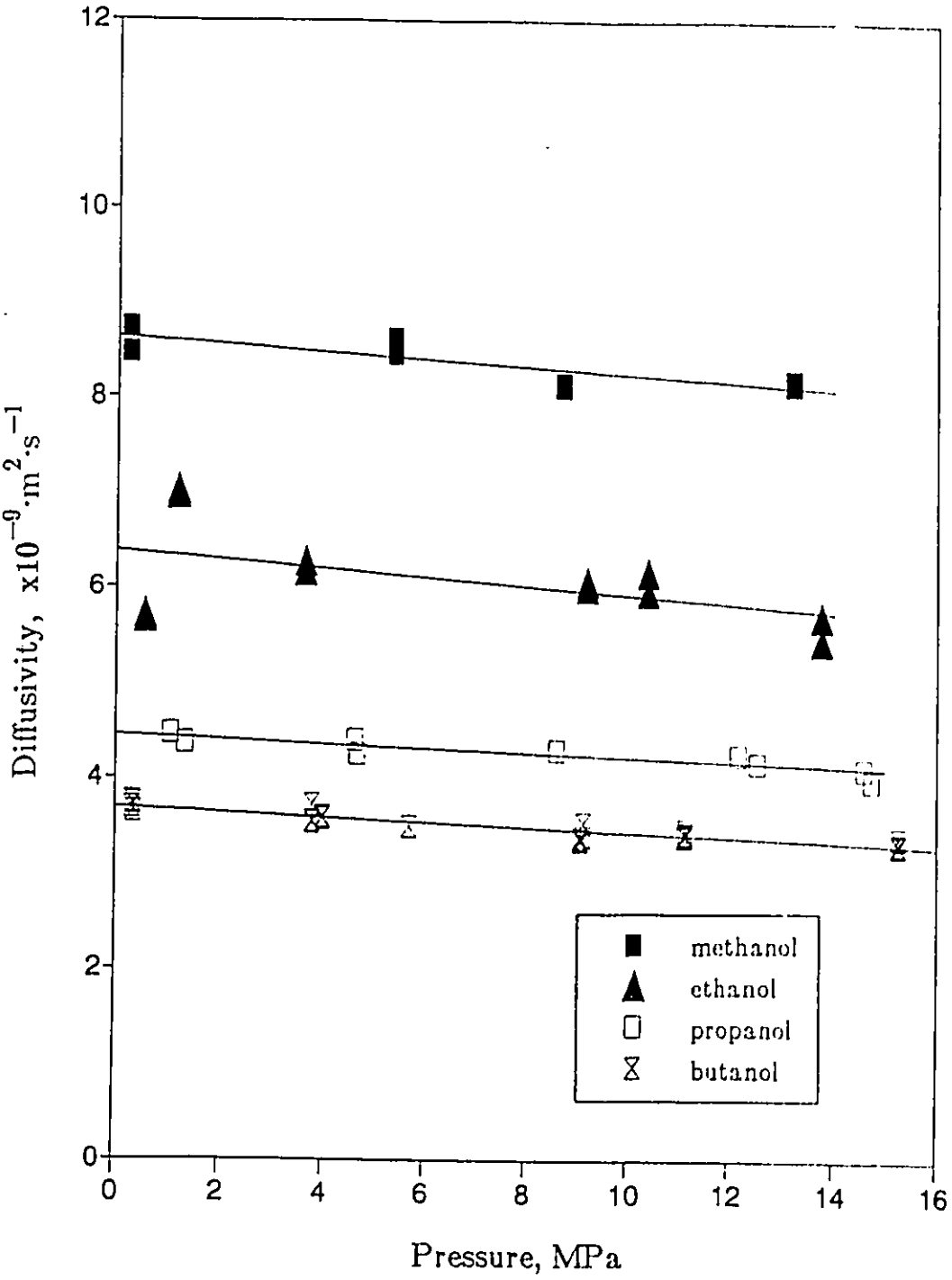

Figure 7.2D: Effect of Pressure on the Diffusivity of Carbon Dioxide in All Solvents at 323.15 K

that V_D is a function of the solvent only. Looking specifically at the diffusion process, as the free volume or intermolecular space increases, the diffusivity should increase if there is little or no intermolecular attractions. Also because of the equivalent nature of V_D and V_η, from equations (3.37) and (3.38), it is observed that as the viscosity increases, the free volume for viscous flow decreases. Thus the free volume for diffusive flow decreases. Thus as the viscosity of the solvent molecules increases, the diffusivity should decrease if there is little or no molecular attractions.

Some general comments can be made concerning the behaviour of the molecular diffusivities of dissolved gases in the alkanol solvents. These observations are made upon examining the results of the effect of pressure and temperature on the density, molar volume and diffusivity of the systems studied in this work as well as similar trends from the literature. Examining the diffusivity data from the tables and the figures, the following were noted.

For any one temperature and solvent, as the pressure increases the diffusivity decreases. This is true for all temperatures in each of the alcohol solvents. This is expected because as the pressure increases, the density increases, with the result that the free space available for diffusion also decreases. Also for any one solute-solvent pair at a given pressure, the diffusivity increases as the temperature increases. This is true for all solute-solvent pairs and over the entire pressure range. This effect is also considered to be associated with the free volume between the solvent molecules and is consistent with the fact that as the temperature increases, the degree of association between the solvent-solvent molecules as well as the solute-solvent molecules decreases.

At any one temperature and over the entire pressure range, the diffusion coefficients of the solutes in a given solvent is greatest for the solute carbon dioxide, followed by propene, propane, and ammonia, in that order (Figures 7.1A to 7.1D). The diffusivity of carbon dioxide appears to be the most affected by pressure and ammonia the least as shown in Tables F.1A to F.1D, Appendix F.

Ross and Hildebrand (1964), Nakanishi et al. (1965) found that the diffusivity of dissolved gases in solvents depends on the molecular size and specifically is inversely proportional to the molar volume of the diffusing gas molecules ($D_{AB} \propto 1/V^{2/3}$). Wilke and Chang (1955) also found a similar inversely proportional relationship based on experimental data but to 0.6 power. As mentioned previously in the hydrodynamic theory, the Stokes-Einstein equation also utilizes an inversely proportional

relationship for large diffusing molecules but to the 1/3 power of the molar volume. From Tables 5.1C and 5.1D, the molar volumes of the solutes at their normal boiling points increase in the following order: ammonia, carbon dioxide, propene, propane. Thus the expected trend in decreasing diffusivity would be in the same order. However these experimental results show that ammonia has the lowest diffusivity, and carbon dioxide the highest followed by propene and propane. A possible explanation why ammonia does not follow the general trend is because ammonia is a strongly polar molecule and thus will have an increased tendency to form hydrogen bonds with the polar alcohol molecules. The formation of hydrogen bonds would tend to decrease the diffusivity. The solute ammonia is not likely to have solute-solute hydrogen bond interactions because the concentration of the solute is so small. Thus the diffusion of the solute molecules does depend on the molecular size in general, but is not valid for highly polar molecules in a medium of other polar, associating molecules. Another indication of the molecular size is the radius or the van der Waals volume of the molecule. Tables 5.1C and 5.1D list the values of the van der Waals volumes and these volumes increase in the same order as the molar volumes at the normal boiling points as expected.

In general, for any one solvent the diffusivity of a dissolved gas is expected to be proportional to the molecular weight of the diffusing solute if no solute-solvent interactions are present (Arnold, 1930). The highly polar nature of ammonia also could explain why, although it has the lowest molecular weight of all the solute molecules, its diffusivity is the smallest. It may be postulated that most of the ammonia molecules are associated with the alcohol solvent molecules, in effect forming larger alcohol-amine complexes. The effective size and molecular weight of this complex is much larger than that of ammonia; as a result, the diffusivity of these larger species is much lower than for simpler molecular ammonia. As shown in Tables 5.1C and 5.1D, the molecular weights of carbon dioxide, propene and propane are approximately the same.

Hayduk and Buckley (1972) found that linear molecules generally tend to diffuse about 30% faster than spherical molecules of the same molar volume at the normal boiling point. In other words, if two different molecules have the same diffusivities, the linear molecule would have the larger molar volume. In this work, it is not possible to make an equivalent direct comparison of solute molecules since they all have different molar volumes at the normal boiling point, and they all have different

diffusivities. However it can be said that from the arrangement of electron pairs, carbon dioxide is an essentially linear molecule with a bond angle of 180 degrees, propene and propane are bent molecules with an angle between any pair of bonds of 109.5 degrees, and ammonia is a triangular pyramidal molecule with a bond angle of 109.5 degrees. Thus, ammonia is the most spherical molecule and carbon dioxide the least. Hayduk and Buckley (1972) found that carbon dioxide does indeed behave as a spherically diffusing molecule. Thus it can be stated that the most spherical molecule, ammonia, does show the lowest diffusivity, and the least spherical molecule, carbon dioxide, shows the highest diffusivity. The molecular diffusivities of the solutes propene and propane lie in between those of the other two gases.

Upon examining the polarity, dipole moments and the association between solute-solute, solvent-solvent, and solute-solvent molecules, the expected behaviour coincides with the previously mentioned results for the measured molecular diffusivities as a function of pressure for the solute gases in the solvent. The polarity and dipole moments of the solute molecules indicate that ammonia contains polar bonds, is a highly polar molecule with the largest dipole moment, can also form hydrogen bonds and is a highly associating molecule. Carbon dioxide contains polar bonds, is a non-polar molecule with zero dipole moment and is therefore not an associating molecule. Propene contains polar bonds because of its double bond, is a polar molecule and has a small dipole moment. Propane the least polar of all of the solute molecules, is a non-polar molecule and has a dipole moment of zero. Thus ammonia could be expected to form relatively strong hydrogen bonds with the solvents, and the other solutes could have weak London forces of attraction to the solvent molecules. This explains the trend observed in the measured diffusivity that the diffusion coefficient of ammonia in all of the solvents has the smallest value. It is postulated that these effects of polarity, dipole moment, association and interactions, as previously described, predominate and are more important than the effects of molecular weight and size for the ammonia molecule, but that these effects along with the effects of molecular weight and size influence the diffusion coefficient for the solutes carbon dioxide, propene and propane. Carbon dioxide, is a non-polar molecule with zero dipole moment, has the smallest molecular size and therefore has the largest diffusivity. Although propene is a polar molecule and has a larger dipole moment that the non-polar molecule propane, the diffusivity of propene is greater than that of propane because its molecular weight and size is smaller.

It has been found by many researchers that the rate of diffusion of a single solute in several solvents within the same family decreases as the size of the solvent molecule increases. This is generally true especially in non-polar alkane solvents where the dipole moment is zero. As shown in Tables 5.1A and 5.1B, the dipole moments of the alcohol solvents used in this work decrease with increasing chain length. All of the alcohols examined in this work contain polar bonds, are polar molecules with a dipole moment, and are highly associating molecules. This is due to the -OH group present. Methanol is the most polar of all the solvent molecules with the largest dipole moment and is the most associating of all the alcohol solvents examined. Although the polarity, dipole moment and association of the alcohol solvent molecules decrease as its size increases, the molecular diffusivity of a single solute at any one fixed temperature and over the entire pressure range, is greatest in methanol and decreases as the chain length increases. Thus for a fixed temperature, the diffusion coefficient of each solute in methanol is greater than in ethanol which is greater than in propanol and which in turn is greater than in butanol (Figure I.1A to I.1H). This suggests that there is more free space available for diffusion for all of the solutes in methanol than in the other solvents. The density data showed that at a fixed temperature and pressure, as the chain length increases, the density increases, and the molar volume increases (Table D.1). The diffusivity data shows that the diffusivity decreases with increasing chain length of the solvent molecule. Thus the available free space for diffusion decreases with increasing chain length. This implies that the 'hard-core' volume of the solvent molecule increases with increasing chain length. The density data also showed that at one temperature as the chain length of the molecule increases from methanol to butanol, the effect of pressure on the molar volume increases with a consequent increase in the effect of pressure on the free space available to diffusion. At all pressures and for all solutes, the diffusivity decreases with increasing chain length of the solvents. This again supports the reasoning that as the chain length increases, the 'hard-core' volume of the solvent molecules increases, at any and all pressures.

From Tables 5.1A and 5.1B, it is observed that the molar volumes of the solvents at their normal boiling points increase with increasing chain length of the alcohol molecule, from methanol to butanol. This thus supports the expected trend that as the molar volume increases, the diffusivity decreases. Thus the diffusion of the solvent molecules, like the solute molecules is inversely related to the molecular

size. Another indication of the molecular size, the van der Waals volume similarly increases as the chain length increases (Tables 5.1A and 5.1B).

Examining the many relationships between diffusivity and solvent viscosity, it is observed that the diffusivity is an inverse function of the solvent viscosity. The Stokes-Einstein equations (3.4) and (3.6) express diffusivity as being inversely related to viscosity. The Arnold equation expresses diffusivity as being inversely proportional to viscosity to the +0.5 power. The empirical correlation of Hayduk and Cheng, equation (3.47), which is based on the hydrodynamic theory expresses the diffusivity as a function dependent only on the solvent viscosity and to some power which depends on the diffusing solute molecule. These correlations, to name a few, all indicate that as the viscosity of the solvent increases, the diffusivity decreases. This is also observed in these experiments. Thus as the chain length of the solvent molecule increases, the viscosity of the solvent increases and the diffusivity decreases for all solutes and at all temperatures and pressures.

7.2 Trends in the Differential Refractometer Response Peaks

The anomalies and some of the trends shown in the peaks which were used to obtain the mutual diffusivities for the systems investigated in this work will now be discussed.

The solute ammonia is of interest because both positive and negative peaks were obtained for the solvents examined. A very dilute solution of ammonia in butanol or propanol resulted in positive peaks. In ethanol however, a high concentration of solute had to be used to obtain a detectable peak. The first experiments with ammonia in ethanol were performed at 348.15 K, and no peak was observed. However, on increasing the concentration of ammonia in ethanol at 298.15 K and 323.15 K, a small peak was observed in each case. This explains the fact that there is no data for this system at 348.15 K. Small negative peaks at all temperatures were obtained for ammonia in methanol. This suggests that the addition of ammonia to methanol increases the refractive index of the solution while the addition of ammonia to ethanol, propanol and butanol decreases the refractive index of the solution, with the largest decrease for butanol and the smallest decrease for ethanol. For ethanol, the change is so small that a peak can only be detected for a high concentration of ammonia.

The relationship between refractive index and concentration for dilute solutions is:

$$(\Delta R) = K^{*}(\Delta C) \qquad (7.1)$$

In the above equation ΔR refers to the difference in refractive index between the sample cell containing the dissolved solute and the reference cell containing the pure solvent, the variable ΔC refers to the difference in concentration between the sample cell and the reference cell and K^{*} is a constant which can be positive or negative and is specific for a solute-solvent pair. It is of interest to relate the value of K^{*} to the molecular size of the solvent. The value of K^{*} is observed to increase from a large negative number to a small negative number and then to become positive for decreasing molecular sizes of the alkanols from butanol to methanol.

No peaks were observed for the solute propene in the solvent methanol at all temperatures and pressures. It was apparent that dissolved propene and methanol have small refractive index differences.

For the solute carbon dioxide, small negative peaks were observed before and after the positive peaks in the solvents methanol, ethanol, and propanol. Henceforth, these negative peaks will be referred to as dips. No dips were observed for carbon dioxide in butanol. The magnitude or size of these dips were found to increase with increasing temperature and to increase with decreasing size of the solvent molecule. Thus, the largest dip occurred at 348.15 K in methanol, the smallest dip occurred in propanol at 298.15 K and no dips occurred in butanol. These dips suggest that two species may exist in the solvent and are the result of the summation of a negative peak and a positive peak by the differential refractometer with the species producing the negative peak being in low concentration and the species producing the positive peak being the dominant one. On injecting a 2 mole percent water solution into the Taylor dispersion apparatus, a small negative peak resulted. The negative peaks in this experiment could therefore have been due to the presence of water. It could also have been due to the carbon dioxide reacting with any moisture present to form carbonic acid - whether the water came from the air, the alcohol or was already present in the gas. The small negative peak could also have been due to the carbon dioxide attaching itself to the alcohol molecule possibly by weak hydrogen bonding. Hayduk and Cheng (1971) state that the quantity and type of molecular association or aggregation for a dilute solute specie or a solvent

molecule could be expected to affect the diffusivity.

The analysis of the dips will now be discussed. Two methods were attempted and one was found to be successful. The successful method of analysis used the five parameter model of equation (4.40).

The first analysis was done using a modification of the five parameter model of equation (4.40) in which each peak was considered to be the sum of two separate positive and negative peaks with the same retention time but with different peak heights and dispersion parameters. The result of this assumption was a seven parameter model. It was found that the regression analysis using this model showed erroneous results. For example, the diffusivity of carbon dioxide in methanol was found to be lower than that in ethanol, which is unlikely.

The other method of analysis used the five parameter model of equation (4.40). However, the data was modified to include only data from the minimum in the dip before the peak to the minimum in the dip following the peak. This in effect treats the data as one peak with a negative shift in the baseline. Thus the assumption was that the entire peak with the new shifted baseline was due only to carbon dioxide. Results obtained using this five parameter model seemed more reasonable. As expected, the diffusivity of carbon dioxide in methanol was larger than that in ethanol using the five parameter model. The diffusivity values obtained using the five and seven parameter models differed most for methanol ($\leq$50%) and the least for propanol ($\leq$5%). Larger and more accurate diffusivity values were obtained using the five parameter model compared to the seven parameter model.

7.3 Comparison with Reported Values

The density results will first be discussed. When the experimental densities of butanol at atmospheric pressure are compared with those of Wong (1989) good agreement is indicated as shown in Table 7.1. The percent differences range from 0.11 to 0.28%. A comparison between the densities from this work and those of Wong (1989) as well as of the effect of pressure on the densities measured are shown in Figure 7.3. It may be concluded that the measured densities show excellent agreement with the reported values. This result confirms that the method used in this work can be used to obtain accurate densities.

Table 7.1

Comparison of Measured Values
with Literature Values, (Wong, 1989),
for Propene in n-Butanol at Atmospheric Pressure

Density

Temperature K	Measured Density $kg \cdot m^{-3}$	Reported Density $kg \cdot m^{-3}$	Difference %
298.15	806.9	806.0	0.11
323.15	784.6	786.8	0.28
348.15	761.1	760.0	0.14

Diffusivity

Temperature K	Measured Diffusivity $x10^{-9}\ m^2 \cdot s^{-1}$	Reported Diffusivity $x10^{-9}\ m^2 \cdot s^{-1}$	Difference %
298.15	1.54	1.35	12.3
323.15	2.45	2.40	2.0
348.15	3.57	3.91	9.5

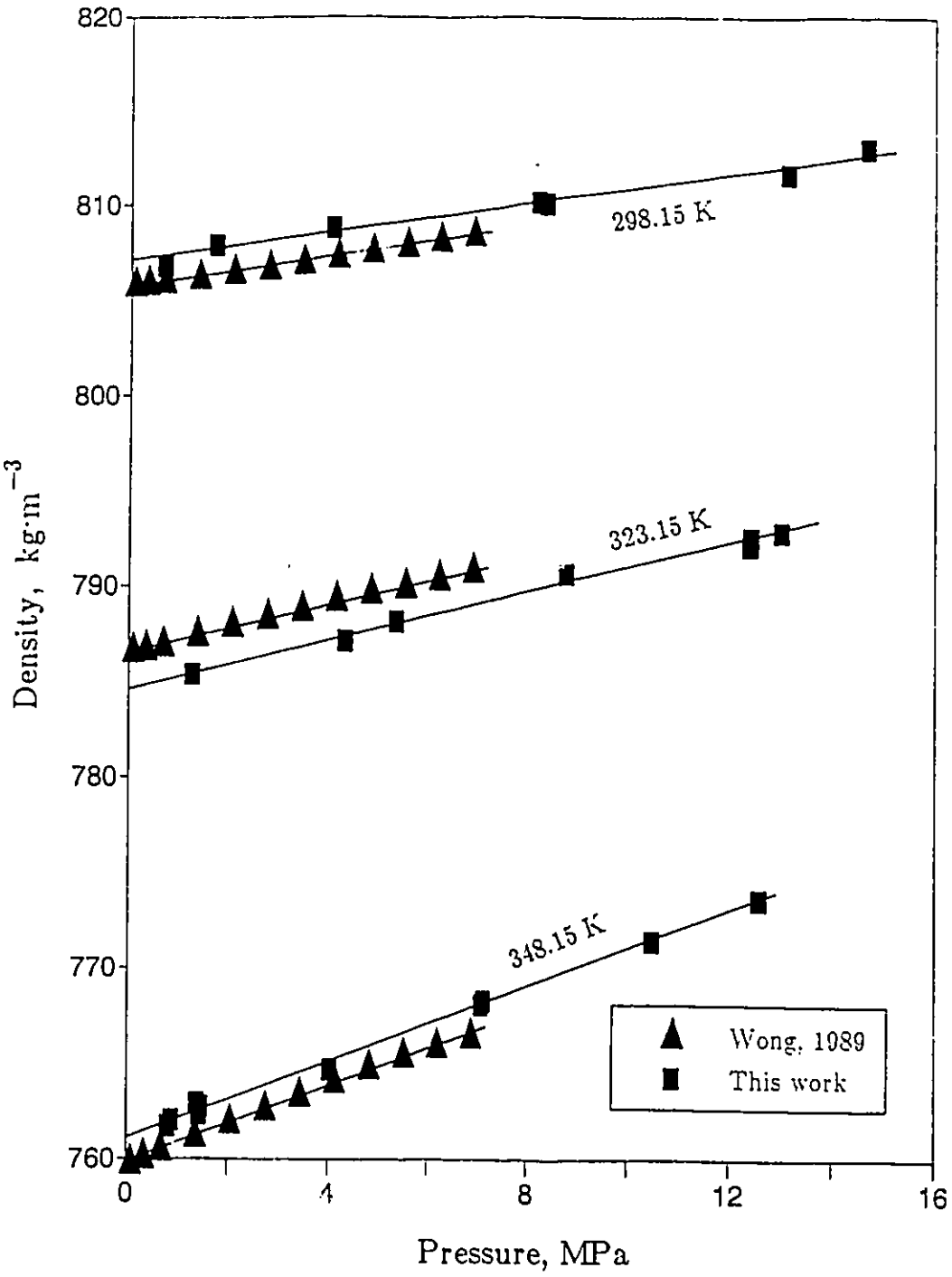

Figure 7.3: Comparison Between This Work and That of Wong (1989) of the Effect of Pressure on the Density of Butanol

A comparison of the viscosity data for ethanol and methanol from this work, see Appendix J, to that reported by Daubert and Danner (1985) showed that the measured viscosities showed excellent agreement with the reported values. This result confirms that this method can be used for accurate determination of the solvent viscosity.

A comparison of the diffusivity results with literature values will now be made The data from the literature were obtained from Wong (1989) for the solute propene and the solvent butanol. A comparison of the experimental data and that available from Wong (1989) shows substantial differences in diffusivities for some of the data as indicated in Table 7.1 and Figure 7.4. The percent differences range from 2.0 to 12%. Figure 7.4 also shows the effect of pressure on the diffusivities from this work and those of Wong (1989). It is noted that there are no other diffusivity data available for this system in the literature. Wong's data were obtained using a similar type of apparatus and the graphical method for interpretation of the results. It was found that upon changing the pressure, the experimental apparatus had to be left for at least seven hours before steady state was attained. At 298 K, for example, it was found that there was a difference of approximately 12% between my experimental results and those of Wong. It was observed that as the time to attain steady state was decreased significantly below seven hours, the value of diffusivity consistently decreased and approached the values reported by Wong. It is postulated that for some of his results, Wong's data may not have been obtained at steady state. It was also found that for these experimental data, there was a difference of approximately 4% in the diffusivities using the graphical method and those obtained by means of a curve-fitting technique based on the analytical solution of Taylor. Thus it seems essential that a sufficiently long period of time be allowed after changing the pressure to ensure that the system attains equilibrium and to use a curve-fitting technique to obtain accurate results. During the experiment, pressure fluctuations are minimized by the installation of a new pulse-free pump, as well as the installation of new capillary tubing to condition the flow before it enters the dispersion tube. The pulse-free pump ensures a constant flow rate of the solvent and thus maintains control of the system pressure. The flow is said to be conditioned with the minimizing of the fluctuations in the flow rate. The flow is conditioned by inserting an additional length (12 m) of capillary tubing. Thus by ensuring that the system attains equilibrium after changing the system pressure, by the use of a computer and a curve

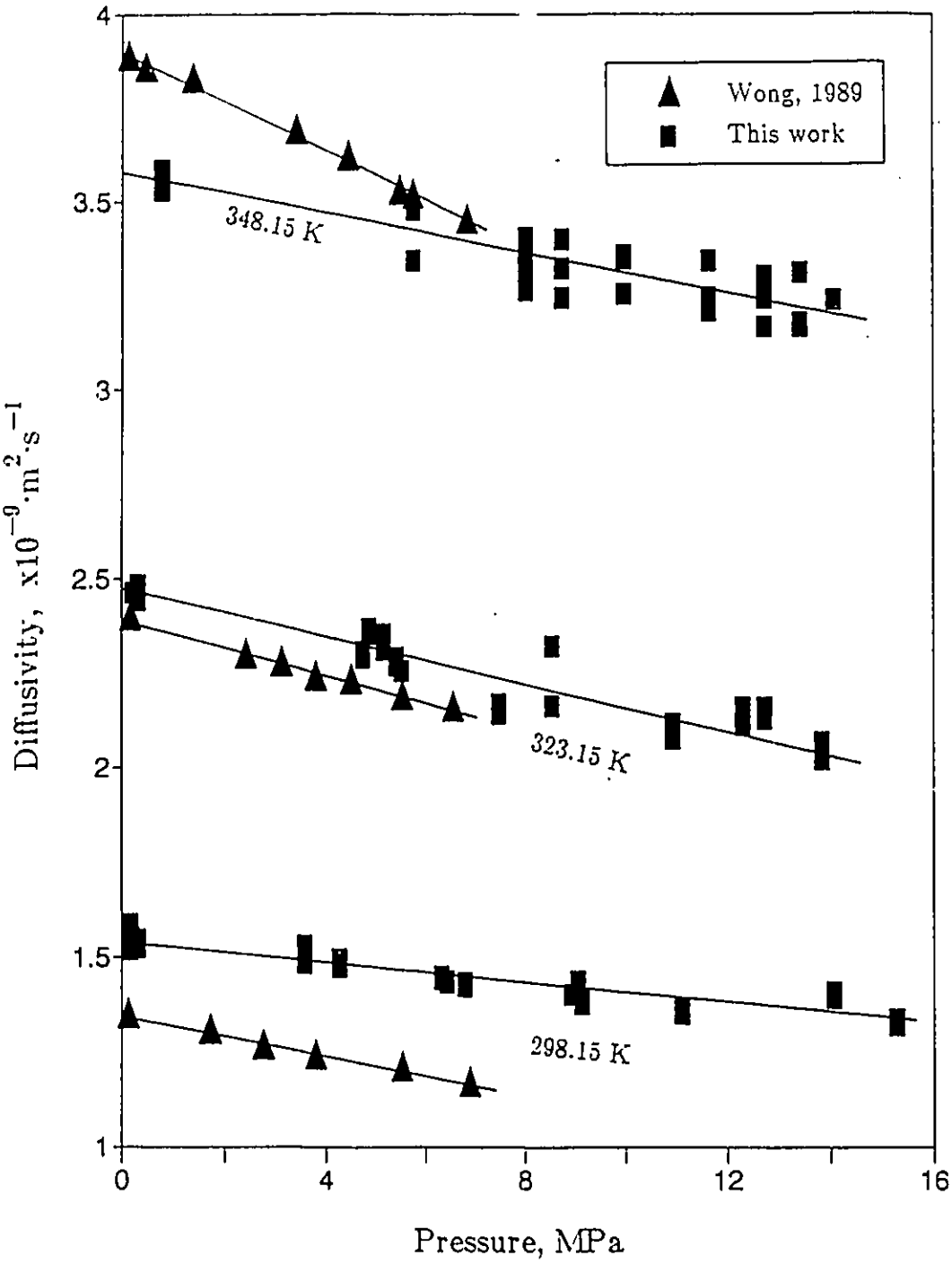

Figure 7.4: Comparison Between This Work and That of Wong (1989) of the Effect of Pressure on the Diffusivity of Propene in Butanol

fitting technique in the analysis of the data and by installing a new pulse-free pump and capillary tubing to ensure a constant flow rate and a constant system pressure, the diffusivities obtained from the revised method of treatment are considered to be more reliable.

Potential sources of error in the measured diffusivities will now be briefly discussed. The effects of finite volume of the injected pulse and of the volume of the sample cell of the detector, the finite length of the tube connecting the diffusion tube to the differential refractometer, the nonuniformity of the radius of the diffusion tube and the effect of the coiling of the diffusion tube all constitute potential sources of error. Matthews (1986), showed that a total error of less than 0.5% could be attributed to these sources and of all the potential errors, the coiling of a diffusion tube is the greatest potential source of error. Since Taylor's model does not account for secondary flows due to coiling, the experiment has to be designed in such a way to ensure that secondary flows are not created.

Thus, it has been found that the linear relationship between diffusivity and pressure is an excellent representation of the data, although a comparison of the measured diffusivities with literature shows substantial differences. Also, the linear relationship between the density and pressure is an excellent representation of the data over the range studied.

7.4 Rough Hard Sphere Correlation

Dymond (1974) first demonstrated the linear relationship between the ratio of self diffusivity to the square root of the absolute temperature and the molar volume for self diffusivity data. Recalling Dymond's equation:

$$\frac{D_{BB}^{DYM}}{\sqrt{T}} = F \cdot \frac{C'}{\sigma_B^2 m_B^{1/2}} \cdot [a(V - b V_o)] \tag{3.25}$$

In equation (3.25), C′ is a constant. Dymond (1974) found for the fitted constants a=1.271, and b=1.384 equation (3.25), after some rearranging, becomes:

$$\frac{10^9 D_{BB}^{RHS}}{\sqrt{T}} = \frac{A \cdot 2.527\, k^{1/2}}{V_o^{2/3} M^{1/2}} \cdot (V - 1.384\, V_o) \tag{3.26}$$

It was Chen (1982) who first applied Dymond's equation for mutual diffusion coefficients at infinite dilution and found a linear relationship for all of the n-alkane systems examined. Chen (1982) did not show why Dymond's equation for self diffusion data should be applicable to mutual diffusivity data.

Rodden (1988) showed that with the use of Dymond's equation, a generalized equation for diffusivity can be obtained based on the RHS theory and the parameters associated with it. Recalling the limiting case of this:

$$\frac{D^{\circ}_{AB}}{\sqrt{T}} = \beta \cdot (V - bV_o) = \beta \cdot (V_B - V_D) \tag{3.35}$$

In equation (3.35), β is represented by:

$$\beta = \frac{K'}{\sigma^2_{AB}} \left(\frac{m_A + m_B}{m_A m_B} \right)^{1/2} \cdot F \frac{g(\sigma_B)}{g(\sigma_{AB})} \frac{[D^{HSL}_{AB} / D^{E}_{AB}]^{\circ}_{MD}}{[D^{HSL}_{BB} / D^{E}_{BB}]_{MD}} \tag{3.36}$$

In equation (3.35), for the case of an infinitely dilute solute in a solvent, V_B represents the molar volume of the pure solvent B and V_D is equivalent to the product bV_o and is the volume for which the diffusivity is zero. In equation (3.36), MD represents the molecular dynamics computer calculations for the determination of C. The term β represents the slope of $D^{\circ}_{AB}/\sqrt{T}$ versus V. Equations (3.35) and (3.36) could thus be used to predict infinitely dilute mutual diffusion coefficients for the systems where infinite dilution MD data are available. The complex nature of the parameter β is reflected in the variables required in its determination. The variables m_A, m_B, σ_A, σ_B can usually be obtained from the literature. However because of the incomplete study done on the molecular dynamic calculations of C and on the determination of F, β cannot be estimated for most systems. A possible solution to this problem is to develop an expression for β based on parameters which can be easily estimated. This was successfully done by Matthews (1986), Rodden (1988) and Wong (1989). Before the development of such an equation, the data needs to be tested to determine whether the required linear relationship exists between $D^{\circ}_{AB}/\sqrt{T}$ and V.

Figures 7.5A to 7.5D demonstrate an apparent linear relationship between $D^{\circ}_{AB}/\sqrt{T}$ and V for the solutes propane, propene, ammonia and carbon dioxide in methanol, ethanol, propanol and butanol, respectively. This linear relationship using experimental data confirms the predictions of the RHS theory of equations (3.35) and

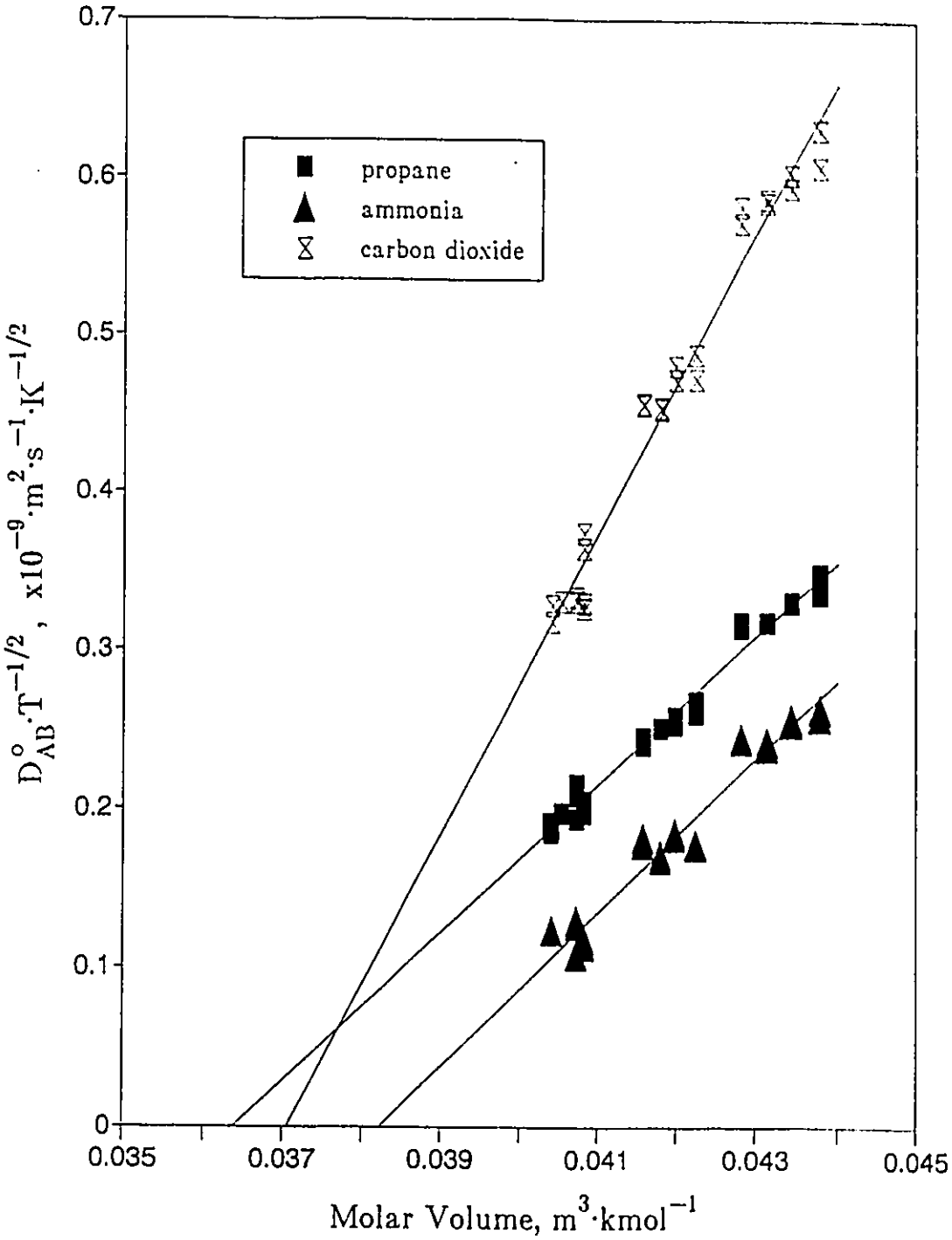

Figure 7.5A: Linear Behaviour of $D^{\circ}_{AB} \cdot T^{-1/2}$ versus V in the Solvent Methanol at Several Temperatures and Pressures

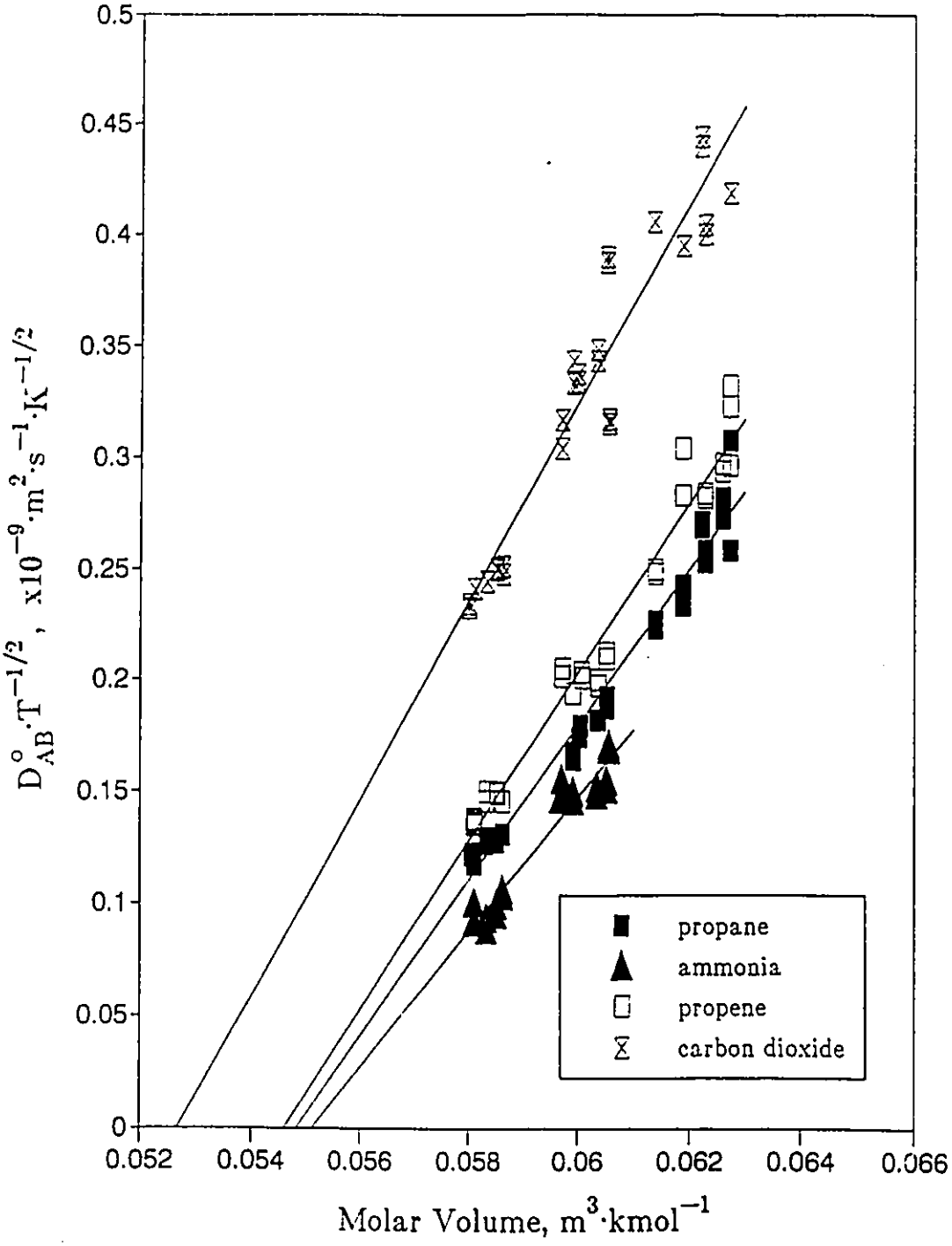

Figure 7.5B: Linear Behaviour of $D^{\circ}_{AB}\cdot T^{-1/2}$ versus V in the Solvent Ethanol at Several Temperatures and Pressures

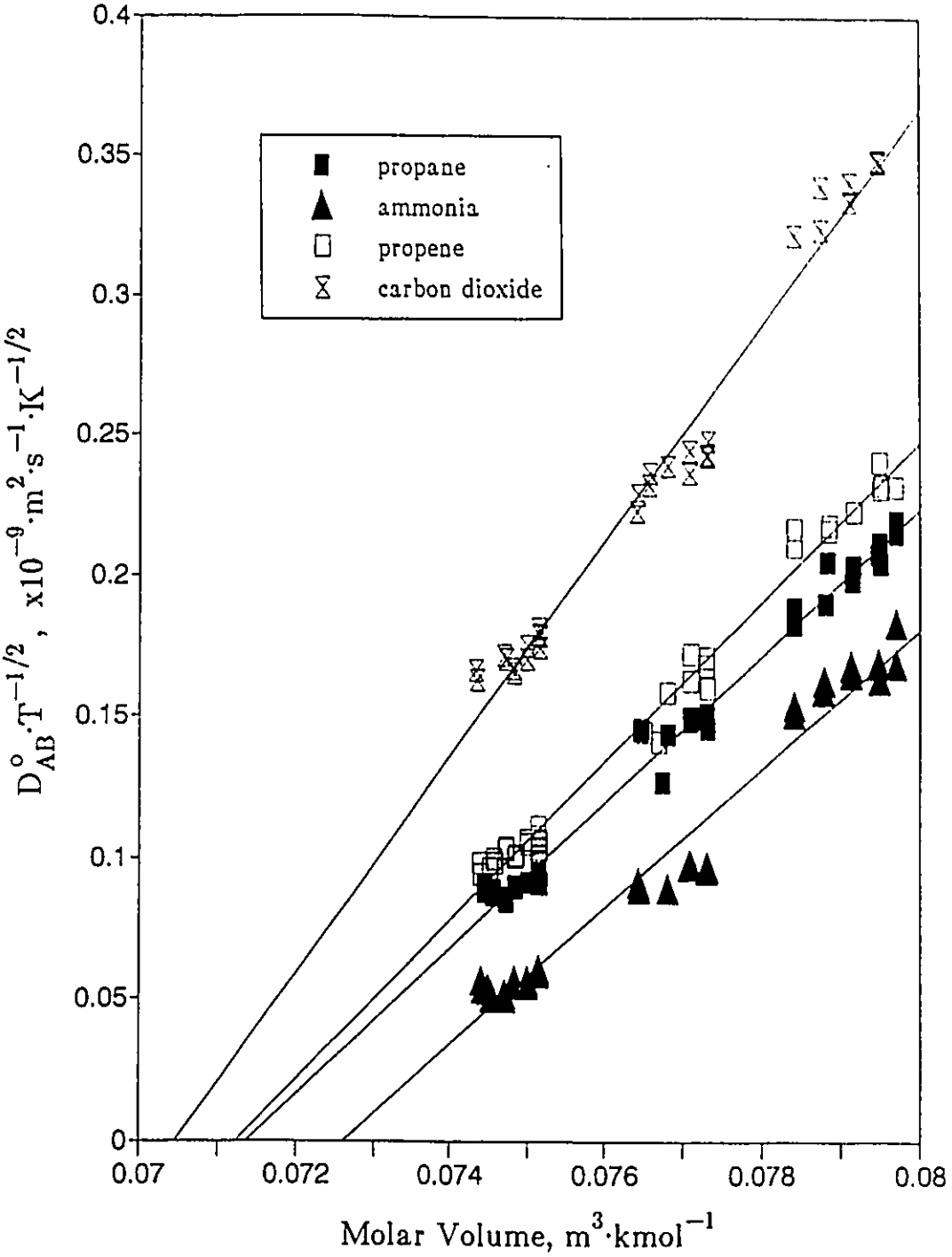

Figure 7.5C: Linear Behaviour of $D^{\circ}_{AB} \cdot T^{-1/2}$ versus V in the Solvent Propanol at Several Temperatures and Pressures

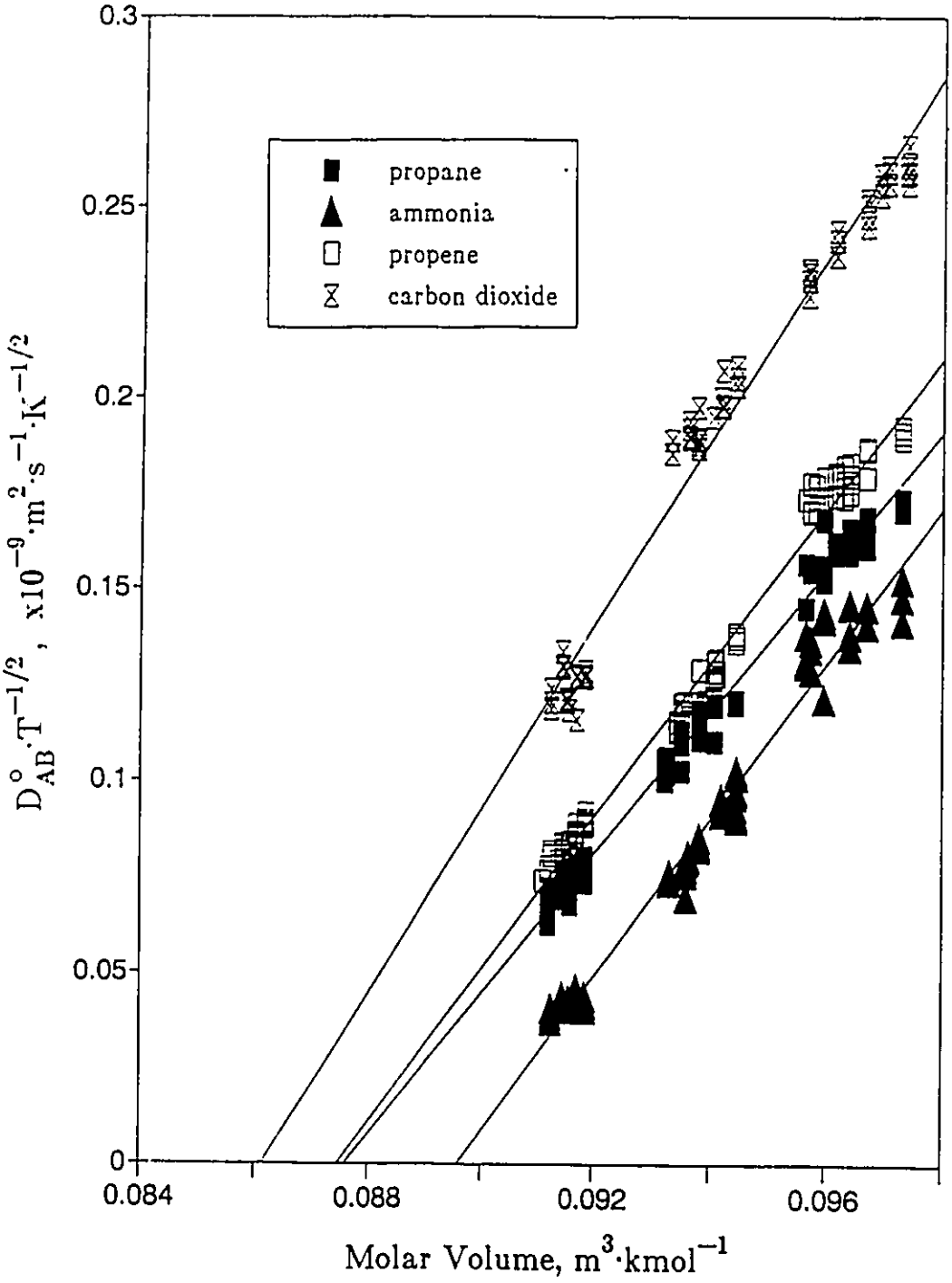

Figure 7.5D: Linear Behaviour of $D^{\circ}_{AB}.T^{-1/2}$ versus V in the Solvent Butanol at Several Temperatures and Pressures

(3.36). It was also found that for methanol and ethanol a similar linear relationship was found between $\sqrt{T}/\eta$ and V, see Appendix J. Although the diffusivity behaviour follows the general trend, the graphs appear to show that β is temperature dependent. This temperature dependency of β will be discussed later. The linear relationship for each solute-solvent pair means that β is independent of the molar volume, V. However, equation (3.36) shows that β is a function of C which is a function of V and thus this lack of dependency of β on V could not have been deduced from equations (3.35) and (3.36). The slopes, β, and intercepts, V_D, from the linear regression analysis is recorded in Table 7.2. A value of β and V_D is recorded for each solute-solvent pair. The range of values of V_D for each solvent instead of one value definitely exists and will be explained later. The critical volume, V_{cB}, and the molar volume at the triple point, V_{tp} of the solvents are also given in Table 7.2.

Looking specifically at the intercepts V_D, it is observed to be strongly dependent on the solvent properties and weakly dependent on the solute properties. The trend in V_D is difficult to describe for each solvent. The expected trend is that as the size of the solute molecule increases, its ability to move in the free space available for diffusion decreases. This trend is also expected around the freezing point where it is expected that there is a limited free volume available for diffusion.

Using equations (3.19) and (3.35), V_D is given by:

$$V_D = b\,V_o = b\,N\sigma_B^3/\sqrt{2} \tag{7.2}$$

In equation (7.2) V_o represents the theoretical closed packed volume of the solvent molecules and is a constant dependent only on the diameter of the solvent molecule. Thus for any one solvent, a range of values of V_D translates to a range of values of b which in turn implies that b is not a constant for each solvent but is a constant for each solute-solvent pair. Dymond (1974) empirically determined b from the limited molecular dynamics data for self diffusion (equation 3.23) and found it to be a constant. The systems used by Dymond were pure, one component, non-polar, non-associating systems. The value of b has been found for an infinitely dilute solute in a solvent by many researchers to be a function of both the solute and the solvent properties (Hildebrand, 1977; Chen et al., 1982; Matthews, 1986; Rodden, 1988; Wong, 1989). However, some researchers claim that for each solvent, the value of b was a constant since it was only a weak function of the solute size (Matthews, 1986; Wong,

Table 7.2

Linear Regression of $D^{\circ}_{AB} T^{-1/2}$ versus the Molar Volume
for the Solvents
Methanol, Ethanol, Propanol and Butanol

$$10^9 D^{\circ}_{AB} T^{-1/2} = \beta(V - V_c)$$

(D°_{AB} in $m^2 \cdot s^{-1}$, T in K, V in $m^3 \cdot kmol^{-1}$)

SOLUTE	β $kmol \cdot m^{-1} \cdot s^{-1} \cdot K^{-1/2}$	V_D $m^3 \cdot kmol^{-1}$
	SOLVENT: METHANOL, V_{cB}=0.1178, V_{tp}=0.0363	
Propane	46.570	0.0364
Propene	-	-
Ammonia	48.635	0.0382
Carbon Dioxide	94.704	0.0370
	SOLVENT: ETHANOL, V_{cB}=0.1669, V_{tp}=0.0511	
Propane	34.731	0.0548
Propene	37.679	0.0546
Ammonia	30.148	0.0551
Carbon Dioxide	44.436	0.0527
	SOLVENT: PROPANOL, V_{cB}=0.2185, V_{tp}=0.0652	
Propane	25.876	0.0714
Propene	28.203	0.0712
Ammonia	24.384	0.0726
Carbon Dioxide	38.363	0.0745
	SOLVENT: BUTANOL, V_{cB}=0.2745, V_{tp}=0.0831	
Propane	18.271	0.0876
Propene	19.869	0.0874
Ammonia	20.261	0.0896
Carbon Dioxide	23.924	0.0861

1989). Rodden (1988) pioneered the development of the solute size in the determination of b to obtain an excellent fit to his equation for predicting mutual diffusivities at infinite dilution. Rodden's expression for b was a linear equation in σ_A/σ_B: $b=1.206+0.0632\ (\sigma_A/\sigma_B)$. Thus the value of b for multi-component systems, as in binary systems with an infinitely dilute solute, is not necessarily constant and seems to depend on the properties of the solute and solvent.

Values of σ are obtained from the van der Waals volume. van der Waals represents the hard core volume of one mole of spherical molecules. Thus σ represents the hard core volume of one spherical molecule. van der Waals method of obtaining σ is used instead of the true hard sphere Lennard-Jones σ because very little self-diffusion and viscosity data are available to calculate the true σ. Also it has been found by many researchers that the van der Waals σ and the Lennard-Jones σ are almost identical. Thus the consistent use of the van der Waals σ represents an accurate means of obtaining the molecular diameters of all of the solutes and solvents used. Values of the van der Waals volume, σ, and the molecular weights of all of the solutes and solvents used are recorded in Table 7.3. It is observed from Table 7.3 that as σ increases, the molecular weight increases for the alcohols solvents. However this trend is not applicable for the solute molecules; carbon dioxide deviates from the trend.

In order to develop the correlation based on the RHS theory to predict D^{o}_{AB} it is necessary to express both V_D and β in terms of variables which are known or can easily be obtained. Looking specifically at V_D, it is observed that in the past several expressions were attempted. The variable V_D has been expressed as being directly proportional to the critical volume of the solvent, V_{cB}, and approximately equal to the triple point volume of the solvent, V_{tp} (Matthews, 1986 and Wong, 1989). The variable V_D has also been expressed as a function of the solute and the solvent size, namely σ_A, σ_B (Rodden, 1988). Thus the expressions for V_D include:

$$V_D = x\,V_{cB} \tag{7.3}$$

$$V_D \approx V_{tp} \tag{7.4}$$

$$V_D = [e(\sigma_A/\sigma_B)+f]\,V_o \tag{7.5}$$

In the above equations, x, e and f are all constants and V_{cB}, V_{tp}, σ_A, and σ_B can all be easily obtained from the literature. Equations (7.3) and (7.4) are dependent on

Table 7.3

van der Waals Volumes, Molecular Diameters and Molecular Weights for all Solutes and Solvents

Compound	van der Waals Volume[a] V_{VDW} ($m^3 \cdot kmol^{-1}$)	Molecular Diameter[b] σ (Angstroms)	Molecular Weight M ($kg \cdot kmol^{-1}$)
Propane	0.0376	4.9205	44.096
Propene	0.0341	4.7632	42.080
Ammonia	0.0138	3.5239	17.030
Carbon Dioxide	0.0197	3.9678	44.010
Methanol	0.0217	4.0984	32.042
Ethanol	0.0319	4.6613	46.069
Propanol	0.0422	5.1136	60.096
Butanol	0.0524	5.4976	74.122

[a] The van der Waals volume, V_{VDW}, represents the hard core volume of one mole of molecules.

[a] Molecular diameter, σ, represents the diameter of an equivalent spherical molecule using the van der Waals volume.

solvent properties only and equation (7.5) is a function of both solute and solvent properties.

Similarly, if β is expressed in terms of known variables, then along with the expression for V_D and equation (3.35), D°_{AB} can be predicted. Before examining expressions for β, the effect of temperature on the roughness factor, F, will be investigated. As shown in equation (3.36), β is a function of F. One of the assumptions of the Enskog theory is that the molecules are spherically symmetrical and smooth and thus only kinetic energy is exchanged. However, the smoothness assumption of Enskog is not valid for colliding polyatomic molecules, where it is possible that in addition to kinetic energy, rotational energy is exchanged and this acts to reduce the diffusion coefficient. Chandler (1975) showed that the use of a roughness factor, F, accounts for the reduction in the diffusion coefficient due to the exchange of both kinetic and rotational energy. Thus for smooth molecules, F=1 and for rough molecules $F \leq 1$. Chandler also claimed that F is a constant for each system and is independent of the density and the temperature of the system. The value of F has been found by many researchers, upon examining only a few systems to be essentially constant and independent of temperature. The systems investigated included alkane-alkane systems, self-diffusing systems and non-associating systems (Chandler, 1975; Parkhurst and Jonas, 1975; Baleiko and Davis, 1974; Evans *et al.*, 1981; and Bertucci and Flygare, 1975). Wong (1989), Matthews (1986) and Rodden (1988) all found β to be a constant and a function of the solute and solvent properties. From equation (3.36), β is a function of F. Thus if F is a function of temperature, then β is a function of temperature and if F is not a function of temperature, then β is a constant independent of temperature and dependent only on the properties of the solute and the solvent. It was assumed by Rodden (1988) that β was independent of temperature and as such F was a constant independent of temperature for the n-alkane systems of infinitely dilute solutes in solvents. Using Rodden's data, Erkey et al. (1989) concluded that the translational-rotational coupling parameter, F, for each binary n-alkane system is a function of temperature. This contradicts Chandler's treatment. Dymond (1985) reported an observation similar to that of Erkey et al. (1989) for tracer diffusion in octamethylcyclotetrasiloxane. Erkey et al. (1989) found for the n-alkane systems that F increases with increasing temperature. This thus implies that as the temperature increases, β increases with a consequent increase in the diffusivity, as is expected. The expected trend of increasing diffusivity with

increasing temperature could possibly explain why the temperature effect on F has not been thoroughly examined. Erkey et al. (1989) also found that F decreases with increasing molecular mass and size which implies that β and subsequently D°_{AB} decreases at any one temperature and for all temperatures. Erkey 's observations and the resulting implications could simply apply to infinitely dilute n-alkane systems. Thus for the alcohols systems used in this work, the effect of temperature on β will be examined to determine whether β is a function of temperature as well as the solute and solvent properties and this will then be used in the correlation for the prediction of the infinite dilution diffusion coefficients.

Before this is done, a linear regression analysis is performed on the data to determine whether the linear relationship tnat exists between $D^{\circ}_{AB}/\sqrt{T}$ and V provides a better fit with $V_D = V_{tp}$ or with $V_D = b\ V_o$ at $D^{\circ}_{AB} = 0$. Further the effect of a temperature dependent β is examined. With the use of $V_D = V_{tp}$ and with β as a function of temperature, the regression analysis on each solute at each temperature in each solvent is illustrated in Figures 7.6A and 7.6B for ethanol and butanol, respectively. Similar plots were obtained for methanol and propanol. A better fit was obtained with β as a function of temperature.

Several expression for β were attempted. The variables used in these expressions included the variables from equation (3.36) where β is a function of σ_A, σ_B, M_A, and M_B. The temperature was also another variable which was used in the attempt to determine whether β is a function of temperature. The final expression for β which best represented the data included the variables the molecular weights and diameters of the solute and the solvent molecules and the temperature.

It was also found that the final expression for V_D which best represented the data included the diameters of the solute and solvent molecules. The final expression for V_D which best represented the data is given in equation (7.5).

$$V_D = [d(\sigma_A/\sigma_B) + e]V_o \tag{7.5}$$

The final expression for β which best represented the data is given by the following equation:

$$\beta = \frac{a_1 M_A^b M_B^c}{(\sigma_A \sigma_B)^d} T^e \tag{7.6}$$

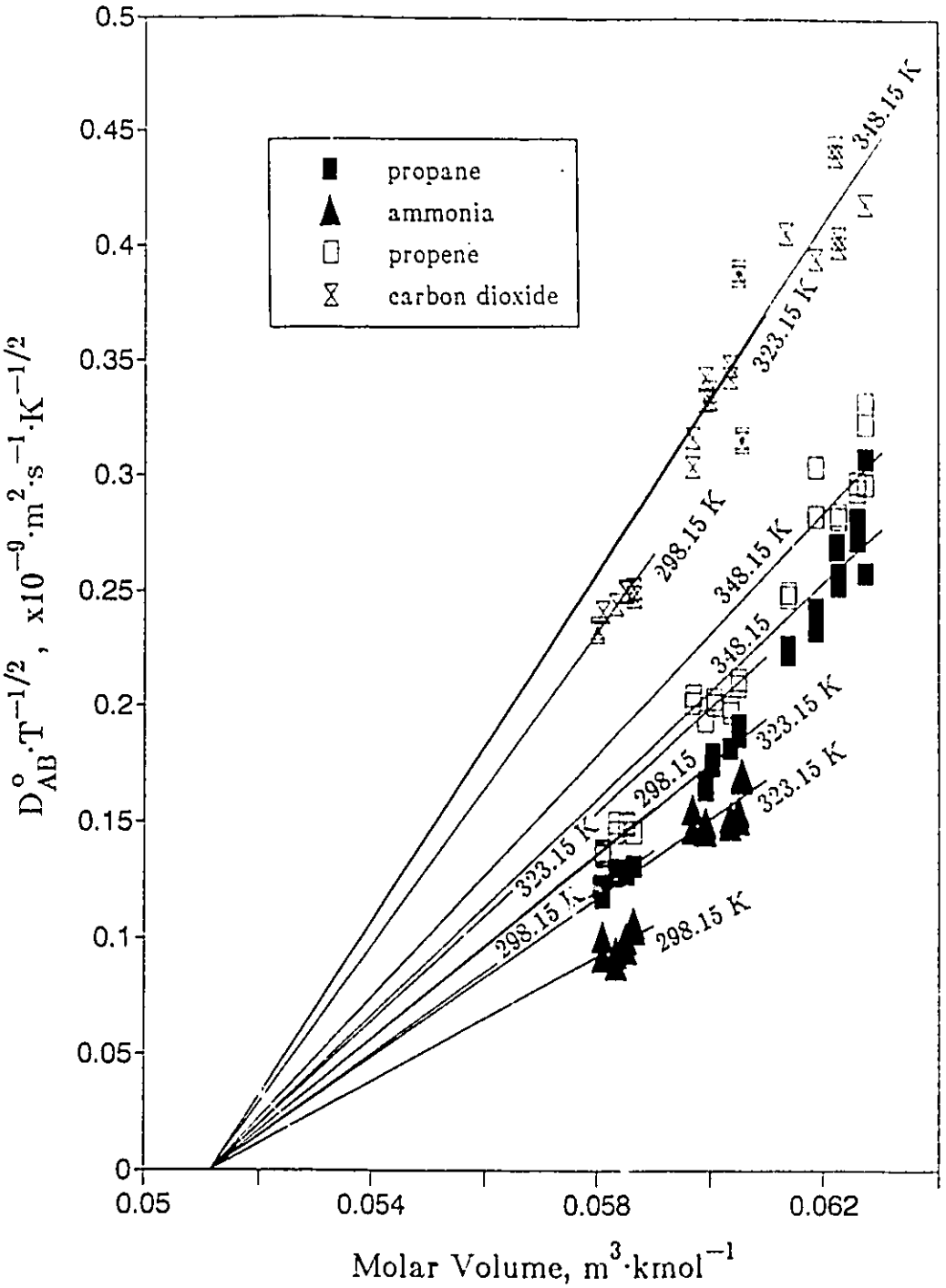

Figure 7.6A: Linear Behaviour of $D^{\circ}_{AB} \cdot T^{-1/2}$ versus V as a Function of Temperature in the Solvent Ethanol Over the Entire Pressure Range Using V_{tp}

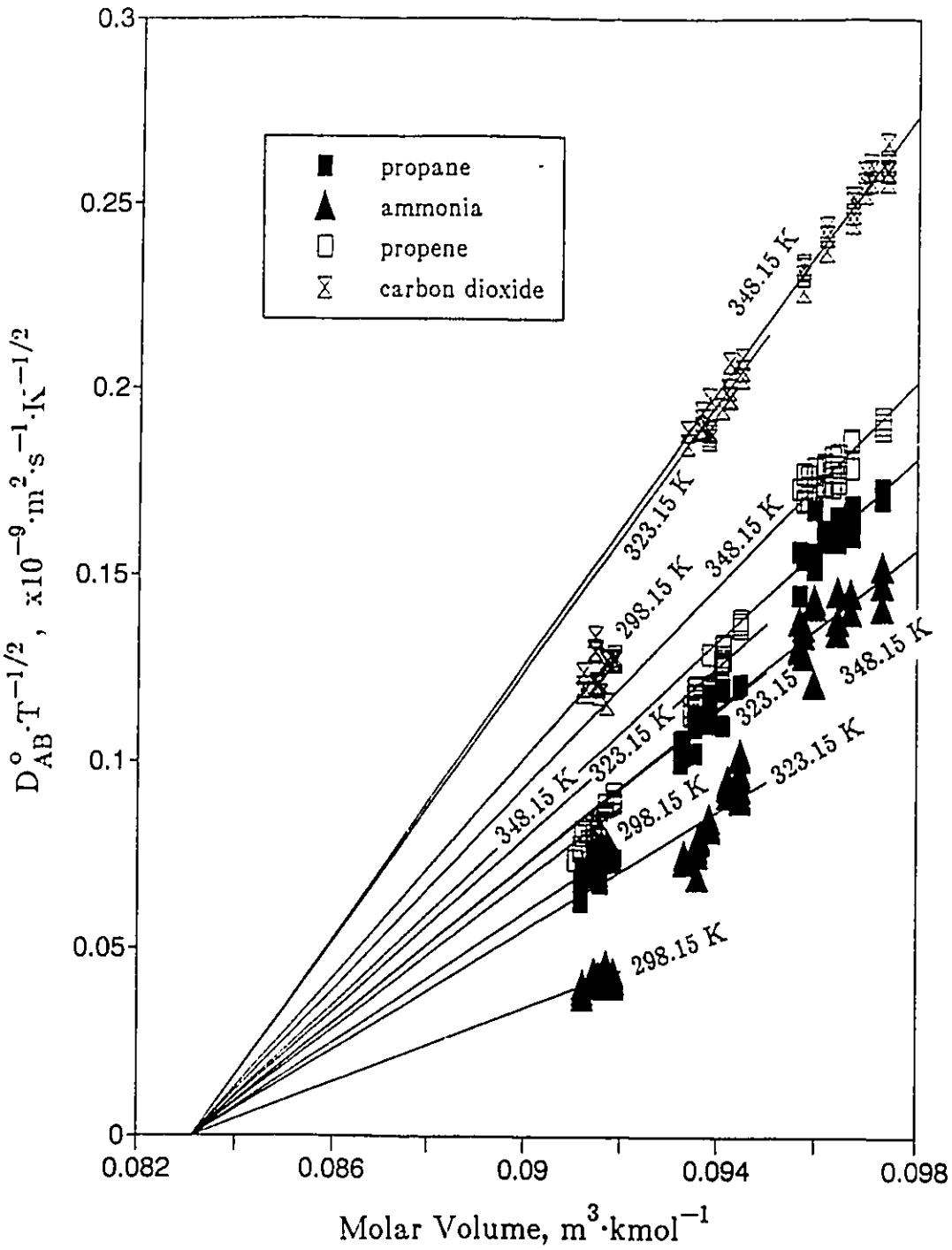

Figure 7.6B: Linear Behaviour of $D^{\circ}_{AB} \cdot T^{-1/2}$ versus V as a Function of Temperature in the Solvent Butanol Over the Entire Pressure Range Using V_{tp}

Some of the steps leading up to the final expressions for V_D and β include the use of equations (7.3), (7.4), and (7.5) for predicting V_D and the stepwise regression analysis of the variables given in equation (3.36) along with the temperature to obtain an equation for β. It was found that V_D can be more accurately predicted using V_{tp} than V_{cB}. It was also found that the standard error of the coefficient for the slope β where β is a function of temperature is smaller than that where β is independent of temperature. This thus supports the claim that β is a function of temperature. The use of $V_D = V_{tp}$ and β as a function of temperature is illustrated in Figures 7.6A, and 7.6B for ethanol, and butanol, respectively. Similar plots were obtained for methanol and propanol. However, it was found that V_D was more accurately predicted using equation (7.5) where it is a function of σ_A and σ_B than V_{tp}. Again a better correlation was obtained with β as a function of temperature. Thus from the non-linear regression analysis on the systems examined in this work which included the solutes propane, propene, ammonia and carbon dioxide in the solvents methanol, ethanol, propanol and butanol at infinite dilution, the final form of the equation which gave the best fit was:

$$\frac{10^9 D^\circ_{AB}}{\sqrt{T}} = \frac{.0951 M_A^{1.2141} M_B^{.1118}}{(\sigma_A \sigma_B)^{3.3131}} (V - b V_o) T^{1.8465} \qquad (7.7)$$

The expression for b which best represents the data from the regression analysis is given by :

$$b = [-0.1641 (\sigma_A / \sigma_B) + 1.3339] \qquad (7.8)$$

In equation (7.7), D°_{AB} is in m^2/s, T is the temperature in Kelvin, the molecular weights M_A and M_B are in kg/kmol, the molecular diameters σ_A and σ_B are in Angstroms, and the molar volumes V and V_o are in m^3/kmol. The expression for V_o is given by equation (3.19) and the expression for b by equation (7.8). The molar volume of the pure solvent, V (=V_B), is obtained from the density data at the system conditions. The physical interpretation of equation (7.7) includes the following. The equation predicts that as the molecular diameter of the solute and the solvent molecules increases, the molecular diffusivity decreases. The equation also predicts that as the molecular weight of the solute increases in any one solvent, the molecular diffusivity increases. This is not the expected trend. However, as observed from the

data, low molecular weight ammonia has the lowest diffusivity possibly due to the attractive forces from the hydrogen bonding. The molecular weight of propane is only slightly larger than that of carbon dioxide but carbon dioxide has the largest diffusivity, possibly because its dipole moment is zero. Equation (7.7) seems to be more strongly influenced by the size, σ of the solute and solvent molecules than their molecular weights.

Figures 7.7A to 7.7D illustrate that equation (7.7) represents the data very well for methanol, ethanol, propanol and butanol, respectively. From these plots of $D^{o}_{AB}/\sqrt{T}$ versus V, the slopes of the lines represent β and it is observed that for each solvent the value of β is dependent on the type of solute and the temperature used. From the nonlinear regression analysis, the average absolute percent error of fit from the experimental data was 6.6%. Thus Figures 7.7A to 7.7D show that β is dependent on the temperature and V_D is dependent on the type of solute used. Figure 7.8 is a plot of the diffusivities predicted from equation (7.7) versus the measured diffusivities. Figure 7.8 shows that carbon dioxide appears to deviate the most from its measured value. This could possibly be due to the negative peaks obtained during measurement. This could also possibly be due to the fact that carbon dioxide does not follow the trend of the other solute gases of increasing σ with increasing molecular weight, M_A. The solute gases increase in M_A in the order: $NH_3 < C_3H_6 < CO_2 < C_3H_8$ and σ_A increase in the order: $NH_3 < CO_2 < C_3H_6 < C_3H_8$.

For the case of self diffusion, the expression for b is reduced to a constant 1.1698. With b=1.1698, the product bV_o agrees closely with V_{tp} (Table 7.4). The intercept V_D for self diffusion data was defined as the molar volume at which diffusion ceases, that is, at the freezing point of the solvent. Thus this agreement supports the theoretical basis of V_D for the case of self diffusion. Table 7.4 also lists the range of V_D due to the different solutes used, and van der Waals volume from the literature. It is observed from Table 7.4 that the van der Waals volume, V_{VDW}, which is a function of the solvent properties only, is not equal to V_D from the experimental data for mutual diffusivity. Also since V_{tp} and bV_o agree closely and they are functions of the properties of the solvent only, this suggests that the intercept V_D is a function of the properties of the solution which comprises of the solute and solvent molecules.

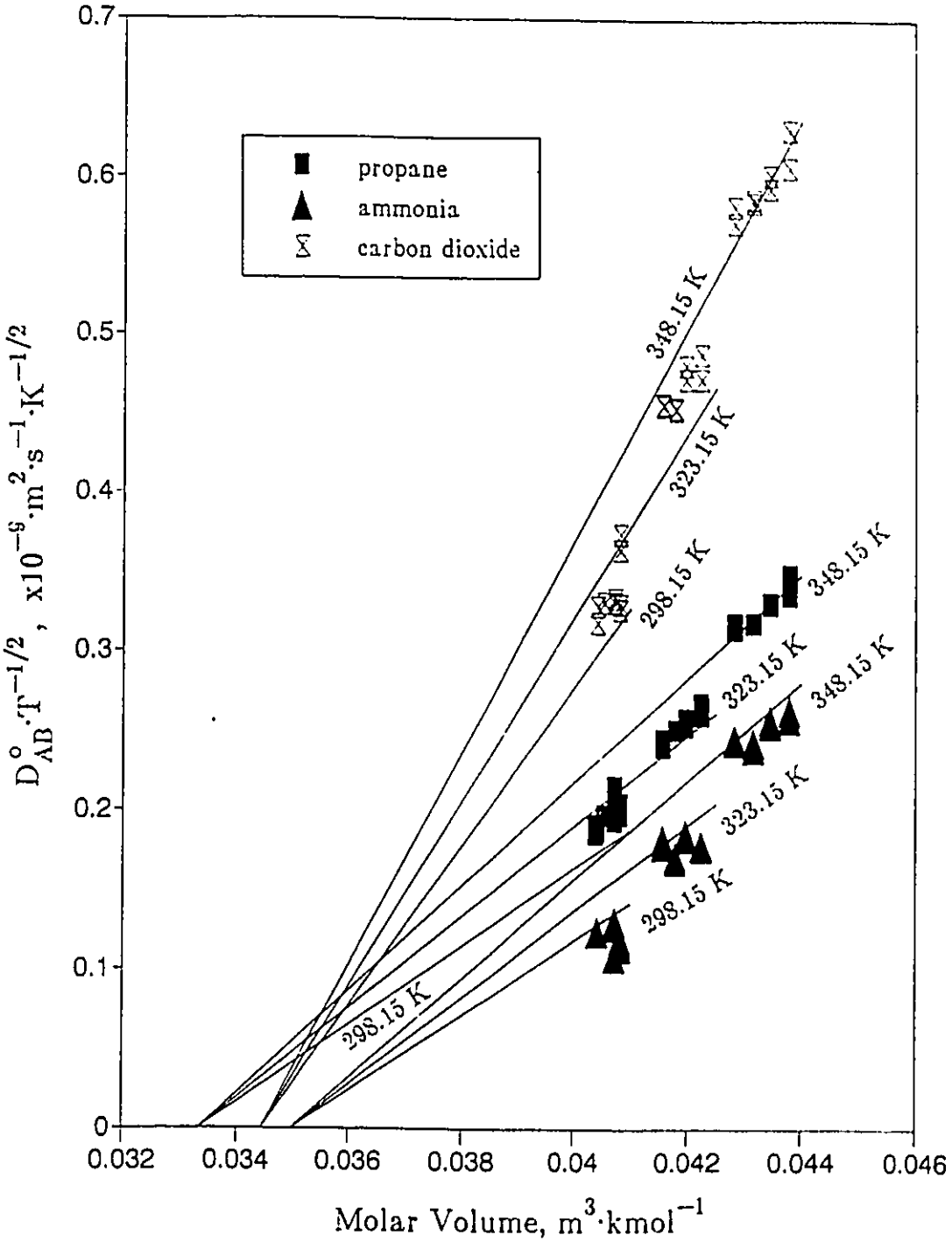

Figure 7.7A: Linear Behaviour of $D^{\circ}_{AB} \cdot T^{-1/2}$ versus V as a Function of Temperature in the Solvent Methanol Over the Entire Pressure Range

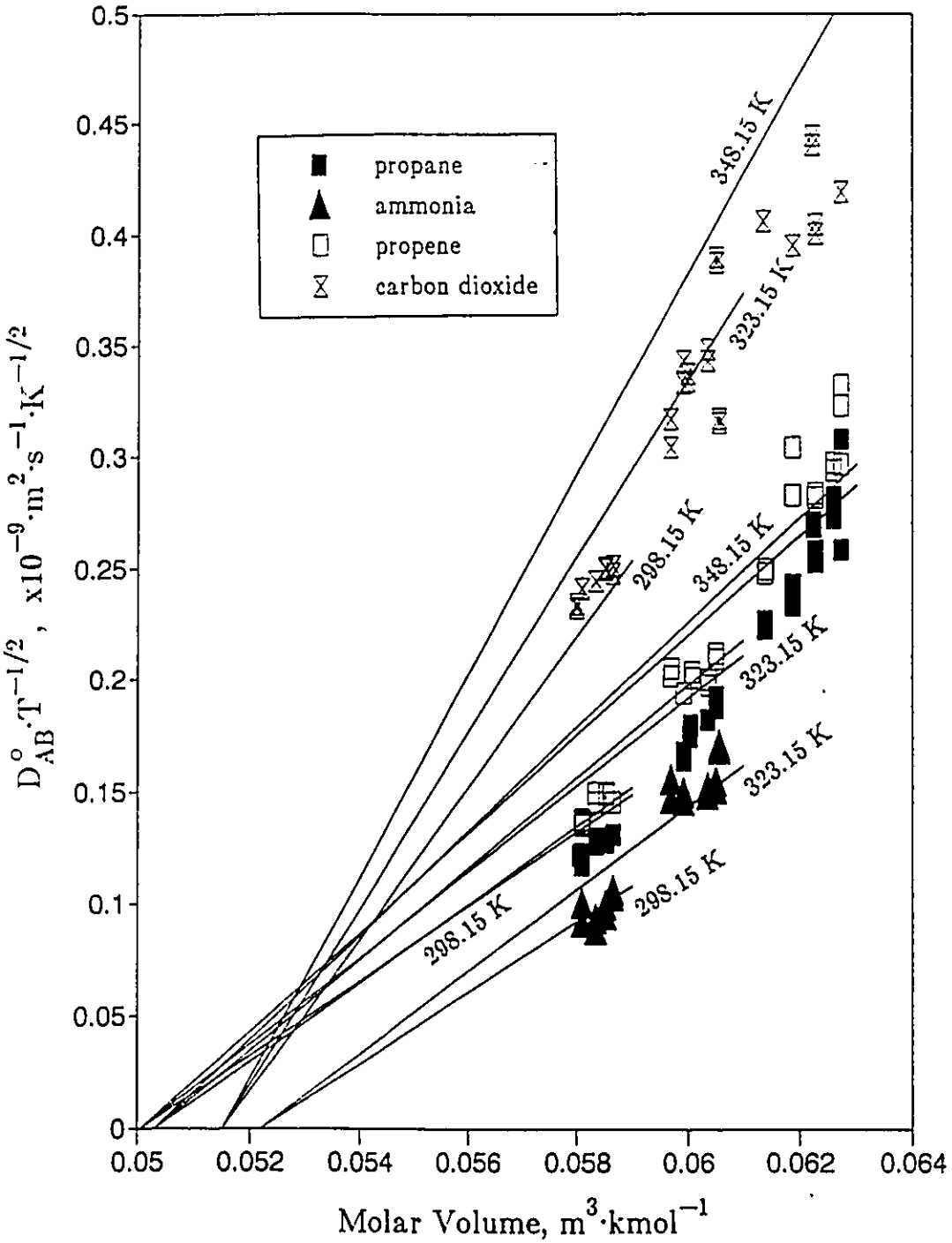

Figure 7.7B: Linear Behaviour of $D^{\circ}_{AB} \cdot T^{-1/2}$ versus V as a Function of Temperature in the Solvent Ethanol Over the Entire Pressure Range

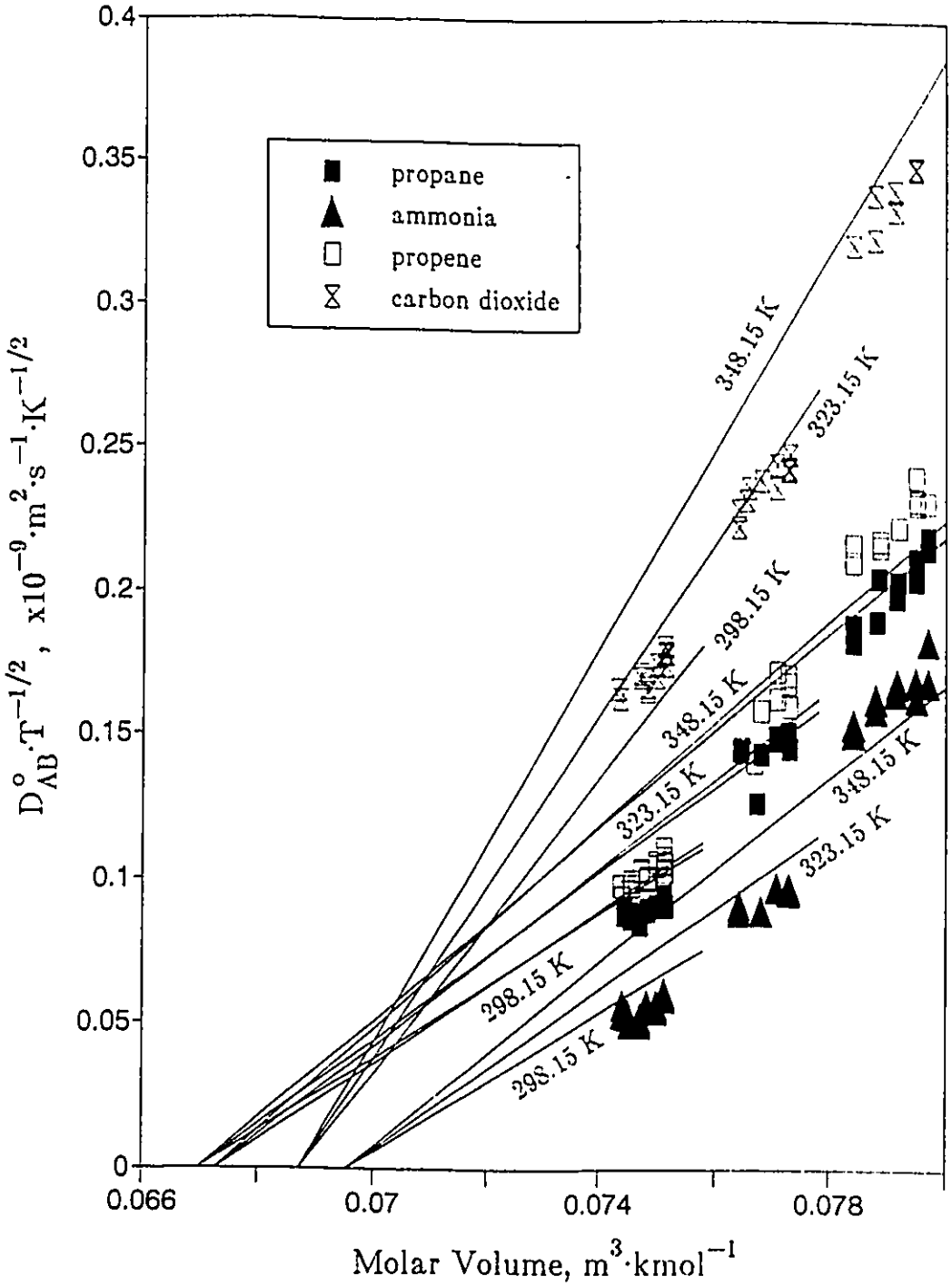

Figure 7.7C: Linear Behaviour of $D^{\circ}_{AB} \cdot T^{-1/2}$ versus V as a Function of Temperature in the Solvent Propanol Over the Entire Pressure Range

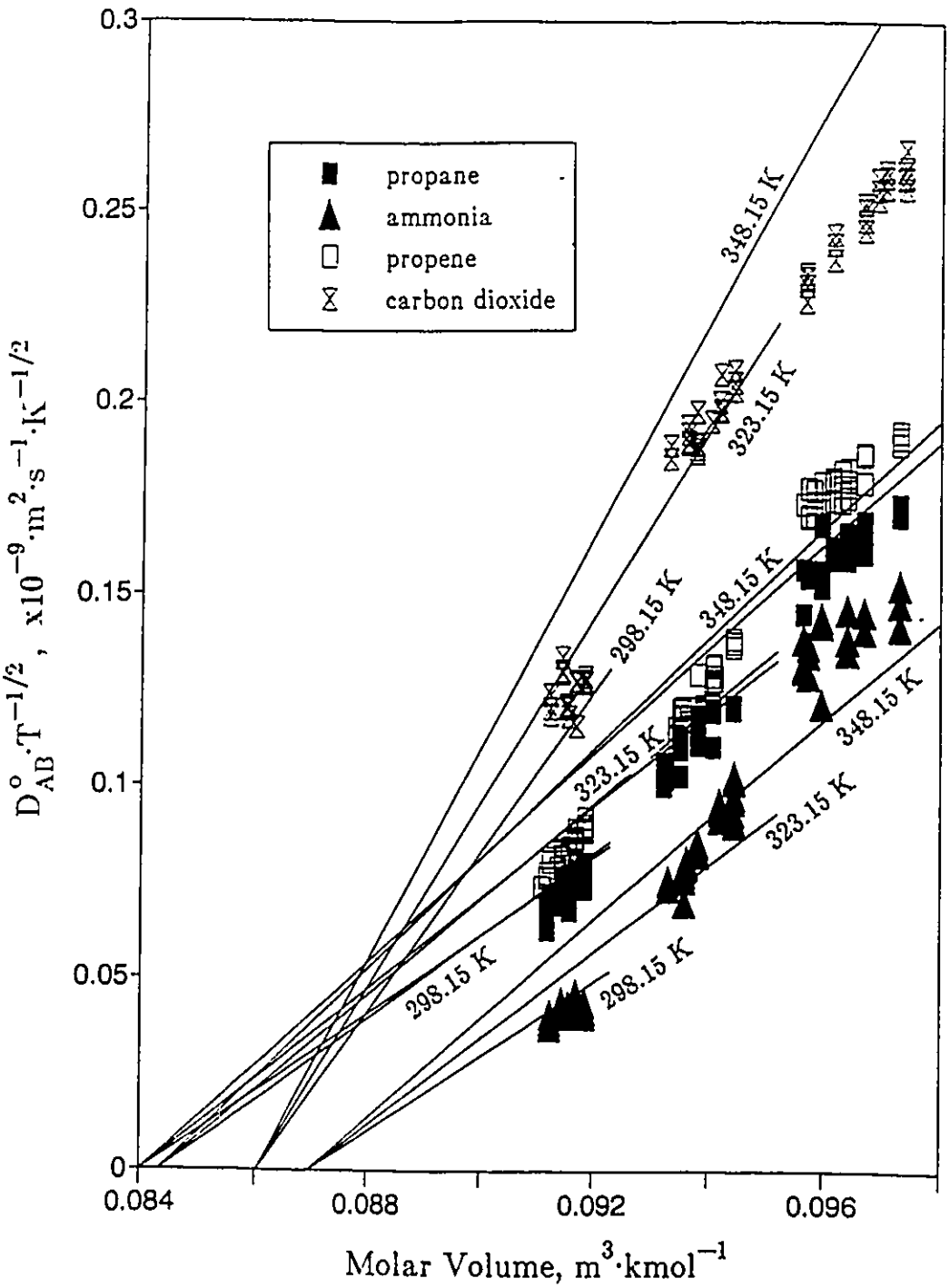

Figure 7.7D: Linear Behaviour of $D^{\circ}_{AB} \cdot T^{-1/2}$ versus V as a Function of Temperature in the Solvent Butanol Over the Entire Pressure Range

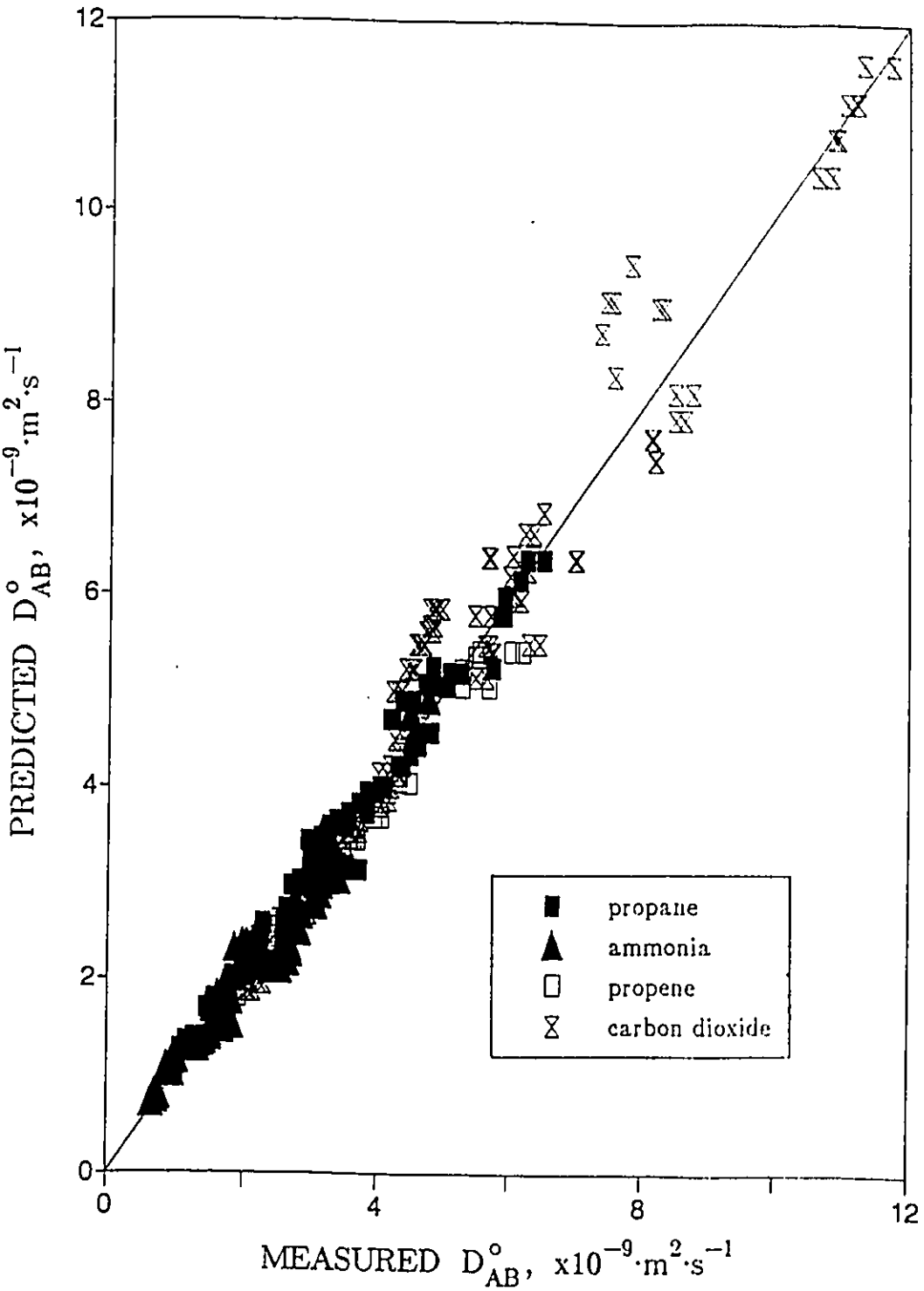

Figure 7.8: Comparison of the Measured Diffusivities to the Calculated Diffusivities for the Gaseous Solutes in the Alcohol Solvents

Table 7.4

Comparison of System
and Solvent Molar Volumes

Solvent	$V_{D,\ expt}$ Expt. $m^3 \cdot kmol^{-1}$	$V_{tp,\ liq}$ Theo. $m^3 \cdot kmol^{-1}$	$1.1698\,V_o$ Expt. $m^3 \cdot kmol^{-1}$	V_{VDW} Theo. $m^3 \cdot kmol^{-1}$
Methanol	0.0364-0.0382	0.0363	0.0343	0.0217
Ethanol	0.0546-0.0551	0.0511	0.0505	0.0319
Propanol	0.0712-0.0745	0.0652	0.0666	0.0422
Butanol	0.0874-0.0896	0.0831	0.0828	0.0524

Equation (7.7) can thus be used, with a good degree of accuracy to predict diffusion coefficients at infinite dilution for dissolved solute gases of various polarities and dipole moments in alcohol solvents over a large pressure range. This equation is based on the RHS theory, and shows the linear relationship between $D^{\circ}_{AB}/\sqrt{T}$ and V. This linear relationship was proved to be true for self diffusion data by Dymond (1974) using molecular dynamics data. Equation (7.7) is a simple one requiring only the physical properties of the solute and the solvent - σ_A, σ_B, M_A, M_B, and V, which can be easily obtained from the literature. The simplicity and the goodness of predictability of the equation shows promise for a generalized correlation for diffusion coefficients over a wide range of temperatures and pressures.

CHAPTER 8

CONCLUSIONS

Several modifications have been made to the basic Taylor dispersion apparatus. These include the use of a computerized data acquisition system, programs written in the C programming language for analysis of this data, improvements in solvent deaeration, improved solvent flow control, calibration of the equipment for density measurement, installation of capillary tubing and a DP cell for viscosity measurement, and improved control of system pressure. The Taylor dispersion apparatus has thus become a versatile tool for obtaining transport data at high pressures and over a reasonable temperature range.

A significant quantity of data was obtained for the infinite dilution diffusion coefficients of the solute gases propane, propene, ammonia and carbon dioxide in methanol, ethanol, propanol, and butanol at temperatures of 298.15, 323.15 and 348.15 K for pressures ranging up to 17 MPa (2500 psig) using this equipment. The diffusivities of all solute-solvent pairs decreased linearly with increasing pressure and increased with increasing temperature. There was a decrease of approximately 0.3-1.2% in diffusivity per MPa increase in pressure, and an increase in diffusivity of about 30-90% resulting from an increase in temperature from 298.15-323.15 K at atmospheric pressure. The effect of pressure on the diffusion coefficient was greatest for the solute gas carbon dioxide and smallest for ammonia in all the solvents. It was also found that the effect of pressure on diffusivity increased as the solvent chain length increased. At any one temperature and over the entire pressure range, the diffusivity of any one solute decreased as the chain length of the solvent molecule increased. Thus, the diffusion coefficient of each solute was greatest in methanol and decreased in order in ethanol, propanol, and butanol.

The different properties of the solute gases were found to distinctly influence the diffusion of these gases through the homologous alcohol solvents used, with respect to the effect of hydrogen bonding, dipole moment, polarity, association, molecular mass, size and the resulting molecular interactions between the solute and the solvent molecules.

Of the solutes used only ammonia could be expected to form relatively strong hydrogen bonds with the solvent alcohols. These strong solute-solvent interactions were found to strongly influence diffusivity since ammonia was the smallest of all the solute molecules used in this study yet it had the lowest diffusivity in each solvent.

The other solutes, carbon dioxide, propene, and propane have weak London forces of attraction to the solvents. For these solutes the effect of molecular size seems to predominate in determining the diffusion coefficient. Although propene is more polar and has a larger dipole moment than propane, the diffusion coefficient of propene is larger because its molecular weight and size are smaller. Carbon dioxide had the smallest molecular size and the highest diffusivity.

The molecular diffusivities of the solute gases could also be attributed in part to their shape or degree of linearity, since it has been found that linear molecules tend to diffuse faster than spherical ones. The triangular pyramidal molecule ammonia is the most spherical of all the solute molecules with the smallest diffusivity, while carbon dioxide is the most linear of all the solute molecules and showed the largest diffusivity.

The RHS correlation was used to describe the diffusivity data. The linear relationship between $D^{\circ}_{AB}/\sqrt{T}$ and V for the experimental data confirms the theoretical basis of the RHS equation for the solute-solvent pairs in this study. This linear relationship for each pair means that the slope, β, was independent of the molar volume. The slopes, β, and intercepts, V_D, were generalized in such a way that only σ_A, σ_B, M_A, M_B, and T, were necessary to predict β and V_D and thus D°_{AB}. From nonlinear regression analysis, the average absolute error of fit from the experimental data was 6.6%.

Density data was obtained as a function of temperature and pressure for the solvents methanol, ethanol, propanol and butanol using Taylor's method. The temperatures examined were 298.15, 323.15 and 348.15 K and pressures ranged up to 17 MPa (2500psig). The measured densities of the solvents showed excellent agreement (<0.3%) with those reported in the literature thus confirming the use of the Taylor dispersion method for measuring densities.

Some preliminary viscosity data was obtained as a function of temperature and pressure for methanol and ethanol using the Hagen-Poiseuille method. The temperatures examined were 298.15, 323.15 and 348.15 K and pressures ranged up to 14 MPa (2000psig). The measured viscosities showed excellent agreement (<1.0%) with those reported in the literature thus confirming the use of the apparatus for measuring viscosity.

The viscosity data, like the diffusivity data, also appeared to be described by the RHS correlation. The linear relationship between $\sqrt{T}/\eta$ and V for the experimental data confirms the theoretical basis of the RHS equation.

CHAPTER 9

RECOMMENDATIONS

Since most industrial chemical processes operate at high temperatures and pressures, there is a need for diffusion coefficients at high temperatures and pressures where diffusion is the rate limiting mass transfer process. There is a need not only for mutual diffusion coefficients at infinite dilution, but concentration dependent diffusion coefficients. There is also a desperate need for the measurement of diffusion coefficients at the melting point of the solvent, to determine if the diffusion coefficient is indeed zero.

Future work on molecular dynamics calculations for both mutual and self diffusion data over a wide range of σ_A/σ_B, m_A/m_B, and V/V_o is necessary in order to develop the RHS theory. The existing molecular dynamics ratios from the literature are only for a limited quantity of self diffusion and infinite dilute mutual diffusion data and over a narrow range of σ_A/σ_B, m_A/m_B, and V/V_o. Concentration dependent molecular dynamics ratios for the mutual diffusion coefficients should also be investigated in order to obtain a concentration dependent RHS model. Also experimentally obtained diffusion coefficients as a function of composition should be used in order to develop a concentration dependent RHS model and these diffusion coefficients can then be compared to the diffusivities predicted from the RHS theory using the molecular dynamic ratios.

Future measurements of diffusion coefficients of solutes having various polarities, dipole moment, ability to form H-bonds, and association in the homologous alcohol solvents are necessary in order to facilitate a better understanding of these effects on the diffusion coefficients in one family of solvents. As more and more data are collected, the RHS theory could then be used to develop a more refined predictive equation in diffusion coefficients at infinite dilution, for alcohol solvents, and later for other classes of fluids.

The viscosities of the remaining alcohol solvents propanol and butanol should be measured. Future work on the measurement of the viscosities and densities of various alcohol solvents over a large temperature and pressure range, as well as the

development of the RHS theory for viscosity in liquid alcohol solvents should be done. The viscosities and densities for other families of liquids should also be measured.

The effect of temperature on β should be examined to determine whether the inclusion of the variable temperature gives a significantly better fit for the RHS model for both viscosity and diffusivity for all future data collected.

CHAPTER 10

REFERENCES

Akgerman, A., and J. L. Gainer, J. Chem. Eng. Data, **17**, 372 (1972a)

Akgerman, A., and J. L. Gainer, IEC Fund., **11**, 373 (1972b)

Albright, J. G., and R. Mills, J. Phys. Chem., **69**, 3120 (1965).

Alder, B. J., D. M. Gass, and T. E. Wainwright, J. Chem. Phys., **53**,3813 (1970)

Alder, B. J., and T. E. Wainwright, Phys. Rev. A., **1**, 18 (1970)

Alder, B. J., and J. H. Hildebrand, IEC Fund., **12**, 387 (1973)

Alder, B. J., W. E. Alley and J. H. Dymond, J. Chem. Phys., **61**, 1415 (1974)

Alizadeh, A., C. A. Nieto de Castro, and W. A. Wakeham, Int. J. Thermophys., **1**, 243-284 (1980)

Alizadeh, A. A., and W. A. Wakeham, Int. J. Thermophys., **3**, 307 (1982)

Ananthakrishnan, V., W. N. Gill, and A. J. Barduhn, AIChE J., **11**, 1063 (1965).

Arnold, J. H., J. Am. Chem. Soc., **52**, 3937 (1930)

Aris, R., Proc. Roy. Soc. Lond., **A235**, 67-77 (1956)

Atwood, J. G., and J. Goldstein, J. Phys. Chem., **88**, 1875 (1984)

Bailey, H. R., and W. B. Grogarty, Proc. Roy. Soc., **A269**, 352 (1962)

Baldauf, W. and H. Knapp, Chem. Eng. Sci., **38**, 1031 (1983)

Baleiko, M. O., and H. T. Davis, J. Phys. Chem., **78**, 1564 (1974)

Bartle, K. D., A. A. Clifford, D. Mills and R. Moulder, J. Chem. Soc., Far. Trans. **1**, **85**, 2347-2353 (1989)

Batchinski, A. J., Z. Physik. Chem. **84**, 643 (1913)

Bertucci, S. J., and W. H. Flygare, J. Chem. Phys., **63**, 1 (1975)

Chandler, D., J. Chem. Phys., **62**, 1358 (1975)

Chapman, S., and T. G. Cowling, "The Mathematical Theory of Non-Uniform Gases", Third Ed., Cambridge Univ. Press, London (1970)

Chen, H.-C and S.-H. Chen, IEC Fund., **24**, 187 (1985)

Chen, S.-H., H. T. Davis, and D. F. Evans, J. Chem. Phys., **75**, 1422-1426 (1981)

Chen, S.-H., Ph. D. Diss., Univ. of Minnesota, Minneapolis (1981)

Chen, S.-H., H. T. Davis and D. F. Evans, J. Chem. Phys., **75**, 1422 (1981)

Chen, S.-H, H. T. Davis, and D. F. Evans, J. Chem. Phys., **77**, 2540 (1982)

Chen, S.-H., D. F. Evans, and H. T. Davis, A.I.Ch.E.J. **29**, 640-644 (1983)

Clegg, G. T. and M. A. Tehrani, J. Chem. Eng. Data, **18**, 59 (1973)

Cloeta, C. E., T. W. Smuts, and K. DeClerk, J. Chrom., **120**, 1-15 (1976)

Collings, A. F., D. C. Hall, M. A. McCool and L. A. Woolf, J. of Phys. E: Sci. Instr., **4**, 1019-1024 (1971)

Czworniak, K. J., H. C. Anderson, and R. Pecora, Chem. Phys., **11**, 451 (1975)

Daubert, T. E. and R. P. Danner, "Data Compilation Tables of Properties of Pure Compounds", AIChE J., New York (1985)

Davidson, J. F., and E. J. Cullien, Trans. Instn. Chem. Engrs., **35**, 51-60 (1957)

Dim, A., G. R. Gardner, A. B. Ponter and T. Wood, J. Chem. Eng. (Japan), **4**, 92-95 (1971)

Dymond, J. H., J. Chem. Soc. Farad. Trans. II, **68**, 1789 (1972)

Dymond, J. H., J. Chem. Phys., **60**, 969 (1974)

Dymond, J. H., and L. A. Woolf, J. Chem. Soc. Farad. Trans I, **78**, 991 (1982)

Dymond, J. H., A. J. Esteal, and L. A. Woolf, Chem. Phys., **99**, 397 (1985)

Erkey, C., J. B. Rodden, M. A. Matthews, and A. Akgerman, Int. J. Thermophys., **10**, 5, 953-962 (1989)

Ertl, H., R. K. Ghai, and F. A. L. Dullien, AIChE J., **20**, 1-20 (1974)

Esteal, A. J., L. A. Woolf, and D.L. Jolly, Physica, **121A**, 286 (1983)

Evans, D. F., T. Tominaga, and C. Chan, J. Sol. Chem., **8**, 461-478 (1979)

Evans, D. F., T. Tominaga and H. T. Davis, J. Chem. Phys., **74**, 1298 (1981)

Evans, E. V., and C. N. Kennay, Proc. Roy. Soc., **A284**, 540 (1965)

Eyring, H., J. Chem. Phys., **4**, 283-291 (1936)

Ferrell, R. T., D. M. Himmelblau, AIChE J. **13**, 702-708 (1967)

Ferrell, R. T., D. M. Himmelblau, J. Chem. Eng. Data, **12**, 111-115 (1967)

Fishman, E., J. Phys. Chem., **59**, 469 (1955)

Fürth, R., in Handbuch der Physikalischen und Technischen Mechanik, Barth, Leipzig, **7**, 635 (1931)

Gainer, J. L. and A. B. Metzner, AIChE J. - Int. Chem. Eng. Symp. Series, No. 6 (1965)

Ghai, R. K., H. Ertl, and F. A. L. Dullien, AIChE J., **19**, 881-900 (1973)

Giddings, J. C., S. L. Seager, J. Chem. Phys., **33**, 1579 (1960)

Giddings, J. C., S. L. Seager, IEC Fund., **1**, 277-283 (1962)

Glasstone, S., K. Laidler, and H. Eyring, "The Theory of Rate Processes", McGraw-Hill, New York (1941)

Golay, M. J., J. Chrom., **186** (1979)

Griffiths, A., Proc. Phys. Soc. Lond., **23**, 190 (1911)

Grushka, E. and J. Kikta, J. Phys. Chem. **78**, 2297 (1974)

Grushka, E. and J. Kikta, J. Phys. Chem. **79**, 2199 (1975)

Grushka, E. and J. E. Kikta, Am. Chem. Soc., **98**, 443 (1976)

Halmour, N., and O. C. Sandall, J. Chem. Eng. Data, **29**, 20-22 (1984)

Hayduk, W., "Encyclopedia of Fluid Mechanics", Chapter 3, Gulf Publishing Company, Houston (1986)

Hayduk, W., and S. C. Cheng, Chem. Eng. Sci., **26**, 635 (1971)

Hayduk, W. and V. K. Malik, J. Chem. Eng. Data, **16**, 143-146 (1971)

Hayduk, W., R. Castaneda, H. Bromfield, and R. R. Perras, AIChE J., **19**, 859-861 (1973)

Hayduk, W., and H. Laudie, AIChE J., **20**, 611-615 (1974)

Hayduk, W., and B. S. Minhas, Can. J. Chem. Eng., **60**, 295 (1982)

Herman, P. T. and B. J. Alder, J. Chem. Phys., **56**, 987 (1972)

Hildebrand, J. H., Science, **174**, 490 (1971)

Hildebrand, J. H.,"Viscosity and Diffusivity: A Predictive Treatment", John Wiley and Sons, Inc., New York (1977)

Himmelblau, D. M., Chem. Rev., **64**, 527 (1964)

Hirschfelder, J., D. Stevenson, and H. Eyring, J. Chem. Phys., **5**, 869-912 (1937)

King, C. J., L. Hsueh, and K. W. Mao, J. Chem. Eng. Data, **10**, 348-350 (1965)

Komiyama, H. and J. M. Smith, J. Chem. Eng. Data, **19**, 384 (1974)

Kramers, H., R. A. Douglas and R. M. Ulmann, Chem. Eng. Sci., **10**, 190-191 (1959)

Lebowitz, J. L., Phys. Rev., **133**, A895 (1964)

Levenspiel, O., W. K. Smith, Chem. Eng. Sci., **6**, 227-233 (1957)

Lusis, M.A. and G. A. Ratcliff, Can. J. Chem. Eng., **46**, 385 (1968)

Malik, V. K. and W. Hayduk, Can. J. Chem. Eng., **46**, 462 (1968)

Marvin, R. S., J. Res. Nat. Bur. Standards, **75A**, 535 (1971)

Matthews, M. A., "Diffusion Coefficients at Infinite Dilution in n-Alkane Solvents at Temperatures to 573 K and Pressures to 3.5 MPa", Ph.D. Diss., Texas A&M Univ. (1986)

Matthews, M. A. and A. Akgerman, AIChE J., **33**, 881-885 (1987)

Maynard, V. R., and E. Grushka, Adv. Chrom., **12**, 99 (1965)

Mazarei, A. F. and O. C. Sandall, AIChE J., **26**, 154-157 (1980)

McCool, M. A., A. F. Collings, and L. A. Woolf, J. Chem. Soc. Fara. Trans. I, **68**, 1489-1497 (1972)

McCool, M. A., and L. A. Woolf, High Temp. High Press., **4**, 85-95 (1972)

Mills, R., J. Phys. Chem., **69**, 3116 (1965)

Moore, J. W., and R. M. Wellek, J. Chem. Eng., Data, **19**, 136 (1974)

Nakanishi, K., E. M. Voigt and J. H. Hildebrand, J. Chem. Phys., **42**, 1860-1863 (1965)

Nunge, R. J., R. S. Lin, and W. N. Gill, J. Fluid Mech., **51**, 363 (1972)

Olander, D. R., AIChE J., **9**, 207 (1963)

Onda, K., T. Okamoto, and Y. Yamaji, Chem. Eng., Tokyo, **24**, 918-925 (1960)

Onda, K., H. Takeuchi, and M. Fujine, J. Chem. Eng. (Japan), **8**, 25 (1975)

Ouano, A. C., IEC Fund., **11**, 268 (1972)

Ouano, A. C. and J. A. Carothers, J. Phys. Chem., **79**, 1314 (1975)

Parkhurst, H. J., and J. Jonas, J. Chem. Phys., **63**, 2698 (1975)

Peter, S., and M. Weinert, Z. Phys. Chem, Neue Folge, **9**, 49 (1956)

Pfeiffer, W. F., and I. M. Krieger, J. Phys. Chem., **78**, 2516-2521 (1974)

Pratt, K. C., D. H. Slater, and W. A. Wakeham, Chem. Eng. Sci., **28**, 1901-1903 (1973)

Pratt, K. C., and W. A. Wakeham, Proc. Roy. Soc. A, **330**, 393 (1974)

Pratt, K. C., and W. A. Wakeham, J. Phys. Chem., **79**, 2198 (1975a)

Pratt, K. C., and W. A. Wakeham, Proc. Roy. Soc. A, **342**, 401 (1975b)

Radeke, K. H., IEC Fund., **20**, 302 (1981)

Reid, R. C., J. M. Prausnitz and T. K. Sherwood, "The Properties of Gases and Liquids", 3rd Edition, McGraw-Hill, New York (1977)

Reid, R. C., J. M. Prausnitz, and B. E. Poling, "The Properties of Gases and Liquids", 4th Edition, McGraw-Hill, New York (1987)

Rodden, J. B., "Diffusion Coefficients for Several Dilute Solutes in n-Eicosane, n-Octacosane, and Fischer-Tropsch Wax at 373-533 K", Ph.D. Thesis, Texas A&M Univ. (1988)

Rossi, C. and E. Bianchi, Nature, **189**, 822 (1961)

Shelton, W. W., Ph. D. Diss., Univ. of Minnesota, Minneapolis (1981)

Siddiqi, M. A., and K. Lucas, Can. J. Chem. Eng., **64**, 839-843 (1986)

Sovova, H., Collect. Czech. Chem. Comm., **41**, 3715 (1976)

Sridhar, T., and O. E. Potter, AIChE J., **23**, 590-592 (1977a)

Sridhar, T., and O. E. Potter, AIChE J., **23**, 946-948 (1977b)

Sun, C. K. J., and S.-H. Chen, AICHE J., **31**, 1510 (1985)

Sun, C. K. J., and S.-H. Chen, AIChE J., **31**, 1904-1910 (1985)

Sun, C. K. J., and S.-H. Chen, Chem. Eng. Sci., **40**, 2217-2224 (1985)

Sun, C. K. J., and S.-H. Chen, IEC Res., **26**, 815-819 (1987)

Sutherland, W., Phil. Mag., **9**, 781 (1905)

Takahashi, M., Y. Kobayashi and H. Takeuchi, J. Chem. Eng. Data, **27**, 328-331 (1982)

Takenihi, H., M. Fujine, T. Sato and K. Onda, J. Chem. Eng. (Japan), **8**, 252-253 (1975)

Tang, Y. P., and D. M. Himmelblau, A.I.Ch.E.J., **11**, 54-58 (1965)

Taylor, G., Proc. R. Soc. Lond., **A219**, 186-203 (1953)

Taylor, G. I., Proc. Phys. Soc. B, **67**, 857 (1954a)

Taylor, G., Proc. R. Soc. Lond., **A225**, 473-77 (1954b)

Tham, M. J., K. K. Bhatia, K. E. Gubbins, Chem. Eng. Sci., **22**, 309 (1967)

Tham, M. K., R. D. Walker Jr., and J. H. Modell, J. Chem. Eng. Data, **18**, 411 (1973)

Topakoglu, H. C., J. Math. Mech., **16**, 1321 (1969)

Tyn, M. T. and W. F. Calus, J. Chem. Eng. Data, **20**, 106-109 (1975)

Tyrrell, H. J. V., and K. R. Harris, "Diffusion in Liquids, A Theoretical andExperimental Study", Butterworths Monographs in Chemistry, London (1984)

Umesi, N. O. and R. P. Danner, IEC Proc. Des. Dev., **20**, 662-665 (1981)

Vivian, J. E., C. J. King, AIChE J., **10**, 220 (1964)

Wakeham, W. A., and D. J. Slater, J. Phys. (B), **6**, 886 (1973)

Wilhoit, R. C. and B. J. Zwolinski, "Physical and Thermodynamic Properties of Aliphatic Alcohols", ACS, AIP, New York (1973)

Wilke, C. R., and P. Chang, AIChE J., **1**, 264 (1955)

Wong, C.-F., "Diffusion Coefficients of Dissolved Gases in Liquids", Ph.D. Thesis, Univ. of Ottawa (1989)

Wong, C.-F. and W. Hayduk, Can. J. Chem. Engr., **68**, 849-859 (1990a)

Wong, C.-F. and W. Hayduk, J. Chem. Engr. Data, **35**, 323-28 (1990b)

APPENDIX A

LINEARITY TEST FOR THE DETECTOR

The linear response of the detector is a check to ensure that the signal given by the detector is a linear function of the concentration of the solute. The voltage signal produced by the differential refractometer is caused by the differences in refractive indices of the dissolved solute in the solvent in the sample cell and the pure solvent in the reference cell. Taylor dispersion experiments were performed several times using several solute concentrations. In order to prevent weight loss, the liquid with the higher boiling point was weighed first. Thus, butanol which was the solvent used in this experiment was weighed first, followed by the more volatile hexane, the solute. Both liquids were degassed prior to weighing in an attempt to eliminate any possible impurities. The mixture was kept in a sealed vial to prevent weight loss due to evaporation. The sum function of concentration with time as given by equation (4.37) was calculated for each peak. These values are tabulated in Table A.1 along with the concentrations of hexane in butanol. Figure A.1 shows a plot of the area under the peak or the sum function versus the mole fraction of n-hexane expressed in percent. A straight line was obtained with intercept zero showing that the detector signal was a linear function of the concentration of the solute.

TABLE A.1

Data for the Linearity Test for the Detector

Mole Percent n-Hexane	Area of Peak cm^2
0.95722	4.83
0.95722	4.88
0.95722	4.92
1.5174	6.88
2.14145	8.96
2.14145	9.01
2.14145	9.13
4.2430	16.61
5.85182	22.35
7.6945	28.77
9.63455	35.25

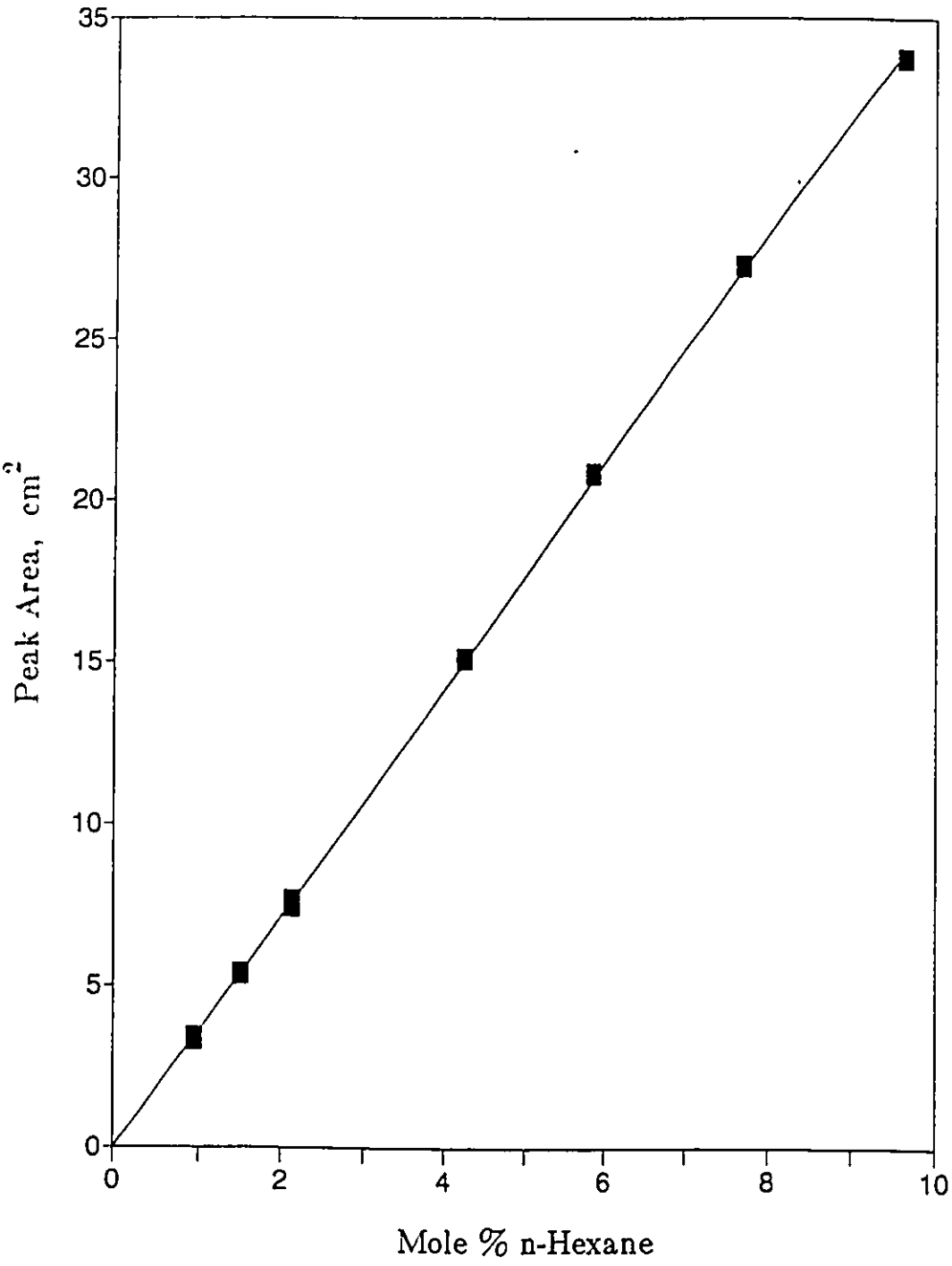

Figure A.1: Plot of Peak Area vs. Mole Percent n-Hexane for the Detector Linearity Test

APPENDIX B

DESCRIPTION OF THE ANALYSIS OF MUTUAL DIFFUSIVITY DATA AT INFINITE DILUTION FROM TAYLOR DISPERSION MEASUREMENT

B.1 Introduction

Analysis of the data accumulated in each run was carried out using two programs written in the C programming language. This appendix will describe these programs and briefly outline the calculation procedures used. The descriptions are divided into two major sections. The first is an overview of the input to the programs and the output produced by them while the second part will provide more details of the calculation procedures.

B.2: Program 1

B.2.1 AN OVERVIEW

The first program has two input files. These files, which are labeled by the name of the run, are saved in a subdirectory of the AD directory on the C drive of the data acquisition computer by the Labmaster Data acquisition system. The first of these, the SETUP file, contains information of a general nature about the run such as the sampling frequency, total run time and the gain for each channel of the A/D converter. The second file, the CHANNEL.0 file, contains the digitized voltage for the signal produced by the differential refractometer. In order to be used by the first program these files were copied onto a floppy disk. The directory structure of the floppy disk was similar to that of the original files (that is, A:\AD\Runname\setup and A:\AD\Runname\channel.0).

Program 1 uses the information in these two input data files to reproduce the voltage time pairs observed during the run. From this data, injection times and time voltage pairs for the peaks are selected in a manner that will be described in more detail in sections B.2.3 and B.2.4.

This program produces four output files, two on the C drive that are replaced the next time the program is run and two on the floppy disk. The most important file is the A:\AD\Runname.RLT file which contains the run data that is used as input to the second program after checking injection times and peak data and adding pressure, temperature and mass flow rate data.

The other file on the floppy disk is the A:\AD\Runname.ABV file. This file contains all the information from the setup file as well as time-voltage data in the region of injections and changes in baseline. This file is used to check to be sure the data acquisition system was configured properly and to check for injections that have been misinterpreted as changes of baseline by the program.

There are two files on the hard drive. The C:\QC2\TEST.TMP is a text file that contains all the time-voltage pairs for the entire run in ASCII format. With the aid of a word processor program data from this file can be scanned for missed injections or time-voltage data can be copied to the .RLT file when for one reason or another a peak is missed by the program.

The other file on the C drive is the C:\QC2\TEMP.TMP file. This is a binary file containing all the time-voltage data for the run. This is the file used by Program 1 to temporarily store the experimental data.

As was previously mentioned, both of these files on the C drive are replaced each time program 1 is run.

B.2.2. STORAGE OF TIME-VOLTAGE PAIRS BY LABMASTER

In order to understand how the time-voltage pairs are recovered from the data files saved by Labmaster after the run it is necessary to understand the data files themselves. The channel.0 file contains no time information as such so each voltage is assumed to be one time increment (=1/frequency) after the previous voltage. The frequency of sampling is obtained from the setup file.

To provide an elementary form of data compression Labmaster does not simply save digitized voltage in the channel.0 file. Labmaster saves voltages in 16 bit words. The last 12 bits represent the voltage, thus there are 2^{12} or 4096 distinct voltages possible as output from the A/D converter. The first 4 bits of the 16 bit word represent the number of times (less 1, since 0=1 time, 15=16 times) an identical voltage was obtained in successive samples up to a maximum of 2^4 or 16 times.

At time 0 Labmaster places a false 0 voltage in the channel.0 file so this value is ignored during the analysis of the data.

B.2.3 DETECTION OF INJECTIONS

Injections are detected by program 1 during the first pass through the data by doing a linear regression on 10 points then using that regression to predict a value for the next, eleventh, data point. If there is an injection then the value predicted will be higher than the observed value. In this case the predicted value of the 16^{th} point is compared to the observed value. If the predicted value is still much higher than the observed value then a change of baseline is assumed and the data in the region near the change of baseline is saved in the .ABV file. If the predicted value of the 16^{th} point is about the same as the actual value than an injection has been found. To determine the time that injection occurred, successively the 15^{th}, 14^{th}, 13^{th}, and 12^{th} points are checked to find the first one where the predicted voltage is higher than the observed voltage. The injection then is assumed to have occurred at the average of this time and the time of the following voltage.

Since this method requires 10 data points preceding the point to be checked it cannot be used at the start of the run so a different method is used here. The first data point at time 0 is arbitrarily set to voltage=0 by Labmaster thus it is ignored and the following method is used for the third through eleventh points.

The voltage of the third through eleventh points are compared to the voltage of the second data point. If any of them (say the i^{th} one) is substantially less than the second and the voltage of the $(i+6)^{th}$ point is comparable to the second one then there is an injection and the actual time of injection is obtained in a manner similar to that mentioned before, otherwise observations 2 to 11 are used for the regression to predict the voltage of the 12^{th} data pair as described above and the entire file is checked for injections.

While checking the data for injections the data is also checked to be sure it does not go offscale, and the time-voltage pairs are written to the two temporary files on the hard drive. If the data does go offscale, an appropriate warning message is added to the display and the .RLT file and the erroneous time-voltage data is not entered into the temporary files on the C disk. Once all the data has been checked for injections the binary data file TEMP.TMP is rewound and analysis of the data for peaks begins.

B.2.4 DETECTION OF PEAKS

In order to identify peaks the program does a linear regression on successive groups of N_P data points (usually 10 points at a time) where N_P represents the number of points within a group. Usually six of such groups, N_G, are considered at a time. If the slopes of the last N_C groups checked, usually four, monotonically increase then the beginning of a peak has been found; otherwise the first group of data points is discarded, the next group added and the procedure repeated. The variable N_C represents the number of groups that are checked during the analysis.

Once the beginning of a peak is identified all the data from the N_G groups is written to the .RLT file. Including the first (N_G–N_C) groups guarantees some baseline data as well as peak data. The problem now becomes how to decide where the peak ends. Several methods were tried with the following being the most consistent. First of all the maximum voltage in the peak was determined. N_P data pairs at a time are read and the voltage of each compared to the previous maximum voltage. If at least one of the N_P data points exceeds the previous maximum voltage then the next N_P data points are read and so on. If none of the N_P voltages exceed the previous maximum voltage then the peaks maximum voltage is assumed to be the previous maximum. The time from the start of the peak to the maximum voltage is then calculated, multiplied by 2.2 and added to the time the peak started; this time defines the end of the peak.

Once all the peak data has been identified and saved in the .RLT file, the first program is complete.

B.3: Program 2

B.3.1 AN OVERVIEW

The second program has two input files. The main input file is the RLT file generated by program 1 with temperature, pressure and mass flow rate data added to it through the use of a word processor which saves the file in ASCII format.

The second input file is the binary channel.1 file containing the differential pressure cell data. The way in which this data is stored is the same as the channel.0 file

discussed in section B.2.2.

There are two output files produced by program 2. The A:\AD\Runname.REG file contains parameter values and residual sum of squares for each iteration of the Marquardt regression as well as experimental and calculated values for the final fitted values.

The A:\DAB\Runname.DAB file is the main output file. It contains calculated diffusivity, various peak information, (height, retention time, mean square error of fit), and the criterion for determining whether the Taylor model is valid for each peak. It also gives the experimentally observed values for the viscosity and density of the solvent.

B.3.2 CALCULATION PROCEDURE

Program 2 first needs the conditions for the run from the RLT file. The tubing length and diameter are then corrected for pressure and thermal effects. Next the mass flow rate data is read followed by the injection times.

The peak data comes next. Chapter 6 describes the Marquardt regression and the method of obtaining initial estimates of the parameters to be determined, so this will not be repeated here. The regression parameters on each iteration are outputted to the REG file as are the calculated and observed values for the final fitted equation.

Once all the peak data has been fitted, the density of the solvent is calculated from the retention time and the mass flow rate. From the data in the channel.1 file the average differential pressure during the measurement of the mass flow rate is calculated and the viscosity of the solvent calculated. After calculation of the values of the Taylor criteria for each peak the final results of the run are outputted to the RLT file.

APPENDIX C

TABULATED VALUES OF THE DENSITIES OF THE SOLVENTS AS A FUNCTION OF TEMPERATURE AND PRESSURE (TABLES C.1A-C.1D)

Table C.1A

Effect of Pressure on the Density of Methanol

Pressure (MPa)	Density ($kg \cdot m^{-3}$)		
	298.15 K	323.15 K	348.15 K
0.22	784.6		
0.24		758.6	
0.38	785.4		732.2
3.20	787.0		
4.79			737.7
5.34		763.2	
8.72		767.0	
8.86			741.6
9.06	791.0		
12.65	792.5		
13.20		770.8	748.9
13.75	793.7		

Table C.1B

Effect of Pressure on the Density of Ethanol

Pressure (MPa)	Density ($kg \cdot m^{-3}$)		
	298.15 K	323.15 K	348.15 K
0.38			734.7
0.43			733.5
0.55		760.6	
1.17		761.4	
1.34	785.5		
1.65			736.5
3.41		763.3	
3.82	787.2		
4.82			740.6
4.96			739.3
7.86		766.7	
8.10	790.1		
8.82			745.4
10.37		770.2	
13.34	792.8		
13.48		770.9	
13.62			749.9

Table C.1C

Effect of Pressure on the Density of Propanol

Pressure (MPa)	Density ($kg \cdot m^{-3}$)		
	298.15 K	323.15 K	348.15 K
0.85	799.5		
1.05		777.3	
1.33		777.6	
1.52			754.3
3.20			755.9
3.42			756.2
3.90	801.3		
4.39		779.6	
6.10			758.7
7.20	803.0		
8.62		782.9	
8.93			762.1
12.86			766.7
12.93		786.2	
12.97	805.7		
13.33		784.6	
14.28	806.4		
16.64	807.6		

Table C.1D

Effect of Pressure on the Density of Butanol

Pressure (MPa)	Density ($kg \cdot m^{-3}$)		
	298.15 K	323.15 K	348.15 K
0.67	806.7		
0.82			761.7
0.89			762.0
1.28		785.3	
1.40			762.9
1.45			762.3
1.46			762.7
1.69	807.9		
4.02			761.7
4.03	808.8		
4.31		787.1	
5.33		788.1	
7.08			768.0
7.13			768.2
8.20	810.1		
8.36	810.1		
8.77		790.6	
10.49			771.3
12.39		792.1	
12.39		792.5	
12.57			773.5
13.01		792.8	
13.10	811.7		
14.66	813.0		

APPENDIX D

PLOTS OF THE DENSITIES OF THE SOLVENTS AS A FUNCTION OF TEMPERATURE AND PRESSURE (FIGURES D.1A-D.1D) AND TABULATED VALUES OF THE PERCENT INCREASE IN DENSITY AND THE CHANGE IN DENSITY WITH PRESSURE OF EACH SOLVENT AND AT EACH TEMPERATURE (TABLE D.1)

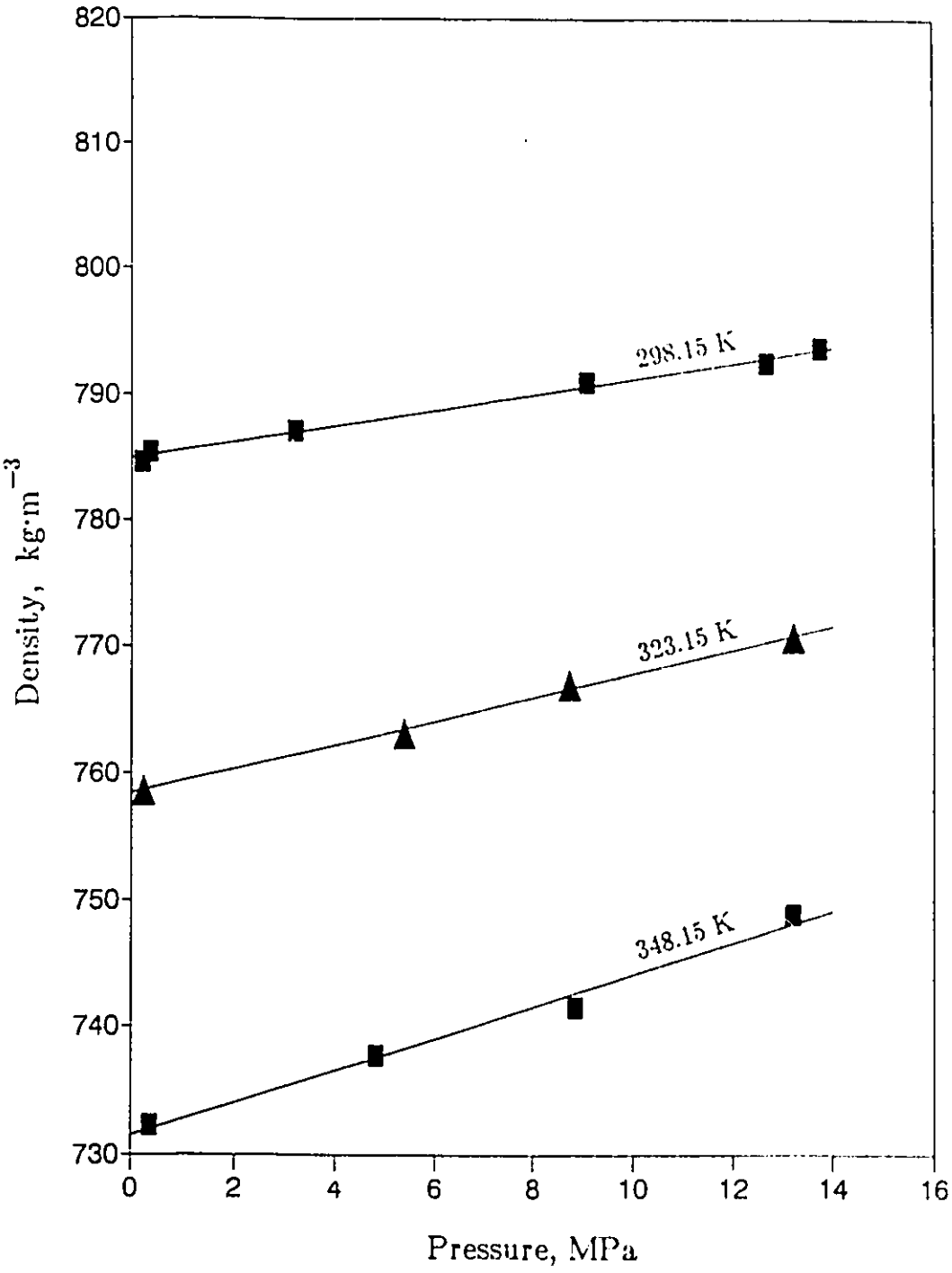

Figure D.1A: Effect of Pressure on the Density of Methanol at 298.15, 323.15, and 348.15 K

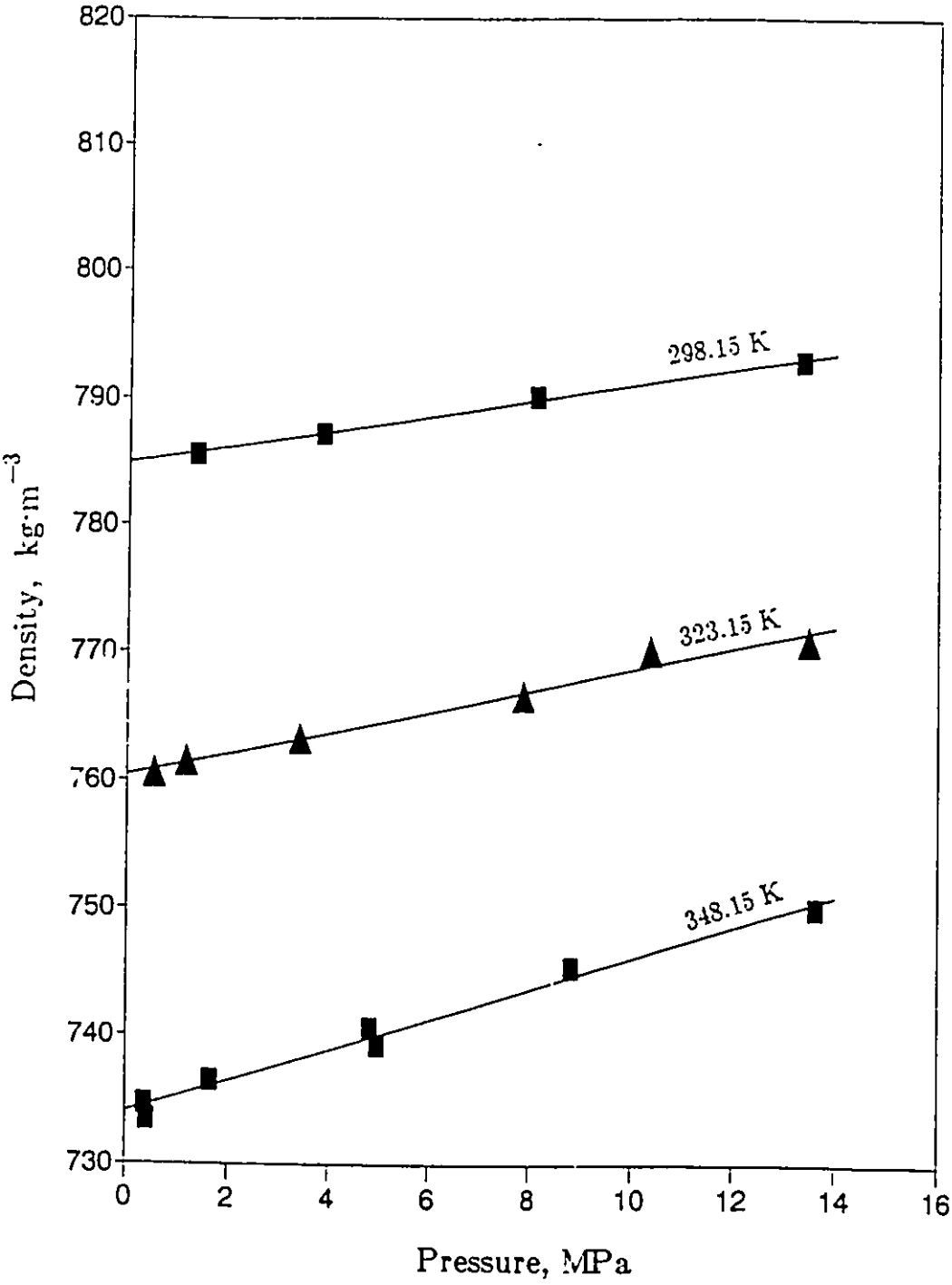

Figure D.1B: Effect of Pressure on the Density of Ethanol at 298.15, 323.15, and 348.15 K

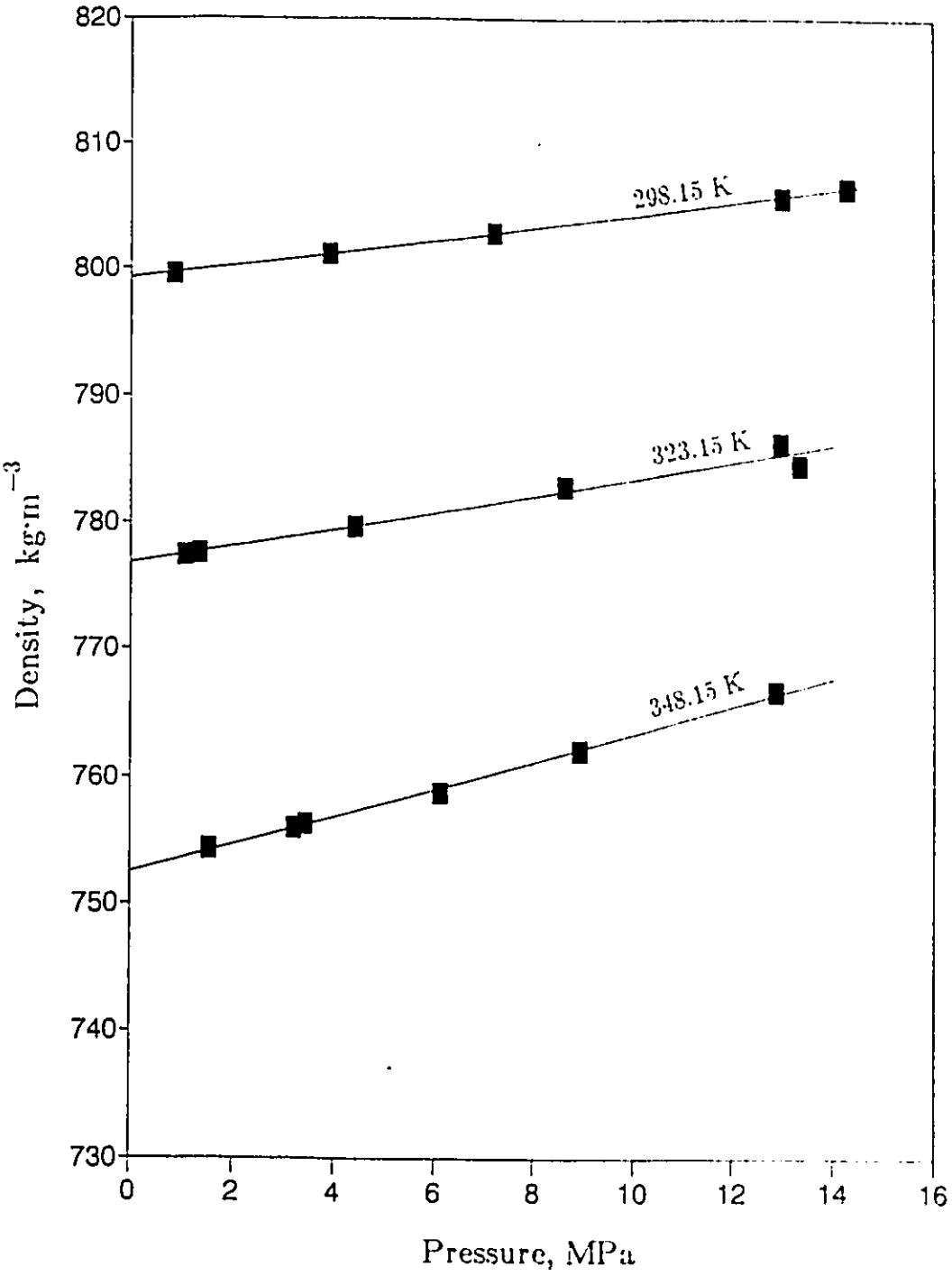

Figure D.1C: Effect of Pressure on the Density of Propanol at 298.15, 323.15, and 348.15 K

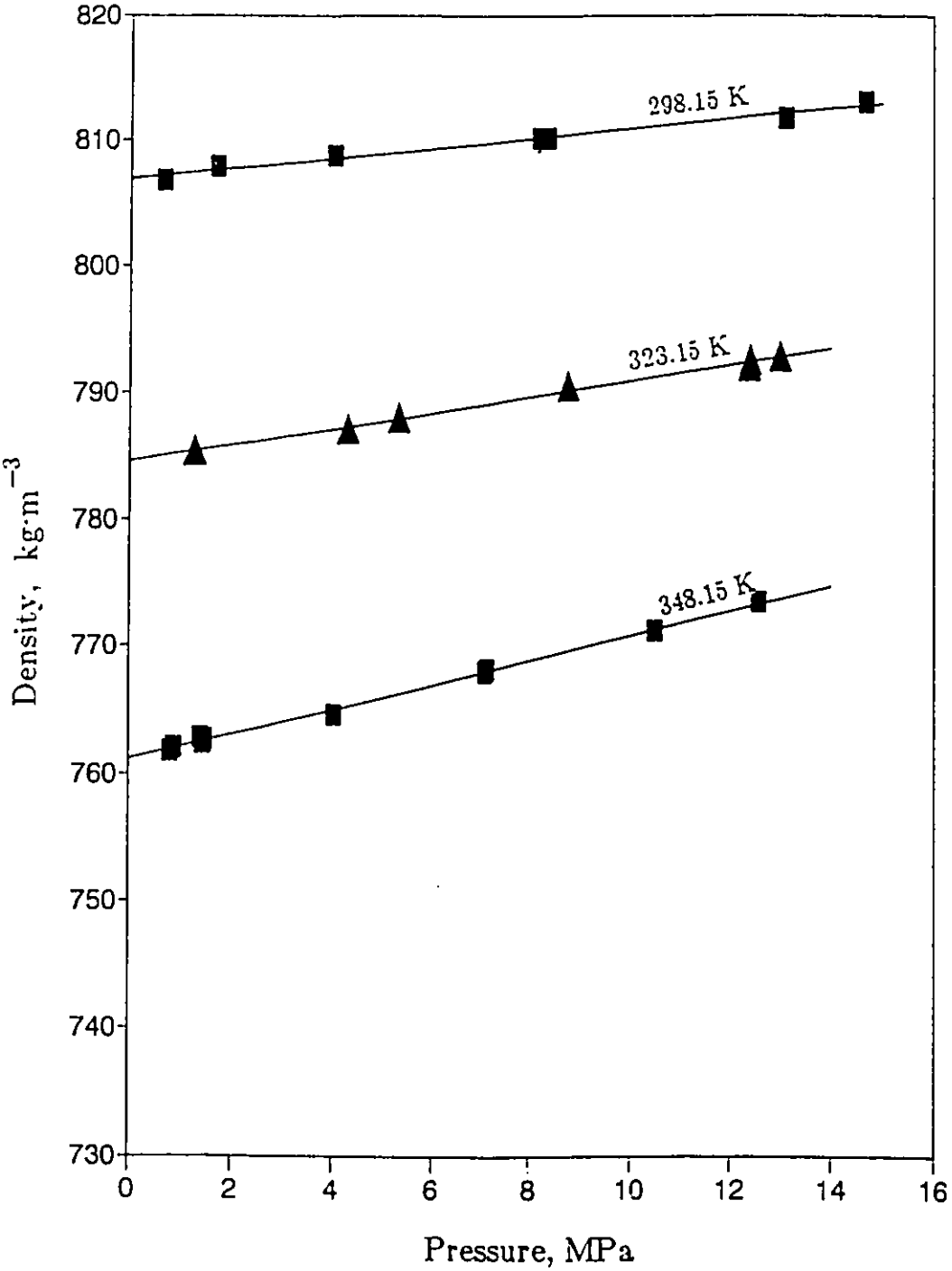

Figure D.1D: Effect of Pressure on the Density of Butanol at 298.15, 323.15, and 348.15 K

Table D.1

Effect of Temperature and Pressure on the Density and Molar Volume of the Solvents Methanol, Ethanol, Propanol, and Butanol

SOLVENT	TEMP. (K)	ρ_1 ($kg \cdot m^{-3}$)	ρ_2 ($kg \cdot m^{-3}$)	$\left(\frac{\rho_2 - \rho_1}{\rho_1}\right)100$ (%)	$\frac{\Delta\rho}{\Delta P}$ ($kg \cdot m^{-3} \cdot MPa^{-1}$)
METHANOL (32.04)*	298.15	786.2 (0.0408)**	792.5 (0.0404)**	0.81 (0.79)**	0.633 (3.24×10^{-5})**
	323.15	760.3 (0.0421)	769.8 (0.0416)	1.25 (1.23)	0.953 (5.2×10^{-5})
	348.15	734.0 (0.0437)	746.7 (0.0429)	1.73 (1.70)	1.270 (7.4×10^{-5})
ETHANOL (46.07)	298.15	786.1 (0.0586)	792.2 (0.0582)	0.78 (0.77)	0.611 (4.5×10^{-5})
	323.15	762.1 (0.0605)	770.4 (0.0598)	1.10 (1.08)	0.835 (6.5×10^{-5})
	348.15	736.4 (0.0626)	748.5 (0.0615)	1.64 (1.62)	1.207 (10.1×10^{-5})
PROPANOL (60.1)	298.15	800.2 (0.0751)	805.3 (0.0746)	0.63 (0.63)	0.504 (1.8×10^{-5})
	323.15	778.1 (0.0772)	784.8 (0.0766)	0.86 (0.85)	0.669 (6.6×10^{-5})
	348.15	754.6 (0.0796)	765.6 (0.0785)	1.45 (1.44)	1.096 (11.4×10^{-5})
BUTANOL (74.1)	298.15	807.7 (0.0917)	811.6 (0.0913)	0.49 (0.48)	0.396 (4.4×10^{-5})
	323.15	785.8 (0.0943)	792.2 (0.0935)	0.81 (0.81)	0.634 (7.6×10^{-5})
	348.15	763.1 (0.0971)	772.9 (0.0959)	1.28 (1.27)	0.980 (12.3×10^{-5})

* molecular weight, $kg \cdot kmol^{-1}$

** value based on molar volume, $m^3 \cdot kmol^{-1}$

APPENDIX E

TABLES E.1A TO E.4C LIST THE TABULATED VALUES OF THE INFINITE DILUTION DIFFUSION COEFFICIENTS OF EACH SOLUTE-SOLVENT PAIR AT EACH TEMPERATURE AND AS A FUNCTION OF PRESSURE

Table E.1A

Effect of Pressure on the Diffusivity in Methanol at 298.15 K

Pressure (MPa)	Diffusivity ($x10^{-9} m^2 \cdot s^{-1}$)		
	C_3H_8	NH_3	CO_2
0.22	3.43	1.98	6.28
0.22	3.48	1.97	6.45
0.38		2.06	5.62
0.38		2.03	5.69
0.38	3.52		
0.38	3.41		
3.17	3.72	2.20	
3.17	3.70		
3.20	3.58	2.21	5.74
3.20	3.34	1.87	5.71
9.06	3.41		5.70
12.65		2.13	5.65
12.65	3.23		5.48
13.27	3.29		
13.27	3.20		
13.75	3.30		
13.75	3.26		

Table E.1B

Effect of Pressure on the Diffusivity in Methanol at 323.15 K

Pressure (MPa)	Diffusivity ($x10^{-9} m^2 \cdot s^{-1}$)		
	C_3H_8	NH_3	CO_2
0.24	4.67	3.17	8.47
0.24	4.80	3.19	8.73
5.34	4.63	3.32	8.47
5.34	4.55	3.28	8.62
8.72	4.50	3.08	8.15
8.72		3.04	8.11
13.20	4.32	3.25	8.16
13.20	4.39	3.21	8.19

Table E.1C

Effect of Pressure on the Diffusivity in Methanol at 348.15 K

Pressure (MPa)	Diffusivity ($x10^{-9} m^2 \cdot s^{-1}$)		
	C_3H_8	NH_3	CO_2
0.38	6.50	4.89	11.74
0.38	6.26	4.82	11.30
4.79	6.16	4.74	11.05
4.79	6.14	4.78	11.21
8.86		4.52	10.87
8.86	5.91	4.46	10.91
13.20	5.91	4.56	10.62
13.20	5.86	4.55	10.83

Table E.2A

Effect of Pressure on the Diffusivity in Ethanol at 298.15 K

Pressure (MPa)	Diffusivity ($x10^{-9} m^2 \cdot s^{-1}$)			
	C_3H_8	C_3H_6	NH_3	CO_2
1.34	2.27	2.52	1.84	4.28
1.34	2.27	2.52	1.80	4.31
3.76		2.58		
3.82		2..60		
3.89	2.24			
3.96	2.22			
4.03			1.65	
4.10			1.73	
4.20				4.31
4.20				4.33
8.10	2.19	2.59	1.62	
8.10	2.23	2.52	1.54	4.22
13.00		2.37		
13.20		2.34		
13.34	2.07	2.36	1.59	4.17
13.34	2.03	2.39	1.73	
13.72	2.12			
14.23	2.11			
15.41				4.02
15.41				4.04

Table E.2B

Effect of Pressure on the Diffusivity in Ethanol at 323.15 K

Pressure (MPa)	Diffusivity ($x10^{-9} m^2 \cdot s^{-1}$)			
	C_3H_8	C_3H_6	NH_3	CO_2
0.55			3.08	5.66
0.55			3.06	5.70
1.17	3.46	3.78	2.73	6.97
1.17	3.38	3.82	2.80	7.01
3.41		3.60		
3.45		3.55		
3.51	3.27			
3.62			2.74	6.18
3.62	3.28		2.69	6.27
7.69		3.62		
7.96		3.66		
8.24	3.24			
8.58	3.14			
9.20				6.06
9.20				6.00
10.37	3.02		2.63	6.17
10.37	2.95	3.49	2.70	5.98
13.34		3.69		
13.62		3.63		
13.75				5.47
13.75			2.81	5.70
13.82			2.65	

Table E.2C

Effect of Pressure on the Diffusivity in Ethanol at 348.15 K

Pressure (MPa)	Diffusivity ($x10^{-9} m^2 s^{-1}$)		
	C_3H_8	C_3H_6	CO_2
0.38		6.19	
0.38	5.74	6.02	
0.43	4.82	5.54	7.82
1.65	5.09	5.48	
1.65	5.26	5.55	
4.82	4.81	5.25	7.46
4.82	4.72	5.29	7.54
5.27	5.05		
5.31	5.01		
5.51			8.22
5.51			8.29
8.82	4.36	5.68	7.37
8.82	4.53	5.27	
13.62		4.65	
13.72	4.17	4.63	
13.72	4.23		
14.17			7.57

Table E.3A

Effect of Pressure on the Diffusivity in Propanol at 298.15 K

Pressure (MPa)	Diffusivity ($x10^{-9} m^2 \cdot s^{-1}$)			
	C_3H_8	C_3H_6	NH_3	CO_2
0.85	1.58	1.82		3.08
0.85	1.57	1.78		3.01
1.18	1.57	1.75		3.09
1.18	1.59	1.84		3.10
1.19	1.64	1.86	1.02	3.14
1.19	1.64	1.92	1.06	
3.90		1.81		
3.94		1.84		
4.00	1.58			
4.05	1.58			
4.11				2.94
4.15				3.02
4.20			0.96	
4.25			0.98	
7.20		1.74		
7.27		1.74		
7.37	1.55			
7.41	1.55			
7.51			0.96	
7.59			0.98	
7.66				2.88
7.70				2.86
9.72		1.78		
9.84		1.80		
9.95	1.46			
10.02	1.48			
10.12				2.95

Table E.3A (Cont.)

Effect of Pressure on the Diffusivity in Propanol at 298.15 K

Pressure (MPa)	Diffusivity ($\times 10^{-9} m^2 s^{-1}$)			
	C_3H_8	C_3H_6	NH_3	CO_2
10.20				2.96
10.23			0.89	
10.24			0.87	
12.97		1.70		
13.17		1.72		
13.37	1.52			
13.55	1.49			
13.77			0.89	
13.95			0.88	
14.09		1.67		
14.32		1.66		
14.52	1.53			
14.73			0.92	
14.97			0.93	
15.81	1.53			
15.83	1.57			
16.48			0.94	
16.61			0.98	
16.64		1.63		
16.86		1.70		
17.90				2.82
18.13				2.87

Table E.3B

Effect of Pressure on the Diffusivity in Propanol at 323.15 K

Pressure (MPa)	Diffusivity ($x10^{-9} m^2 s^{-1}$)			
	C_3H_8	C_3H_6	NH_3	CO_2
1.05	2.62	2.88	1.75	4.45
1.33	2.73	3.08	1.74	4.37
1.33	2.68	3.02	1.73	4.36
4.32		2.92		
4.37		3.09		
4.42	2.70			
4.45	2.67			
4.49			1.75	
4.53			1.76	
4.61				4.40
4.65				4.25
8.62	2.59	2.86	1.61	4.30
9.75	2.28			
10.44		2.54		
12.17				4.25
12.51				4.18
13.17		2.60		
13.89		2.62		
14.06	2.62			
14.27			1.60	
14			1.65	
				4.12
.72				4.00

Table E.3C

Effect of Pressure on the Diffusivity in Propanol at 348.15 K

Pressure (MPa)	Diffusivity ($\times 10^{-9}$ $m^2 s^{-1}$)			
	C_3H_8	C_3H_6	NH_3	CO_2
1.52	4.01	4.33	3.15	
1.52	4.09		3.42	
3.20		4.33		
3.26		4.31		
3.32	3.82			
3.38	3.96	4.48		
3.41			3.05	
3.48	3.87			
3.51			3.15	
3.55				6.49
3.55				6.51
6.10		4.16		
6.27	3.81			
6.33	3.69			
6.44			3.14	
6.51			3.09	
6.55				6.22
6.65				6.36
8.86		4.07		
8.93		4.03		
9.06	3.83			
9.34	3.55			
9.49			3.04	
9.58			2.98	
9.75				6.04
9.75				6.33
12.86	3.52	4.05	2.87	6.00
12.86	3.41	3.93	2.82	

Table E.4A

Effect of Pressure on the Diffusivity in Butanol at 298.15 K

Pressure (MPa)	Diffusivity ($x10^{-9} m^2 s^{-1}$)			
	C_3H_8	C_3H_6	NH_3	CO_2
0.17		1.53		
0.17		1.58		
0.17		1.55		
0.17		1.54		
0.17		1.52		
0.17		1.52		
0.20		1.55		
0.27	1.27		0.752	2.19
0.27	1.29		0.751	2.20
0.27	1.27		0.749	
0.31	1.33			
0.31	1.38			
0.31	1.32			
0.31	1.36			
0.31	1.33			
0.31	1.32			
0.31	1.32			
0.31	1.32			
0.32	1.31		0.719	2.20
0.32	1.34		0.703	2.21
0.32	1.29		0.722	2.22
0.33		1.52	0.717	
0.33		1.55	0.718	
0.33		1.54	0.723	
0.34	1.32			
0.34	1.34			

Table E.4A (Cont.)

Effect of Pressure on the Diffusivity in Butanol at 298.15 K

Pressure (MPa)	Diffusivity ($\times 10^{-9}$ m^2 s^{-1})			
	C_3H_8	C_3H_6	NH_3	CO_2
3.41	1.31			
3.41	1.28			
3.41	1.29			
3.41	1.28			
3.55	1.28	1.53	0.788	2.00
3.55	1.34	1.48	0.784	2.19
3.55	1.29	1.49	0.782	2.19
4.24		1.49		
4.24		1.47		
4.24		1.48		
6.31	1.28	1.44		
6.31	1.17	1.45		
6.31	1.28			
6.41		1.43		
6.41		1.44		
6.41		1.44		
6.78	1.30	1.42	0.714	2.09
6.78	1.30	1.43	0.713	2.04
6.78	1.32		0.735	2.09
7.69	1.24		0.699	2.07
7.69	1.24		0.698	2.08
7.69	1.25		0.702	2.09
8.04	1.23			
8.04	1.24			
8.04	1.22			

Table E.4A (Cont.)

Effect of Pressure on the Diffusivity in Butanol at 298.15 K

Pressure (MPa)	Diffusivity ($\times 10^{-9}$ $m^2 \cdot s^{-1}$)			
	C_3H_8	C_3H_6	NH_3	CO_2
8.87	1.26			
8.87	1.22			
8.87	1.25			
8.87	1.22			
8.93	1.32	1.40		
8.93	1.30			
9.06		1.43	0.745	2.24
9.06		1.44	0.753	2.30
9.06		1.41	0.730	2.24
9.13		1.38		
9.13		1.37		
9.13		1.39		
11.10		1.35		
11.10		1.37		
11.13	1.23			
11.13	1.20			
11.13	1.19			
14.06	1.22	1.39	0.676	2.07
14.06	1.24	1.40	0.700	2.14
14.06	1.19		0.649	2.05
15.27		1.32		
15.27		1.33		
15.41	1.08			
15.41	1.18			
15.41	1.16			
15.41	1.16			
17.41		1.28		

Table E.4B

Effect of Pressure on the Diffusivity in Butanol at 323.15 K

Pressure (MPa)	Diffusivity ($\times 10^{-9}$ $m^2 \cdot s^{-1}$)			
	C_3H_8	C_3H_6	NH_3	CO_2
0.17			1.620	
0.17			1.641	
0.17			1.745	
0.22			1.817	
0.22		2.46	1.842	
0.33				3.68
0.33				3.74
0.34	2.15	2.46	1.677	3.73
0.34	2.17	2.48	1.730	3.64
0.34	2.16	2.44	1.648	
3.60			1.710	
3.60			1.702	
3.60			1.686	
3.60			1.647	
3.76				3.72
3.76				3.56
3.76				3.55
3.76				3.55
3.97				3.59
3.97				3.59
4.72		2.29		
4.72		2.29		
4.72		2.30		
4.72		2.31		

Table E.4B (Cont.)

Effect of Pressure on the Diffusivity in Butanol at 323.15 K

Pressure (MPa)	Diffusivity ($x10^{-9} m^2 \cdot s^{-1}$)			
	C_3H_8	C_3H_6	NH_3	CO_2
4.84		2.35		
4.84		2.36		
4.84		2.36		
5.13	2.14			
5.13	1.97			
5.13		2.31		
5.13	2.15	2.35		
5.38		2.29		
5.38		2.28		
5.38		2.27		
5.38		2.28		
5.49		2.25		
5.69				3.50
5.69				3.50
7.48		2.14		
7.48		2.16		
7.48		2.17		
8.55	1.99		1.523	
8.55			1.481	
8.55	2.12	2.16	1.495	
8.55	2.08	2.32	1.478	
9.06				3.38
9.06				3.40
9.06				3.35
9.13				3.39
9.13				3.55

Table E.4B (Cont.)

Effect of Pressure on the Diffusivity in Butanol at 323.15 K

Pressure (MPa)	Diffusivity ($x10^{-9} m^2 \cdot s^{-1}$)			
	C_3H_8	C_3H_6	NH_3	CO_2
10.93		2.12		
10.93		2.07		
10.93		2.08		
10.93		2.09		
11.06			1.429	
11.06			1.429	
11.06			1.435	
11.06			1.444	
11.10				3.40
11.13				3.44
11.13				3.41
11.13				3.48
11.62			1.385	
11.62			1.417	
11.62			1.253	
11.62			1.361	
12.31		2.16		
12.31		2.11		
12.31		2.11		
12.72	1.84	2.15		
12.72	2.03			
12.72	1.97	2.13		
13.84		2.02		
13.84		2.03		
13.84		2.06		

Table E.4B (Cont.)

Effect of Pressure on the Diffusivity in Butanol at 323.15 K

Pressure (MPa)	Diffusivity ($x10^{-9} m^2 \cdot s^{-1}$)			
	C_3H_8	C_3H_6	NH_3	CO_2
15.27				3.32
15.27				3.33
15.27				3.39
15.51			1.352	
15.51			1.324	
15.89	1.90			
15.89	1.87			
15.89	1.83			
15.89	1.87			
16.58	1.89			
16.58	1.86			
16.58	1.79			
16.58	1.86			

Table E.4C

Effect of Pressure on the Diffusivity in Butanol at 348.15 K

Pressure (MPa)	Diffusivity ($x10^{-9} m^2 \cdot s^{-1}$)			
	C_3H_8	C_3H_6	NH_3	CO_2
0.26				4.83
0.26				4.86
0.26				4.78
0.26				4.88
0.27				4.82
0.27				4.86
0.27				4.86
0.76	3.17	3.53	2.637	
0.76	3.23	3.58	2.846	
0.76	3.18	3.56	2.753	
2.99				4.77
2.99				4.86
2.99				4.83
3.93				4.77
3.93				4.82
3.93				4.72
5.71	3.15			
5.71	2.99			
5.71	3.07			
5.72	3.01	3.34		
5.72	3.11	3.47	2.710	
5.72	3.06	3.48	2.624	

Table E.4C (Cont.)

Effect of Pressure on the Diffusivity in Butanol at 348.15 K

Pressure (MPa)	Diffusivity ($x10^{-9} m^2 \cdot s^{-1}$)			
	C_3H_8	C_3H_6	NH_3	CO_2
5.82				4.67
5.82				4.69
5.82				4.62
5.82				4.57
7.93	2.99			
7.93	3.09			
7.93	3.03			
8.00		3.40		
8.00	2.98	3.32	2.718	
8.00	3.07	3.35	2.519	
8.00		3.26		
8.00	3.00	3.40	2.579	
8.75		3.24		
8.75		3.40		
8.75		3.32		
9.96	2.97	3.34		
9.96	2.97	3.36		
9.96	3.02	3.25		

Table E.4C (Cont.)

Effect of Pressure on the Diffusivity in Butanol at 348.15 K

Pressure (MPa)	Diffusivity ($x10^{-9} m^2 \cdot s^{-1}$)			
	C_3H_8	C_3H_6	NH_3	CO_2
10.05				4.42
10.05				4.50
10.05				4.54
11.62	3.13	3.21	2.680	
11.62	2.84	3.24	2.257	
11.62	2.91	3.34	2.655	
12.72		3.30		
12.72		3.17		
12.72		3.24		
13.41	2.88	3.31	2.408	
13.41	2.91	3.17	2.549	
13.41	2.91	3.17	2.506	
13.82				4.36
13.82				4.34
13.82				4.30
13.82				4.22
14.06	2.92		2.449	
14.06	2.92		2.571	
14.06	2.70	3.24	2.431	

APPENDIX F

TABULATED VALUES OF THE PERCENT INCREASE IN MOLECULAR DIFFUSIVITY AND THE CHANGE IN DIFFUSIVITY WITH PRESSURE AT EACH TEMPERATURE AND FOR EACH SOLUTE-SOLVENT PAIR (TABLES F.1A-F.1D)

Table F.1A

Effect of Temperature, Pressure, and Solute on Diffusivity in Methanol

SOLUTE	TEMP. (K)	$D_1 \times 10^9$ ($m^2 \cdot s^{-1}$)	$D_2 \times 10^9$ ($m^2 \cdot s^{-1}$)	$\left(\frac{D_1 - D_2}{D_1}\right)100$ (%)	$\frac{\Delta D}{\Delta P} \times 10^9$ ($m^2 \cdot s^{-1} \cdot MPa^{-1}$)
CO_2	298.15	5.904	5.565	5.74	-0.0339
C_3H_6		-	-	-	-
C_3H_8		3.507	3.305	5.76	-0.0202
NH_3		2.049	2.149	-4.88	+0.0100
CO_2	323.15	8.550	8.165	4.50	-0.0385
C_3H_6		-	-	-	-
C_3H_8		4.686	4.391	6.29	-0.0295
NH_3		3.198	3.188	0.31	-0.0010
CO_2	348.15	11.363	10.745	5.44	-0.0618
C_3H_6		-	-	-	-
C_3H_8		6.284	5.890	6.27	-0.0394
NH_3		4.796	4.524	5.67	-0.0272

Table F.1B

Effect of Temperature, Pressure, and Solute on Diffusivity in Ethanol

SOLUTE	TEMP. (K)	$D_1 \times 10^9$ ($m^2 \cdot s^{-1}$)	$D_2 \times 10^9$ ($m^2 \cdot s^{-1}$)	$\left(\frac{D_1 - D_2}{D_1}\right)100$ (%)	$\frac{\Delta D}{\Delta P} \times 10^9$ ($m^2 \cdot s^{-1} \cdot MPa^{-1}$)
CO_2	298.15	4.329	4.133	4.527	-0.0196
C_3H_6		2.575	2.411	6.37	-0.0164
C_3H_8		2.267	2.118	6.57	-0.0149
NH_3		1.745	1.621	7.11	-0.0124
CO_2	323.15	6.296	5.845	7.16	-0.0451
C_3H_6		3.690	3.605	2.30	-0.0085
C_3H_8		3.373	2.968	12.00	-0.0405
NH_3		2.850	2.691	5.58	-0.0159
CO_2	348.15	7.863	7.602	3.32	-0.0261
C_3H_6		5.676	4.899	13.69	-0.0777
C_3H_8		5.135	4.290	16.46	-0.0845
NH_3		-	-	-	-

Table F.1C

Effect of Temperature, Pressure, and Solute on Diffusivity in Propanol

SOLUTE	TEMP. (K)	$D_1 \times 10^9$ ($m^2 \cdot s^{-1}$)	$D_2 \times 10^9$ ($m^2 \cdot s^{-1}$)	$\left(\frac{D_1 - D_2}{D_1}\right)100$ (%)	$\frac{\Delta D}{\Delta P} \times 10^9$ ($m^2 \cdot s^{-1} \cdot MPa^{-1}$)
CO_2	298.15	3.041	2.903	4.54	-0.0138
C_3H_6		1.823	1.715	5.92	-0.0108
C_3H_8		1.585	1.528	3.60	-0.0057
NH_3		0.999	0.932	6.71	-0.0067
CO_2	323.15	4.387	4.169	4.97	-0.0218
C_3H_6		3.005	2.652	11.74	-0.0353
C_3H_8		2.665	2.512	5.74	-0.0153
NH_3		1.739	1.640	5.71	-0.0099
CO_2	348.15	6.560	6.047	7.82	-0.0513
C_3H_6		4.369	3.986	8.76	-0.0383
C_3H_8		3.985	3.511	11.88	-0.0473
NH_3		3.230	2.899	10.26	-0.0331

Table F.1D

Effect of Temperature, Pressure, and Solute on Diffusivity in Butanol

SOLUTE	TEMP. (K)	$D_1 \times 10^9$ ($m^2 \cdot s^{-1}$)	$D_2 \times 10^9$ ($m^2 \cdot s^{-1}$)	$\left(\frac{D_1 - D_2}{D_1}\right)100$ (%)	$\frac{\Delta D}{\Delta P} \times 10^9$ ($m^2 \cdot s^{-1} \cdot MPa^{-1}$)
CO_2	298.15	2.170	2.112	2.67	-0.0058
C_3H_6		1.510	1.369	9.34	-0.0141
C_3H_8		1.307	1.209	7.50	-0.0098
NH_3		0.737	0.703	4.56	-0.0034
CO_2	323.15	3.632	3.391	6.63	-0.0241
C_3H_6		2.394	2.099	12.34	-0.0296
C_3H_8		2.148	1.952	9.11	-0.0196
NH_3		1.680	1.396	16.9	-0.0284
CO_2	348.15	4.810	4.396	8.61	-0.0414
C_3H_6		3.516	3.253	7.48	-0.0263
C_3H_8		3.162	2.924	7.53	-0.0238
NH_3		2.727	2.523	7.48	-0.0204

APPENDIX G

FIGURES G.1A TO G.1O SHOW THE RESULTS FOR THE MOLECULAR DIFFUSIVITIES AS A FUNCTION OF PRESSURE FOR ONE SOLUTE-SOLVENT PAIR WITH TEMPERATURE AS A PARAMETER IN EACH GRAPH

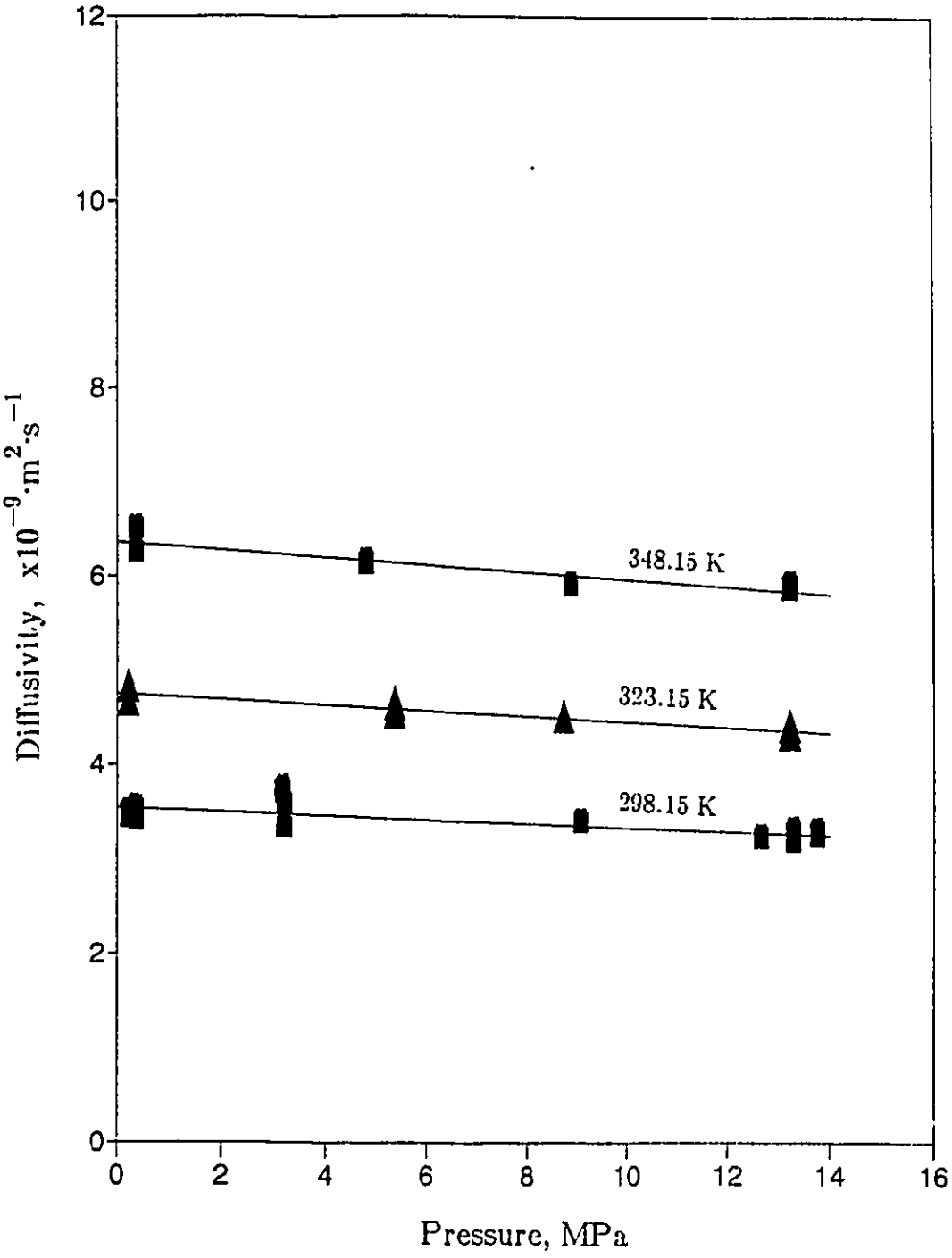

Figure G.1A: Effect of Pressure on the Diffusivity of Propane in Methanol at All Temperatures

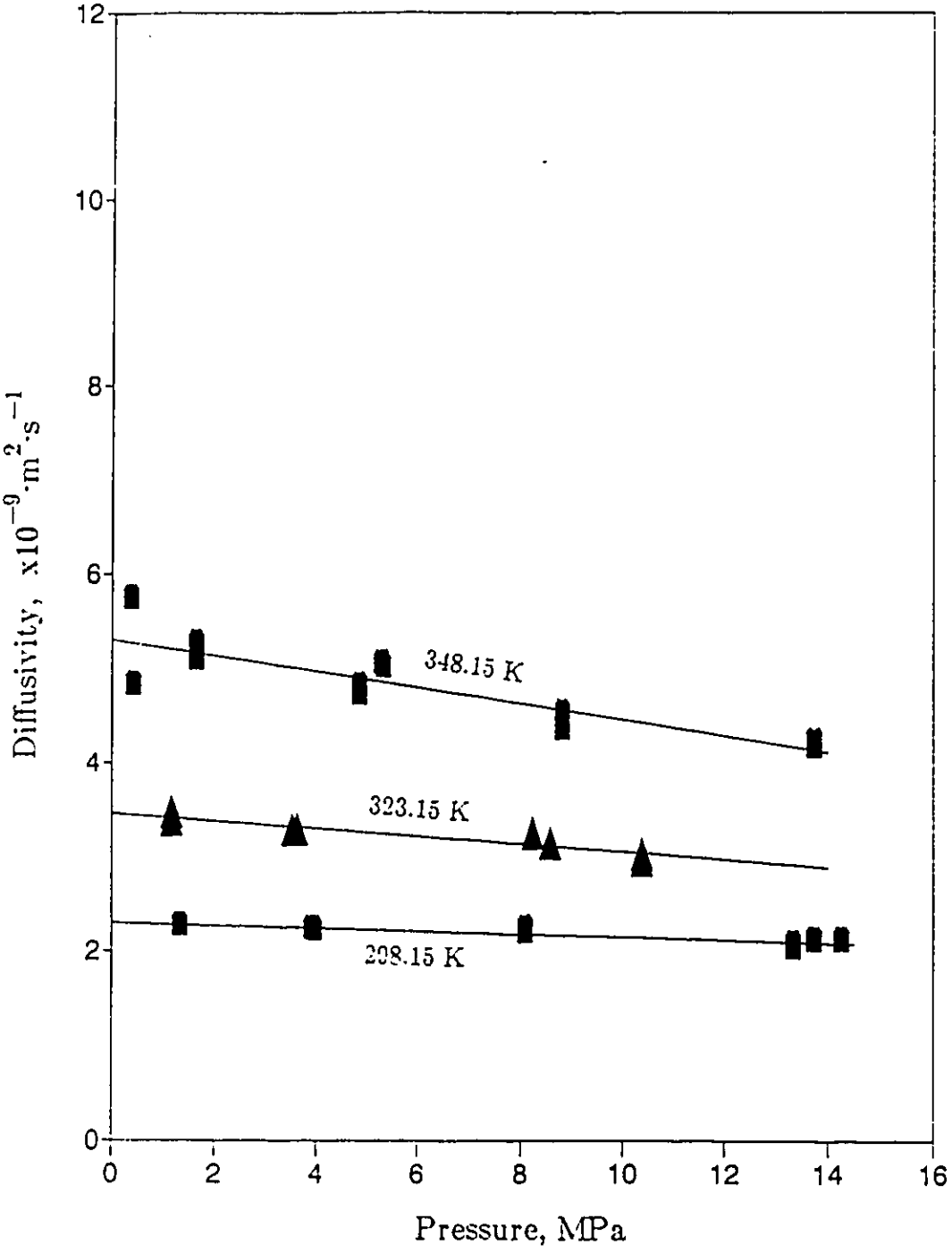

Figure G.1B: Effect of Pressure on the Diffusivity of Propane in Ethanol at All Temperatures

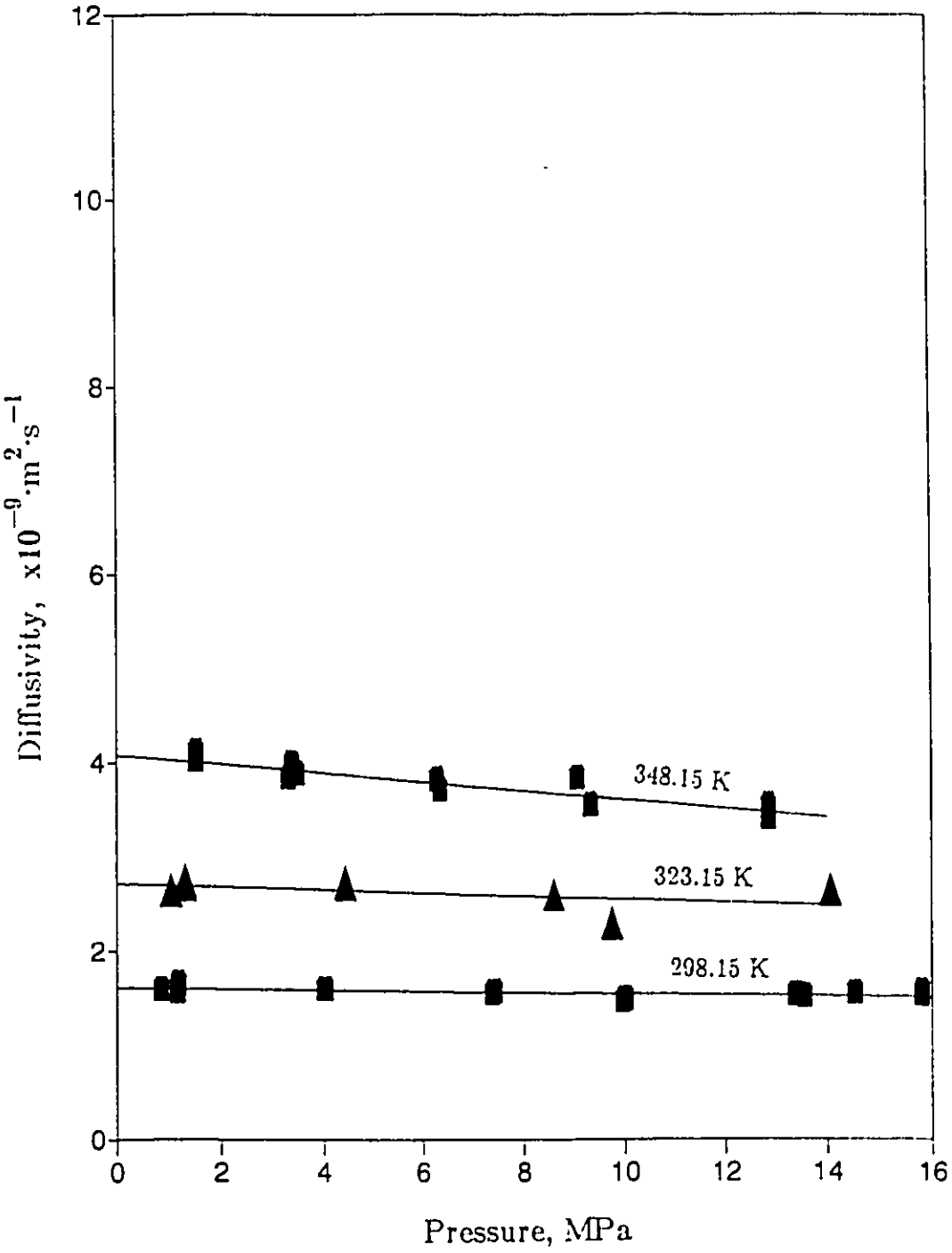

Figure G.1C: Effect of Pressure on the Diffusivity of Propane in Propanol at All Temperatures

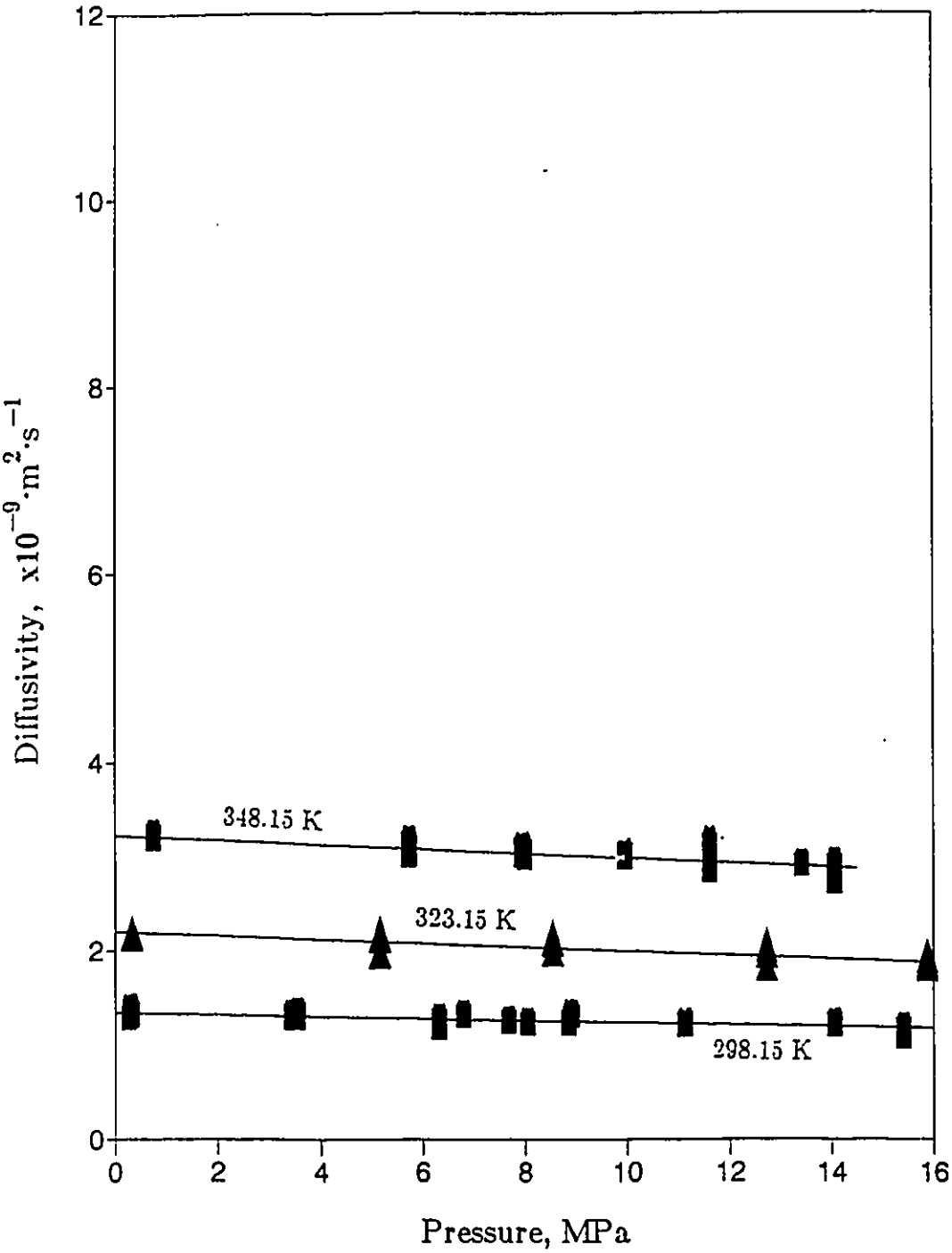

Figure G.1D: Effect of Pressure on the Diffusivity of Propane in Butanol at All Temperatures

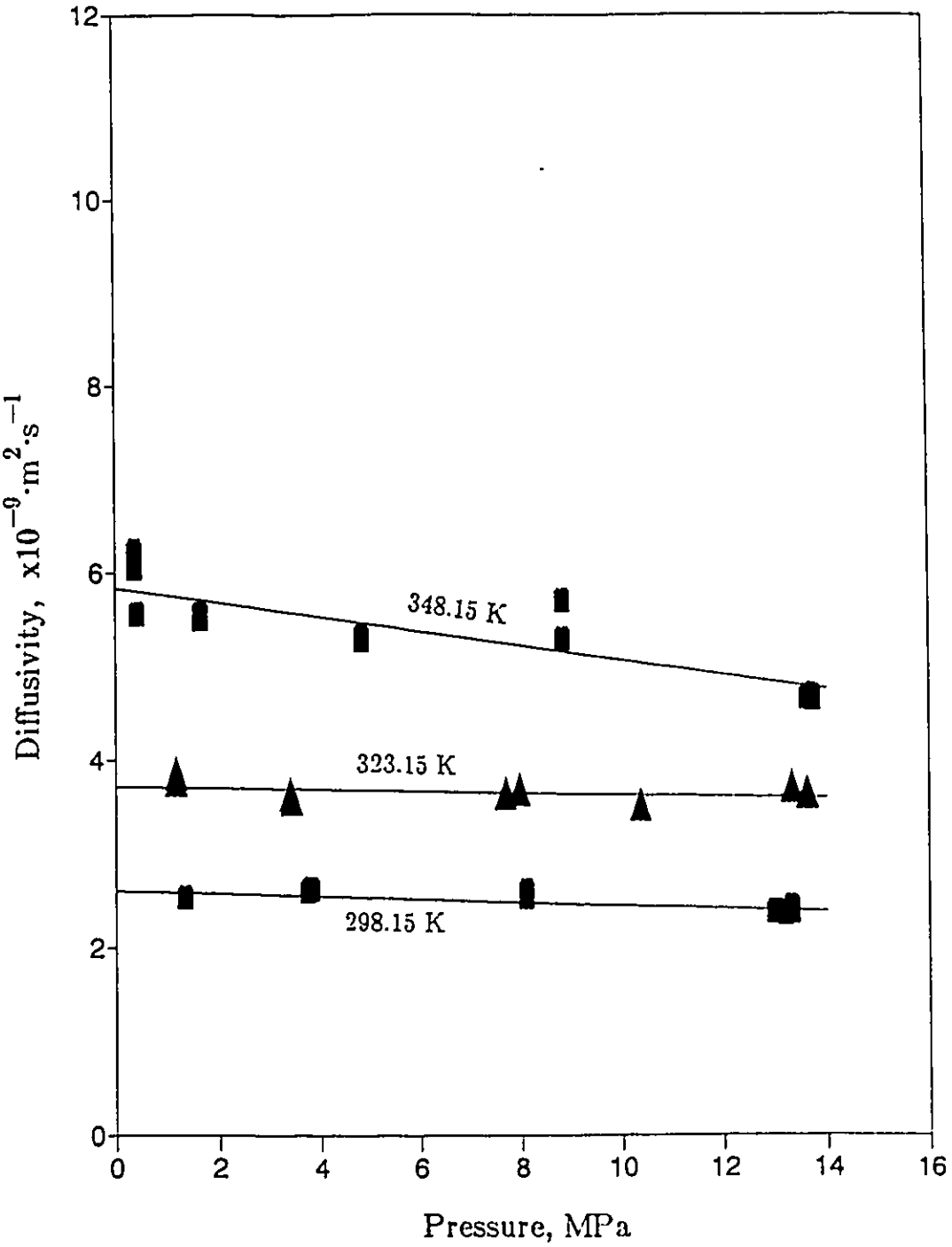

Figure G.1E: Effect of Pressure on the Diffusivity of Propene in Ethanol at All Temperatures

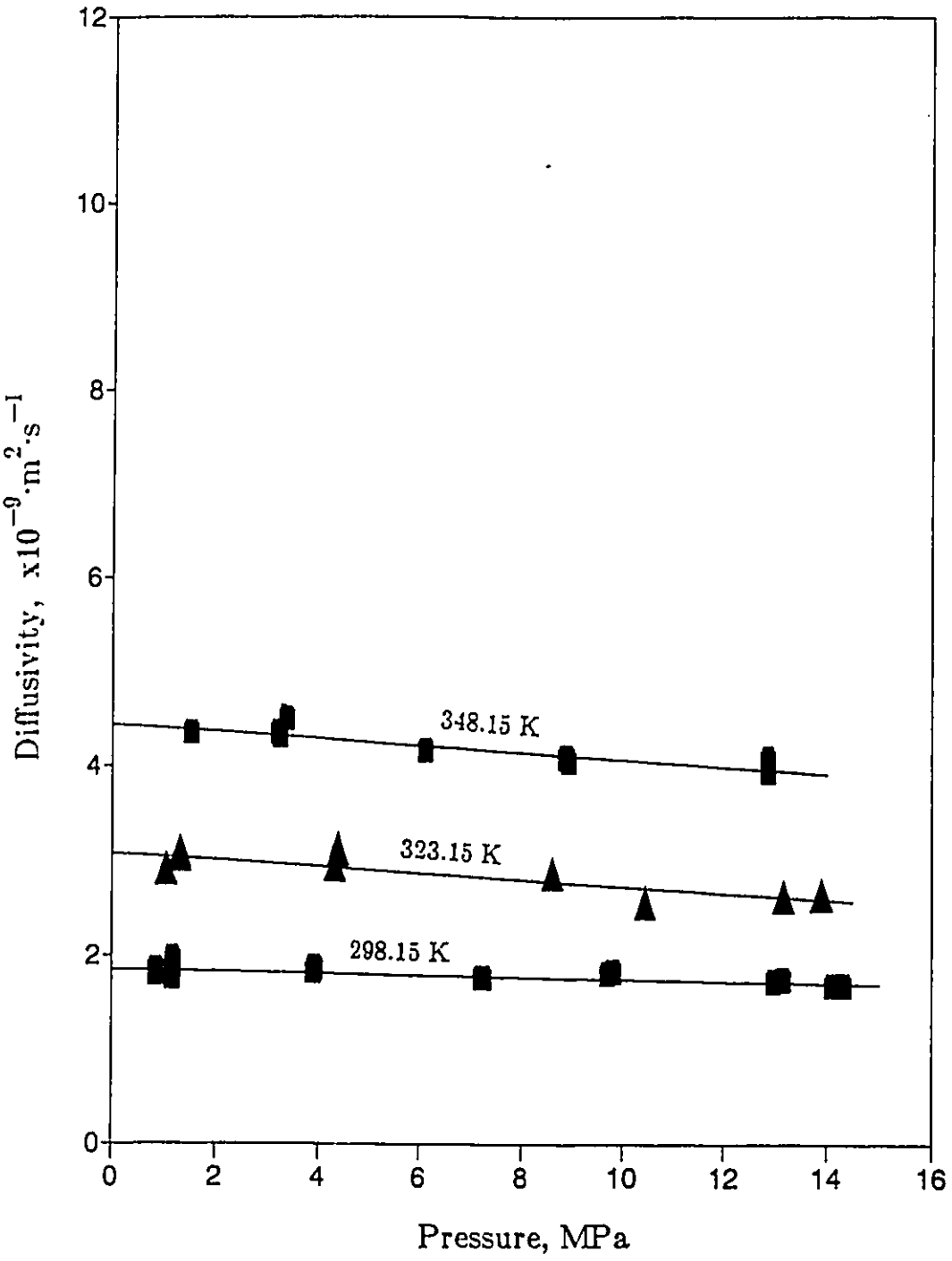

Figure G.1F: Effect of Pressure on the Diffusivity of Propene in Propanol at All Temperatures

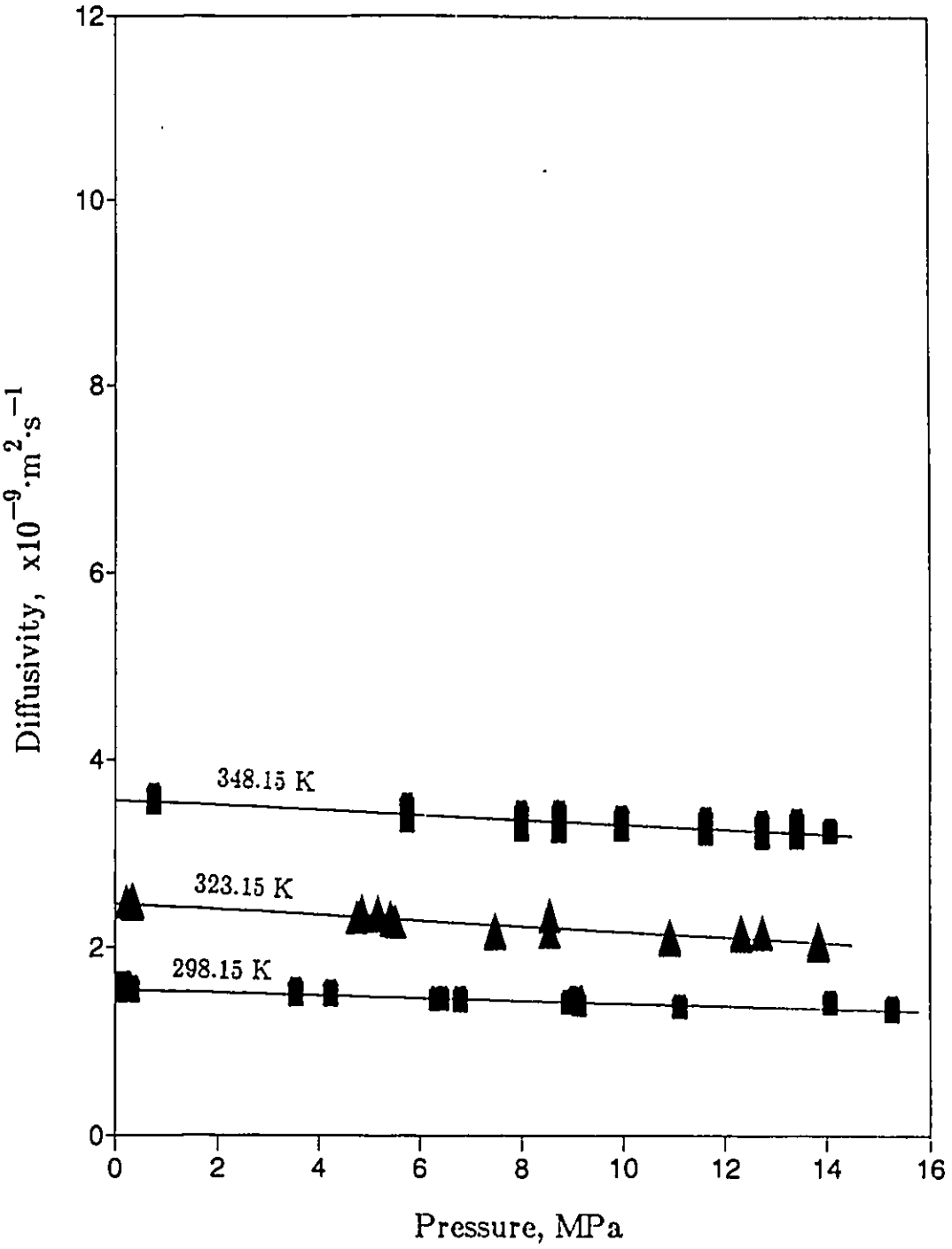

Figure G.1G: Effect of Pressure on the Diffusivity of Propene in Butanol at All Temperatures

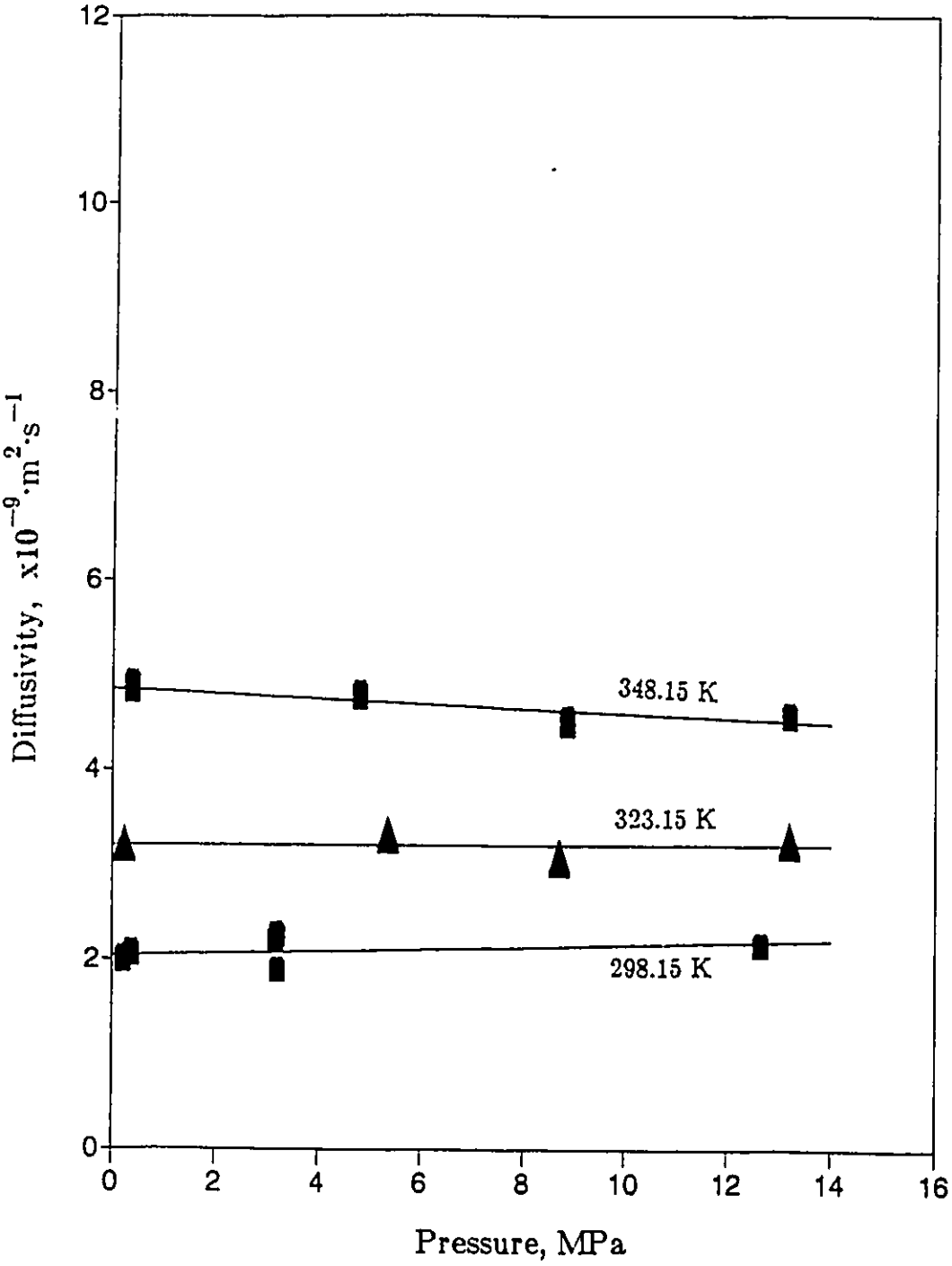

Figure G.1H: Effect of Pressure on the Diffusivity of Ammonia in Methanol at All Temperatures

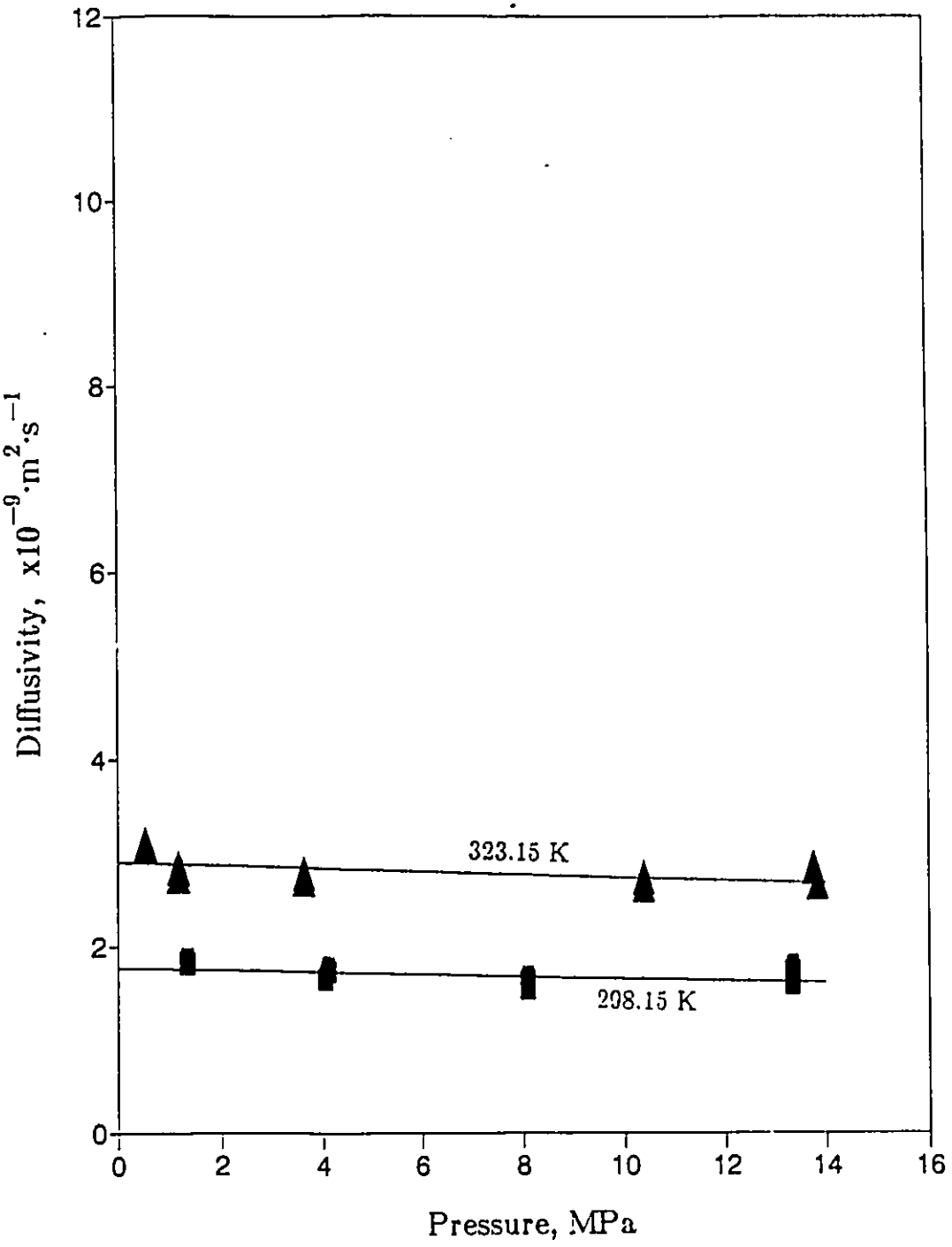

Figure G.1I: Effect of Pressure on the Diffusivity of Ammonia in Ethanol at All Temperatures

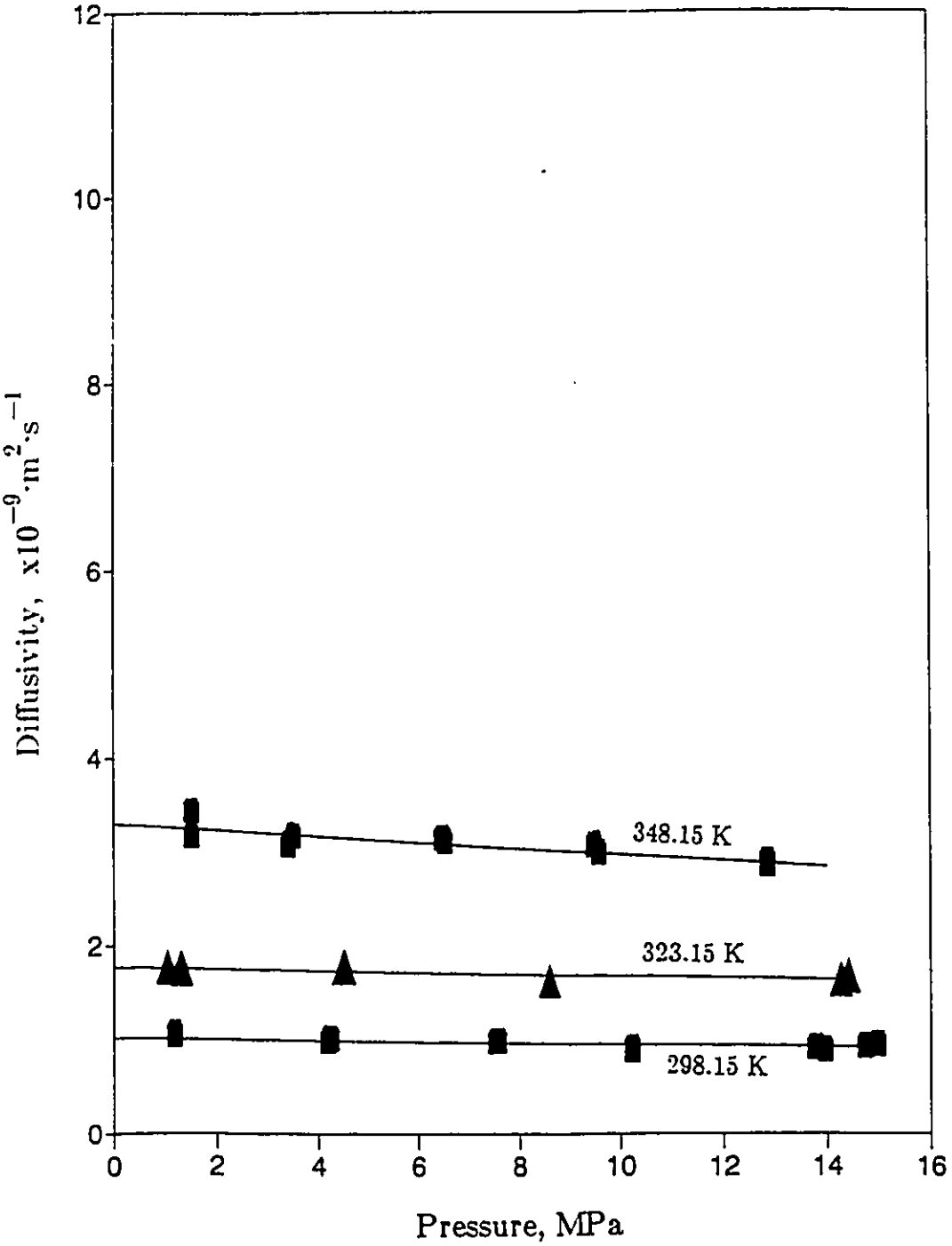

Figure G.1J: Effect of Pressure on the Diffusivity of Ammonia in Propanol at All Temperatures

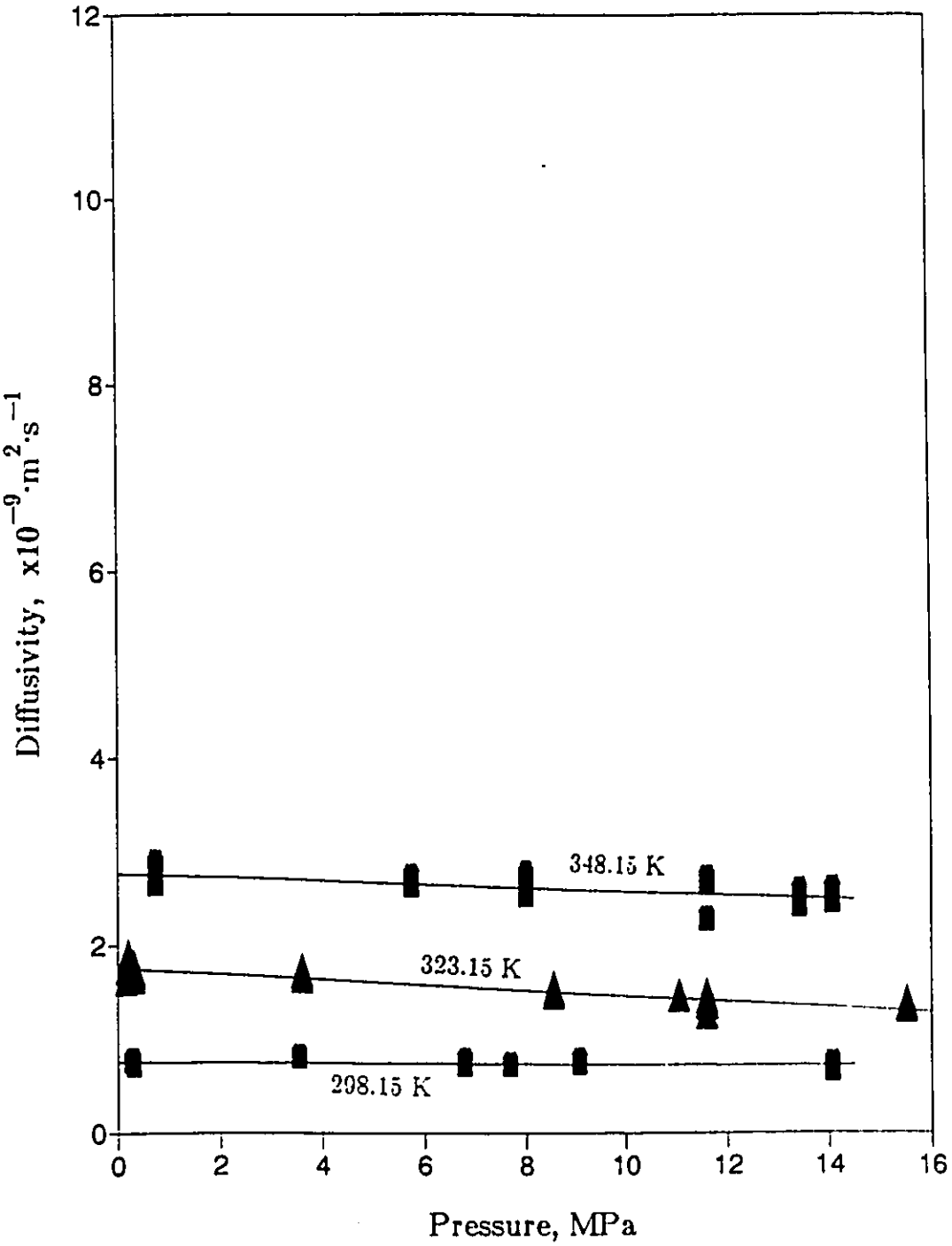

Figure G.1K: Effect of Pressure on the Diffusivity of Ammonia in Butanol at All Temperatures

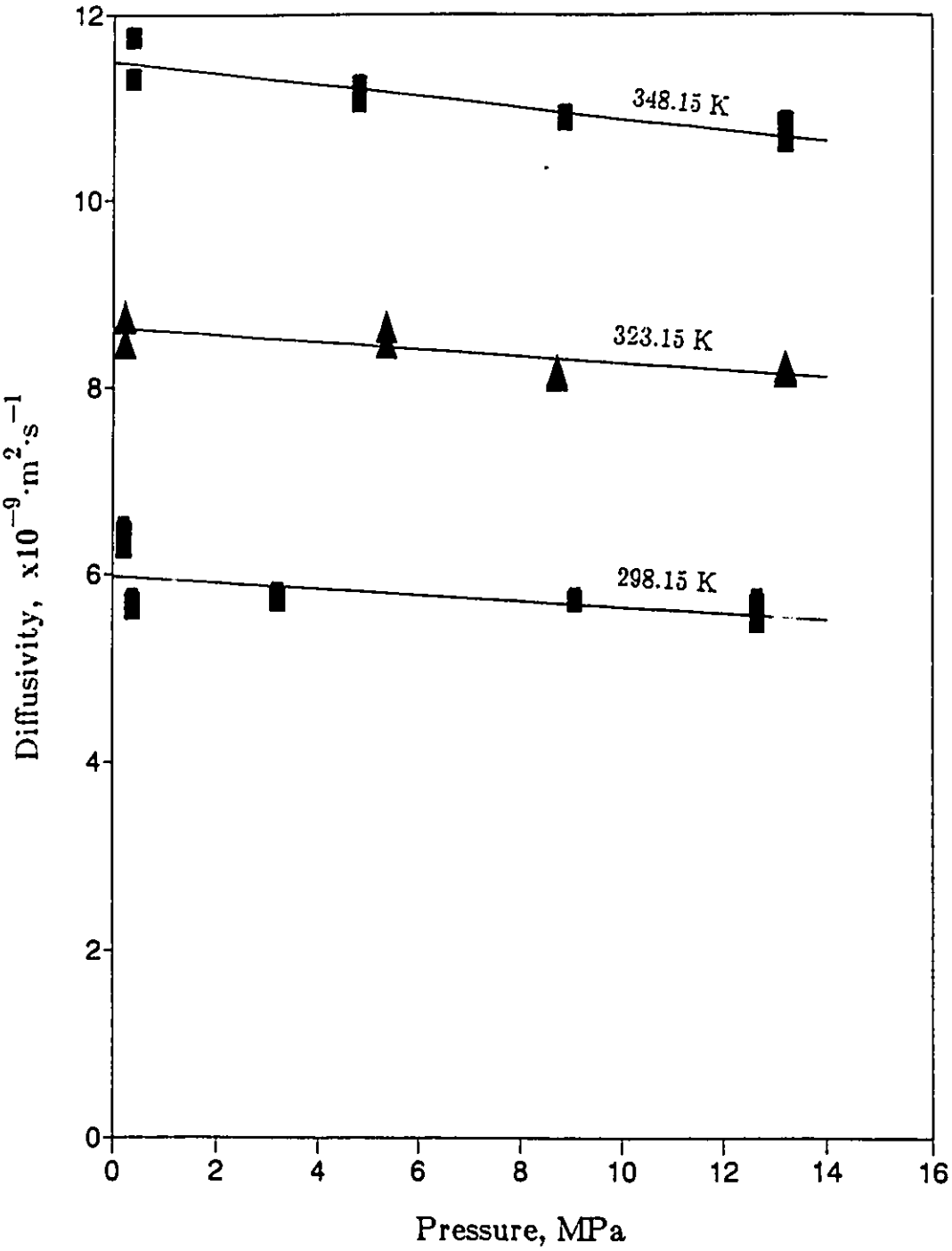

Figure G.1L: Effect of Pressure on the Diffusivity of Carbon Dioxide in Methanol at All Temperatures

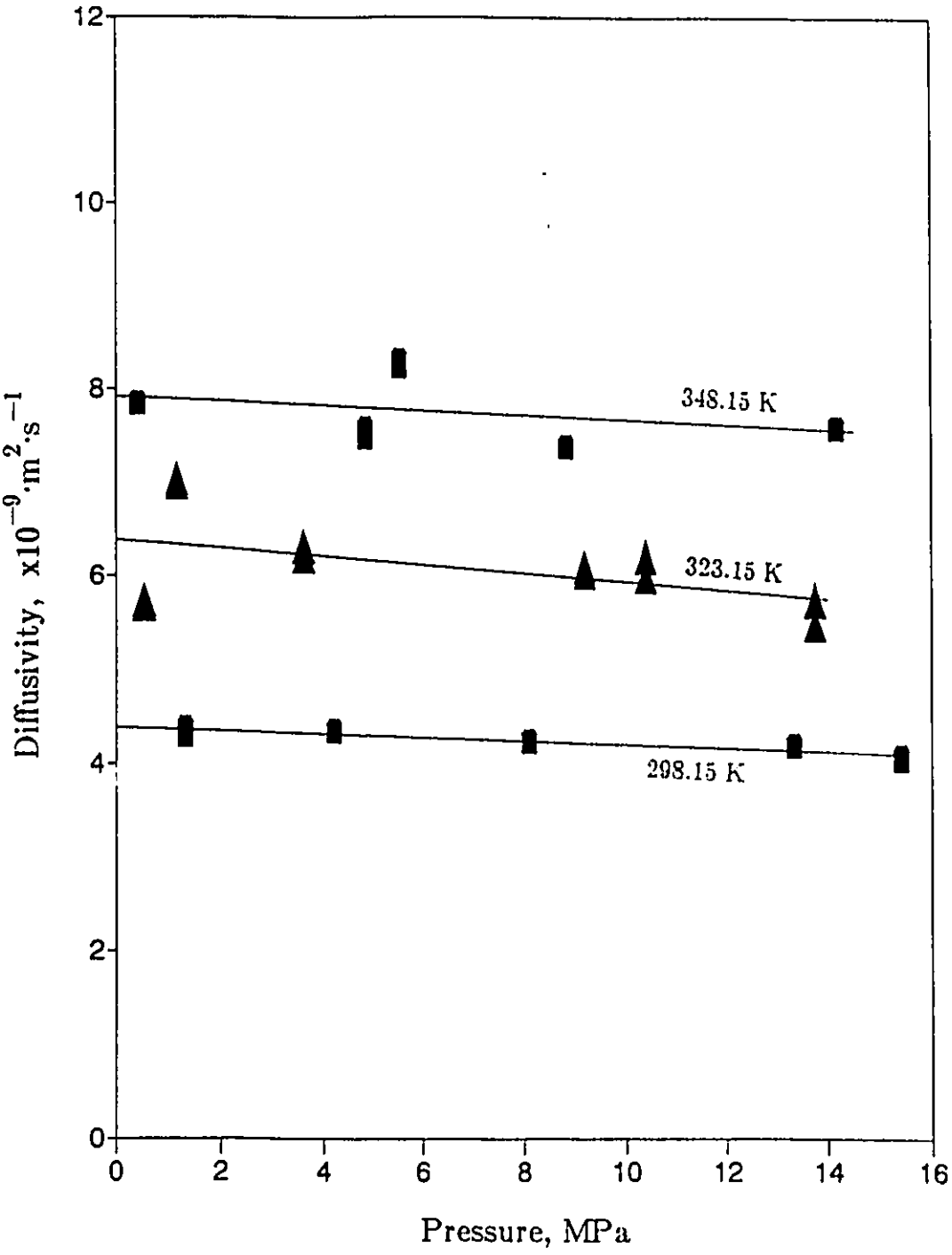

Figure G.1M: Effect of Pressure on the Diffusivity of Carbon Dioxide in Ethanol at All Temperatures

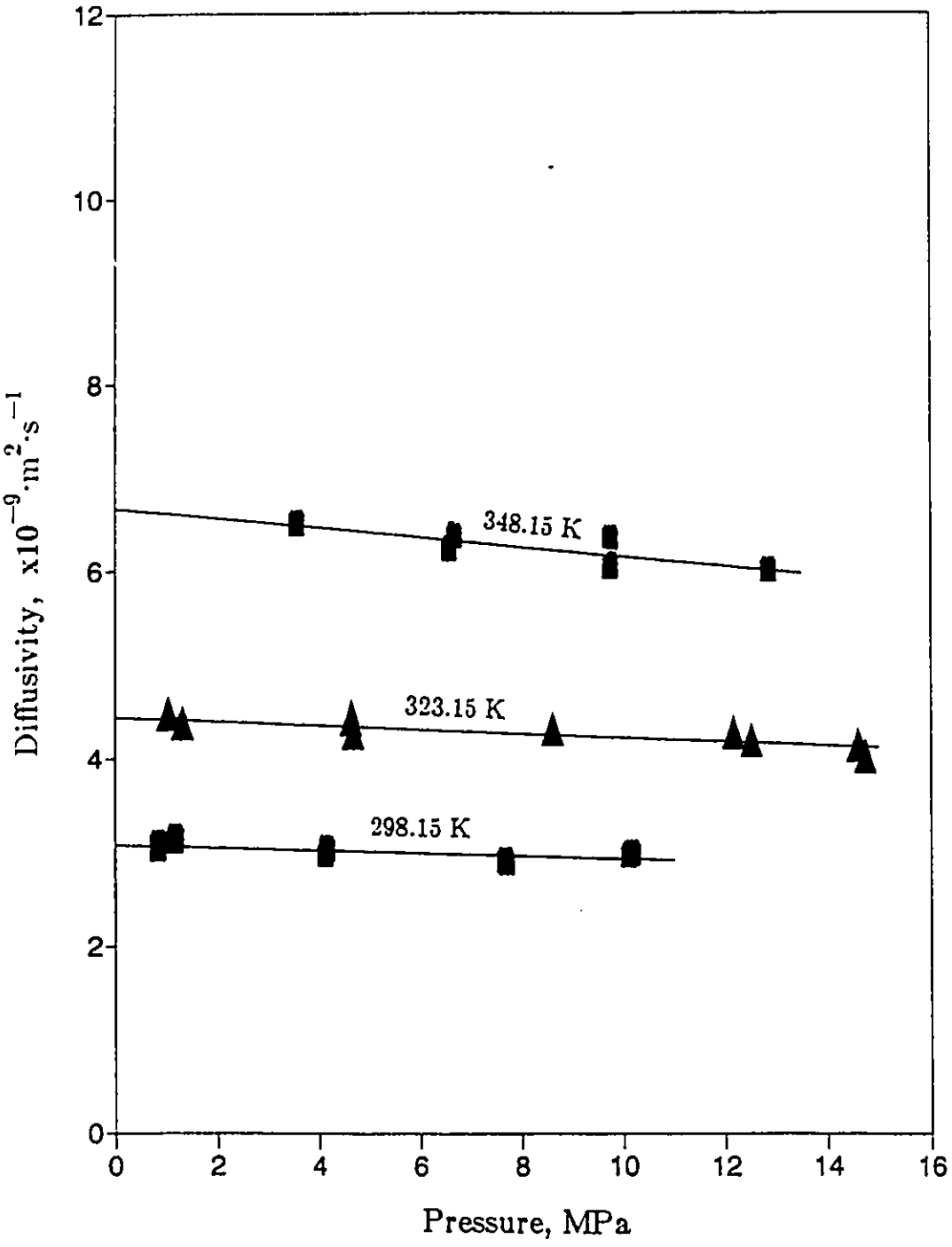

Figure G.1N: Effect of Pressure on the Diffusivity of Carbon Dioxide in Propanol at All Temperatures

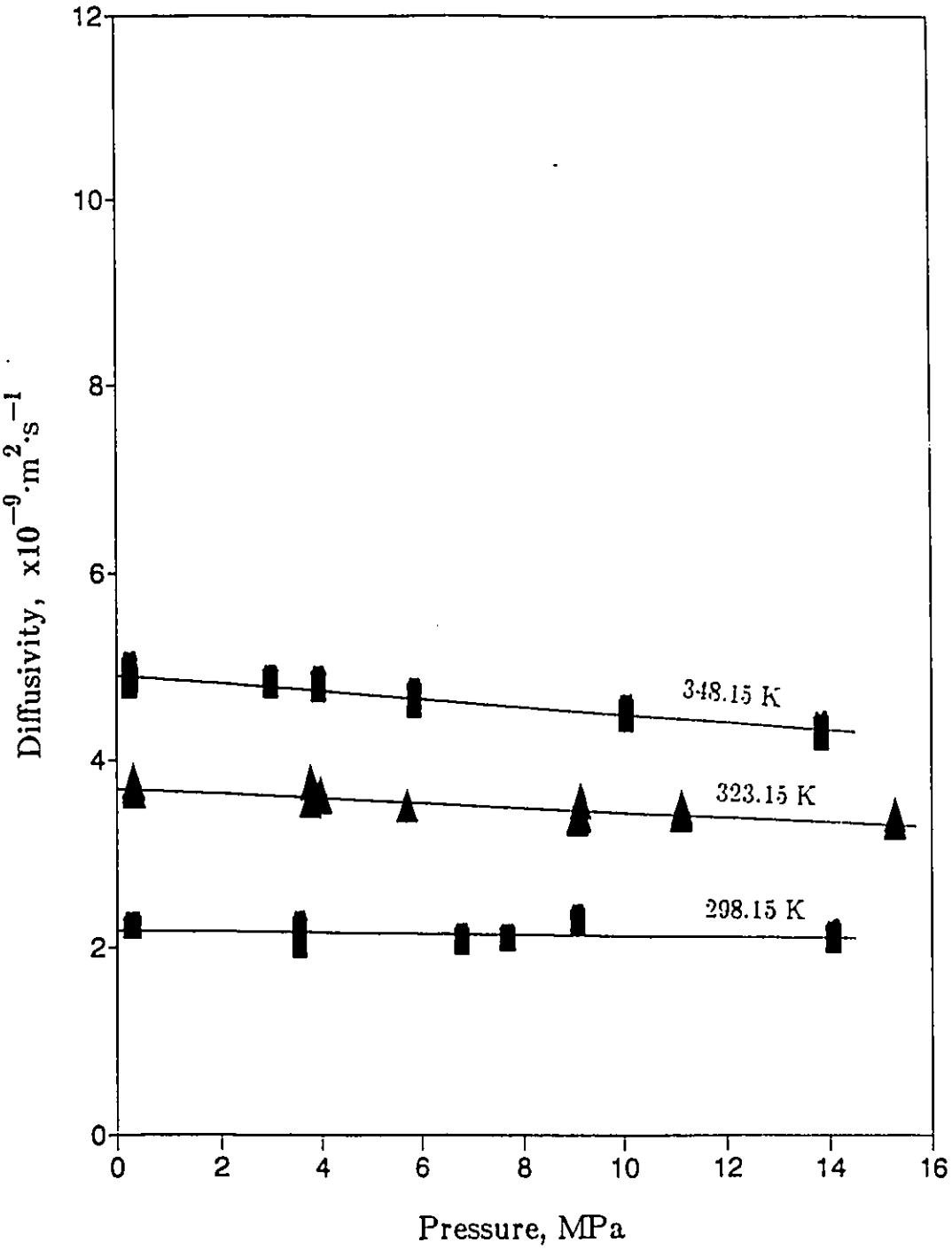

Figure G.1O: Effect of Pressure on the Diffusivity of Carbon Dioxide in Butanol at All Temperatures

APPENDIX H

FIGURES H.1A TO H.1H SHOW THE RESULTS FOR THE MOLECULAR DIFFUSIVITIES AS A FUNCTION OF PRESSURE FOR THE FOUR SOLUTE GASES PROPANE, PROPENE, CARBON DIOXIDE AND AMMONIA IN EACH ALCOHOL SOLVENT AND AT ONE TEMPERATURE IN EACH CASE

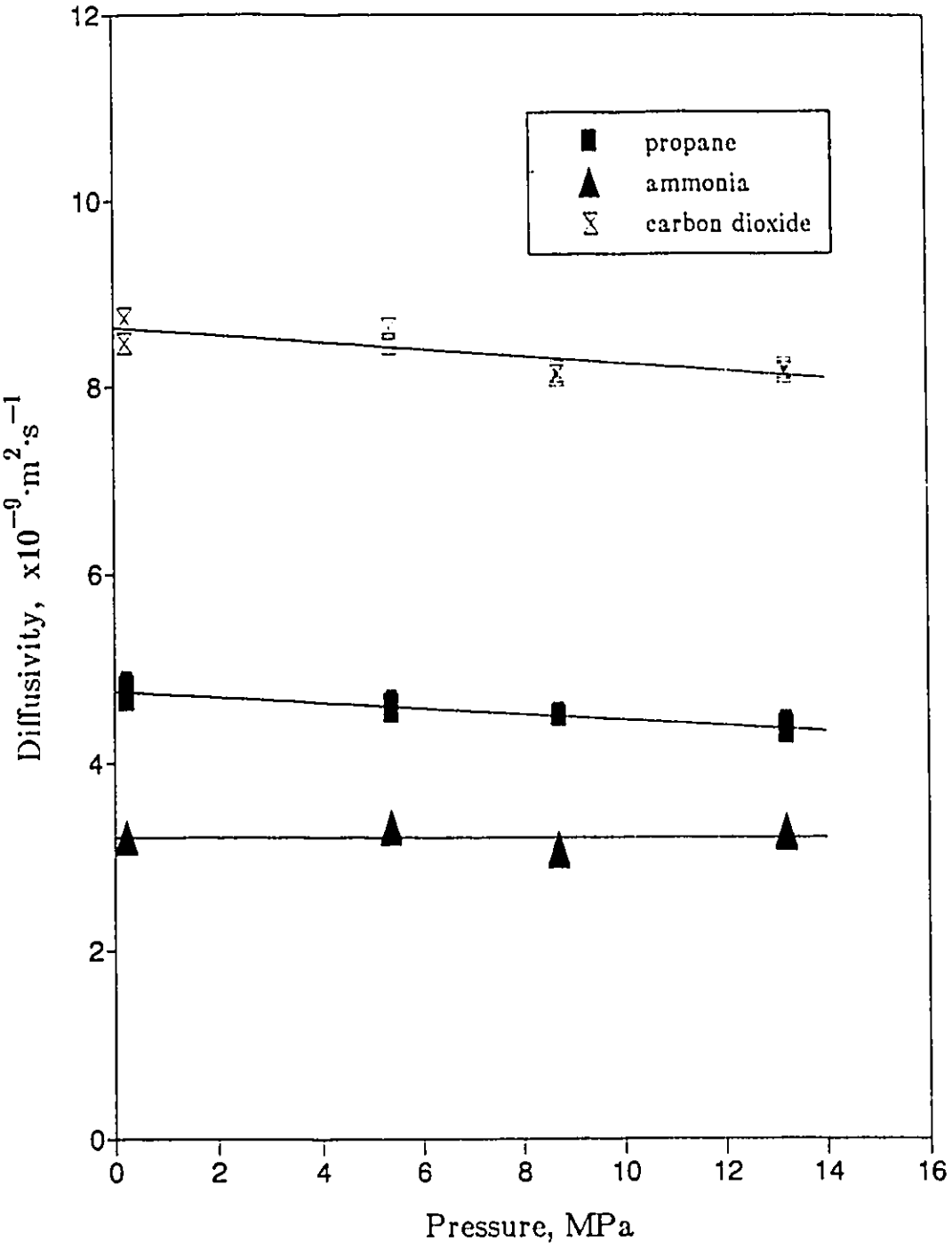

Figure H.1A: Effect of Pressure on the Diffusivity of All Solutes in Methanol at 323.15 K

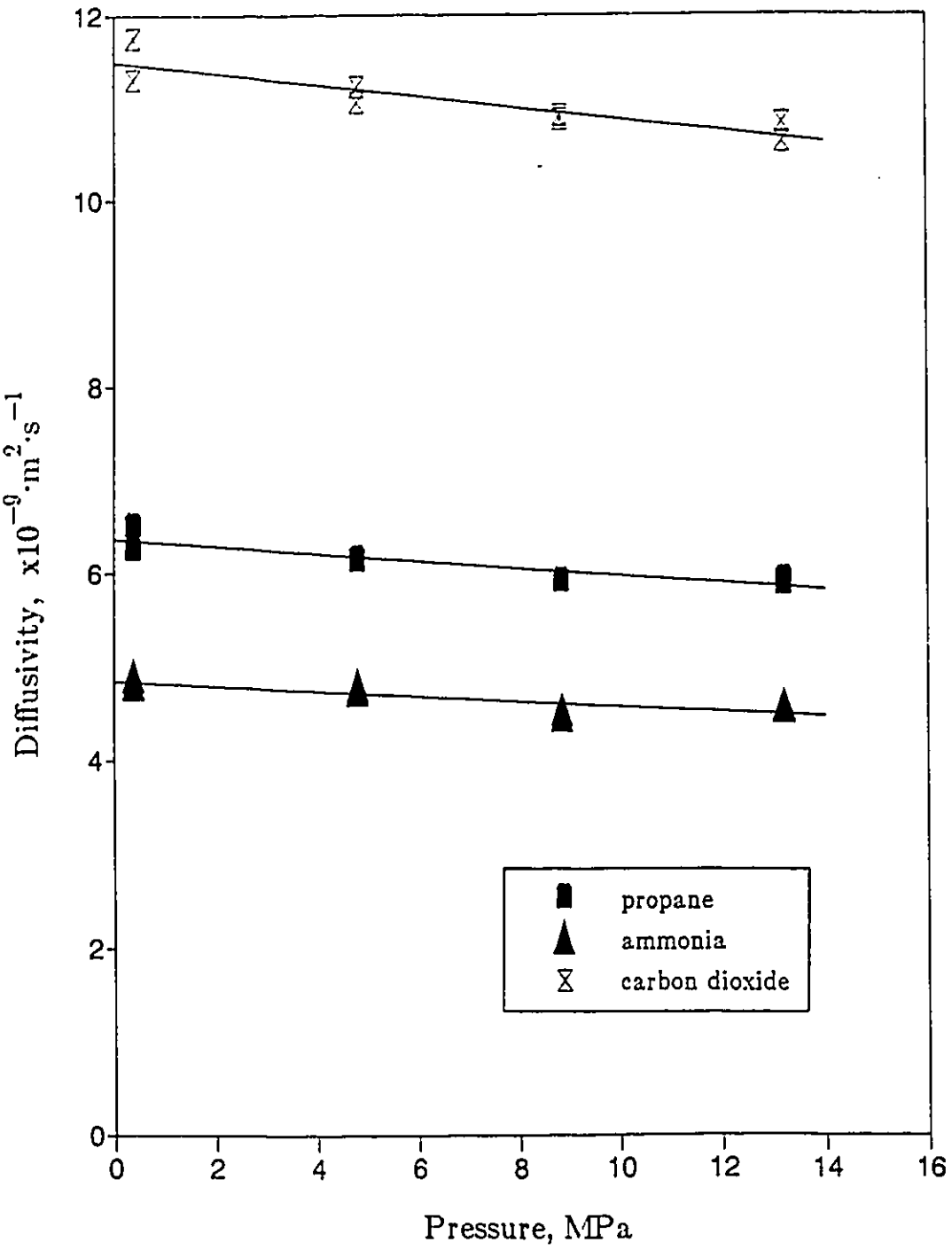

Figure H.1B: Effect of Pressure on the Diffusivity of All Solutes in Methanol at 348.15 K

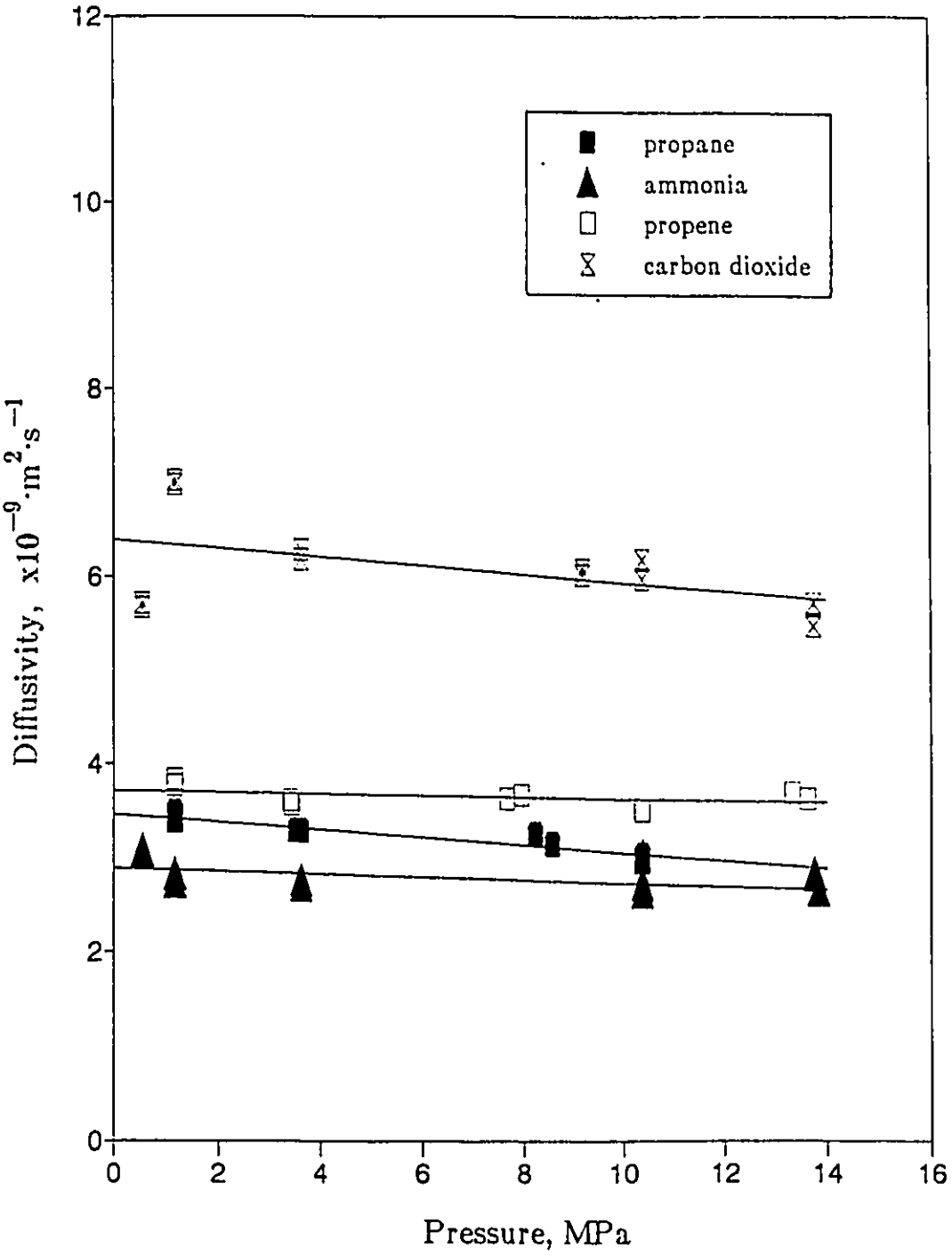

Figure H.1C: Effect of Pressure on the Diffusivity of All Solutes in Ethanol at 323.15 K

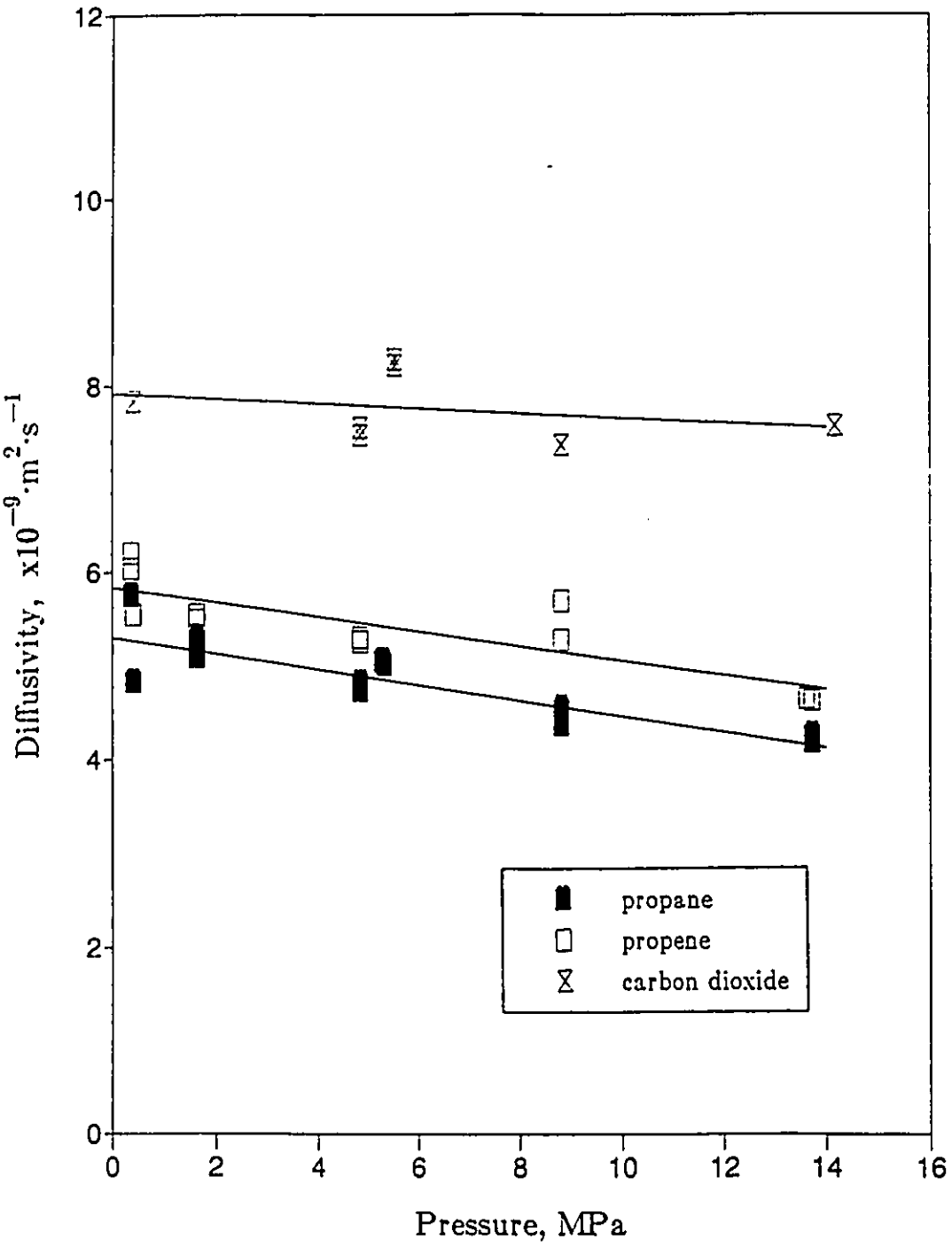

Figure H.1D: Effect of Pressure on the Diffusivity of All Solutes in Ethanol at 348.15 K

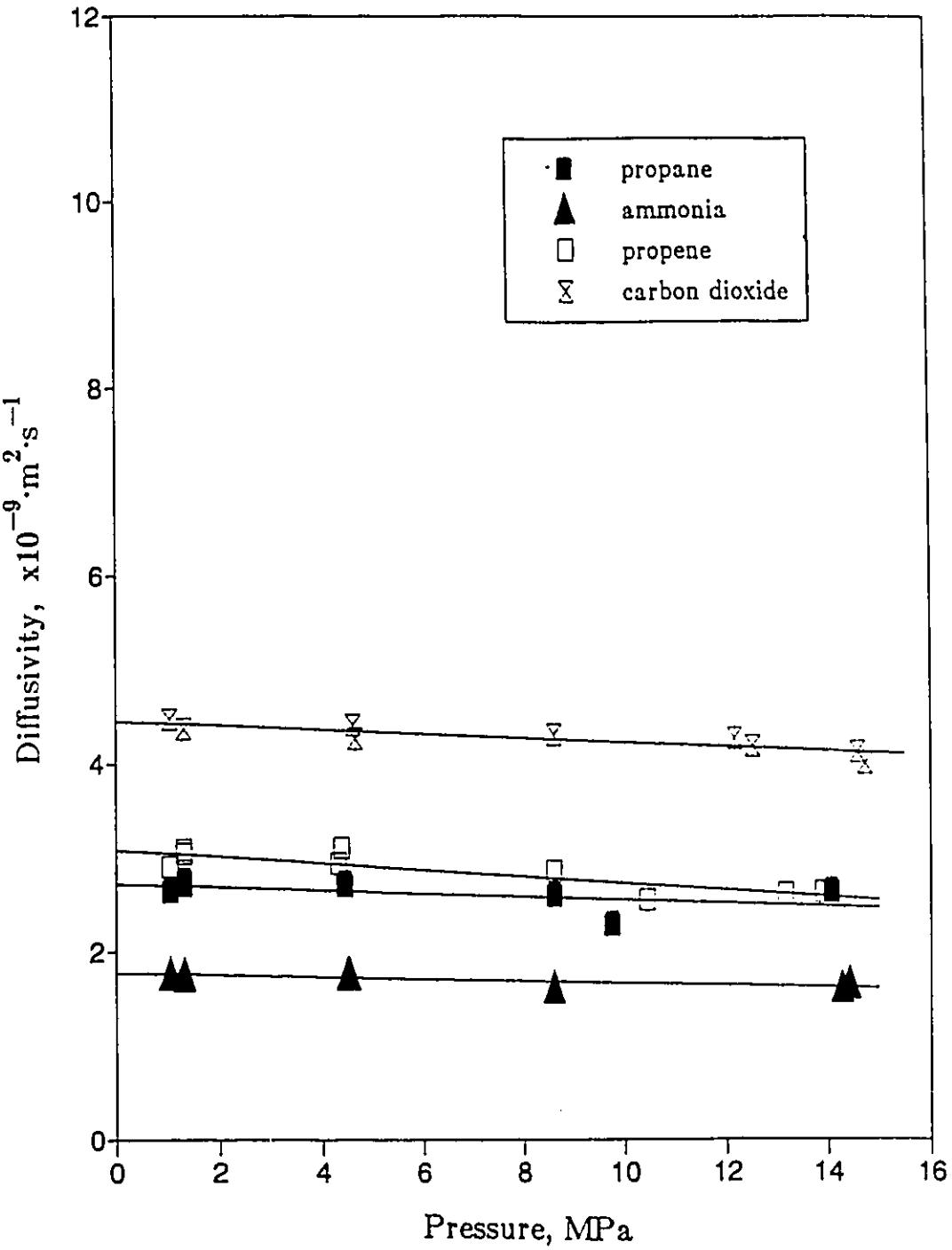

Figure H.1E: Effect of Pressure on the Diffusivity of All Solutes in Propanol at 323.15 K

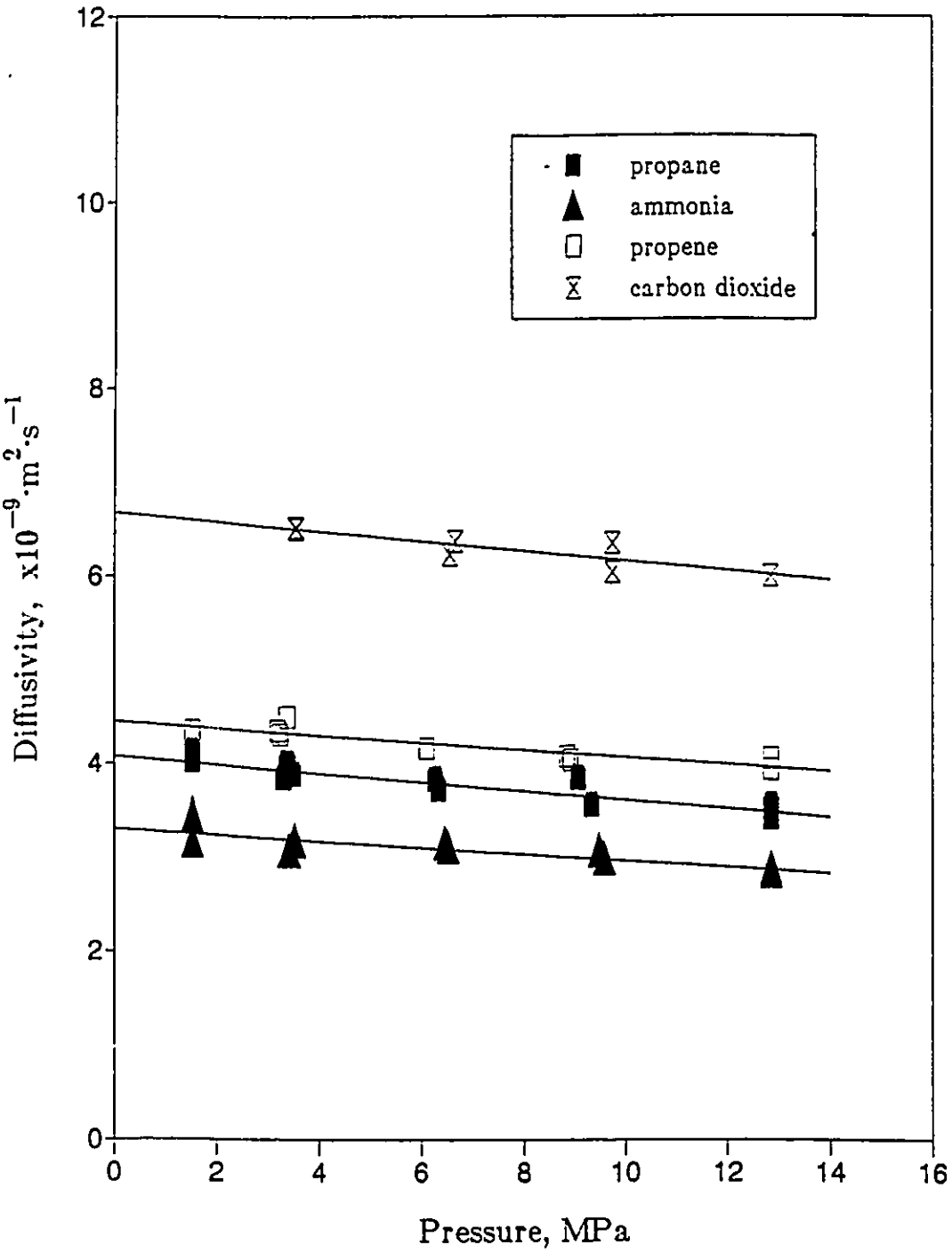

Figure H.1F: Effect of Pressure on the Diffusivity of All Solutes in Propanol at 348.15 K

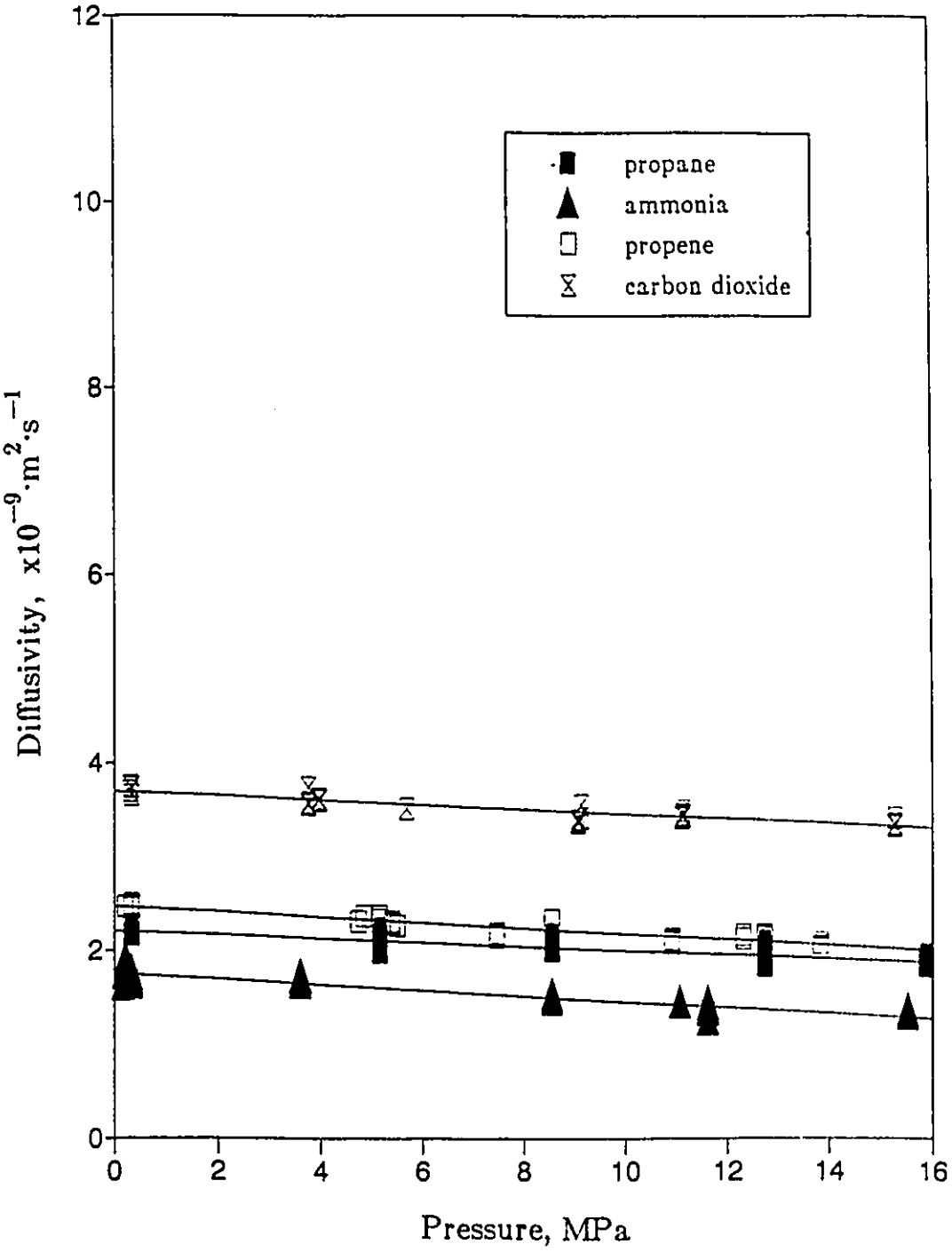

Figure H.1G: Effect of Pressure on the Diffusivity of All Solutes in Butanol at 323.15 K

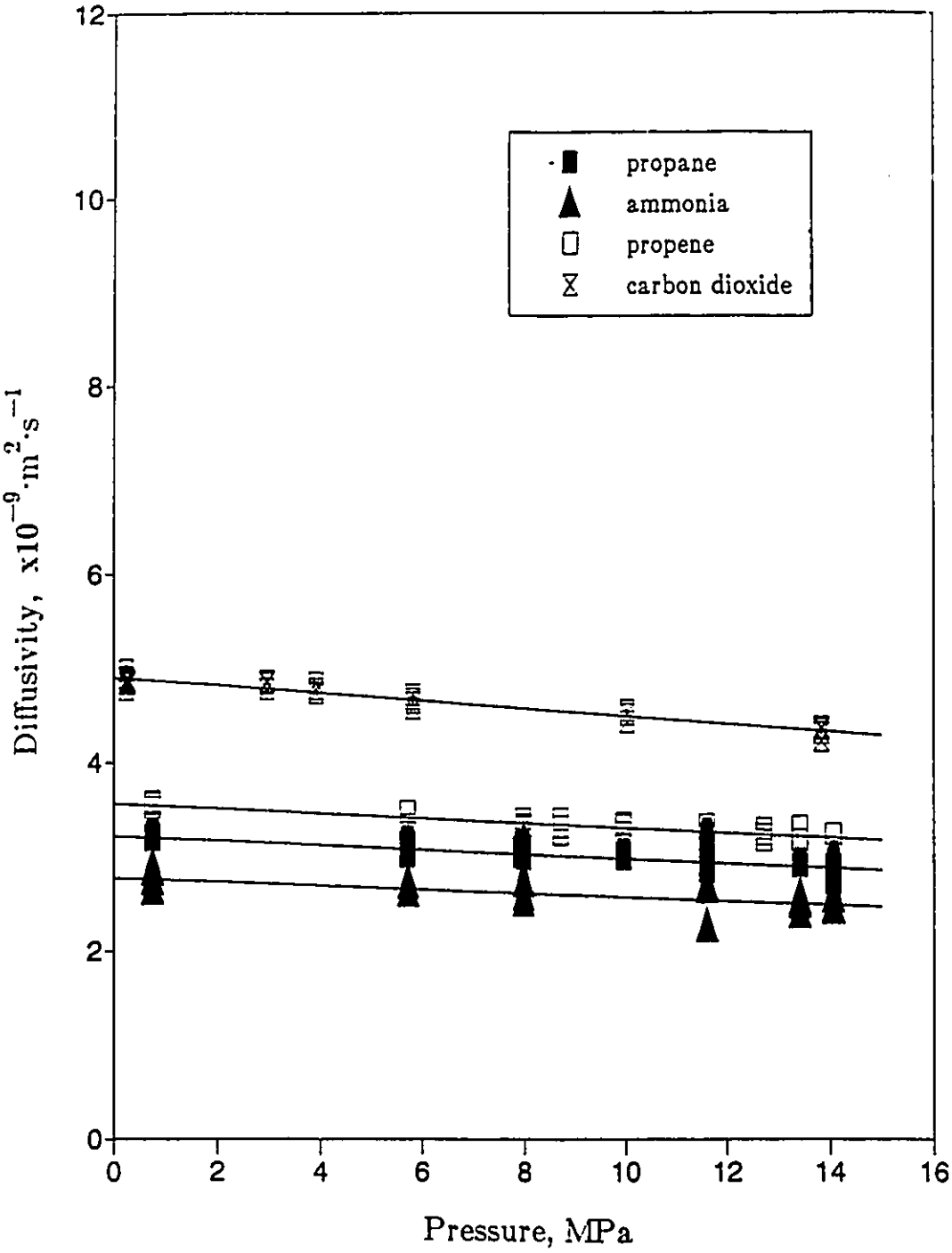

Figure H.1H: Effect of Pressure on the Diffusivity of All Solutes in Butanol at 348.15 K

APPENDIX I

FIGURES I.1A TO I.1H COMPARE THE EFFECT OF PRESSURE ON THE MOLECULAR DIFFUSIVITY OF EACH OF THE SOLUTES IN ALL OF THE SOLVENTS METHANOL, ETHANOL, PROPANOL AND BUTANOL AND AT ONE TEMPERATURE IN EACH CASE

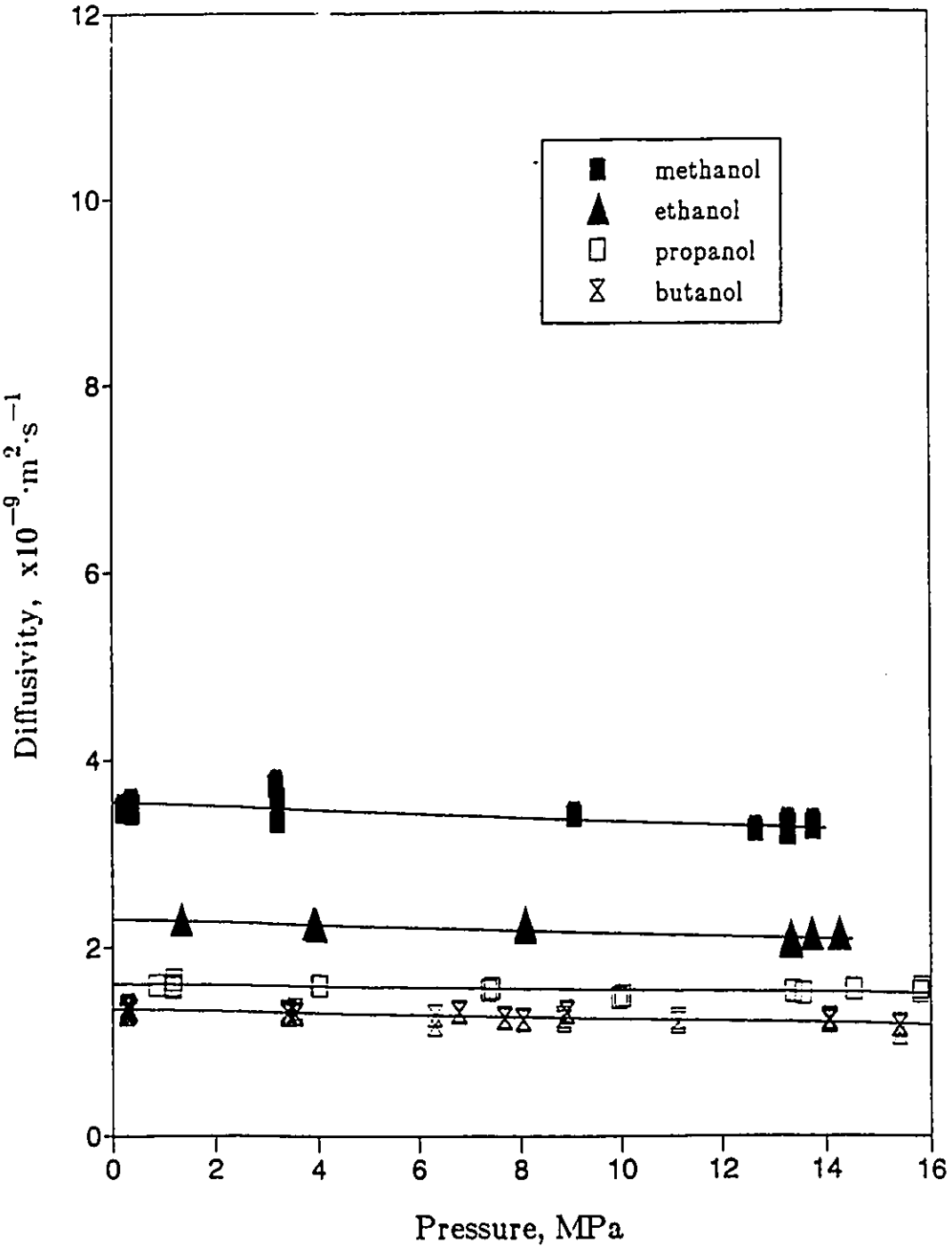

Figure I.1A: Effect of Pressure on the Diffusivity of Propane in All Solvents at 298.15 K

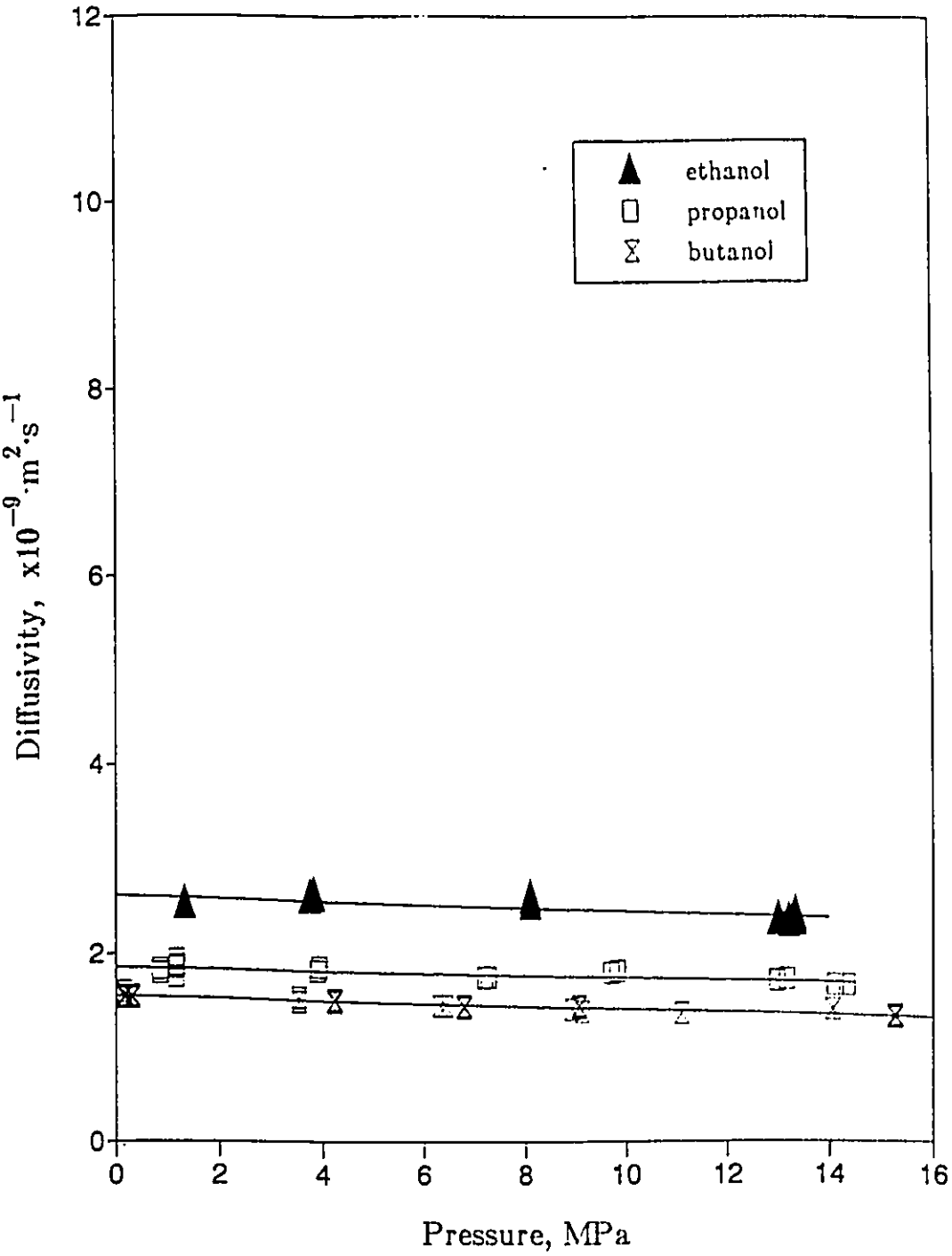

Figure I.1B: Effect of Pressure on the Diffusivity of Propene in All Solvents at 298.15 K

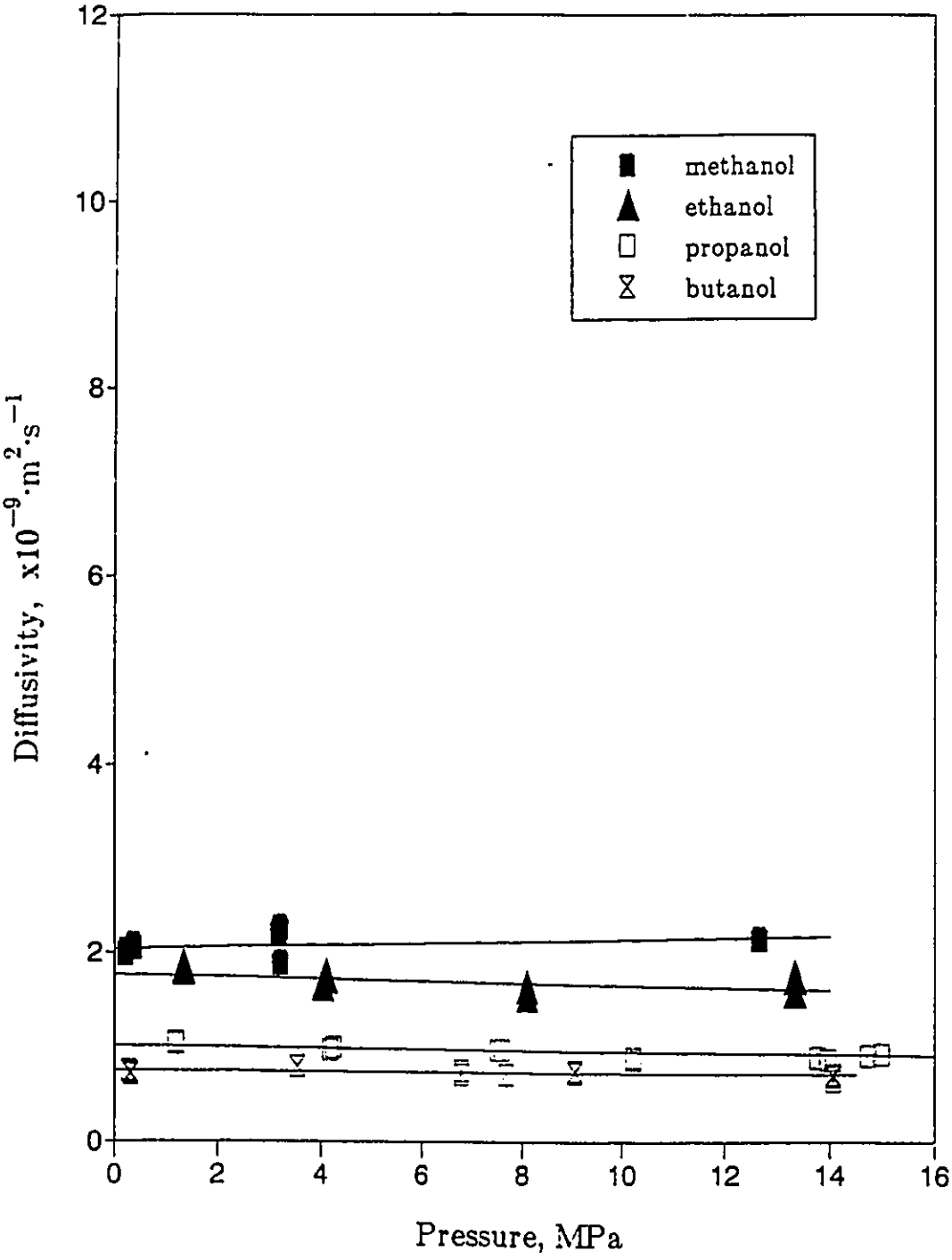

Figure I.1C: Effect of Pressure on the Diffusivity of Ammonia in All Solvents at 298.15 K

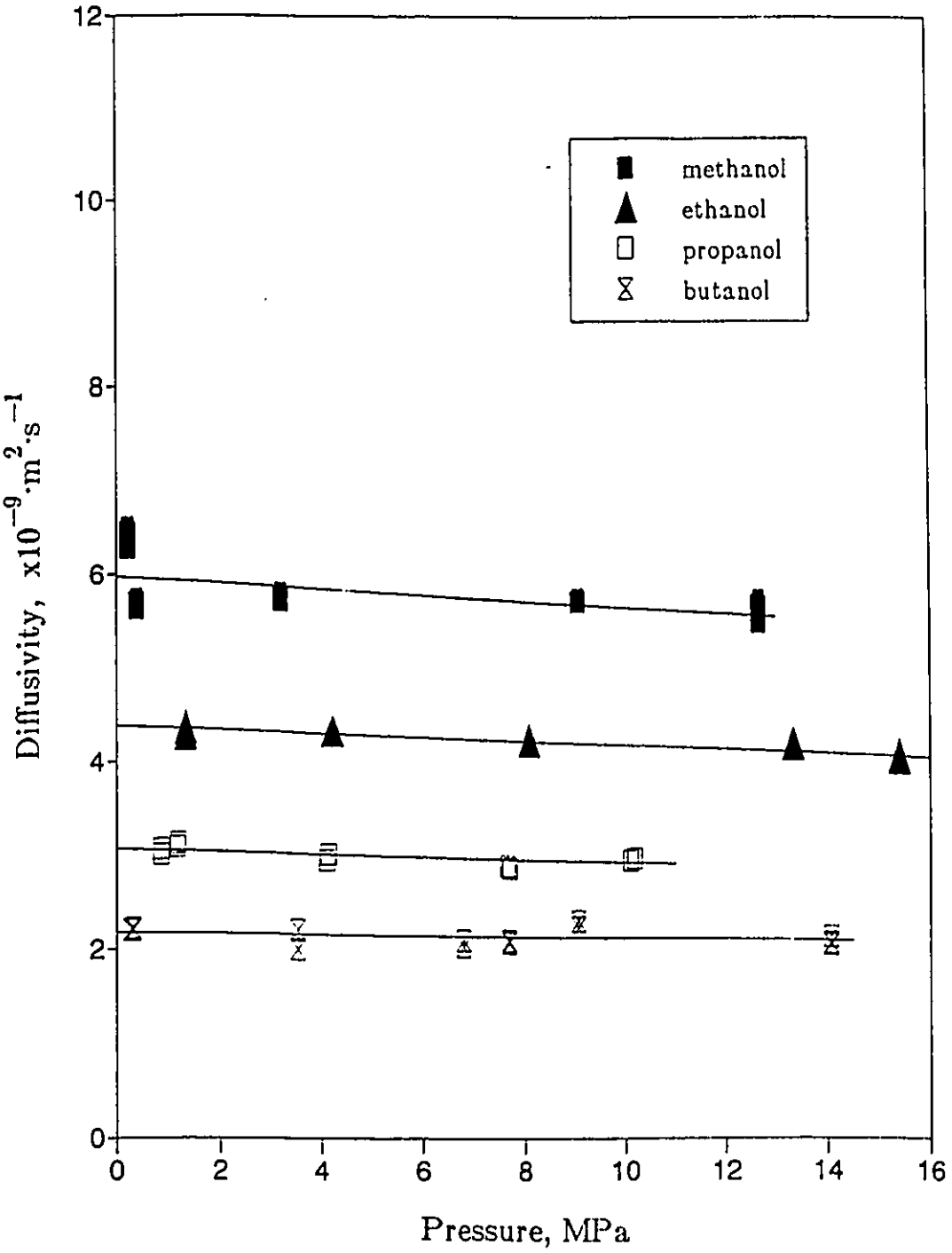

Figure I.1D: Effect of Pressure on the Diffusivity of Carbon Dioxide in All Solvents at 298.15 K

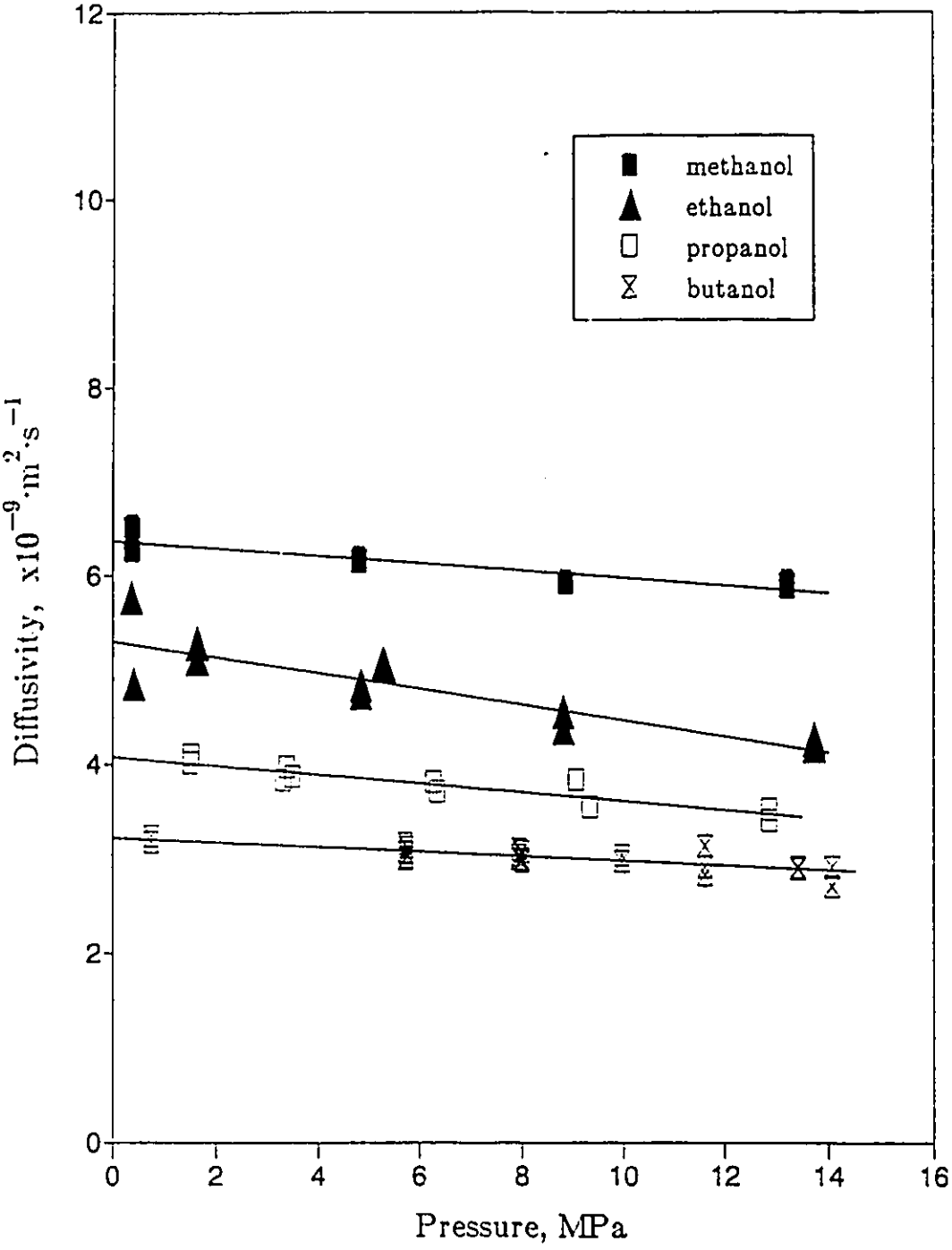

Figure I.1E: Effect of Pressure on the Diffusivity of Propane in All Solvents at 348.15 K

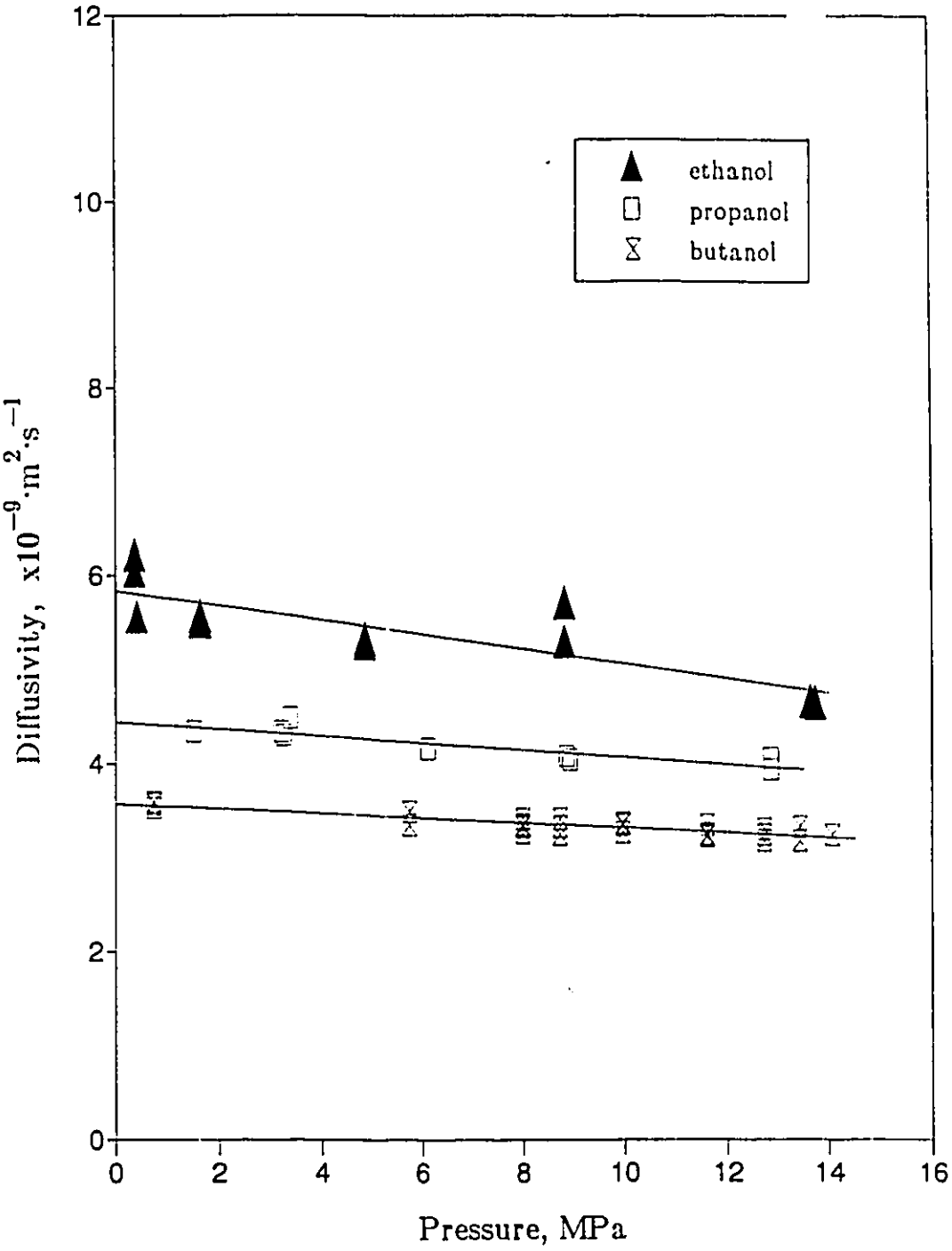

Figure I.1F: Effect of Pressure on the Diffusivity of Propene in All Solvents at 348.15 K

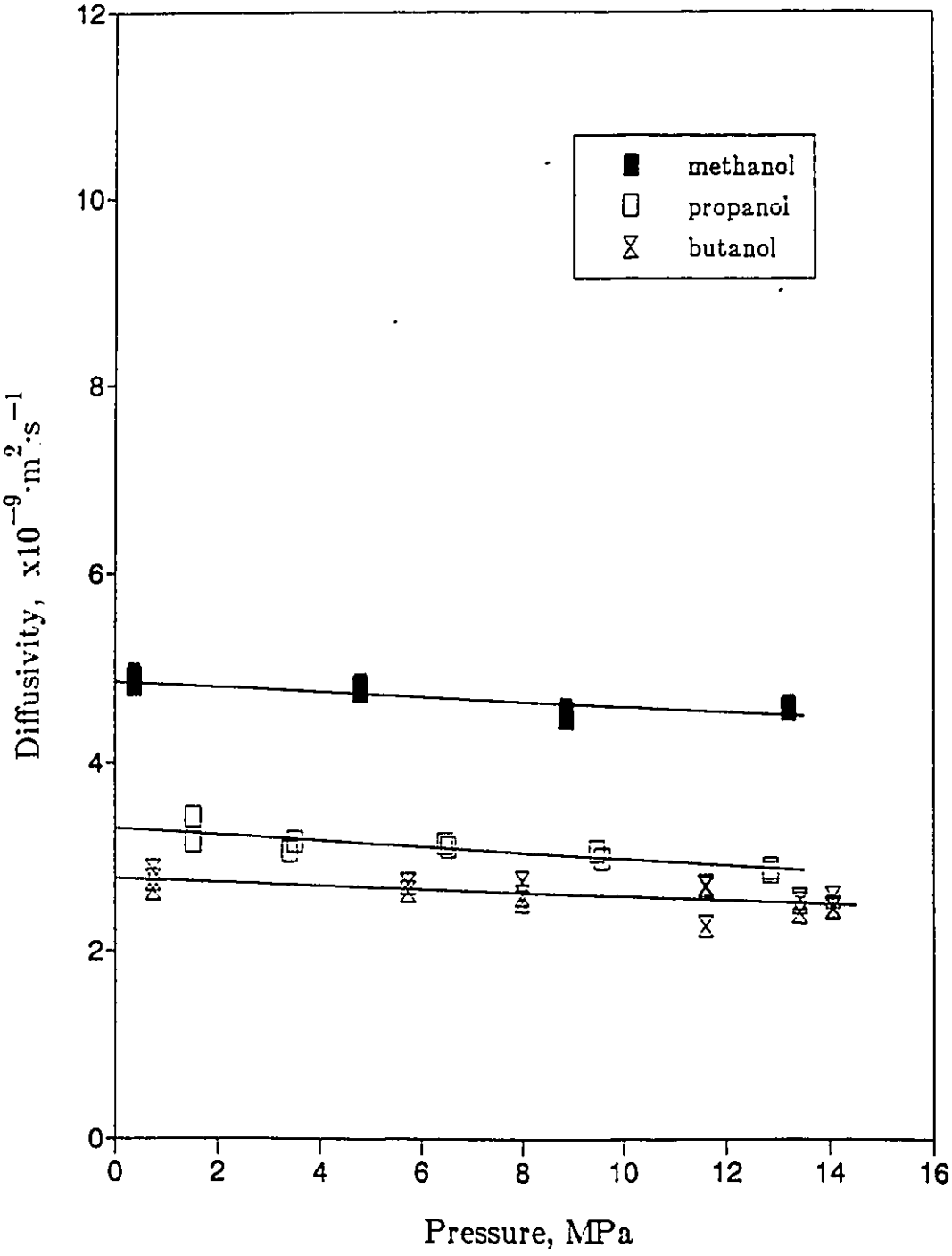

Figure I.1G: Effect of Pressure on the Diffusivity of Ammonia in All Solvents at 348.15 K

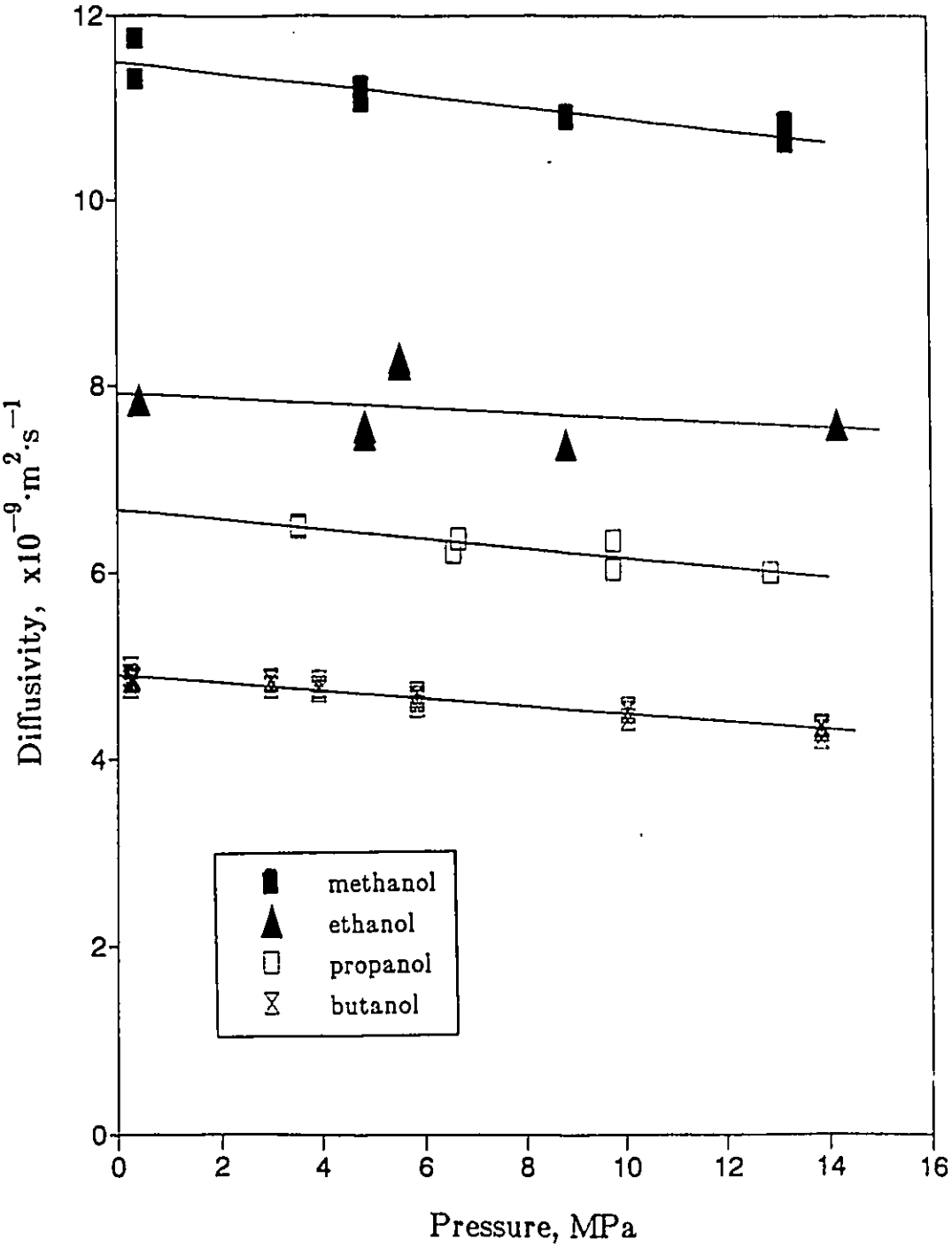

Figure I.1H: Effect of Pressure on the Diffusivity of Carbon Dioxide in All Solvents at 348.15 K

APPENDIX J

TABULATED VALUES OF THE VISCOSITY OF METHANOL AND ETHANOL AS A FUNCTION OF TEMPERATURE AND PRESSURE (TABLE J.1), AND THE APPLICATION OF THE RHS MODEL TO THIS DATA (FIGURES J.1A TO J.3B)

Preliminary viscosity data were measured for the solvents methanol and ethanol at 298.15, 323.15, and 348.15 K and up to pressures of 14 MPa. The method of measuring the viscosities of the solvents involved the use of conditioning capillary columns, the viscosity capillary column, and a differential pressure transducer. The conditioning columns, one of length L=0.50 m, and internal diameter I.D.=0.000127 m, and the other of L=12 m and I.D.=0.00076 m served the purposes of preheating the solvent before it flowed into the capillary viscometer and damping out pressure fluctuations. The differential pressure transducer was installed across the capillary viscosity column of L=0.50 m and I.D.=0.000127 m to measure the pressure drop across the column. The measured pressure difference, ΔP, across the length of capillary tubing was then used to obtain the viscosity of the solvent using the Hagen-Poiseuille equation. These measurements were done upstream of the dispersion column and were thus a part of the apparatus used to measure the diffusivities and the densities. Data were collected for the solvents methanol and ethanol only because the differential pressure cell was not installed until late into the experiments.

A linear regression analysis was performed on the measured viscosities as given in Table J.1 and it was observed that the viscosity increased linearly with increasing pressure and decreased with increasing temperature. Although the effect of temperature on viscosity was more significant than the effect of pressure, an F-test showed that the effect of pressure on viscosity was significant at the 95% confidence level.

Figure J.1 shows the comparison of the viscosity data for methanol and ethanol from this work to that reported by Daubert and Danner (1985). It was observed that there was excellent agreement between the measured and the reported viscosities (<1%). The ethanol results at 348.15 and 323.15 K have somewhat higher errors; however, these were the first two runs after installation of the DP cell and the baseline measurement had not stablized. The consistency of the remaining data confirms that this method can be reliably used for the accurate determination of the viscosity of a liquid.

It was Batchinski who first observed the linear relationship between viscosity and molar volume for 87 non-associated liquids. Batchinski found that this relationship could be expressed as:

$$\frac{1}{\eta} = B \cdot \frac{V_B - V_\eta}{V_\eta} \tag{3.37}$$

Table J.1

Effect of Pressure on the Viscosity of Methanol and Ethanol

Pressure (MPa)	Viscosity ($\times 10^{-4}$ Pa·s)					
	Methanol			Ethanol		
	298.15 K	323.15 K	348.15 K	298.15 K	323.15 K	348.15 K
0.26		3.77				
0.40			2.86			
0.59					7.13	
1.21					7.26	
1.39				10.87		
1.74						5.31
3.22	5.53					
3.87				11.14		
4.82			3.05			
5.36		4.14				
8.15				11.50		
8.74		4.21				
8.87						5.46
8.89			3.10			
10.42					7.54	
12.68	6.05					
13.22		4.29				
13.23			3.22			
13.52					7.78	
13.68						5.62
13.77	5.85					

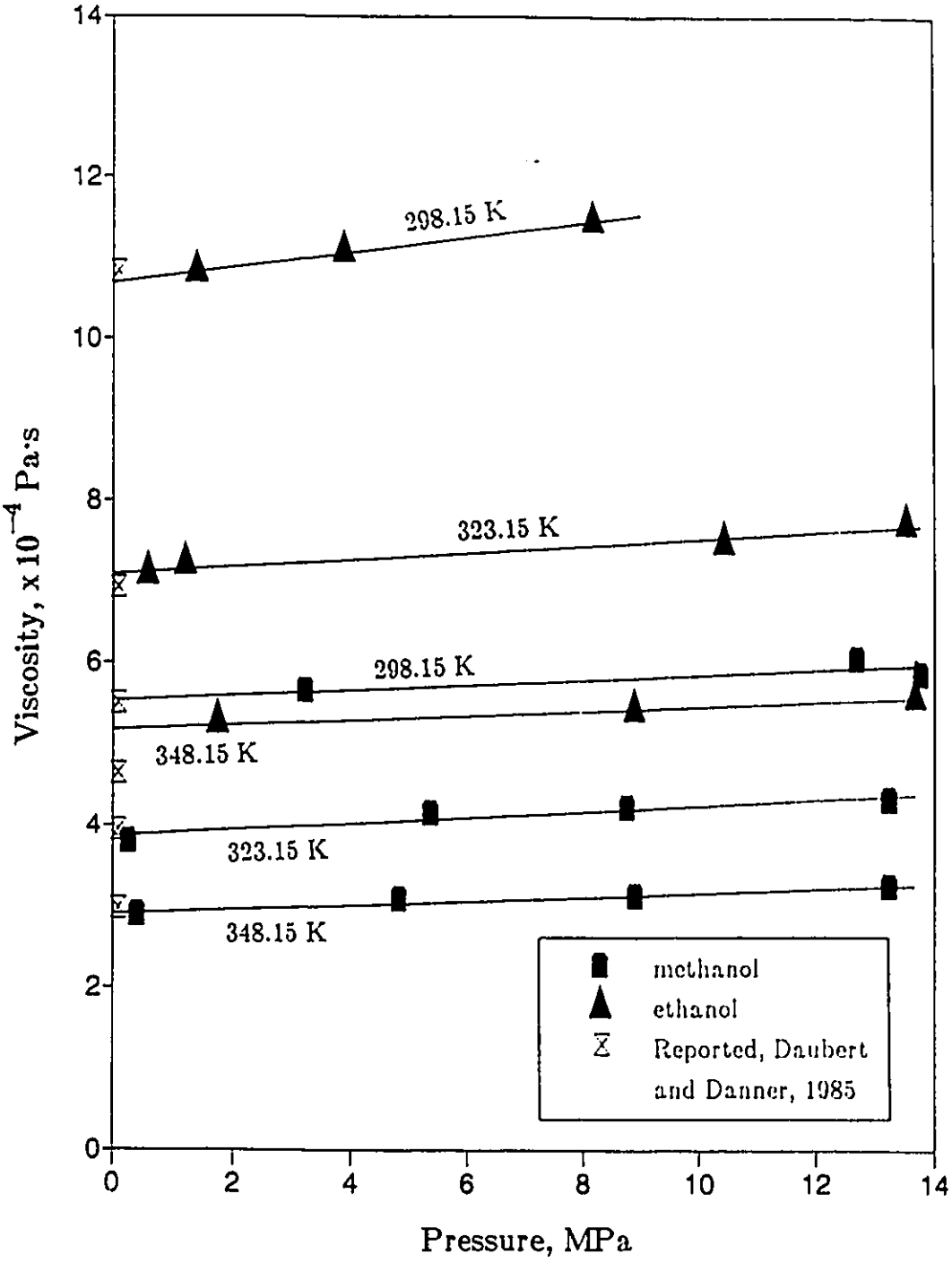

Figure J.1: Effect of Pressure on the Viscosity of Methanol and Ethanol at 298.15, 323.15 and 348.15 K

In equation (3.37), B is a constant dependent on the solvent, V_B is the molar volume of the solvent, and V_η is the hypothetical liquid molar volume at infinite viscosity, that is, where the fluidity is zero at its melting point. Thus $V_B - V_\eta$ was considered by Batchinski to be the free volume that exists between the fluids actual volume and the close packed volume at its melting point.

Hildebrand (1971) applied this reasoning to diffusivity and postulated a similar relationship:

$$D = B' \cdot \frac{V_B - V_D}{V_D} \tag{3.38}$$

In equation (3.38), V_D is equivalent to V_η and is the molar volume of the solvent at its melting point at which the diffusivity is zero, and $V_B - V_D$ is the free volume available for the diffusion process.

Both Batchinski and Hildebrand showed no theoretical basis for their equation. However the RHS theory and the resultant equations show a similar linear behaviour and with a theoretical basis for the equations.

Dymond (1974) first demonstrated, using the RHS theory, the linear relationship between the ratio of self diffusivity to the square root of temperature and the molar volume for the self diffusivity data, which is represented by:

$$\frac{D_{BB}^{DYM}}{\sqrt{T}} = F \cdot \frac{C'}{\sigma_B^2 m_B^{1/2}} \cdot [a(V - bV_o)] \tag{3.25}$$

Recalling that the limiting case of the infinitely dilute diffusion coefficient of A in B is:

$$\frac{D_{AB}^{\circ}}{\sqrt{T}} = \beta \cdot (V - bV_o) = \beta \cdot (V_B - V_D) \tag{3.35}$$

Dymond developed an analogous expression for viscosity:

$$\frac{\sqrt{T}}{\eta} = \beta' \cdot (V_B - V_\eta) \tag{J.1}$$

A similar linear relationship between $D_{AB}^{\circ}/\sqrt{T}$ and V_B was obtained for the solutes carbon dioxide, propane, propene and ammonia in the solvents methanol, ethanol,

propanol and butanol. This confirms the predictions of the RHS theory of equation (3.35). A similar linear relationship between $\sqrt{T}/\eta$ and V_B was obtained for the solvents methanol and ethanol, as shown in Figures J.2A and J.2B, respectively. This linear relationship again confirms the predictions of the RHS theory for viscosity (equation J.1).

The development of equations (3.35) and (J.1) using the RHS theory and the linear relationship between $\sqrt{T}/\eta$ and V_B and D°_{AB} and V_B suggest that β' and V_η are analogous to β and V_D. The values of V_η were observed to be close to the values of V_D for methanol and ethanol. Although the RHS theory predicts that these two values should be exactly the same, the differences could be due to experimental error or imperfections in the RHS theory near the melting point. Another possible and more likely reason why $V_\eta \neq V_D$ is that V_D was found to be a function of the properties of the solute and the solvent while V_η is a function of the properties of the solvent only. Also since β for the diffusivity data was found to be temperature dependent, the dependency of β' on temperature was examined. It was found that β' was significantly dependent on temperature with $V_\eta = V_{tp}$. Thus the point of intersection on the x-axis where the fluidity is equal to zero occurs at the molar volume of the solvent at its triple point. Therefore this explains why $V_\eta = V_{tp} \neq V_D$. Figures J.3A and J.3B show this temperature dependency of β' for methanol and ethanol, respectively.

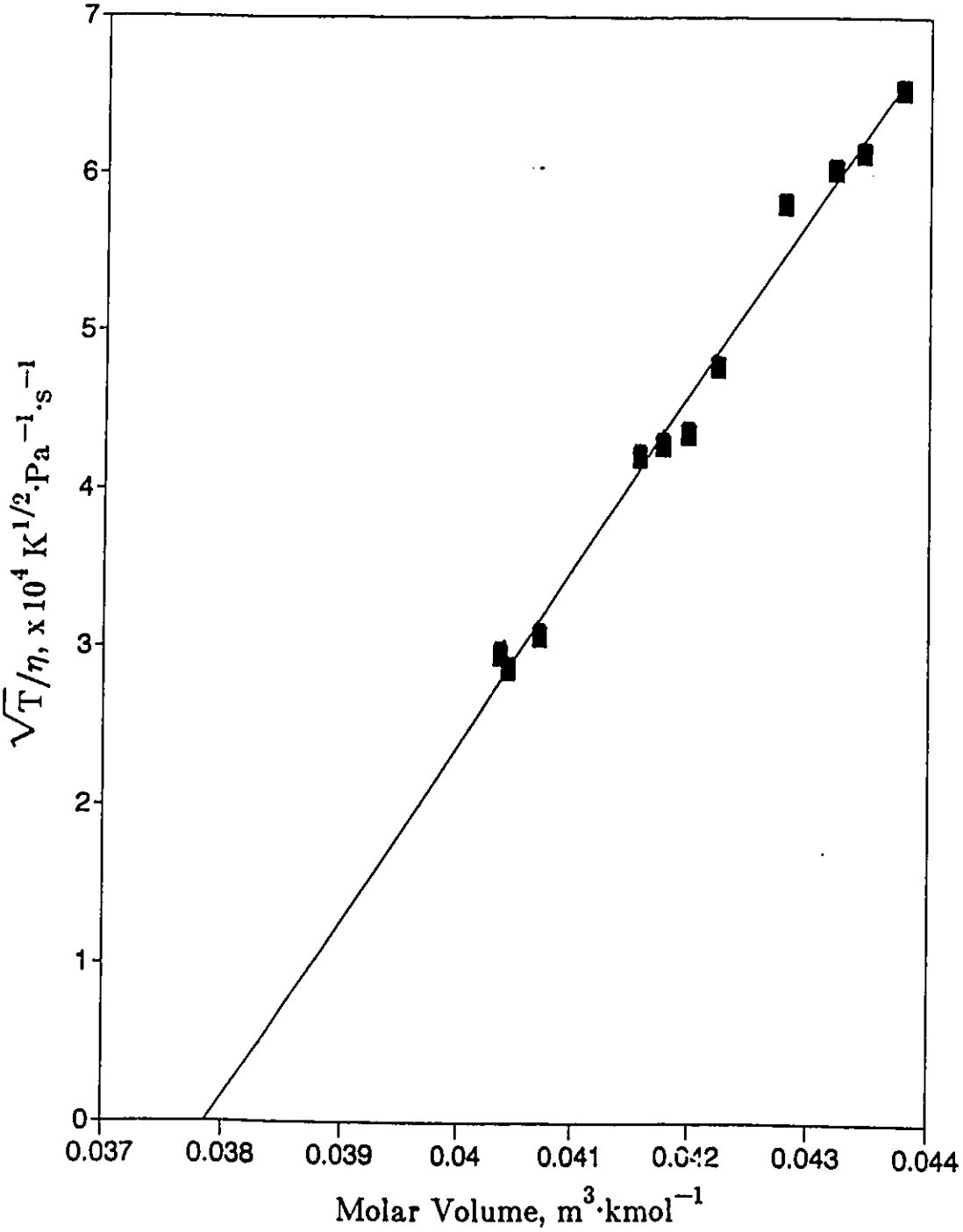

Figure J.2A: Linear Behaviour of $\sqrt{T}/\eta$ Versus Molar Volume in the Solvent Methanol at Several Temperatures and Pressures

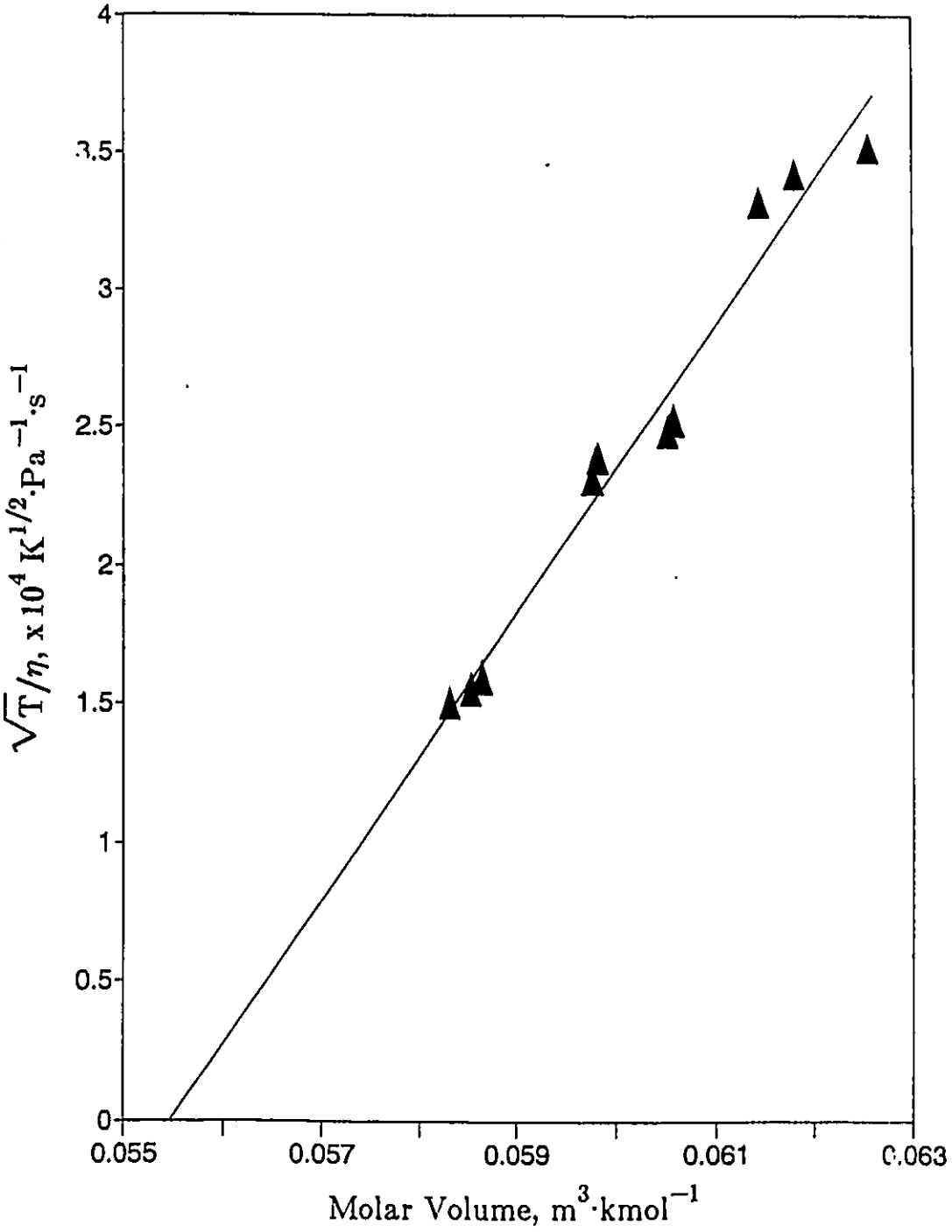

Figure J.2B: Linear Behaviour of $\sqrt{T}/\eta$ Versus Molar Volume in the Solvent Ethanol at Several Temperatures and Pressures

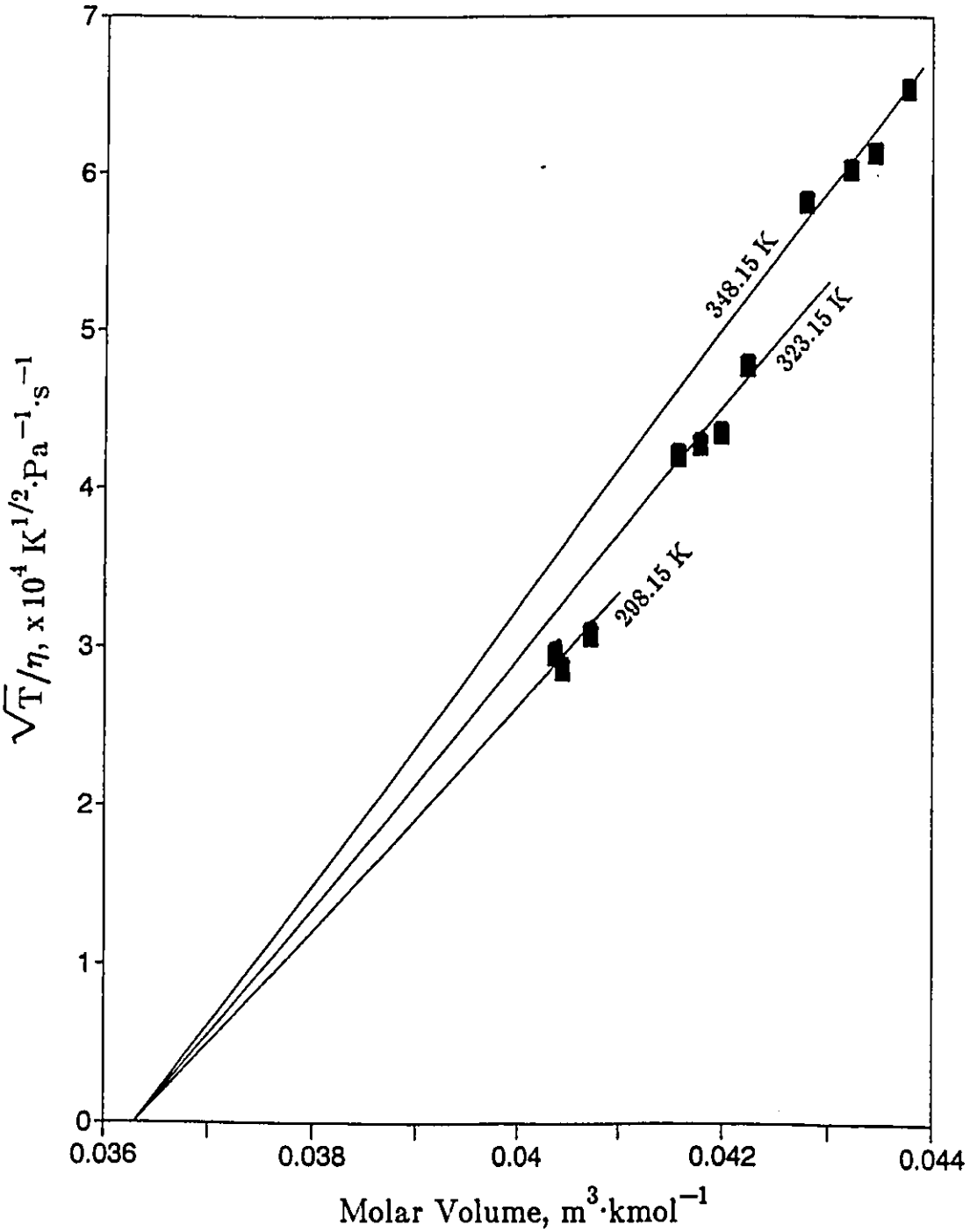

Figure J.3A: Linear Behaviour of $\sqrt{T}/\eta$ Versus Molar Volume in the Solvent Methanol over the Entire Pressure Range Using V_{tp}

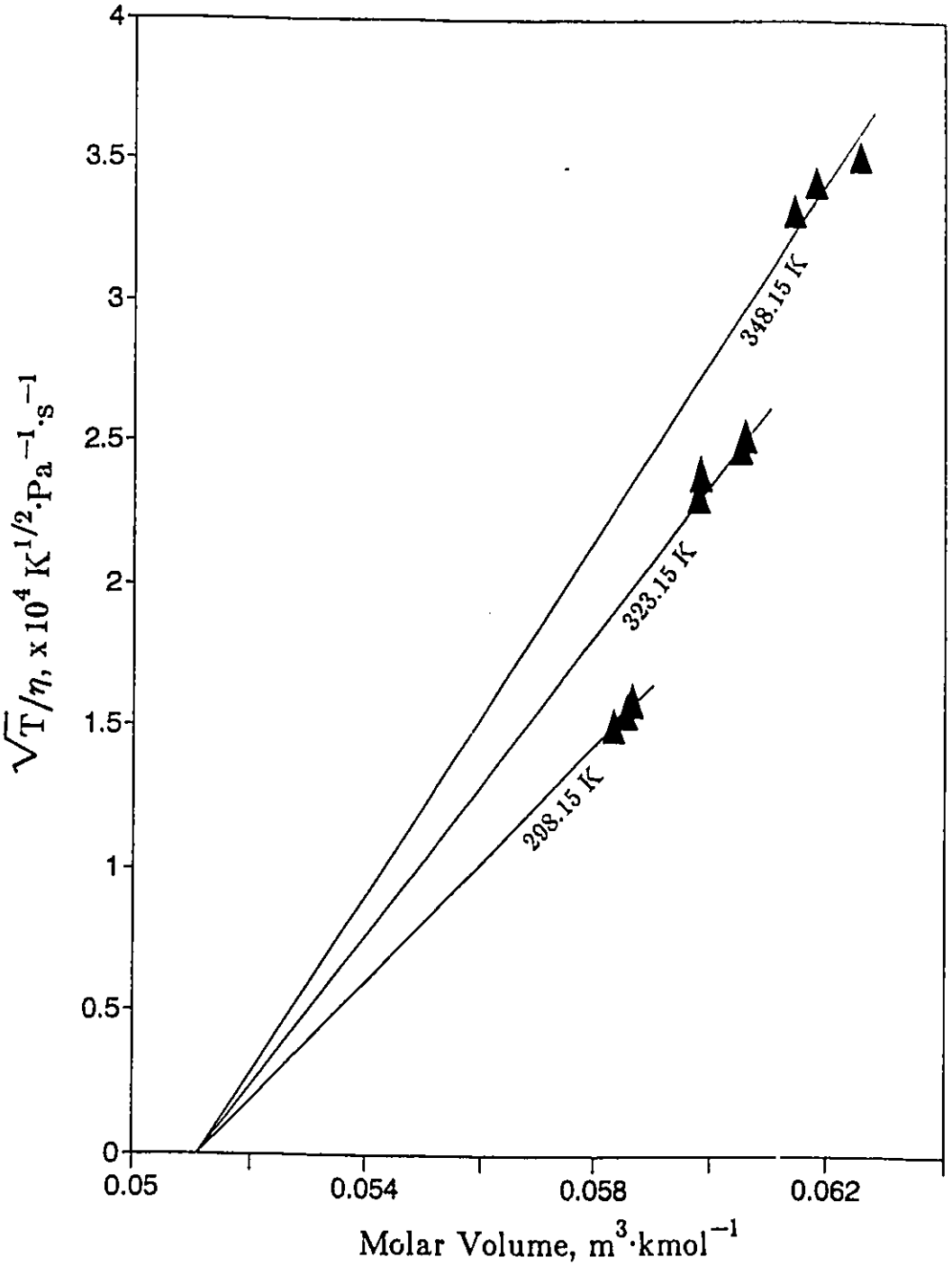

Figure J.3B: Linear Behaviour of $\sqrt{T}/\eta$ Versus Molar Volume in the Solvent Ethanol over the Entire Pressure Range Using V_{tp}